Integration of Hydrological and Economical Aspects for Water Management in Tropical Regions. Case Study: Middle Magdalena Valley, Colombia.

MARIA CRISTINA ARENAS BAUTISTA, M.Sc

Universidad Nacional de Colombia
School of Engineering
Doctoral Program in Civil Engineering
Bogota D.C., Colombia
2020

Integration of Hydrological and Economical Aspects for Water Management in Tropical Regions. Case Study: Middle Magdalena Valley, Colombia.

MARIA CRISTINA ARENAS BAUTISTA, M.Sc

A dissertation submitted as partial fulfillment of the requirements for the degree of:

Doctor in Engineering, *Ph.D*
in the Program of Civil Engineering

Research Line in Water and Environment Engineering
Hydrodynamics of Natural-Media Research Group - HYDS

Adviser:
Leonardo David Donado Garzón, Ph.D
Associate Professor

Universidad Nacional de Colombia
School of Engineering
Graduate Programs in Civil and Agricultural Engineering
Bogota D.C., Colombia
2020

This work was funded by Colciencias and Universidad Nacional de Colombia with the Financing Program 647.

This work was also supported by Universidad Nacional de Colombia Research Program, with National Call for the International Mobility N. 9599.

A mi familia, lo más importante en mi vida.
A mi mamita, Ligita, quien nunca me dejo desfallecer.
A Laura, a quien espero dejarle como ejemplo que educarse si vale la pena.
A Pedro, mi compañero de vida, quien pese a las dificultades me apoyó incondicionalmente.
A Leonardo, mi Director y amigo, por creer en mí.

Acknowledgment

I want to give the special thanks to the guidance given by professors Monica Riva and Alberto Guadagnini from the Politecnico di Milano (Italy) during my internship. Also, I want to thank the members of the Hydrodynamics of Natural-Media - HYDS and GIREH research groups, whose questions, discussions, and examples gave me new ideas to improve each part of this work. Juan Pescador, I not only want to thank you I also want to recognize your work in the consolidation of the geological model; This would not be possible without your help. Thanks to Edwin Saavedra, Pedro Arboleda, Alejandro Proaño and Sarah Coral for your help in style review of this document. Thanks to Universidad Nacional de Colombia, that partially funded my Ph.D studies.

I would like to thank my advisor Leonardo Donado for his patience and unconditional support in my doctoral training process. Thank you Leonardo, for showing me a different path of life, for contributing to improve my professional skills and as a friend, for your kind guidance in difficult moments.

Graphical Abstract

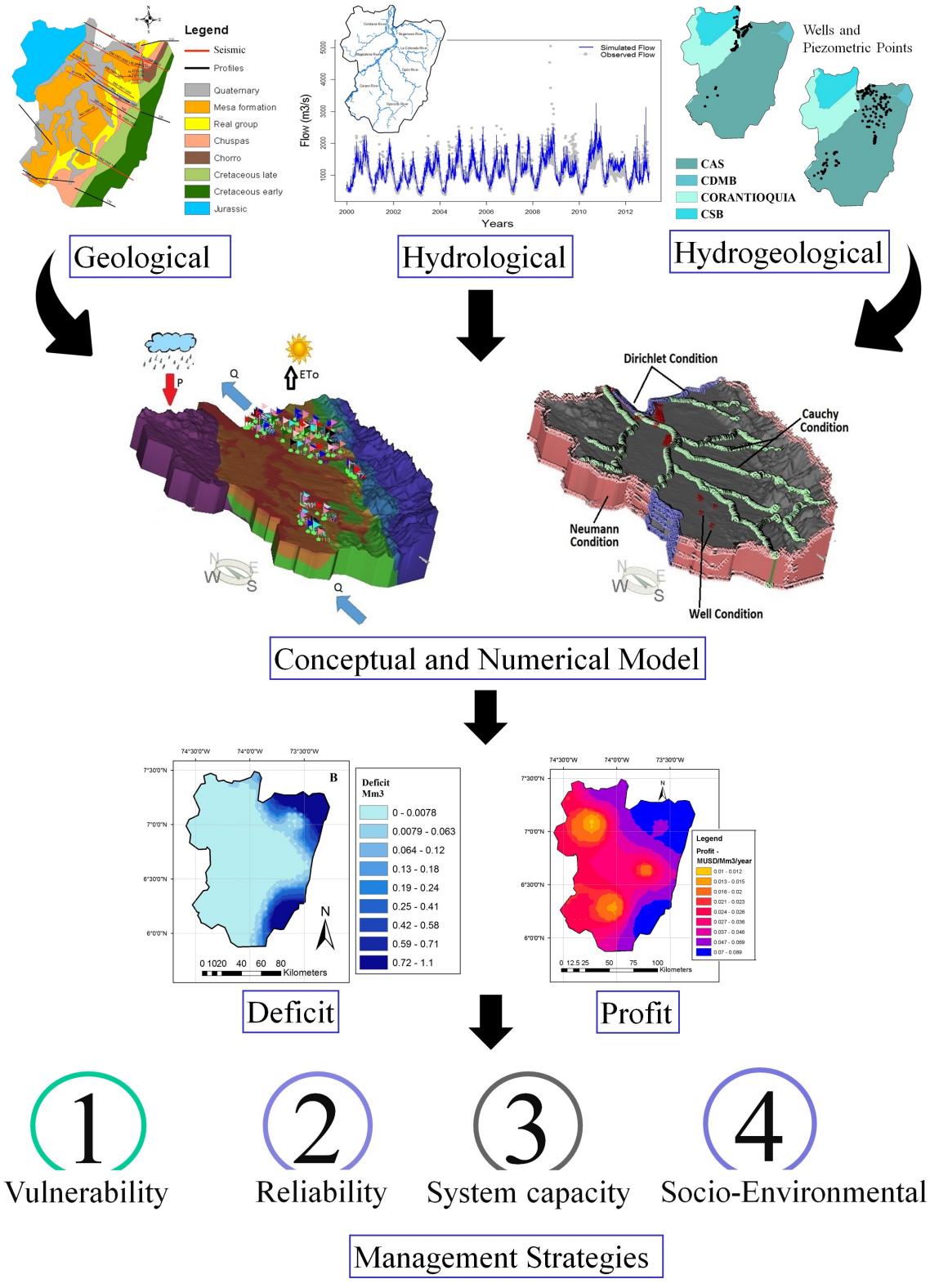

Resumen

El recurso hídrico es un factor determinante en el desarrollo económico y social de las comunidades dada la amplia necesidad que se genera en torno a su aprovechamiento. El uso del agua ha generado a través de los años, presiones sobre su disponibilidad, las cuales usualmente se resolvían aumentando el suministro, explorando y desarrollando nuevas fuentes y, expandiendo las extracciones de las ya existentes. En Colombia, la concesión de agua es el derecho al uso limitado del agua, otorgado para desarrollar una actividad económica. Esta concesión debe estar relacionada con la disponibilidad de agua para garantizar la preservación y el uso eficiente del agua. Para asignar el recurso hídrico de manera eficiente se requieren herramientas que ayuden a tomar decisiones mediante el análisis del régimen hidrológico integral (aguas superficiales y subterráneas), lo cual es un problema complejo en áreas que carecen de datos hidrológicos confiables; y que permiten una evaluación sobre la disponibilidad en un contexto económico. En este orden de ideas, el objetivo principal de esta investigación fue proporcionar una aproximación metodológica que permita integrar aspectos hidrológicos, hidrogeológicos y económicos en la asignación de agua entre diferentes usuarios, priorizando las necesidades humanas y los procesos ecosistemicos, para establecer estrategias de gestión a escala regional.

En consecuencia, esta investigación realizó una integración de aspectos hidrológicos, hidrogeológicos y económicos, utilizando la cuenca geológica del Valle Medio del Magdalena (MMV) como laboratorio a escala real. Debido a que esta zona es centro de abastecimiento para la pequeñas poblaciones rurales y se desarrollan de manera conjunta actividades económicas relacionadas con minería, agricultura, acuicultura, producción pecuaria, industria, generación hidroeléctrica, servicios de seguridad y emergencia y exploración y producción de hidrocarburos, se analizó el comportamiento hídrico y económico del sistema respecto a la disponibilidad de agua superficial y subterránea, y su asignación a los diferentes usuarios. Para ello, se definieron tres etapas: **(1.)** caracterización del sistema hidrológico, **(2.)** caracterización del sistema hidrogelógico, y **(3.)** su integración en un modelo de optimización económica.

En la **primera etapa**, se analizó mediante herramientas numéricas el comportamiento hidrológico del sistema para caracterizar la oferta hídrica. En adición, se identificaron las zonas de recarga y se investigaron las alteraciones hidrológicas que afectan la cantidad de agua en el sistema. La modelación hidrológica permitió realizar una evaluación exhaustiva de la interacción entre la dinámica del ciclo hidrológico y las condiciones climáticas. Luego, se realizaron los análisis de sensibilidad e incertidumbre para evaluar la influencia de los

principales parámetros asociados con el modelo y a partir de ello, se validó una metodológia que permite: (*i*) seleccionar valores apropiados para los parámetros de los modelos y (*ii*) evaluar en qué medida la variación de estos parámetros afecta una respuesta simulada.

En la **segunda etapa**, se integraron la caracterización geológica, la hidrológica y la hidráulica en un modelo hidrogeológico para estimar el volumen de agua y la descripción del sistema de flujo subterráno. El resultado de esta etapa permitió consolidar una metodología para restringir asertivamente un modelo inverso altamente parametrizado con pocos o sesgados datos de campo, estimar parámetros hidráulicos de acuíferos y analizar la variación espacial y temporal que presentan estos parámetros a escala regional.

Finalmente, en la **tercera etapa**, se integraron los aspectos hidrológicos superficiales y subterráneos desarrollados anteriormente, en un marco de optimización económica para determinar la asignación conjunta de agua y la gestión de la calidad del recurso hídrico. Este aparte tuvo como objetivo principal análizar el beneficio de uso del agua en un modelo de flujo regional que integra múltiples ofertas de agua y de demandas por parte de los usuarios. Aquí, se analizó el modelo de asignación desde una escala regional con el fin de consolidar tipologías de uso por sector económico y determinar estrategias de gestión a escala regional que permitan reducir los conflictos por uso y calidad, y fortalecer la gestión y administración del recurso hídrico en la zona.

Los resultados generales de esta investigación permitieron identificar y evaluar de manera conjunta los problemas y estrategias de gestión, en una cuenca tropical con escases de información. Adicionalmente, se concluyó sobre cómo la cuantificación de la oferta hídirica afecta el proceso de asignación entre diferentes usuarios y este proceso a su vez, esta en función de la calidad. Como parte de la etapa final de esta investigación, se analizó a través de escenarios futuros el comportamiento del sitema hídrico.

Abstract

Water resources are a determining factor in the economic and social development of communities, given the need that is generated around its use. Over the years, this use has generated pressure on water availability, which were solved by increasing supply, exploring and developing new water sources, and expanding the existing extractions. In Colombia, water concession is the right to the limited use of water, and it is granted to develop economic activity. This concession must be related to water availability to ensure the preservation and efficient water use. However, to allocation water resources efficiently, tools that help to make decisions by analyzing the hydrological regime (surface and groundwater) in areas with lacking reliable data on water availability in an economic context are required. In this context, the main goal of this research was to provide a methodological approximation that allows integrating hydrological, hydrogeological, and economic aspects in water allocation between different users, prioritizing human needs and ecosystem processes, to establish management strategies at a regional scale.

In this research performed an integration of diverse hydrological, hydrogeological, and economical aspects, using the Middle Magdalena Valley (MMV) geological basin as a real scale laboratory. Because this area is a primary supply center for the Colombian population, and economic activities related to mining, agriculture, aquaculture, livestock, industrial, services, and O&G exploration and exploitation are developed in conjunction; hydric and economic behavior of the system was analyzed. This analysis was carried out in regards to water availability (surface and groundwater), and its allocation to different stakeholders. For it, three phases were defined: **(1.)** to characterize the hydrological system, **(2.)** to characterize the hydrogeological system, and **(3.)** its integration into an economic optimization model.

In the **first phase**, the hydrologic system behavior was analyzed through a numeric tool, to characterize the water supply, the recharge zones were identified, and the hydrologic alterations affecting the water supply were evaluated. The hydrological modeling allowed to perform an exhaustive interaction analysis between the hydrologic cycle dynamic and the weather condition and land use. Then, it was made an analysis of uncertainty and sensitivity to evaluate the influence of the principal parameters associated with the model. From this analysis, it was validated a methodology allowing to: (*i*) select proper values for the model parameters, and (*ii*) evaluate how the model parameters variations influence a simulated response.

In the **second phase**, the geological, hydrological and hydraulic characterization was integrated into a hydrogeological model to estimate the water volume and groundwater flow system description. The result of this phase allowed to consolidate a methodology to assertively restrict a highly parameterized inverse model with lack of information, estimate hydraulic parameters of aquifers and analyze the spatial and temporal variation presented by these parameters at the regional scale.

Finally, in the **third phase**, the hydrological aspects (surface and groundwater) were integrated with an economic optimization framework. This allows them to determine water allocation and water resources quality management. The main objective of this phase was to analyze the water use profit in a regional flow model, integrating multiple water supplies (surface and groundwater) and multiple demands. Here, the allocation model was analyzed from a regional scale in order to consolidate typologies of use by economic sector, and determine management strategies at a regional level.

The general results of this research allowed to identify problems and evaluate management strategies, in a tropical basin at the regional level. Additionally, it was concluded that the quantification of water supply affects the allocation process between different stakeholders and this process, in turn, is a function of water quality. As part of the final stage of this research, the water system behavior was analyzed through future scenarios.

Keywords

Keywords: Hydro-economic Optimization, Integrated Water Resources Management, Economic Aspects, Water Allocation, Management Strategies, Hydrological modeling, hydrogeological Model, Tropical Regions, uncertainty, sensitivity analysis, Sobol and *AMA* indices, pilot-points technique, PEST, inverse parameterization.

Palabras clave: Optimización Hidroeconómica, Gestión Integral del Recurso Hídrico, aspectos económicos, asignación de agua, estrategias de gestión, Modelación hidrológica, Modelación hidrogeológicoa, incertidumbre, análisis de sensibilidad, índices Sobol y *AMA*, técnica de puntos piloto, PEST, parametrización inversa.

Related Publications

Papers

Arenas-Bautista, M.C., Pescador-Arévalo, J.P., Donado, L.D., Saavedra-Cifuentes, E.Y. and Arboleda-Obando, P.F. (2020). Hydrogeological Modeling in Tropical Regions via FeFlow. *Earth Sciences Research Journal*. (Accepted for Publication).

Arenas-Bautista, M.C., Saavedra-Cifuentes, E.Y., Arboleda-Obando, P.F and Donado, L.D. (2020). Impact of pilot points number and plausibility for determination of hydraulic properties in a real regional model of groundwater. In preparation to *Groundwater Journal*.

Arenas-Bautista, M.C., Gardeazabal, N., Arboleda-Obando, P.F, Guadganini, A., Riva, M. and Donado, L.D. (2020). Comparing Global Sensitivity Analysis approaches of a Semi-Distributed Hydrological Model in Tropical Regions. Study case: Middle Magdalena Valley, Colombia. In preparation to *Water Resources Management Journal*.

Arenas-Bautista, M.C. and Donado, L.D. (2020). Hydro-economic Optimization of the Assignment and Management of Water Quality in Tropical Basin. In preparation to *Water Resources and Economics Journal*.

Conferences

Arenas-Bautista, M. C. and Donado, L.D. (2020). Integrated Water Resources Optimization Model a tropical basin in Colombia. In European Geosciences Union -EGU, 3 - 8 may. Vienna (Austria).

Arenas-Bautista, M. C., Pescador-Arévalo, J.P. and Donado, L.D. (2019). Pilot-Points Impact in Determination of Hydraulic Properties in a Tropical Basin. Study Case: Middle Magdalena valley . In Darcy Lecture -ICGW, 22 November. Bogotá (Colombia).

Donado, L.D., **Arenas-Bautista, M.C.** and Pescador-Arévalo, J.P. (2018). Hydrogeological Characterization in Tropical Regions with lack of information subject to competing uses of groundwater. In American Geophysical Union -AGU, 10-14 December. Washington (USA). DOI: 10.13140/RG.2.2.12349.10727

Arenas-Bautista, M. C., Pescador-Arévalo, J.P. and Donado, L.D. (2018). Three-dimensional geological model applied for groundwater flow simulations in the Middle

Magdalena Valley, Colombia. In American Geophysical Union -AGU, 10-14 December. Washington (USA). DOI: 10.13140/RG.2.2.19059.99365

Arenas-Bautista, M.C., Gardeazabal, N., Arboleda-Obando, P.F, Guadganini, A., Riva, M. and Donado, L.D. (2018). Sensitivity Analysis to uncertain Parameters of TopModel in Tropical Regions with application to the Middle Magdalena Valley (Colombia). In European Geosciences Union -EGU, 8-13 April. Vienna (Austria). DOI: 10.13140/RG.2.2.29463.68008.

Arenas-Bautista, M. C., Gardeazabal, N., Arboleda-Obando, P.F, Guadganini, A., Riva, M. and Donado, L.D. (2017). Hydrological Modeling in Tropical Regions via TopModel. Study Case: Central Sector of the Middle Magdalena Valley - Colombia. In European Geosciences Union -EGU, 23-28 April. Vienna (Austria). DOI: 10.20944/preprints201807.0210.v1.

Arenas-Bautista, M.C., Suescún-Casallas, L.C., Guadganini, A., Riva, M. and Donado, L.D. (2017). Hydrogeological model of the Middle Magdalena Valley – Colombia. In International Conference on Groundwater -ICGW, 28-31 August. Bogotá (Colombia). ISBN: 978-958-59856-0-5.

Arenas-Bautista, M.C., Gardeazabal, N., Arboleda-Obando, P.F, Guadganini, A., Riva, M. and Donado, L. D. (2017). Hydrological Modeling the Middle Magdalena Valley (Colombia). In American Geophysical Union -AGU, 11-15 December. New Orleans (USA).

R Package - Tool

García-Echeverri, C., **Arenas-Bautista, M. C**, and Donado, L. D. (2020). GSA.UN: Global Sensitivity Analysis Tool - R package (Version v1.0.0). Zenodo. http://doi.org/10.5281/zenodo.3870871. https://CRAN.R-project.org/package=GSA.UN

Contents

List of Symbols

Symbol	Units	Description
T	°C	Temperature
P	LT^{-1}	Precipitation
Q	L^3T^{-1}	Flow
E	LT^{-1}	Evapotranspiration
ET_o	LT^{-1}	Potential Evapotranspiration
E_a	LT^{-1}	Real Evapotranspiration
R_s	LT^{-1}	Solar Radiation
R_a	LT^{-1}	Extraterrestrial Radiation
a_i	L	Upslope Contributing Area
β_i	radians	Average Slope
D	L	Local Storage Deficit
h	L	Hydraulic Head
K	LT^{-1}	Hydraulic Conductivity
k	L^2	Permeability
∇h	L	Hydraulic Gradient
η	-	Porosity
S_S	L^{-1}	Specific Storativity
t	T	Time
T	L^2T^{-1}	Transmisivity

$-Dimensionless$

Acronyms

COD	Chemical Oxygen Demand
CZ	Constant Zones
DTA	Digital Terrain Analysis
DO	Dissolved Oxygen
EC	Electrical Conductivity
ERA	Environmental Regional Authority
FDC	Flow Duration Curve
GLUE	Generalized Likelihood Uncertainty Estimation
GSA	Global Sensitivity Analysis
IWRM	Integrated Water Resources Management
ITCZ	Inter-Tropical Confluence Zone
LSA	Local Sensitivity Analysis
MCB	Magdalena-Cauca Basin
MSE	Mean Square Error
MMV	Middle Magdalena Valley
MESD	Ministry of Environment and Sustainable Development
NWS	National Water Study
NSE	Nash Sutcliffe Efficiency
O&G	Oil and Gas
PP	Pilot-points
PIA	Price Index Analysis
pdf	Probability Density Function
RMSE	Root Mean Square Error
SVD	Singular Value Decomposition
TWI	Topographic Wetness Index
TSS	Total Suspend Solids
WQI	Water Quality Index

1. General Introduction

The current dynamics of the human civilization generates a constant rise in demand for water. This increase is due to the increment of: population, city sizes, industrialization, energy needs, and human consumption. The world will face a 40% water shortage if the current water usage is kept (Sordo-Ward et al., 2019). This world water crisis will be a matter of management and will not be related to resource availability (Vieira, 2009), but, taking into account the upraise in needs for water from different uses the latter will boost the possibility of localized conflicts and will drive more difficult choices regarding water resource allocation. This situation will also limit the growth of crucial economic sectors for development. In this context, water–food–energy relation will pose major political decisions even though each sector is managed separately, and will imply concessions around allocation and prioritization of water resources (Ki-moon et al., 2014; Schwabe et al., 2017). The social, political, economic and legal connotations in water management are undoubtedly important, as it allows the understanding of the lifestyle, traditions, and cultural development of the population.

Water resources have to be managed according to laws and plans that regulate the water allocation to different stakeholders including all productive sectors. According to its economic nature, water is conceived as a limited value asset that economic sectors use to create goods (Young, 1996; Gunawardena et al., 2018). In an economically efficient allocation, the maximum amount of money a user is willing to pay for water use must be equal for all sectors for the sake of maximizing social well-being. If this does not occur, society will benefit allocating water in the sector where payments the higher are (Kirshen et al., 2018; De O. Torres et al., 2016). The objectives of equitable systems refer to justice in water allocation within different economic sectors. However, it is possible that these objectives are not consistent with objectives related to efficiency (Cai, 2008).

Water management as an economic asset is an important strategy to achieve efficient and equitable profitability and to favor the protection and preservation of water (Groves et al., 2008; Räsänen et al., 2017; Wu et al., 2016; Cobourn et al., 2017). Thus, the economic theory provides tools for decision making through the increase or decrease price analysis. These tools are useful for water allocation in systems with multiple stakeholders, giving a base for

comprehension and performance in water planning (Valdés-Pineda et al., 2014; Casadevall, 2016).

The relationship between hydrologic supply (surface water and groundwater) and economic analysis of water resources, produce new approaches in administration, management and planning for water resources, through the use of hydro-economic models that allow optimizing profits and reduce operating costs of water management (De O. Torres et al., 2016; Lopez-Nicolas et al., 2018; Ward, 2009). For instance, hydrological modelling in a regional scale provides valuable information for adequate management of water resources, even more in a high-pressure anthropic context (Neverre & Dumas, 2015; Barthel & Banzhaf, 2016). The main reason to consider the regional scale is to explore the social well being of a region (resource allocation between stakeholders) from the perspective of political accountability (Brouwer & Hofkes, 2008; Hanemann, 2006). Nowadays, authors are adopting regional-scale models, mainly to guarantee the quality of information that they use reducing the amount of collected data (Reynaud & Leenhardt, 2008). The main limitation in regional models is a high level of aggregation, because of resource homogeneity not being a solid assumption in real-world environments, particularly when water is considered (Meyer et al., 2018). Thus, regional model construction is important, since it seeks to analyze patterns and trends of hydrological, hydrogeological and economic variables, and understanding interactions amount them (Fu et al., 2017; Mukundan et al., 2019).

Additionally, when the value of water is included in hydrological modeling, economic focalization in water resources management is completed (Rosenberg et al., 2008). Thereby, the integration of economic aspects is built as a tool to ease the construction of a hydro-economic model. Álvarez Mendiola (2010) identifies two approaches for the model construction: (*i*) a modular approach that establishes a connection between the hydrogeological and economical model, and (*ii*) a holistic approach which contains in a single unit both models. The latter focuses on finding a proper technique that allows the representation of these components in a significant manner. An application of this technique is the water commercialization strategies that Lund & Israel (1995) presented. Booker et al. (2012) also introduced applications of market analysis and water banks, enabling the balance between water offer and demand to decrease the effect of drought. Water markets are also susceptible to market failure, especially due to the presence of natural monopoly and public goods that compete with private demand, as showed by Young (1996). Market failures could be reduced trough the insertion of water rights and the structure of appropriated incentives, as showed by Spulber (1988). Viability of water management strategies depends on legal, institutional, environmental and economic implications. An insufficient organizational context and lack of a solid economical foundation are the main causes of failure in water resources management projects (Loucks et al., 2005).

Likewise, integration of hydrologic and economical aspects is increasingly more relevant in the design of policies for management and administration of water resources through the definition of usages and rates that transmit to the user a sign of the resource real value, and the cost associated to their supply (Lopez-Nicolas et al., 2018; Pulido-Velazquez et al., 2008; George et al., 2011). Moreover, this integration will allow local and national authorities to define strategies to reduce the gap that exists between water demand and the available offer. These strategies can be applied in all stakeholders (mining, agriculture, livestock, services, industrial sectors, and new Oil and Gas (O&G) exploration and exploitation projects), in order to define the cost of associated impacts to water quality, and to determine the water marginal price depending on its usage (Pedro-Monzonís et al., 2016; Pérez-Blanco & Gutiérrez-Martín, 2017).

In Colombia, water concession is the right to a limited use of water, granted to develop a productive activity. This concession must be related to water availability to ensure the preservation and efficient use of water. The Environmental Regional Authority (ERA) has the responsibility to apply rates defined by the Ministry of Environment and Sustainable Development (MESD) in these concessions. However, modifying concessions volume requires considering supply and water availability, hydrological regime (surface water and groundwater), use and water allocation, and land use. These concessions are governed by policies that determine the allocation, rates and water prioritization analyzing the water supply. However, these policies have no differences between economic activities and conflicts that are generated by their use. Given the current interest in economic development of MMV system and the expectation of new O&G exploration and exploitation projects, it is necessary to evaluate the supply and water allocation between different stakeholders, due to its use in the economic activities, which can limit supply and water availability (surface water or groundwater). This limitation could be due to water volumes required and water quality associated with these economic activities. For instance, in 2012, 55.8 Mm^3 of water were collected from 217 water sources for O&G projects (Valencia, 2014). Water management, from its shortage or abundance, may constitute a conflict focus between stakeholders, demonstrating needs for improvement in the Integrated Water Resources Management (IWRM), and in the analysis of the territory occupation through an economic and environmental dynamic that allows to evaluate water resource vulnerability among different stakeholders.

This situation does not show the current reality regarding IWRM in Colombia, so it requires tools for decision making by analyzing hydrological regime (surface water and groundwater) in areas with lacking reliable information on water availability and quality (Agencia Nacional de Hidrocarburos - ANH, 2012). Consequently, the main goal of this research is to provide a methodological approximation that enables the integration of hydrological, hydrogeological, and economic aspects in water allocation between different stakeholders

to establish management strategies at a regional scale. Thus, three specific objectives are proposed: (*i*) to characterize the water system (surface water and groundwater) to quantify the water supply and recharge, (*ii*) to develop an optimization model that permits to define the water resource allocation based in the usage, cost and quality and (*iii*) to evaluate the model performance in the MMV to determine water resources management strategies.

To approach the challenges proposed in the research objectives, three main activities were developed and implemented in the MMV zone (described in **Chapter 2**): (*i*) hydrological characterization and recharge determination, (*ii*) geological reinterpretation and hydraulic conductivity estimation in different geological units and, (*iii*) establishment of a relationship among the water availability, quality, and demand in economic terms.

The first activity is developed in **Chapter 3**, where hydrological zoning is proposed through the usage of a semi-distributed model. The picking of this model was motivated by the simplicity in the inclusion of hydrometeorological variables for temporal analysis of an area. The output used in the model implementation was analyzed with global sensitivity techniques, starting from statistical moments analysis, local analysis and uncertainty. This characterization allowed them to determine the water offer and identify the recharge zones, making a complete evaluation of dynamic interaction between the hydrologic cycle and climatic conditions. In summary, this activity helped to improve the comprehension of: (*i*) the surface flow regimen within the MMV zone, (*ii*) identification of likely physical limits for the model parameters and (*iii*) validation of a new metric for the hydrologic model calibration in tropical zones. This project has auxiliary data in its development shown in Arenas-Bautista et al. (2018b, 2017).

The second activity focused on the hydraulic conductivity estimation, which was made using two approaches: (*i*) analysis of hydrogeological units as constant zones and (*ii*) determination of hydrogeological units that vary spatially and temporarily, analyzed trough the distribution of pilot-points (*PP*) in the zone. Thus, it was necessary to collect the geologic structural, seismic information, and determine the geological units present in the zone to consolidate the geological model. With this information, it was interpreted the geologic zones and a three-dimensional model was created, constituted by blocks of similar characteristics. The lack of observation points in the hydrogeological model allowed to explore the validity of the *PP* technique to assure the soil heterogeneity representation in a numeric model with real information, showing a satisfactory behavior. **Chapter 4**, details the methodology and results that highlight an advancement in the knowledge of: (*i*) streamlines and path lines, (*ii*) surface water and groundwater interaction, (*iii*) determination of biased parameters and validation of *PP* usage in real scale models, and (*iv*) assertive restriction in highly parametrized models with field data in tropical zones. The results in this chapter have been presented in Donado et al. (2018) and published in Arenas-Bautista et al. (2020).

Consolidation of these models, allowed to perform the integration of economic aspects. For that, it was developed a hydro-economic optimization model, as a utility tool in the decision making processes, to allocate water between different stakeholders. The regional optimization model is described in **Chapter 5**. It integrates multiple water offers (surface water and groundwater) and multiple demands. The model considered the inclusion of a water quality parameter and an objective function has established penalties in a way that the model contemplates the possibility that not all the water demand can be fulfilled. The differed analysis in four scenarios that vary temporally, allowed to widen the knowledge in: (*i*) water availability affectation caused by its quality, (*ii*) the cost-benefit relation of interaction between multiple users and different requirements, and (*iii*) management strategies consolidation that could provide an effective analysis for efficient price policy determination in tropical basins.

Finally, the management strategies results are consolidated in **Chapter 6**, providing an effective analysis for determination of efficient policies in tropical basins. The document ends with the principal conclusions of the research and discussion of some possible guidelines for future research work.

2. The Middle Magdalena Valley (Geological System)

In this section, a general description of the case study is presented. Then, the hydrological process is described using variables like precipitation, temperature and evapotranspiration. The hydrogeological processes considered in the model development were introduced from the general geological description in the area. All this information and the processes it describes will help to build the hydrological and hydrogeological models, which will be shown in the next two chapters. This chapter is based on Arenas-Bautista et al. (2020).

The MMV system is located in the central part of the Magdalena-Cauca Basin (MCB). This is the most important basin in Colombia in demographic, social and economic terms (Arboleda-Obando, 2018). The approximate MCB area is 257 000 km^2 and represents a complex terrain by its topographic and climatological characteristics. This is mainly due to the presence of the Andes mountain range and the interaction with the Pacific and Atlantic Oceans, making it difficult to analyze the environmental conditions (Ideam, 2014). About 80% of the country's population is concentrated in this area, where 95% of thermoelectric energy and 75% of national hydroelectric energy is produced. In national terms, the MCB concentrates 80% of the nation's economic output (according to Gross Domestic Product calculations by IDEAM (2019)).

The MMV system is defined as an intramontane basin with an extension about 34 000 km^2, which separates the Eastern and the Central mountain ranges in northern Colombia. This area extends longitudinally from *South* to *North* between the Ibague fault and the Girardot belt, which in turn separate it from the Upper Magdalena Valley Basin. The system is bounded to the *South East* by Bituima and the La Salina faults system; to the *North* by the Espiritu Santo faults system; to the *West* by the onlap of Neogene sediments against the base of San Lucas and the Central mountain range, and finally to *North East* by the Bucaramanga - the Santa Marta faults system (Ingrain, 2012).

The MMV system is a geographical axis in the middle section of the Magdalena River in a stretch of 386 km, which supplies different economic sectors making it a central axis for the country's development. Several departments (national administrative states) interact in this region, whose relationship strengthens activities of mining, agriculture, domestic, livestock, aquaculture, services, industrial, construction and O&G exploration and exploitation processes. This economic development allows contributions to road construction, environmental development programs and job creation. However, the most critical factors in the area are water use in agriculture, hydropower, O&G projects and domestic supply compared to water offer so that knowledge of spatial and temporal distribution from its sources is a necessity to achieve an optimal management and planning of the consumptive use. In this zone, the population is about one million inhabitants distributed in forty-five municipalities (DANE, 2016). The MMV landscape is a tropical rain forest but currently, there are few remains of its, due to the strong anthropic intervention that brought the agricultural and livestock expansion.

2.1. Study Area

The characterization of the study area is presented in this chapter, as a basis for analyzing the hydrological behavior of the system and understanding the impact that the physical environment's transformation generates at the social, cultural and economic level in the region. The study area is located in the southern part of the MMV system (Figure **2-1**) and represents 17 000 km^2. This area is located geomorphologically along the central part of the Magdalena River valley, between Eastern and Central Andes mountain ranges (Ingrain, 2012). The Magdalena River extends approximately 170 km across the study area. The region is abundant in natural resources that includes: quartz, marble, gold, O&G, water, flora, and fauna (Ingrain, 2012).

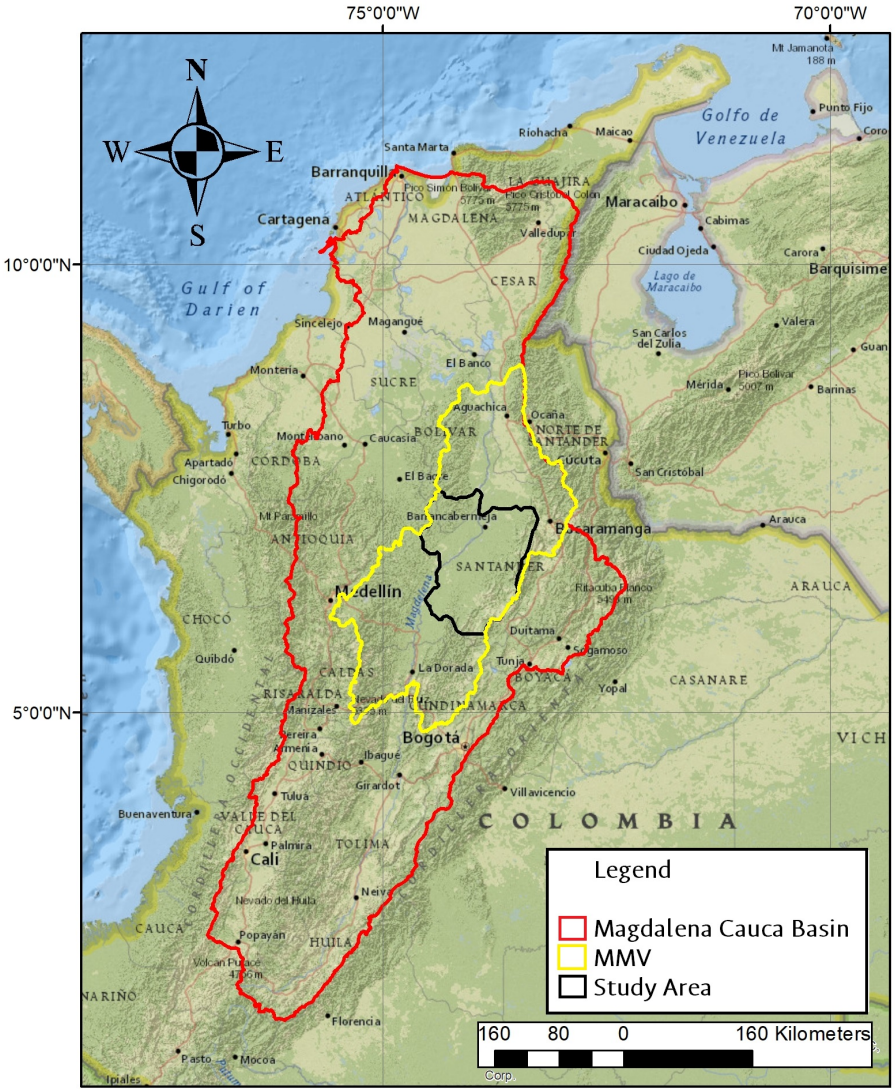

Figure **2-1**.: Location Study Area in MCB (Red), MMV system (Yellow) and Study Area (black).

2.2. Hydrology Context

The MMV starts in *Honda* (Tolima) and extends to *El Banco* (Magdalena) at is shown in Figure **2-2**, a municipality located at an altitude of 33 m.a.s.l. In this system, Magdalena river presents a length of 542 km with an average slope of 0.35 $m\ km^{-1}$ and a drainage area of 105 850 km^2. In this area, a large number of wetlands begin to form due to fluvial dynamics and the flat area geoforms. These wetlands exert a regulatory effect and behave as affluents or effluents, depending on the river water level.

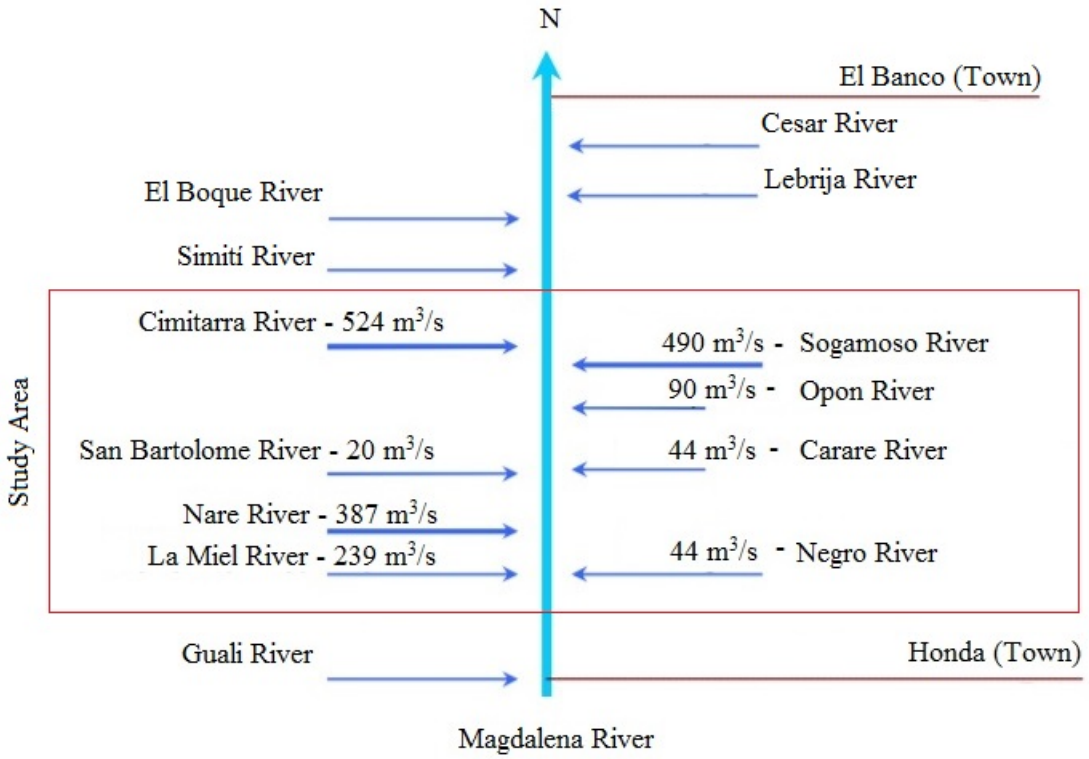

Figure **2-2**.: Water Flow Diagram of the Magdalena River in the study area.

In the study area, most abundant sources of water include the Magdalena River and its major affluents (Cimitarra, Sogamoso, Opon, Carare, Nare and San Bartolome Rivers). The area is composed of two morphological parts: (i) the alluvial, and (i) the mountains. In the former zone there exists a system of wetlands connected to the rivers, creating a wetland ecosystem. Rainfall in this area is distributed across two wet periods: march-june and october-december; the remaining periods being typically dry. The average rainfall amount is about 2 000 $mm\ yr^{-1}$ and the Magdalena River is characterized by an annual average flow of 2 361 $m^3\ s^{-1}$ (with high and low flows of $Q_{5\%}$ 4 298 $m^3\ s^{-1}$ and $Q_{95\%}$ 1 578 $m^3\ s^{-1}$; $Q_{5\%}$ correspond to a discharge exceed the 5% of time, and so, characterizes high flows, meanwhile $Q_{95\%}$ correspond to a discharge exceed the 95% of time, and so, represents low flows). The annual average temperature is above $24°C$ throughout the territory and elevations are between 50 and 3 700 m.a.s.l.

The Magdalena River in the study area is a semi-meandering river with curves controlled by a rock outcrop, it means the location of the curves depends on the geological controls. The geological control sites are stable points and in the curves where competent rock does not appear there are points of instability.

This research used the regionalization of monthly precipitation using criteria at the macroclimate level (Inter-tropical Convergence Zone - ITCZ). The amount of monthly precipitation at a local level is determined by the cloud systems associated with the local circulation of each slope and, in turn, is conditioned by the altitude, the mountain ranges location and the convective activity of each locality. Daily rainfall information in the MMV area basin has been acquired from the Institute of Hydrology, Meteorology and Environmental Studies (IDEAM). A total of thirty-seven monitoring stations were considered, as depicted in Figure **2-3**. The data covers a period of time between 2000 and 2012. Missing data was completed via linear interpolation from the three closest stations. The average precipitation in the area was estimated by the Thiessen method (Ruelland et al., 2008; Wagner et al., 2012).

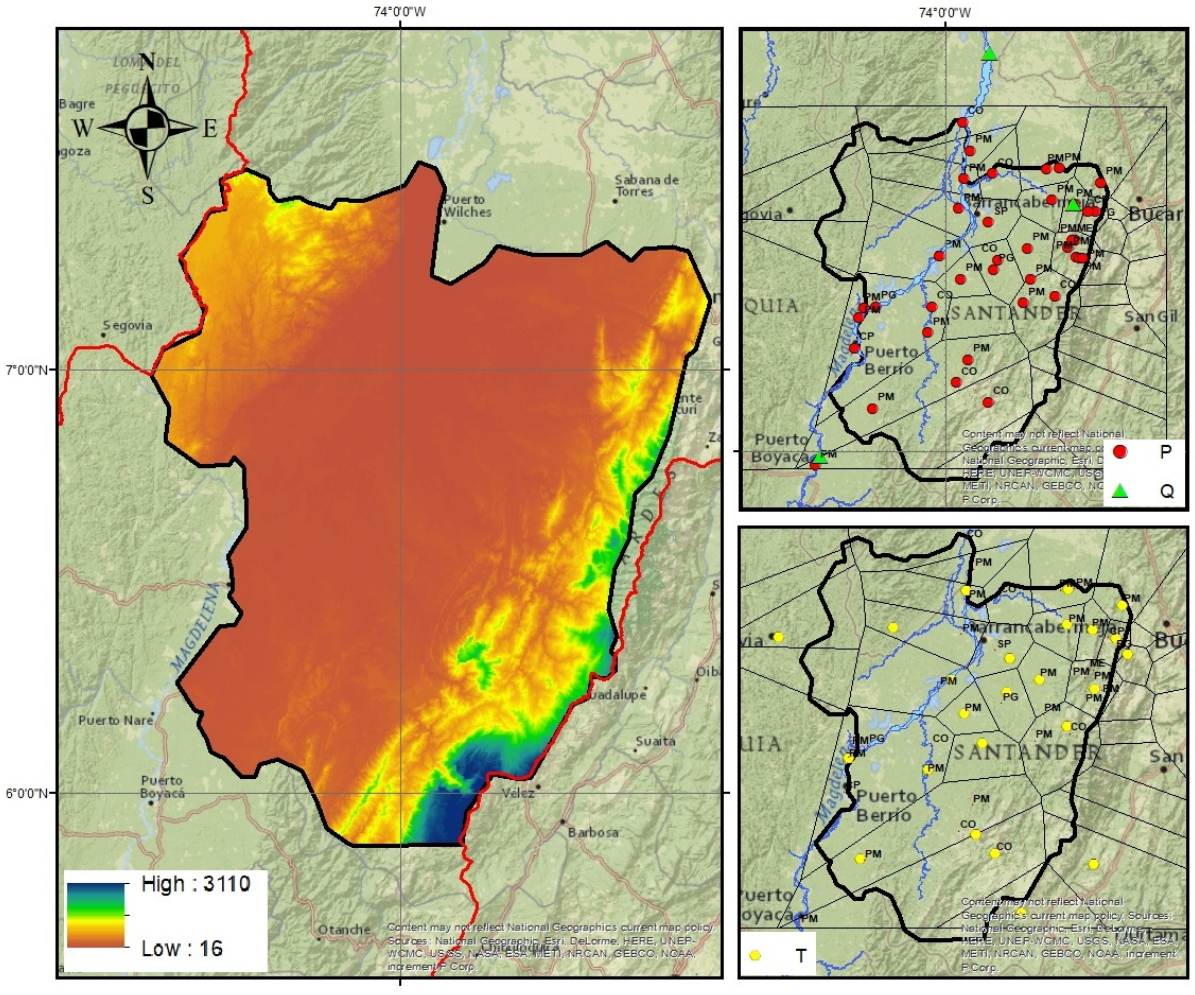

Figure **2-3**.: Data used in hydrological model development. Left- DEM. Right- Precipitation -P and Temperature -T stations and Thiessen polygons.

Discharge data was also obtained from the IDEAM database, through the selection of three limnimetric stations. The selection of stations considered two at the basin entrance and one

at the basin exit, in order to obtain the flow in the area. The input and output stations were the Puerto Berrio and the San Pablo, respectively (Figure **2-4**). These stations were selected because they were used as a reference in the National Water Study (NWS) by Ideam (2014).

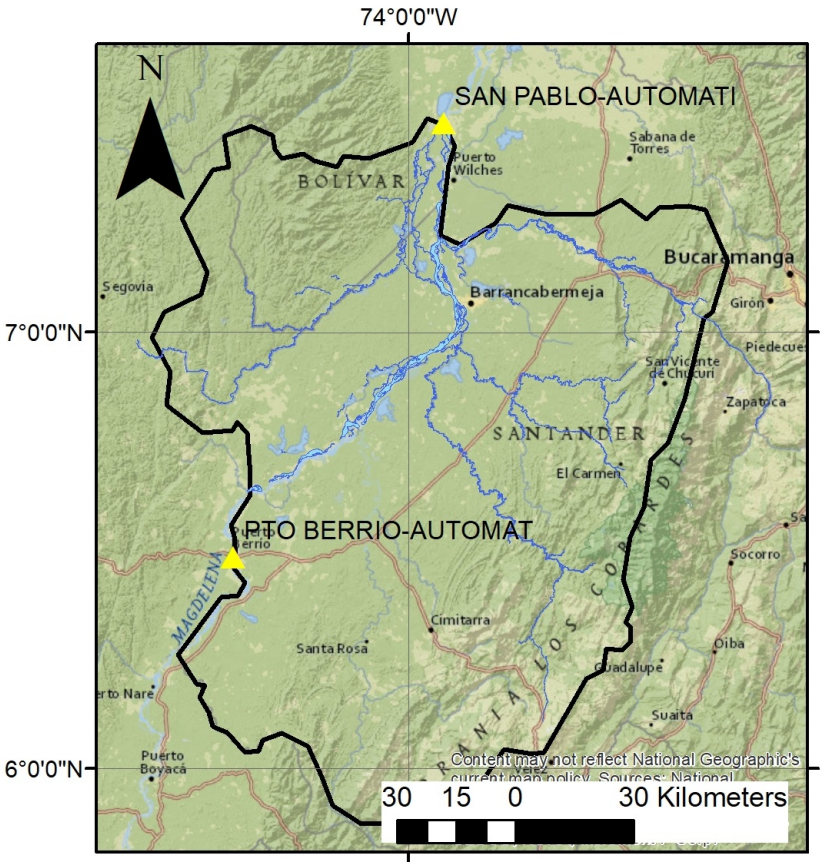

Figure **2-4**.: Limnimetric stations used in the hydrological model calibration.

Daily temperature information in the study area has been acquired from IDEAM (Figure **2-3**). A total of sixteen monitoring stations were considered. The data covers a period of time between 2000 and 2012. Missing data was completed via linear interpolation from the three closest stations. The average temperature in the area was estimated by Thiessen method, correcting the polygon value by its elevation (Zhang et al., 2016; Ayantobo et al., 2017).

Evapotranspiration was evaluated through the Hargreaves method (Hargreaves & Samani, 1982; Hargreaves & Allen, 2003). This parameter is based on the estimate of solar radiation (R_s) via assessing the daily air temperature range ($\mathrm{TR} = \mathrm{T_{max}} - \mathrm{T_{min}}$) and R_a to estimate R_s, as Eq. 2-1

$$R_s = K_{RS} R_a T R^{0.5}, \tag{2-1}$$

here, T_{max} and T_{min} being the daily maximum and minimum air temperatures ($^{\circ}C$), respectively; K_{RS} is an empirical coefficient fitted to R_s/R_a versus TR data with a value of 0.16; and R_a is extraterrestrial radiation ($mm\ day^{-1}$) and was calculated according to (Allen et al., 1998). R_s is the solar radiation in equivalent water evaporation (given in $mm\ day^{-1}$ since 1 $mm\ day^{-1} = 2.45\ MJ\ m^{-2}\ day^{-1}$ due to the relationship between latent heat of vaporization, water evaporated and the energy received by water) (Allen et al., 1998). Evaluation of ET_o is then performed through Eq. 2-2

$$ET_o = CR_a(Tmean + 17.8)TR^{0.5}, \tag{2-2}$$

here, ET_o is the potential evapotranspiration ($mm\ d^{-1}$), C is the original empirical constant proposed by H. Hargreaves & A. Samani (1985), with value of 0.0023 and T_{mean} is the observed daily mean air temperature ($^{\circ}C$). Mean daily air temperature of day i, measured at the gauge j, is computed as the arithmetic mean of measured values from a dry-bulb thermometer at 7, 13, and 19 (or 18) hours (local time, GMT-5).

P, Q and ET_o data between years 2000 to 2008 were employed for model calibration. Meanwhile, for the validation process, observations between years 2009 to 2012 (Figure **2-5**).

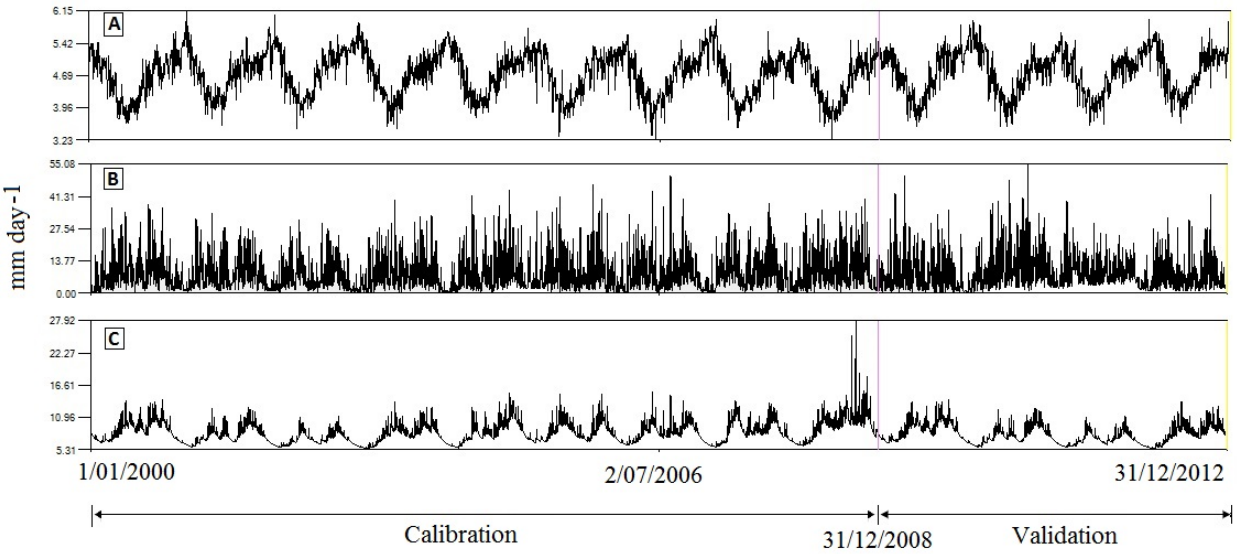

Figure **2-5**.: Time series used in the sensibility analysis and the calibration-validation processes in MMV. (A)- Daily ET_o obtained from Hargreaves equation using temperature data. (B)- Daily P obtained from rainfall gauges. (C)- Daily river flows obtained from gauging stations.

2.3. Geology Context

Traditionally, surface water has been the main source of supply in Colombia. However, in the last decade, groundwater has become more important because it is an alternative source due to its better quality, the relatively low cost of handling and its influence on the industrial and economic development of the Country (Ideam, 2014). Colombia has possibilities of using groundwater in 74% of its extension. However, 56% of this area corresponds to geographic regions with high surface water yields and low percentage of the settled population (Vargas Martínez et al., 2013). The MMV has 106 131 km^2 of surface area with resources and groundwater reserves. These reserves are equivalent to 12.5% of the total area covered by hydrogeological basins in the country. This potential has led to the hydrogeological study of the area, through the development of conceptual and mathematical models to understand its operation (IDEAM, 2019).

In Colombia, sixteen hydrogeological provinces have been identified. The hydrogeological provinces correspond to larger units referred to smaller scales (1:1 000 000 to 1:500 000), defined on the basis of tectonostratigraphic units separated from each other by regional structural features. In the MMV, the hydrogeological province has a main aquifer system (Figure **2-6**). The MMV Aquifer System is composed of six aquifers: (*i*) Aquifers of Magdalena River terrace, (*ii*) Aquifers of the alluvial deposit of the Magdalena River, (*iii*) Mesa Formation, (*iv*) Real group, (*v*) Luna Formation, and (*vi*) Tablazo and Rosablanca aquifers.

These features coincide with the boundaries of larger geological basins and, from the hydrogeological point of view, they correspond to impervious barriers represented by regional and structural faults. Additionally, they are characterized by their geomorphological homogeneity (Vargas, 2006). Within each province, hydrogeological units are identified by characteristics of porosity and permeability, which have different storativity conditions and allow the groundwater flow.

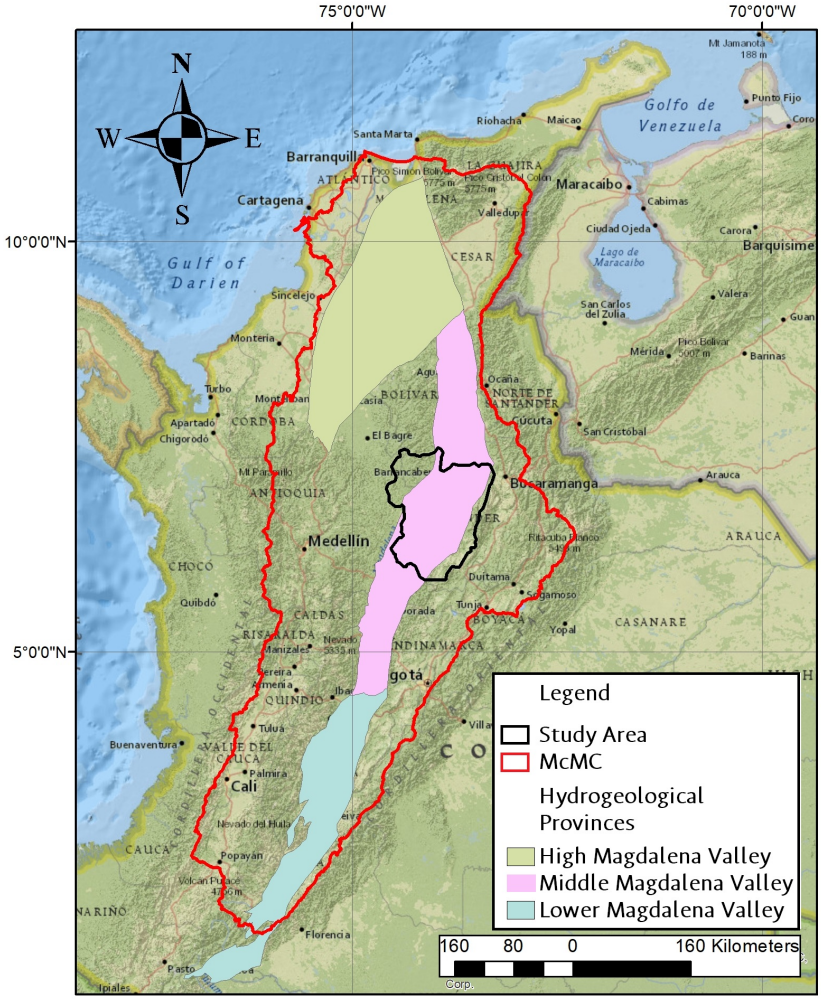

Figure **2-6**.: Hydrogeological Provinces of the Magdalena Cauca Basin and the MMV.

3. Hydrological Model

This section presents the consolidation of the hydrological model. This model allows us to make a comprehensive assessment of the interaction between the dynamics of the hydrological cycle and climate conditions in the study area. Throughout this chapter, you will find the hydrological simulation and the application of the sensitivity and uncertainty analyses to assess the influence of the main parameters in estimating surface runoff. This chapter is based on Arenas-Bautista et al. (2018a,b, 2017).

TopModel (TOPography based hydrological MODEL) as a tool for the hydrological simulation in the south of MMV is presented. Additionally, it shows the application of the sensitivity and uncertainty analyses to assess the influence of the main parameters associated with TopModel in estimating surface runoff. The model is focused on indices for variance-based analysis. This methodology is conducive to a Global Sensitivity Analysis (GSA), according to the statistical moment's characterization of the output simulations. It does so upon relying on (a) the Sobol indices, associated with a classical decomposition of variance and (b) the recently developed indices estimating the delivery of each model parameter to the mean, variance, skewness, and kurtosis of the outputs. The analysis uses a collection of 150 000 model simulations, each spanning over a 12-years temporal. These are constructed by assuming those model parameters are random and associated with a uniform distribution within a range, whose values are supported by literature studies and preliminary model calibration against available data.

3.1. Introduction

In the last decade, mathematical models are getting an important role for solving problems in water resources management (Reynaud & Leenhardt, 2008; Dunne, 1983; Reynaud & Leenhardt, 2008; Bossa et al., 2012), giving rise to discussions about their use and application to evaluate and analyze complex hydrological systems (Bellin2016).

Hydrological models have been developed to understand different processes, which must be evaluated for different environmental conditions (Jenson, 1991; Loosvelt et al., 2014; Hollanda et al., 2015). However, they are generally focused on fulfilling two main objectives: (*i*) to improve the understanding of the hydrological phenomena in the basins and how the changes generated in them affect the hydrological phenomena and, (*ii*) the generation of synthetic sequences of hydrological data for the design of infrastructure or for its use in forecasting (Refsgaard, 1997; Kauffeldt et al., 2016; Ibarra-Zavaleta et al., 2017).

These models are classified into three types (Sieber et al., 2005; Hughes, 2016): (*i*) Empirical: where the solution is based on empirical parameters, calculated by identifying statistically significant relationships between certain variables; (*ii*) Theoretical: that are described by differential equations and follow the laws of physical and chemical processes; and (*iii*) Conceptual: which are simplified representations of physical processes, in mathematical terms to simulate complex processes based on key parameters that describe the important functions of the system of interest.

In this research, it was implemented a rainfall-runoff model known as TopModel (Lamb et al., 1998; Beven & Freer, 2001b,a). TopModel is usually applied to assess the management of water resources at the regional scale, using conceptual models for detailed assessment of surface flow (Beven & Freer, 2001b; Mockler et al., 2016; Teng et al., 2017). Likewise, distributed and semi-distributed models (which do not simulate the basin as a group, but as a set of divided parts) are necessary for the simulation of spatial patterns of hydrological response within a basin (Mazzoleni et al., 2015; Ibarra-Zavaleta et al., 2017). Moreover, hydrological models also provide valuable information to study changes in land use or climate (Karlsson et al., 2016). Thus, changes in land use are directly related to water supply (and therefore to hydrological modeling), mainly related to human consumption, food production, and power generation. These activities have become a global priority in the economic and social sphere due to the growth of the population and the need to establish economic activities for the communities' empowerment (Buytaert, 2011; Crespo et al., 2012; Harou et al., 2009). Through models, it has been possible to represent dominant hydrological processes in the hydrological cycle of a particular ecosystem, mainly by calculating the water balances which allow exploring the validity of the representation, interactions and various levels of model behavior (Buytaert, 2011).

The more hydrological information have the model (precipitation, temperature, evaporation, evapotranspiration, and flow), the results will be better. However, the uncertainty due to scarcity of these data is quite common in several areas of Colombia, due to the complexity of the topography and to the low gauges density in some areas (Meerveld & Weiler, 2008). In addition, it is necessary to generate tools for calibration and validation of synthetic data to the hydrological modeling process (Blanco-Gutiérrez et al., 2013; da Silva et al., 2015). The calibration and validation of data through modeling, has enabled the verification of the assumptions that underlie the hydrological model used, which has contributed significantly to the generation of new knowledge (Ibarra-Zavaleta et al., 2017).

Sensitivity analyses allow the identification of key parameters that affect model performance. Also, these analyses show the parameters' importance and its role on model structure, calibration, optimization and quantification for uncertainty, helping to improve the flow prediction or simulation processes (Yasari et al., 2013; Song et al., 2015; Li & Zhang, 2017). Depending on the uncertainty analysis perspective, global sensitivity methods can be independent of statistical moments, or based on the model variance decomposition. The aim of GSA is to determine the contributions of each individual parameter or the combinations of their values that generate the variance (Kellner et al., 2015; Ballinas-González et al., 2016; Borgonovo et al., 2017). To exemplify this scenario, Hou et al. (2015), have used sensitivity analyses to identify important and unimportant parameters in simulated processes in the Huaihe River basin, China.

3.2. Methodology

This section describes the field sampling, the statistical and graphical analysis proposed for the hydrological database.

3.2.1. Hydrological Model: TopModel

TopModel is a semi-distributed model based on similarities of the topography which are expressed through a Topographic Wetness Index (TWI). It can be considered as a rainfall-runoff conceptual model based on the landscape characteristics which contains three dynamic storage regions: (i) a root zone, (ii) an unsaturated zone and (iii) a fully saturated zone (Hollanda et al., 2015; Metcalfe et al., 2017). Figure **3-1** depicts the workflow upon which TopModel relies and its main conceptual elements. Main assumptions at the basis of the modeling suite include:

1. processes in the saturated zone are described through a steady-state scenario,

2. model assumes that the soil properties and hydrologic parameters are homogeneous in the catchment model, parameters are uniformly distributed in space,
3. hydraulic gradient driving fully saturated groundwater flow can be approximated by the topographic gradient (at the scale investigated),
4. hydraulic conductivity decreases exponentially with depth

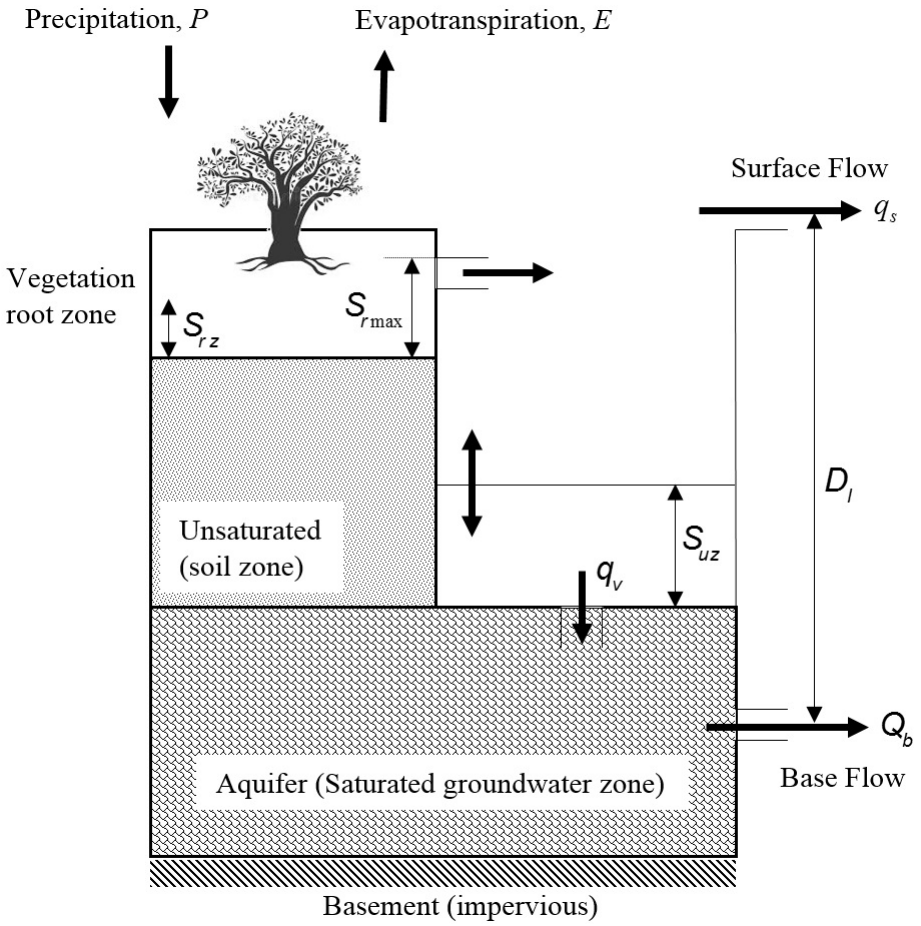

Figure **3-1**.: TopModel model description (Xue et al., 2018). Sr_{max} is the maximum root zone deficit, S_{rz} is the root zone deficit, S_{uz} is the local water storage in the unsaturated zone, P is the precipitation per unit width, and q_v, q_b, and q_s are infiltration, base flow and saturated surface flow respectively. Source: Jeziorska & Niedzielski (2015)

The model theory assumes that the local hydraulic gradient is equal to the local surface slope and implies that all points with the same value of the TWI have the same hydraulic properties (Andersen et al., 2001; Mukherjee et al., 2013; Yi et al., 2017; Jeziorska & Niedzielski, 2015). Its value is computed from the basin topography using Eq. 3-1.

$$TWI = \ln \frac{a_i}{\tan \beta_i}, \tag{3-1}$$

here, a_i and $\tan \beta_i$ are the upslope contributing area, i.e., the area that can potentially contribute to discharge to the point of interest, and the average slope of the surface of the $i - th$ pixel, respectively (Suliman et al., 2016).

The process described herein uses a type of digital terrain analysis (DTA) resulting in a TWI that quantifies topographic controls of basic hydrological processes (Yi et al., 2017; Jeziorska & Niedzielski, 2015). TWI is derived through interactions of fine-scale landform coupled to the up-gradient contributing land surface area according to the following relationship: the cells with similar hydrological characteristics were generated from the grouping of pixels into different categories based on the topographic index function (Figure **3-2**) (Dai et al., 2017). For the consolidation of the TWI, it was necessary to export the DEM in ASCII format to TopModel using the Sp, Raster and Topidx packages (Metcalfe et al., 2015).

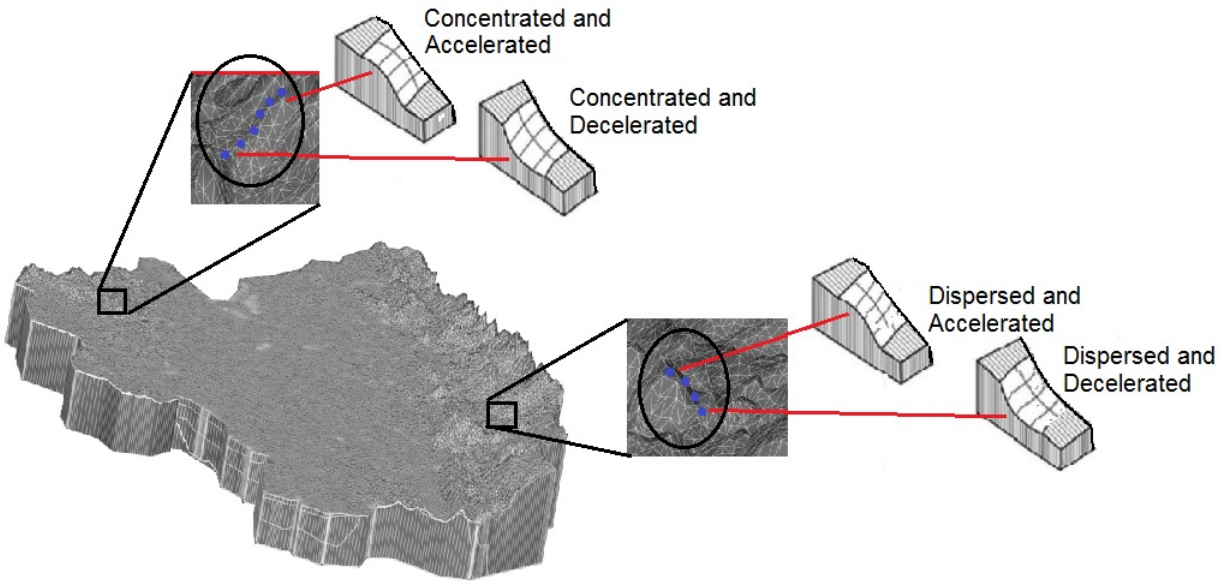

Figure **3-2**.: Schematic diagram of morphology types used to compile TWI. Adapted from Zimmerman (2016).

The runoff generation in TopModel is given by the relation between topography and transmissivity of basin (Dewandel et al., 2017; Jeziorska & Niedzielski, 2015; Xue et al., 2018). Rain infiltrates the root zone until its maximum storage capacity is reached, and then it can be reduced to a linear velocity by the actual evapotranspiration of the surface, described by Eq. 3-2.

$$E_a = ET_p(1 - \frac{S_{rz}}{S_{rmax}}), \tag{3-2}$$

where, E_a is the real evapotranspiration, ET_p is the potential evapotranspiration, Sr_{max} is the maximum root zone deficit and Srz is the root zone deficit.

After the infiltration process in the root zone ends, the excess water fills the unsaturated zone and recharges the saturated zone generating a decrease in the water table depth. According to the first assumption of TopModel, the depth of the local water table is represented by the local storage deficit (D), which can be calculated for each TWI class using Eq. 3-3.

$$D_i = D + m(\alpha - \ln \frac{a_i}{\tan \beta_i}), \tag{3-3}$$

where, D_i is the catchment average water table depth, D is the average TWI and m is a scaling parameter.

The water table is equal to the ground level when D reaches zero. Therefore, the average value of the TWI for which D_i constitutes the threshold for the maximum storage capacity. Moreover, each point having higher value of TWI is considered to be in a saturation condition. Additional rain on saturated surfaces cannot infiltrate the soil, therefore, excess water is transferred directly to saturated surface runoff.

The water storage deficit is reduced by the recharge water flux from the unsaturated zone to the groundwater, and its rate can be calculated using Eq. 3-4

$$q_v = \frac{S_u z}{D_l T_d}, \tag{3-4}$$

where, D_l is the local storage deficit, and T_d is the mean residence time in $S_u z$.

Therefore, the total recharge rate (q_v) is expressed (Eq. 3-5) as the sum of all values of q_v multiplied by the upslope area a_i representing a set of hydrologically homogenous points, associated with topographic index class of the $i - th$ location (Metcalfe et al., 2015).

$$Q_v = \sum_{i=1} q_{v_i} a_i, \tag{3-5}$$

where, Q_v is the total flux and (q_{v_i}) is the flux of water entering the water table locally (per unit area).

The base flow (Q_{base}) is represented as the subsurface saturated zone flux q_s, and can be defined by Eq. 3-6

$$Q_{base} = q_s = Q_o \epsilon^{(\frac{-D}{m})}, \tag{3-6}$$

where, Q_o is the hydrological flux for the entire catchment area when $D = 0$. Both surface flow q_s and base flow Q_{base} account for the total discharge (Van Der Heijden & Haberlandt, 2015).

The transmissivity (T) in the low zones (Eq. 3-7), according to the fourth assumption of TopModel, decreases with the depth following the negative exponential law versus the saturation deficit (D) being m a recession parameter (Ahmed Suliman et al., 2014).

$$T = T_o \epsilon^{(\frac{-D}{m})}, \tag{3-7}$$

where, T_o is the local saturated transmissivity.

3.2.2. Global Sensitivity Analysis

A major goal of a GSA is to increase our understanding of the behavior of the model considered (Anderton et al., 2002; Borgonovo et al., 2017; Gupta & Razavi, 2018). In this context, the sensitivity of a desired model output is diagnosed to given model input(s) across the entire parameter space, *i.e.*, globally (Peña-Haro et al., 2009; Pianosi et al., 2016). As such, a GSA approach enables us to (i) naturally account for model input uncertainties that are typically encountered in hydrological models and (ii) identify sets of parameters that have the largest influence on the output of the model (Mishra & Lilhare, 2016; Khorashadi Zadeh et al., 2017). Our study relies on two approaches to GSA: (i) the variance-based Sobol Indices (Sobol, 2001); and (ii) the Moment-based AMA indices proposed by Dell'Oca et al. (2017). Sobol Indices are tied to one of the most widespread GSA approaches and rely on the variance as a key descriptor of uncertainty. The AMA Indices allow characterizing global sensitivity in terms of various features of the probability density (*pdf*) of the model output, as rendered by its main statistical moments.

Sobol indices for variance-based GSA

Variance-based GSA approaches (Sobol, 1993, 2001; Sudret, 2008; Fajraoui et al., 2011; Sochala & Le Maître, 2013; Wang et al., 2015) consider variance as the metric to quantify the contribution of each uncertain parameter to the uncertainty of a target model output.It

can be shown (Sobol, 1993) that if the model response $f(p)$ (p representing a vector of N model parameters) belongs to the space of square integrable functions, then the total variance, $V[f]$, of f (p) can be expressed according to the decompositon in Eq. 3-8

$$V[f] = \sum_{i=1}^{N} V_{p_i} + \sum_{1<i<j<=N} V_{p_i} + ... + V_{p_1...p_N}, \tag{3-8}$$

here, V_{p_i} is the contribution to V $[f]$ due solely to the effect of parameter p_i, and $V_{p_1...P_N}$ is its counterpart due to interaction of model parameters belonging to the subset $p_1...p_S$. The Sobol' indices, S_{p_i} and $S_{p_1...p_S}$ are defined in Eq. 3-9

$$S_{p_i} = \frac{V_{pi}}{V[f]}; \qquad S_{p_1...p_S} = \frac{V_{pi...p_S}}{V[f]} \tag{3-9}$$

quantifying the contribution of only p_i and the joint effect of $p_1...p_S$ on V $[f]$, respectively. The total contribution of pi to V $[f]$ is quantified by the total Sobol' index (Eq. 3-10)

$$S^i_{p_i} = S_{p_i} + \sum_{j} S_{p_i,...,p_j} + \sum_{j,k} S_{p_i,p_j,p_k} + ... + S_{p_i,...,p_N}, \tag{3-10}$$

In this sense, the total Sobol' index represents the relative expected (average) reduction of process variance due to knowledge of (or conditioning on) a model parameter.

AMA Indices for moment-based *GSA*

The AMA indices (Dell'Oca et al., 2017) allow quantifying the expected variation of a given statistical moment M $[f]$ of the *pdf* of $f(p)$ due to conditioning on parameter values. These are defined in Eq. 3-11 and Eq. 3-12

$$AMAM_{p_i} = \left\{ \begin{array}{cccc} \frac{1}{M[f]} \int_{\Gamma_{p_i}} |M[f] - M[f|p_i]\, \rho_{\Gamma_{p_i}} & dp_i & if & M[F] \neq 0 \\ \int_{\Gamma_{p_i}} |M[f] - M[f|p_i]\, \rho_{\Gamma_{p_i}} & dp_i & if & M[F] = 0 \end{array} \right\} \tag{3-11}$$

$$AMAM_{p_1...p_S} = \left\{ \begin{array}{cccc} \frac{1}{M[f]} \int_{\Gamma_{p_1...p_S}} |M[f] - M[f|\, p_1...p_S]\, \rho_{\Gamma_{p_1...p_S}} & dp_1...dp_S & if & M[F] \neq 0 \\ \int_{\Gamma_{p_i...p_S}} |M[f]|\, p_1...p_S]\, \rho_{\Gamma_{p_1...p_S}} & dp_1...dp_S & if & M[F] = 0 \end{array} \right\} \tag{3-12}$$

here, $AMAM_{p_i}$ (3-11) and $AMAM_{p_1...p_S}$ (3-12) are the AMA indices associated with a given statistical moment M and related to variations of only p_i or considering the joint variation

of $p_1...p_S$, respectively; $\rho_{\Gamma_{p_i}}$ is the marginal *pdf* of p_i, $\rho_{\Gamma_{p_1...p_S}}$ being the joint *pdf* of $p_1...p_S$; and $M[f\,|p_1...p_S]$ indicates conditioning of the (statistical) moment M on known values of parameters $p_1...p_S$. Note that $AMAV_{p_i}$, i.e., the AMA index related to the variance ($M = V$) of f (p), coincides with the total Sobol' index S_{p_i} only if the conditional variance, $V[f\ |p_i]$ is smaller than (or equal to) its unconditional counterpart $V[f]$ for all values of p_i. If $V\ [f\ ]$ can undertake values that are smaller or larger than $V[f\,|p_i]$ while varying p_i, than $AMAV_{p_i}$ $\geq S_{p_i}$. Note also that, in this latter case, $AMAV_{p_i}$ can be either smaller or larger than $S^T_{p_i}$, depending on the relative impact of the interaction terms (Dell'Oca et al., 2017).

Calibration and Validation Processes

Model calibration relied upon the *MCAT* library (Pianosi et al., 2015). This is grounded on the generalized likelihood uncertainty estimation (*GLUE*) approach (Kellner et al., 2015; Ballinas-González et al., 2016; Simmons et al., 2017), from which it was evaluated a probability density of model parameters conditional to available observations. Inputs to the *MCAT* come from a Monte Carlo sampling in the parameter space, using a classical uniform random sampling, where all parameter are simple from an uniform distribution, without consideration of parameter interaction.

In this model, it was considered the Nash Sutcliffe Efficiency (NSE) as a calibration metric to analyze the model performed (Eq. 3-13) (Jeong & Adamowski, 2016; Wu et al., 2017; Dakhlaoui et al., 2017).

$$NSE = 1 - \frac{\sum_{i=1}^{n}(Q_{obs} - Q_{sim})^2}{\sum_{i=1}^{n}(Q_{obs} - \tilde{Q}_{obs})^2}, \tag{3-13}$$

where, Q_{obs} represents observed flows, Q_{sim} shows the simulated flows and $\tilde{Q}_{obs}$ represent the average of observed flows.

In addition, the percentage bias ($PBIAS$) is used as a complement in the analysis of the performance of the model to measure the average tendency of the simulated values to be larger or smaller than those observed (Wiant & Harner, 1979). The optimal value of the $PBIAS$ is 0, the positive values indicate an overestimation bias and the negative values indicate a bias of underestimation of the model. The equation used for its calculation is shown in Eq. 3-14.

$$PBIAS = 100\frac{\sum Q_{sim} - Q_{obs}}{\sum(Q_{obs})}. \tag{3-14}$$

3.3. Results and Discussion

The *TWI* for the study area is presented in Figure **3-3**. This map shows a correspondence between the highest values of the index and the drainage network. Areas with *TWI* values between 15 and 22.5 correspond to the location where the drainage network is generated. According to this, the high values of the topographic index are related to areas topographically convergent or smooth slopes which generate discharge flows (Beven & Freer, 2001a). These areas are characterized by low transmisivities, thus, the level of water table reaching the surface (Tian et al., 2016).

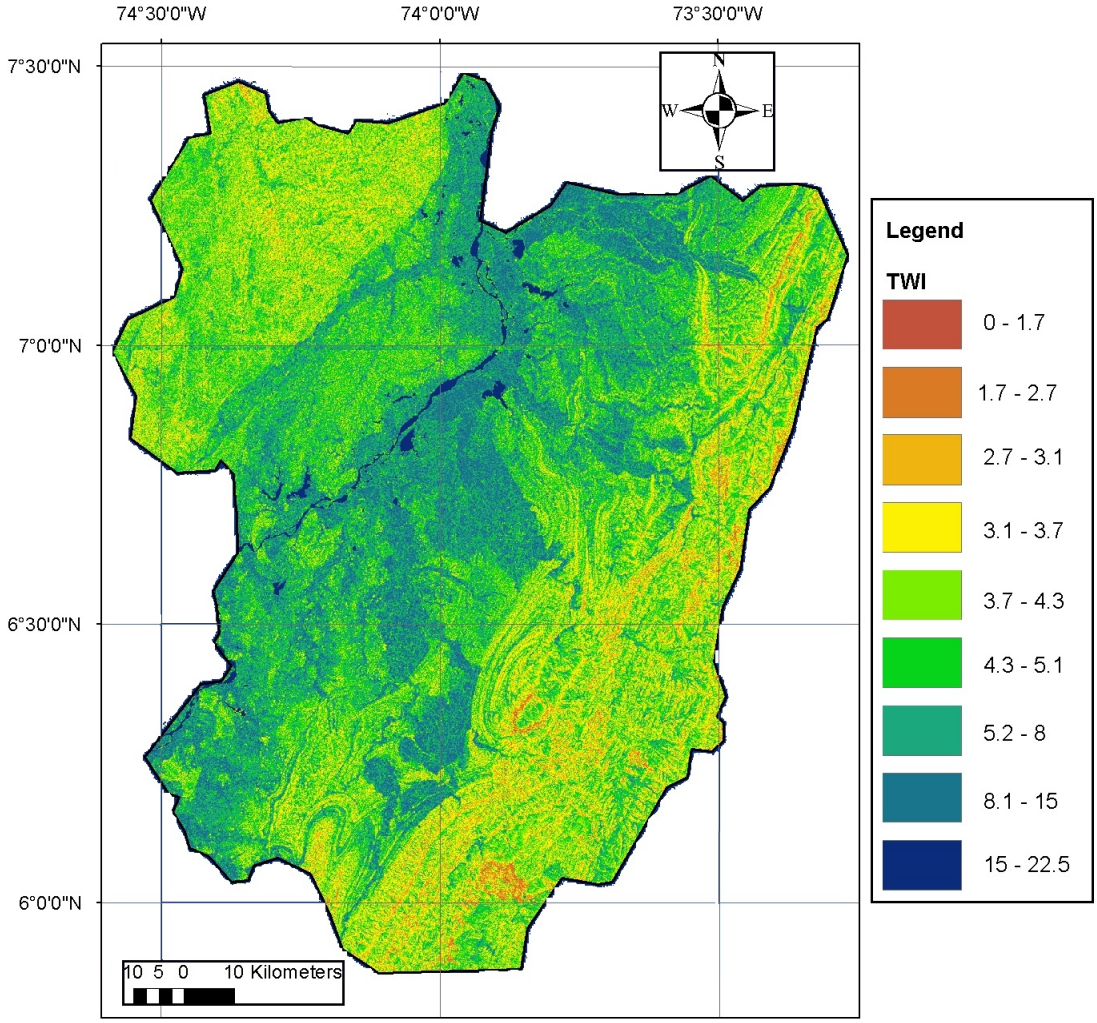

Figure **3-3**.: Topographic Wetness Index (*TWI*) in the study area. Source: Arenas-Bautista et al. (2018b).

3.3.1. Parameter estimation

TopModel uses, in addition to the TWI, ten parameters that represent the characteristics of the basin through hydrology, soils, and location of the study area (Table **3-1**). The values of each of these parameters or tune using prealable information that is available for the study area. In this work, the values of the model parameters were initially established from the reported literature for MMV area by the hydrological and geological institutions of Colombia (IDEAM and Colombian Geological Service - SGC) and they are shown in Table **3-1** (Ingrain, 2012; Ideam, 2014; Servicios Integrales Hidrogeológicos, 2015).

Table **3-1**.: Value of TopModel parameters reported literature for MMV area.

Parameters	Description	Unit	Value
qso	Initial subsurface flow per unit area	L	0-0.00005
$LnTe$	Log of the areal average of T	L^2T^{-1}	-7 - 6
m	Model parameter controlling the rate of decline of T in the soil profile	[-]	0-3
$Sr0$	Initial root zone storage deficit	L	0-3
Sr_{max}	Maximum root zone storage deficit	L	0-3
Td	Unsaturated zone delay time per unit storage deficit	TL^{-1}	20-250
Vch	Channel flow outside the catchment	TL^{-1}	1200-10800
Vr	Channel flow inside the catchment	TL^{-1}	50-2500
$K0$	Surface Conductivity	TL^{-1}	0-20
Cd	Capilary drive	L	0-5

In this context, the interval of variability of model parameters is expected to be greater. The key purpose of the GSA in this setting is to (i) improve our understanding of the functioning of the model, in terms of the relevance of each model parameter on the target model output, and (ii) to identify the relative importance of model parameters to the desired output model (Liu et al., 2016; Hutcheson & McAdams, 2010).

The drawbacks generated by the model in the calibration process are associated with the uncertainty of the parameters because the different sets of possible parameter values can have similar performance values (Loosvelt et al., 2014; Mazzoleni et al., 2015; Ballinas-González et al., 2016). For this reason, a Monte Carlo analysis (He et al., 2012; Simmons et al., 2017) has been used to estimate the best sets of parameters that generate a better performance. For this purpose, a data sampling with uniform distribution based on the interval reported in the Table **3-1** was used. The number of simulations varied between 10 000 and 35 000, since making new iterations did not improve the model performance.

This analysis showed that the parameters m and Sr_{max} are the most significant (Figure **3-4**), so the change in their values influences the performance of the model and the shape of the

simulated hydrograph. The n parameter represents the change in the saturated hydraulic conductivity with respect to depth. Small values of m imply quick flow and insignificant subsurface runoff, while large values indicate that more rainfall can infiltrate the soil, thus less water reaches the outlet via surface route (Sigdel et al., 2011). This parameter is related to subsurface flow control and the deficit of local storage, which is important in the case of percolation and recharge of an aquifer (Buytaert & Beven, 2011). Therefore, this parameter has a significant effect on the calculation of the local storage deficit, contributing areas and the shape of the curve in the hydrograph recession.

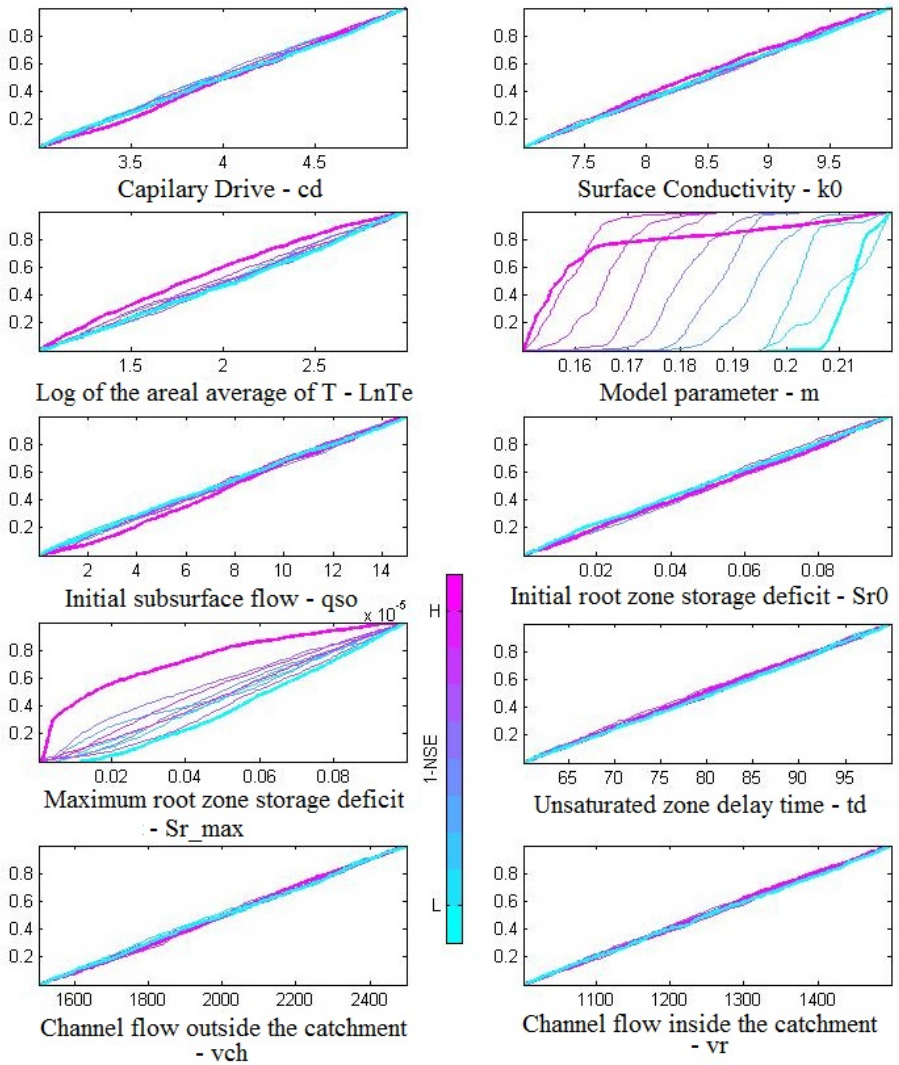

Figure **3-4**.: Cumulative distribution function plot of the model parameters according to the simulations performed for the 12 years of analysis. Source: Arenas-Bautista et al. (2018b)

The value of the Sr_{max} indicates the influence of evapotranspiration on the hydrological

behavior of the catchment. A low Sr_{max} value allows less water to be stored in the root zone and, hence, available for evapotranspiration which can lead to the increased runoff (Hollanda et al., 2015).

3.3.2. Global Sensitivity Analysis

Sensitivity analysis was carried out by two methods: Sobol and *AMA* indices. In the Sobol method, the calculation of the total and first-order indices presented a high computational cost, due to a large number of operations performed by decomposing the variance of the model for each of the parameters. *AMA* indices had a high computational cost too, due to computation of dependant statistical moments across the parameters ranges. The analyses were performed for 150 000 random parameter sets with a uniform distribution for the study period (2000 - 2012).

Sobol results (Figure **3-5**) showed that the parameters of lower sensitivity are those which tend to zero during most of the modeling time and that correspond to the partial results of $MCAT$. The parameter driving the transmissivity recession curve (associated with an exponential decrease of saturated hydraulic conductivity with depth) -m, the maximum root zone storage deficit -Sr_{max}, and the initial subsurface flow- qso can be considered as the most sensitive ones. For Sr_{max} and m the analysis of first-order indices was not as critical as when the total sensitivity index was analyzed. This suggested that the parameters interacted strongly within each other.

When considering the statistical moments and the *AMA* indices, other features can be assessed. The first observation reveal that the sensitivity of Q with respect to qso, m and Sr_{max} depends on the statistical moment of interest. It was analyzed the temporal evaluation of the first four unconditional statistical moments of Q (Figure **3-6**).

Figures **3-7**-a and **3-8**-a show that, at beginning of time period (year 2000), the mean and the variance of Q, respectively, are more sensitive to the qso parameter. This parameter is directly related to the initial conditions of the calibration period: if it is a wet period, the value of qso should be lower, but it would increase if the dry period. However, the range of values is associated with the physical conditions of the basin, mild slopes for our case study. These areas in the basin generally correspond to valleys, which present a saturation condition that causes a decrease in the amount of subsurface flow.

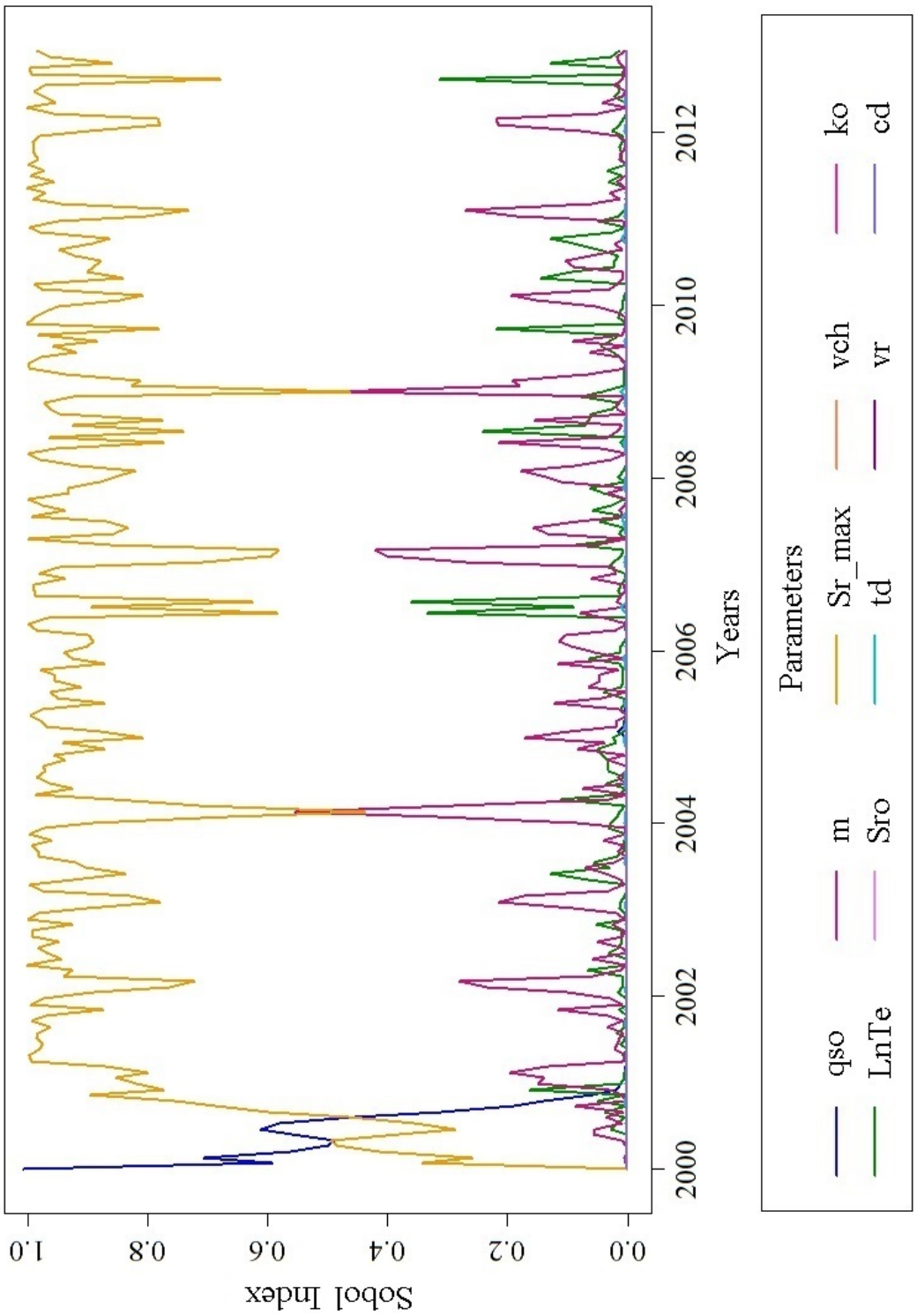

Figure **3-5**.: Time evolution of the Sobol index. The parameters vch, ko, Sro, td, vr and cd tend to zero and may not be clearly seen in the Figure.

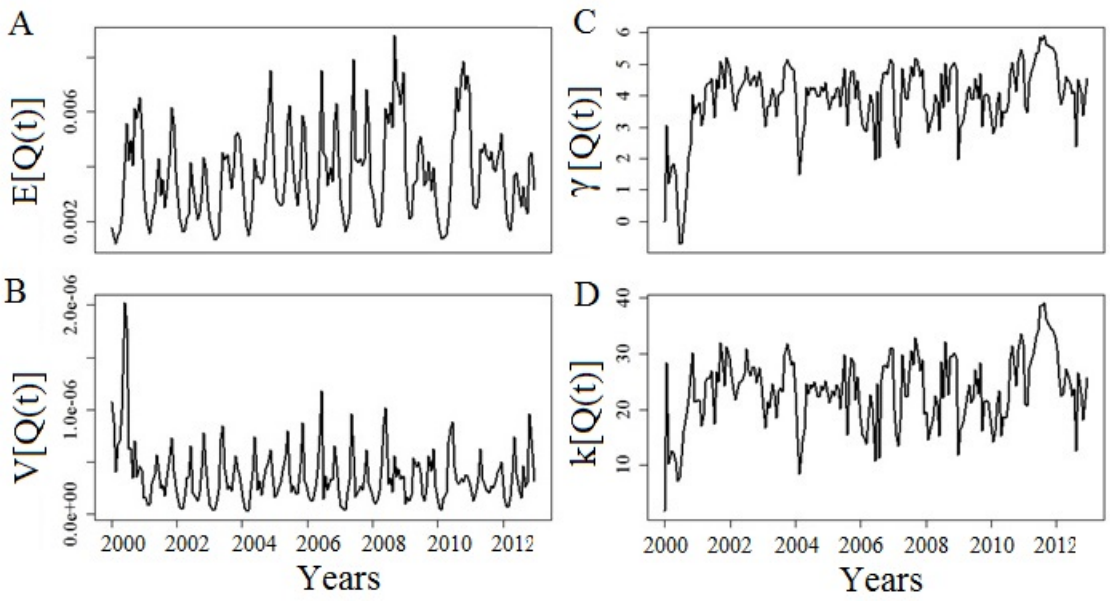

Figure **3-6**.: Temporal evolution of the first four moments of Q. (a) expected value, (b) variance, (c) skewness, and (d) kurtosis

.

The Figures **3-7**-b and **3-8**-b show the mean and variance of Q respectively. It is found that in 2003, the model is more susceptible to Sr_{max} and $LnTe$ parameters. This indicates the influence of evapotranspiration on the hydrological behavior of the catchment. The sensitivity of these parameters can be justified by analyzing the variations in the values of the Sr_{max} parameter, because it represents a greater or lesser runoff in response to the model. Now, if it is associated with a variation of the values of Sr_{max} parameter, changes could be observed in the saturated transmissivity, which represents delays in the runoff and system variation response.

For the years 2007 (Figure **3-7**-c and Figure **3-8**-c) and 2012 (Figure **3-7**-d and Figure **3-8**-d), figures indicate that Q is also sensitive to m. This sensitivity is presented by the change in the saturated hydraulic conductivity with respect to depth. That is, variations in subsurface flow conditions and local storage deficit modify the response of the model in the calculation of water recharge.

These analyzes are consistent with the results of the $AMAE$ and $AMAV$ indices (Figure **3-9**-a and b, respectively), where for the year 2000 the $AMAE$ and $AMAV$ indices for the qso parameter are greater than for the others parameters. For the other years, the $AMAE$ and $AMAV$ indices for the qso parameter are less important than for others parameters. The $AMAV$ index is related to Sobol index, as evidenced by the behavior shown in the Figure **3-9**-b.

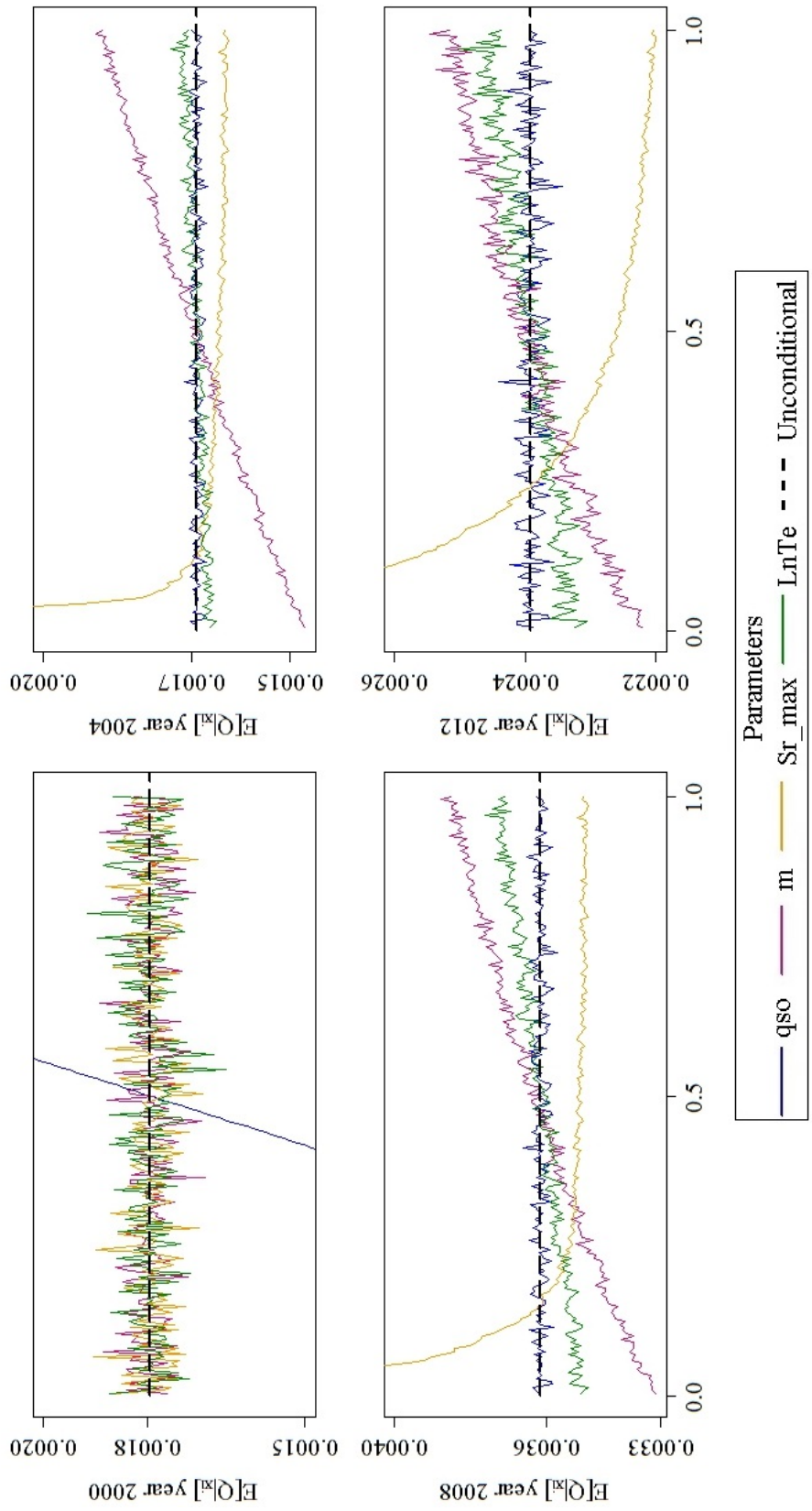

Figure **3-7**.: First moment (mean) of Q conditional to values of parameters: qso (blue lines), m (violet lines), Sr_{max} (gold lines) and $LnTe$ (green lines) for the years: 2000 (a), 2003 (b), 2007 (c) and 2012 (d). The corresponding unconditional moments (black curves) are also depicted. Intervals of variation of parameters has been rescaled between zero and one for graphical representations.

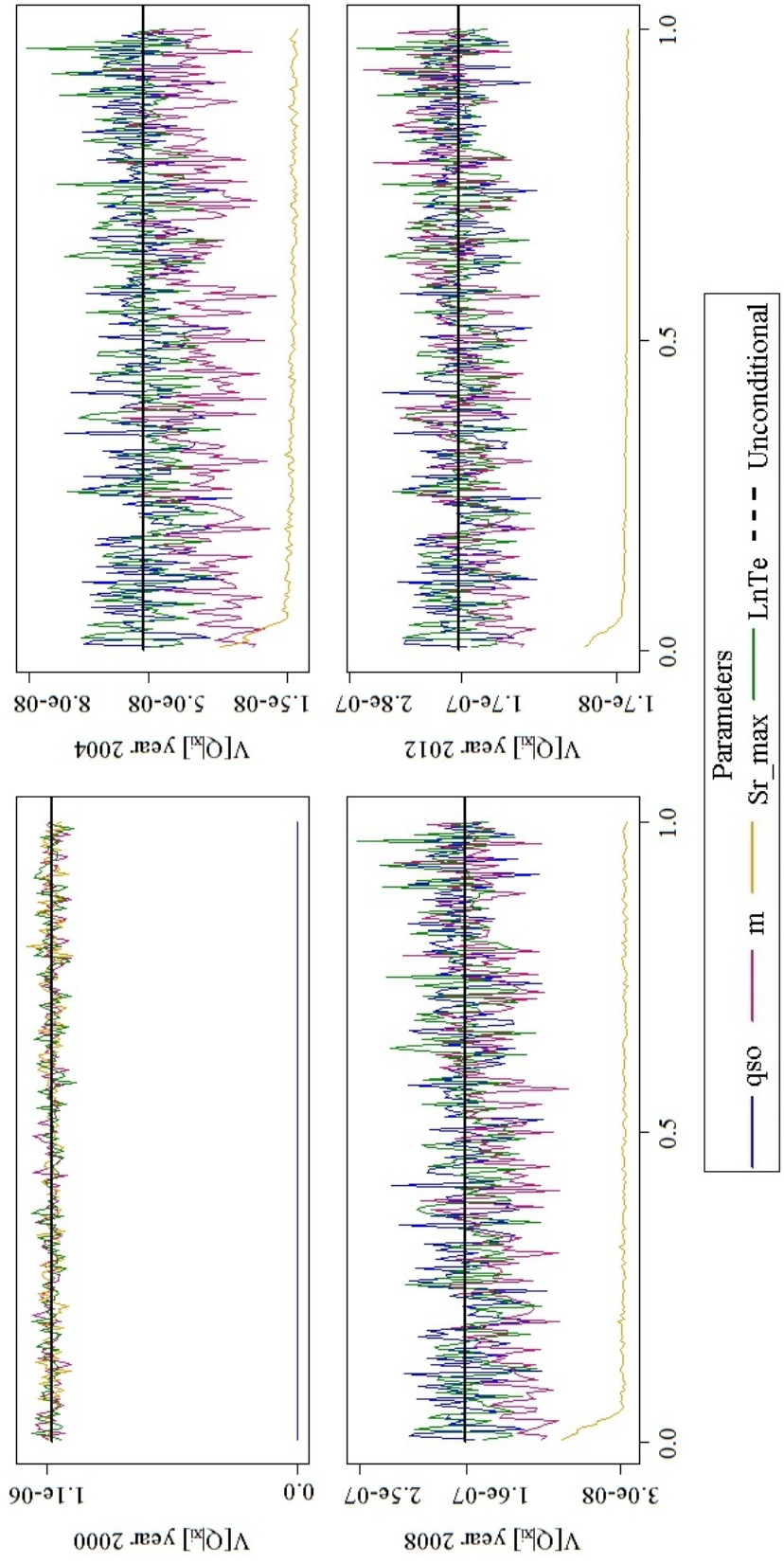

Figure **3-8**.: Second moment (Variance) of Q conditional to values of parameters: qso (blue lines), m (violet lines), Sr_{max} (gold lines) and $LnTe$ (green lines) for the years: 2000 (a), 2003 (b), 2007 (c) and 2012 (d). The corresponding unconditional moments (black curves) are also depicted. Intervals of variation of parameters has been rescaled between zero and one for graphical representation.

Skewness and kurtosis present a similar behavior to that shown by qso, m, $LnTe$ and Sr_{max} parameters in median and variance. On 2003, the conditioning to the Sr_{max} parameter makes the probability distribution function of flow to become more symmetric and tailed than the unconditional. For years 2007 and 2012 the conditioning is given by the Sr_{max} and m parameters, and corresponds to the behavior shown in the AMA_γ and AMA_k indices in Figures **3-9**-c and d.

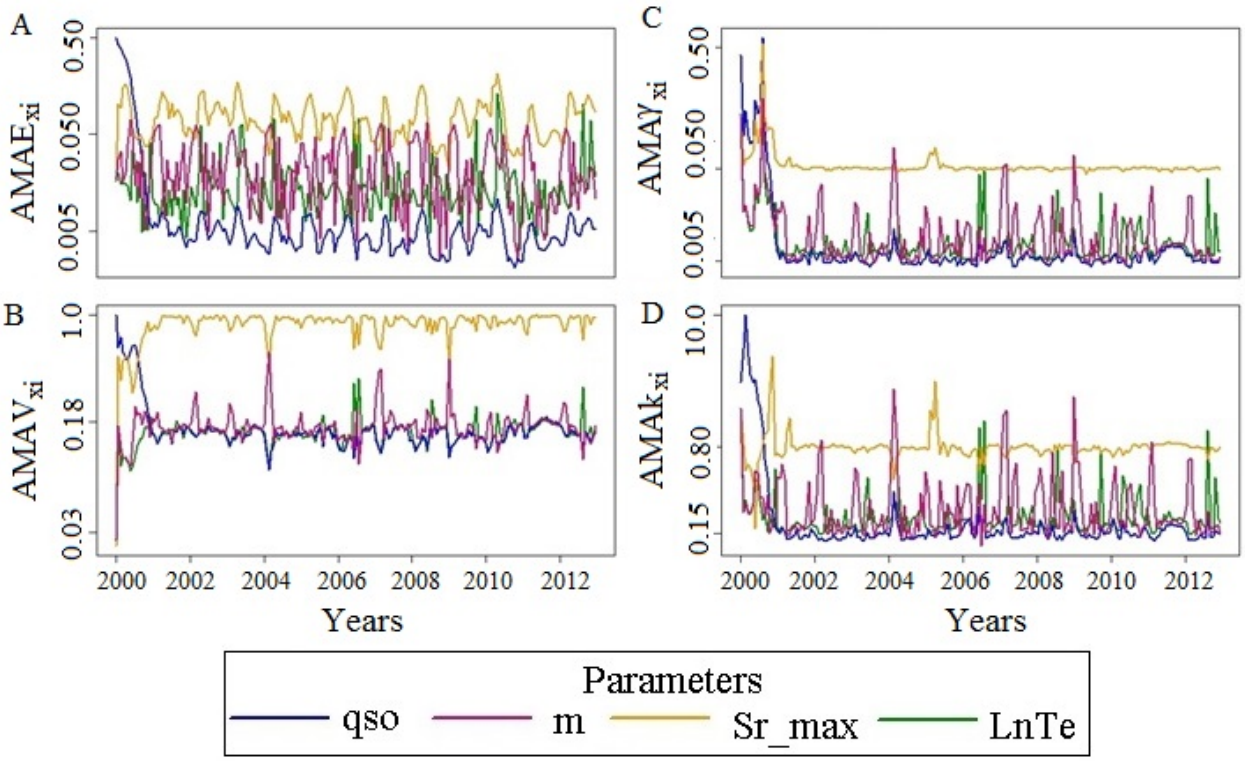

Figure **3-9**.: Time evolution of the global sensitivity index. (a) $AMAE$, (b) $AMAV$, (c) AMA_γ (d) AMA_k of $log(qso)$, $log(LnTe)$, $log(m)$ and $log(Sr_{max})$.

3.3.3. Model Performance

The model was implemented for the period 2000 - 2012, with a time step of 24 hours. The data between 2000 and 2008 were used for the calibration process. In this step, the characteristics of the basin were adjusted and the assumptions of the model were defined, consolidating the set of initial parameters that adequately describe the hydrological behavior of the study area. The data from 2009 to 2012 was used for the validation of the calibrated model.

The results from calibration (in San Pablo Station - Figure **2-4**) with *GSA* (Figure **3-10**), generated a set of parameters with efficiency of 0.74 for the objective function and 2.6

for $PBIAS$. The differences in the efficiencies of the best parameter sets were low, so the overall performance of all the simulations can be considered similar. This result is associated with the sensitivity analysis of the parameters and their impact on the representation of hydrological processes in the basin.

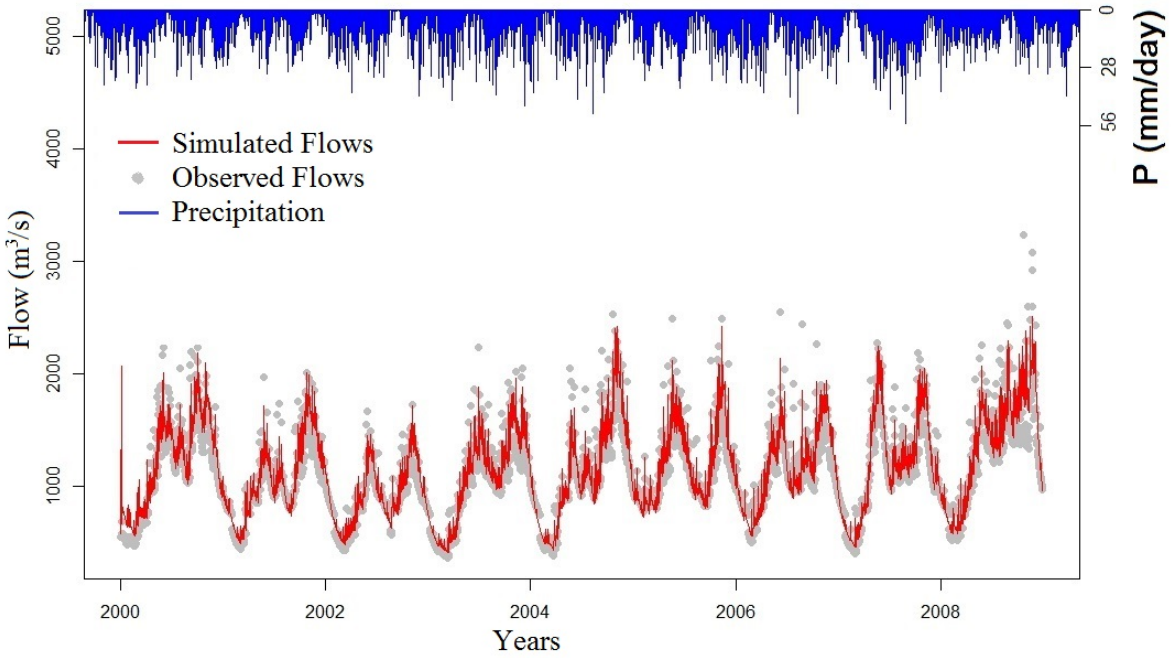

Figure **3-10**.: Observed Flows (gray), simulated flows (red) and Precipitation -P (blue) used in the calibration process in the San Pablo Station.

This set of parameters (Table **3-2**) was used to calculate the simulated flows by TopModel during the period studied, presenting an under estimation of the maximum flows. For the process of the model validation (in San Pablo Station - Figure **2-4**), results generated from the calibrated parameters with higher NSE values gave efficiency values near to 0.73 and its simulated flows are shown in the Figure **3-11**. The NSE values found are close to the values obtained for a proven models in Ecuador, Colombia, Poland, Nepal and China with efficiency values near to 0.7 (Sigdel et al., 2011; Padrón et al., 2015; Gil Morales & Tobón Marín, 2016; Jeziorska & Niedzielski, 2015).

Table **3-2**.: Value of TopModel parameters used for the validation process.

Parameters	Description	Unit	Value
NSE		[-]	0.74
$PBIAS$		[-]	2.6
qso	Initial subsurface flow per unit area	L	0.000123
$LnTe$	Log of the areal average of T	L^2T^{-1}	1.255
m	Model parameter controlling the rate of decline of T in the soil profile	[-]	0.217
$Sr0$	Initial root zone storage deficit	L	0.086
Sr_{max}	Maximum root zone storage deficit	L	0.002
Td	Unsaturated zone delay time per unit storage deficit	TL^{-1}	94.7
Vch	Channel flow outside the catchment	TL^{-1}	1740
Vr	Channel flow inside the catchment	TL^{-1}	1044
$K0$	Surface Conductivity	TL^{-1}	8.39
Cd	Capilary drive	L	4.22

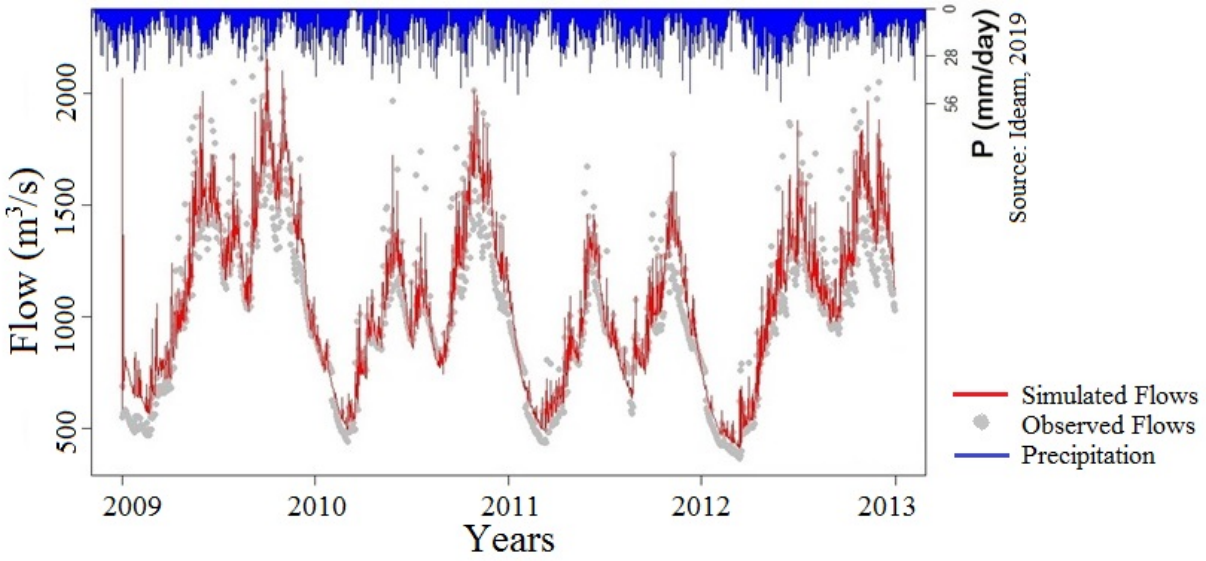

Figure **3-11**.: Observed flows (gray), simulated flows (red) and Precipitation -P (blue) used in the validation process in the San Pablo Station.

However, it is possible that longer periods of time could help ensure better simulations and adjustments, because when more data is added to model, the variability increases, and so the parameter values are adjusted in concordance. Additionally, it is widely known that TopModel has problems to accurately represent low flows during droughts (Hollanda et al., 2015). For periods where precipitation exceeds evapotranspiration, the wide range of parameters provide acceptable simulations for basin discharge, although base flow is less accurately simulated, as it happen in other sites (Zhang et al., 2016).

The efficiencies were classified according to the methodology reported by Boskidis et al. (2012). The NSE values found are close to the values obtained for a proven model in Ecuador and Colombia with efficiency values near to 0.67 and 0.7 respectively (Padrón et al., 2015; Gil Morales & Tobón Marín, 2016). For periods where precipitation exceeds evapotranspiration, the wide range of parameters provide acceptable simulations for basin discharge, although base flow is less accurately simulated, as it happen in other sites (Zhang et al., 2016).

The initial determination of the dominant and sensitive parameters was performed with $MCAT$ through the cumulative distribution curves which were created from the division of the Monte Carlo sampling results into a group of equal size, showing that the parameters $LnTe$, m, qso and Sr_{max} present a greater slope of the distribution curve (Figure **3-4**), which supports the importance premise of these four parameters in the hydrological response of the basin (Bulot et al., 2016).

AMA sensitivity analysis outlines the importance of the parameters considered by $MCAT$ and Sobol, but Sobol index and AMA indices remark the need to concentrate the calibration effort on some parameters, according to the modelling's final goals. For example, if the main goal is forecast, or retrospective time-series reconstruction, Sr_{max} and m are the parameter to take into account in the calibration process, but if the modelling is centered on lowering the output uncertainty, $LnTe$ could improve the model performance in some moments of the time period. Finally, the assessment of extreme events will eventually need the tuning of Sr_{max}, but might make an insight on $LnTe$ and m on some moments, specially on dry periods.

Those remarks and guidelines could lead other calibration processes in tropical catchments with similar behavior, saving computational resources and time in the processes, and allowing to link the modelling framework to the catchment scale hydrologic processes observed in nature.

In addition, the model performance has been analyzed through the flow duration curve (FDC - Figure **3-12**) between the observed and simulated data (Badjana et al., 2017).

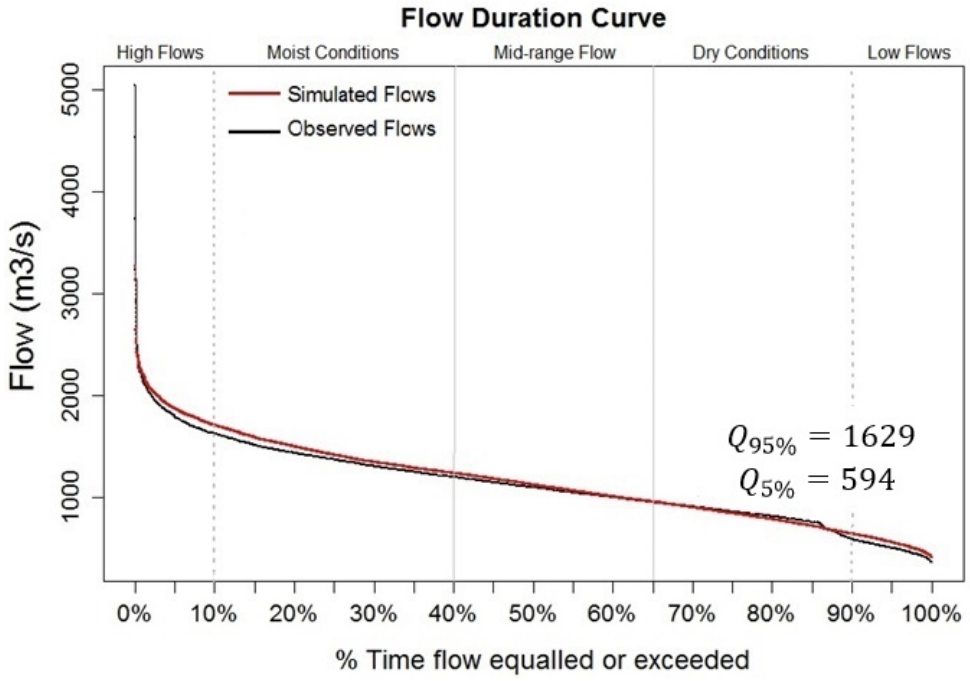

Figure **3-12**.: Flow duration curve - *FDC* to analyze the flow variability in the study area.

These curves show a variability of 22% between 10% and 90% of the exceedance time, which indicates that its variability is low and therefore it is related to groundwater storage processes that dominate the flow of the stream and maintain a flow more stable in time (Salazar, 2016). This corroborates the analysis carried out with respect to the variability of the parameters and allows us to identify a coherent process between the behavior of the basin studied and the performance of the model. In particular, it seems that the model fits well the high-flow observations, but presents a slightly higher variance for the mid-flows, as observed in a line with a higher slope; as for the low-flows, the observations is featuring a step at the end of the *FDC*, indicating that the basin is not able to maintain the same conditions for baseflow as for other flow sources, maybe due to anthropic or natural interferences on the percolation fluxes, and simulated flows roughly follow these patterns, with a smoother curve, due to its impossibility to represent these unknown interferences.

3.3.4. Recharge

The recharge (Figure **3-13**) shows the spatial behavior of recharge in the study area, where there are values of percolation ranging from 20 to 400 mm/month. The recharge generated in the area comes mainly from the rain and the zone has a moderate to low potential to recharge the aquifer. Note that for the model configuration, in the months with the highest rainfall (April - May and October - November) the spatial behavior of percolation is similar.

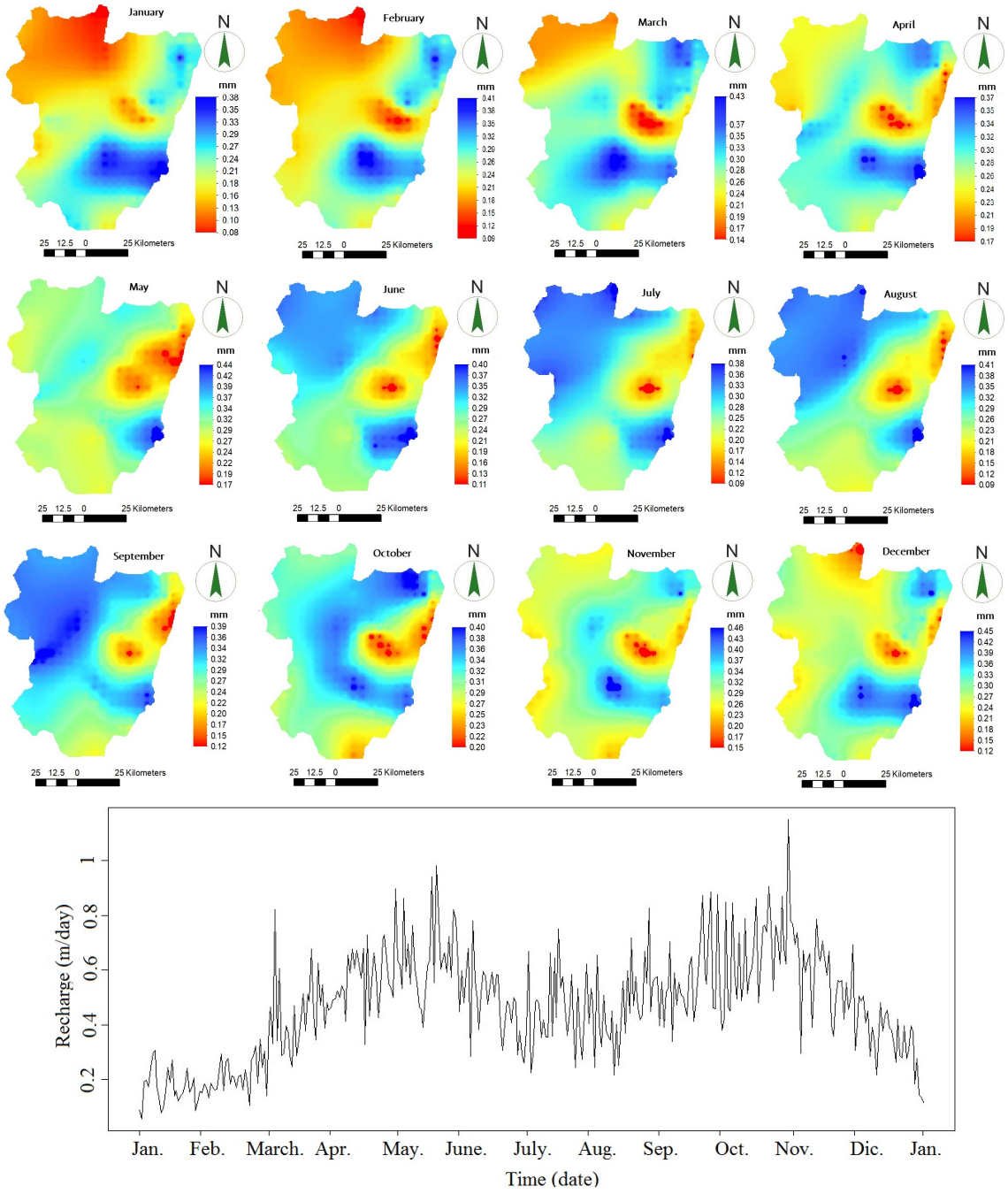

Figure **3-13**.: Recharge data used in hydrogeological model. The maps show a monthly distribution of the recharge value in the study area and are the inputs in the hydrogeological model. This series was built for an average year, based on results of hydrological model (Arenas-Bautista et al., 2017).

3.3.5. Limitations and Conclusions

Models are used to represent real-life conditions. So, the major limitation of models, is that they are a 'simplification' of real conditions. Additionally, the model selection process should be conditioned by the modeling objective; however, the available information is a limitation that ends up prevailing. So, the available data and their quality are important because a model is only as good, as the information used to build it. If we use simpler information or wrong information, it will give us, the wrong results. And finally, the models should be limited by a physical meaning, but, what happens when the information is not available to compare? I should skip the physical behavior for the model precision?. In these cases, to increase the parameter values range, or decrease the system simplifications, would take us again at previous limitation.

The application of the hydrological model developed in this research contributes to national efforts, and the availability of results helps the development of comparative studies in the Middle Magdalena Valley at the basin scale. This work constitutes a sample of the advantage of applying a widely used semi-distributed model that is freely accessible to the scientific community, contrary to the limitations of using a model that depends on the singularity of the study area. TopModel was able to reproduce the main pattern of the hydrograph with acceptable accuracy for the case-study. A low performance to simulate some patterns (baseflow) can be attributed to input data error, calibration inaccuracy, parameter uncertainty and model structure. The most probable cause for those results is linked to the uncertainty of the data series analyzed. Low accuracy of the model can also be an effect of the model's inability to represent distributed rainfall pattern. The results obtained will be used as input data in the hydrogeological analysis of the area.

The sensitivity analysis allowed to establish the intervals of the parameters that offer a better response of the model. Additionally, it allowed identifying which of these parameters govern the behavior of the model. The sensitivity results obtained from the output of the model, with respect to one parameter, is directly related to the global sensitivity index. This is because the variability of a parameter modifies the statistical moments of the model.

The preliminary results of $MCAT$ are related to those obtained in the Sobol and AMA index. Sobol sensitivity analysis is a useful tool for hydrological models evaluation and thus allowed to identify the most sensitive parameters of the TopModel model in the study area. The AMA indices take into account the mean, variance, skewness and kurtosis of the probability density function of an output of the model. From these metrics, they quantify the variation of the results with respect to the change of one or several input parameters of the model, allowing to analyze in a simple way the characteristics of the probability distribution function of the output of the model (i.e. the degree of dispersion, symmetry, and tailed).

4. Hydrogeological Model

This chapter presents the consolidation of the hydrogeological model. This model allows us to identify and analyze the behavior of hydraulic conductivity in the study area. Throughout this chapter, you will find the hydrogeological simulation and the comparison between PP and CZ to properly identify any biased parameters and the relationship between the hydraulic properties heterogeneity and the PP numbers. This chapter is based on Donado et al. (2018).

In this chapter, the analysis of a regional groundwater flow model is presented. This model implements two types of analysis: *i* pilot-points (PP) and *ii* constant zones (CZ). The former is analyzed with the comparison of three regularization methods: (i) Tikhonov, which is proposed as a restricted optimization problem, (ii) singular value decomposition (SVD), which defines a small group of "super parameters" given by the model that can be appraised by non-linear regression of data, and (iii) SVD-assisted, which is based in the determination of super parameters that can be associated as multiplicating eigen-vectors within a weighted sensitivity matrix to obtain a minimization in the objective function. SVD-assisted technique allows to properly identify any biased parameters and the relationship between the hydraulic properties heterogeneity and the PP numbers. Additionally, the possibility to evaluate the plausibility's reviewed, analyzing if this can improve the identification of hydraulic conductivity (K) heterogeneity and if it would be sensitive to the number of PP. For this purpose, a numerical variable density model is developed. This tool is limited to reinterpreted data from real measurements. For the CZ technique, the initial parameters are assigned according to each layer, that is considered constant for hydraulic parameter values. In contrast to PP technique, the initial parameters are assigned according to interpolations using in-situ point measurements. The established model shows a low correlation with the observed state variable (hydraulic head), proving the importance of spatial heterogeneity. The model is calibrated in order to establish K (as an anisotropic parameter that varies spatially), the porosity (η) and the specific storativity capacity (S_s) in the PP and CZ, reducing a mean square error of state variable dependable on the observation points.

4.1. Introduction

Two-dimensional and three-dimensional representations in hydrogeological modeling allow us to exemplify static and dynamic conditions of hydrogeological systems in natural or hypothetical scenarios and their relationships with surface water bodies inputs (Alberti et al., 2018; Gogu et al., 2001). This type of modeling can be used to analyze the effects of groundwater extraction, to evaluate irrigation strategies in order to establish an appropriate correspondence with aquifers, or to simulate different water management scenarios (White, 2018). In this context, a calibrated model is a significant tool for water resources management.

The calibration process must be used to acquire reliable modeling results (Wu et al., 2017). A good model calibration minimizes the residual data between the observed and simulated data and reduces the uncertainty of the hydrodynamic parameters in the area. This procedure was developed using the inverse method. The inverse methods can solve problems: (*i*) linear and (*ii*) non-linear. The method application with non-linear parameter estimation techniques (Carrera et al., 2010; Wang et al., 2017b; White et al., 2016; Usman et al., 2018) is common, given the swiftness that this method shows to determine the best adjustment parameters, applying low subjectivity in the calibration process (Sun et al., 2015; Usman et al., 2018; Zhou et al., 2014). Despite this advantage, the method is limited to the satisfactory sampling of field data (Llopis-Albert et al., 2016; Pool et al., 2015; Zhang et al., 2016). Additionally, hydrogeological models have a high spatial-temporal variability rate that causes non-linearity which also increases the correspondence within different model input parameters (Gaganis & Smith, 2006; Marchant & Bloomfield, 2018). An undesirable effect in this situation is the appearance of unrealistic parameter distributions that causes the calibration process to fall to a local minimum without exploring other posibilities (Hu & Chan, 2015; Klaas et al., 2017). Bearing in mind that the calibration process does not guarantee the total model reliability and that the results obtained are as real as the veracity in the assumptions used in the conceptual model (Betancur et al., 2009; Kpegli et al., 2018; Linde et al., 2015), then, it is appropriate to analyze the sensitivity and uncertainty associated with the parameters. The uncertainty in the hydrogeological models is related to: (*i*) inaccurate measurement of input data, (*ii*) inadequate simplification of the represented system and (*iii*) calibration process (Carrera et al., 1993; Chen et al., 2018; Meeks et al., 2017). In particular, the calibration process of any hydrogeological model is based on some method of spatial characterization or zone focused parameters (Dewandel et al., 2012; Benoit et al., 2018).

The model was divided into different hydrogeological units based mainly on geological properties (Custodio et al., 2016; Islam et al., 2017; Wang et al., 2017a). This subdivision leads to suppose hydraulic uniformity properties in each zone (Cherry et al., 2004). This simplification means that the hydraulic parameters values at any location are weighted

averages of the actual values measured at different points within an area (Hassane & Ackerer, 2017; Irsa & Zhang, 2012; Zhang et al., 2014). The sensitivity analysis allows to address uncertainties identifying the most important model input parameters (Karay & Hajnal, 2015). Additionally, this analysis provides an overall system understanding, reduces uncertainties and improves the calibration and validation processes (Carrera et al., 1993; Ehtiat et al., 2015; Sanchez-León et al., 2016).

The use of these *CZ* for allocation the hydraulic parameters' values, lead to unnecessary uncertainties in the modeling and, therefore, produce erroneous parameter values and high heterogeneity in the geological units (Linde et al., 2017; Tiedeman & Green, 2013; Woodrow et al., 2016). Having this into consideration, the *PP* technique has been proposed to improve the spatial variability interpretation of parameters, in cases of groundwater flow modeling that cannot be obtained by working with *CZ* (Christensen & Doherty, 2008; Jiménez et al., 2016; Le Ravalec-Dupin, 2010; Usman et al., 2018). This technique interpolates the spatially correlated hydraulic properties values of a set of points distributed along the model domain (Ma & Jafarpour, 2017); generating an uniform distribution of parameter values with less uncertainty. However, the use of a larger number of *PP* or the area subdivision in large spaces could result in extensive modeling times (Christensen & Doherty, 2008; White et al., 2016).

The application of this technique has been widely used throughout many related issues as shown (Alcolea et al., 2006a, 2008; Christensen & Doherty, 2008; Hernandez et al., 2003; Jung et al., 2011; Le Ravalec-Dupin & Roggero, 2012; Le Ravalec-Dupin, 2010; Ma & Jafarpour, 2018; Panzeri et al., 2012). Nonetheless, the use of this technique can generate over parameterization, situation that would lead to the optimization problem instability (Amini et al., 2009). The instability can imply infinite or very large ranges where the variations of the parameters are established, large variations in the parameter's value, non-existent correlations due to the small amount of data, and large second derivatives of the hydraulic properties (Riva et al., 2011; Tóth et al., 2016; Yeh, 2015). The use of variograms to correlate the initial value of hydraulic properties and limit their search ranges, can help to improve their stability (Friedel & Iwashita, 2013; Jardani et al., 2012; Kashyap & Vakkalagadda, 2009; Sheikholeslami et al., 2017). Although the biggest issue with application of *PP*, is associated with the number of parameters to be calibrated, which is actually the definition of *PP* parameters itself, where each of those parameters is another constraint. Determination of *PP* number within the model can be defined in a fixed way associating a spatial location or a random variation during the optimization process (Christensen & Doherty, 2008; Jiménez et al., 2016; Sun et al., 2011). The usage of a reduced *PP* value can improve model stability, although this approach could generate a larger homogeneity of hydraulic properties, approaching it to *CZ* technique and making the problem sensitive to the point locations (Ma & Jafarpour, 2017). However, Alcolea et al. (2006a) established

that when implementing *PP*, and regularization processes, it is recommended to implement as many number of *PP*s as computational viability is allowed. This implementation permits to obtain a conductivity field that is as close as possible to the true field.

4.2. Methodology

4.2.1. Governing Equations and Modeling

Mathematical equations describing groundwater flow through a porous medium are based mainly on Darcy's law (Jiao & Zhang, 2016) (Eq. 4-1) and the continuity equation. According to Darcy's law, the average flow velocity is proportional to the hydraulic gradient (Freeze and Cherry 1979) and the effective porosity.

$$V = -K\nabla h, \tag{4-1}$$

where, V is the Darcy velocity which is defined as the flow per unit cross-sectional area of the porous medium, K is the hydraulic conductivity, and h is the hydraulic head.

Substituting the Darcy equation in the Continuity equation is obtained flow equation (Eq.4-2).

$$\nabla.(K\nabla h) \pm W = S_s \frac{\partial h}{\partial t}, \tag{4-2}$$

where, S_s is the specific storativity, W represents the source/sink term, and t is the time.

In the mass balance, the rate of change in storage of volume overtime must be equal to the input rate minus the mass output rate. Under steady-state conditions there is no change in the hydraulic head, so time is variable dependent. The steady-state flow can be described by the Eq. 4-3.

$$\nabla.(K\nabla h) \pm W = 0, \tag{4-3}$$

In a homogeneous and isotropic medium (Eq. 4-3) can be expressed by the Eq. 4-4

$$\nabla^2 h \pm W = 0, \tag{4-4}$$

The solution $h(x, y, z, t)$ describes the value of the hydraulic head at any point in the system at time t. The flow in 3D transient state in a porous, heterogeneous and anisotropic medium is described by this equation combined with the initial and boundary conditions. Thus, the three-dimensional aquifer is conceptualized in layers, which are discretized in nodes within the model (Anderson and Woessner, 1992). The flow between nodes is defined by storativity and transmissivity through $T = Kb$, where, b is the saturated thickness of that aquifer.

Given this, the equation that governs the flow of groundwater in the each layer is expressed by Eq. 4-5.

$$\frac{\partial h}{\partial x}\left(T_x \frac{\partial h}{\partial x}\right) + \frac{\partial h}{\partial y}\left(T_y \frac{\partial h}{\partial y}\right) = S\frac{\partial h}{\partial t} + W, \tag{4-5}$$

The z dimension is not considered in this layer, and the storativity term is expressed as the $S = S_s \times b$. When the aquifer is confined, the saturated thickness and transmissivity remain constant. Additionally, the saturated thickness may vary over time. To calculate this thickness it is necessary to know the elevation of the bottom of the aquifer and the hydraulic head (Eq. 4-6).

$$\frac{\partial h}{\partial x}\left(K_x \frac{\partial h}{\partial x}\right) + \frac{\partial h}{\partial y}\left(K_y \frac{\partial h}{\partial y}\right) = S_y\frac{\partial h}{\partial t} + W, \tag{4-6}$$

here, the specific yield (S_y) that represents the unconfined equivalent of the hydrogeologic system.

Finally, when the groundwater system has been characterized, the numerical model is developed. The methodological development used in this model is presented in Figure **4-1**.

4.2.2. Boundary Conditions

The conditions of the hydrogeological limits can be explained through the following mathematical conditions (Sahoo & Jha, 2017; Tóth et al., 2016).

- 1^{st} type: Dirichlet Condition. The main assumption for this condition is that, regardless of the flow of water within the domain, there is no influence on the potential of the outside water body, so that this potential remains constant (Eq. 4-7).

$$h(x_i, t) = h_l^R(t), \qquad \Gamma_l \quad \in \quad t(0, \propto). \tag{4-7}$$

  Here, h_l^R is the prescribed limit values of the hydraulic head, and Γ is the given limit.

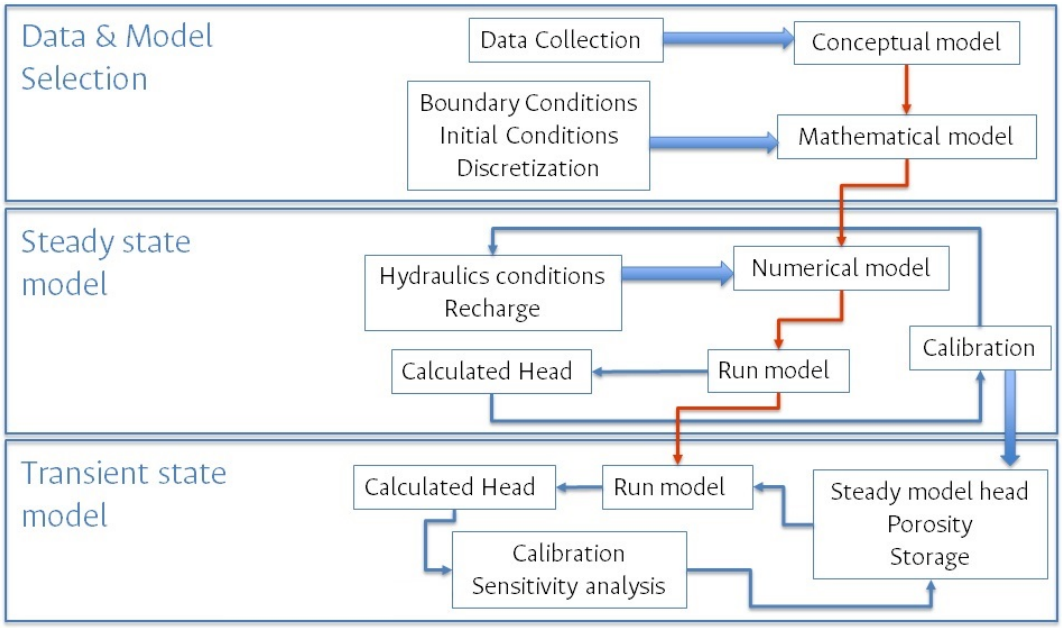

Figure **4-1**.: Hydrogeological Modeling Methodology. The thick blue arrow indicates inputs. The thin blue arrow indicates an iterative process for the model's optimization. The red arrow indicates the methodology steps.

- 2^{nd} type: Neuman Condition. This condition states that regardless of the state and the flow of water within the domain and at the limit, the normal flow is set by external conditions and is still determined by the state of the limit (Carrera & Neuman, 1986; Tóth et al., 2016) (Eq. 4-8).

$$qn_h(x_i, t) = q_h^R(t) = -K_{i,j}\frac{\partial h}{\partial x_j}n_i, \qquad \Gamma_2 \quad \in \quad t(0, \propto). \tag{4-8}$$

  Here, qn_h represents the Darcy flux of the fluid, q_h^R is the normal boundary fluid flux, and n_i is the normal unit vector.

- 3^{rd} type: Cauchy Condition. In this condition, the flow through the limit depends on the magnitude of the difference in the head through the limit, with the head on one side of the limit entered into the model and the head on the other side calculated by the model (Eq. 4-9).

$$qn_h(x_i, t) = \Phi_h(h_2^R - h), \quad \Gamma_3 \quad \in \quad t(0, \propto). \tag{4-9}$$

  Here, the Φ_h is the fluid transfer coefficients.

- 4^{th} type: Pumping/Injection Condition. In this condition it is established that the

aquifer is subjected to extraction or injection processes, which in turn cause changes in the hydraulic head, and can be represented mathematically as shown in Eq. 4-10.

$$Q_p^w(x_i,t) = \sum_m Q_m^w \prod_i \{\delta(x_i - x_i^m)\}, \qquad for \quad \forall (x_i, x_i^m) \in \Omega. \tag{4-10}$$

Here, Q_p^w represents the well function, Q_m^w is the pumping or injection rate of well m, and x_i^m is the location of well m.

4.2.3. Regularization and Parametrization

In order to understand the regularization methods proposed in this chapter, an introduction to the conditioned probability computation over a parameter space whose probability distribution function (*pdf*) is unknown is presented. This approach focuses on finding an optimum function from an eligible set of *pdf*'s that represents the best approximation of the data set. The goodness-of-fit of the approach is measured through the MSE, which implies the approximation being a correlation as accurate as possible between the input and output data, represented by the interpolated function.

However, in this research, parameters as the hydraulic conductivity were not well represented when the spatial analysis was carried out due to the few field measurements. This misrepresentation is due to field data errors during the measurement process, to clustering on the field data location, and to an important data scarcity across the area, with zones presenting a few measurements, and others with no information. Given this, the use of minimization functions such as MSE does not eliminate the noise generated by measurement errors. As for the location clustering and small or null amount of information, a function which is robust enough and permits generalization is an advantage that allows to predict information across the area, when no data is available.

The regularization process in hydrogeological models applies some constraints in the function to reduce the error. The soft constraint is the most used to regularize a solution due to is limited with the same parameter values to obtain models with fewer failures. Another possibility is the use of sparsity constraints, which forces the function to simplify the number of parameter combinations around a set of representative data in the model's domain.

The methodology presented in this chapter for parameterization of a regional groundwater flow model consists in the comparison of three regularizations.

1. Tikhonov: guides the solution of the inverse problem towards parameter estimates that approximate the minimum error variance. In this research, the inverse problem

was formulated as a restricted optimization problem in which an adequate parameter value is sought, defined by the field measurements of hydraulic parameters and which is subject to restrictions of the objective function. When looking for these values, without exceeding the model constraint, it is sought to minimize the objective function for the parameter and reduce the predictive error. In this modeling a soft constraint was used, assuming that the *PP*s that are close to each other must have similar values. The soil heterogeneity level was controlled by the corresponding semi-variogram. However, due to the lack of information in some areas, it was not possible to correlate the hydraulic parameters in areas with ranges greater than 2000 m, so the soft constraint was combined with the sparsity constraint. In this constraint, the a-priori information relates the *PP*s to their initial value, which leads the model to find value closed to the initial value of the assigned *PP*.

2. Singular Descomposition Value - SVD: solves the inverse problem by removing parameters' combinations. This method is more flexible than Tikhonov since is not necessary to estimate combinations of parameters which are not relevant for the calibration process. The method works by subdividing the parameter space into two orthogonal subspaces. One space is encompassed by combinations of parameters that correspond to the solution and the other is the null calibration space, in which the parameters of the inverse problem that cannot be estimated are omitted.

3. SVD-assisted: subspace methods provide numerical stability in the modeling process by removing parameters or combining them in the calibration process (Aster et al., 2005). As a result of the removal, the calibration process is no longer necessary to estimate individual parameters or combinations of correlated parameters that are indeterminate in the parameters' space. These combinations are determined automatically by the weighted Jacobian matrix which is calculated only once. Then, the parameter space is broken down into the combinations of estimated parameters (super-parameters) and the combinations of indeterminate parameters. The calibration problem is reformulated so that it only solves in these super-parameters (Christensen & Doherty, 2008; Tavakoli & Reynolds, 2009; Khaninezhad et al., 2012; Khaninezhad & Jafarpour, 2018).

In general, the parametrization processes: (*i*) achieves uniqueness of a fundamentally nonunique calibration problem (nonuniqueness is always the case for groundwater models), and (*ii*) achieves a level of fit that stops overfitting. Overfitting a model describes the random error in the data instead of the relationships between the variables. That is, overfitting models have too many variables for observations number. Thus, the regression coefficients represent noise rather than genuine relationships between the variables.

Each sample has its unique peculiarities, thus, a model that adapts to the random peculiarities of one sample is unlikely to fit the random peculiarities of another sample.

Therefore, overfitting a regression model reduces its generalization outside the data set. In other words, an overfitting model describes the noise and is not applicable outside the sample, which is not useful.

An important consideration is that the sample size limits the quantity and quality of the conclusions that can be drawn about a population. The more you need to learn, the bigger the sample should be. That is, as the number of observations per estimate decreases, the estimates become more erratic. In addition, a new sample is unlikely to reproduce inconsistent estimates produced by smaller sample sizes. Overfitting often occurs when a high R2 is sought. When choosing a regularization model, the goal is to approximate the true model for the entire population. If it achieves this goal, the model should fit most of the random samples taken in an area.

The general parametrization for a hydraulic property $Y(x,t)$ of a groundwater flux system is defined by: (i) a deviation $Y_D(x,t)$ representing the real values from n observation in Y, and (ii) a residual error (ε), corresponding to a model's parameters lineal combination (P_j). The deviation $Y_D(x,t)$ is represented through a model's discretization using Kriging. This discretization allows to consider field measurements of the property $Y(y^*)$ and geophysical data (g^*). For the lineal estimation, deviation is written in Eq. 4-11.

$$Y(x,t) = \sum_{i=i}^{Dim_Z} \beta_i^z(x) Z(x_i,t), \tag{4-11}$$

where, x is the deviation location, t and x_i are time and measurements' locations, and β_i^z are the weights assigned in the discretization for every measurment, arranged in the vector $Z = (y^*, g^*)$. The residual error's paramterization express the required modification on the deviation to preserve the dependent variable measurements. The residual error can be written as the lineal combination of hydraulic properties' values in the PP (see Eq. 4-12).

$$\varepsilon = \sum_{j=i}^{N_{PP}} (\mu_j^z) P_j, \tag{4-12}$$

here, N_{PP} is the number of PP, μ_j^z are the weights assigned in the discretization of P_j.

4.2.4. Estimation and Objective Function

A priori estimation of PP values and the covariance matrix is done through conditional estimation of measurements in vector Z. PP variance located near the measurement points will be lesser. When using the SVD method, the values for super parameters are estimated

iteratively, minimizing the total error used to quantify the deviation between observations and simulations. In the development of this model, the identity matrix has been used as the weighting matrix using the Monte Carlo method described in Alberti et al. (2018). The regularization process helps to reduce the non-singularity in the estimation of parameters (Mahmoud & Saleem, 1993; Alcolea et al., 2006a; Jafarpour, 2013; Carniato et al., 2015). Tikhonov regularization involves a series of information based data equations to set the initial parameters values (Christensen & Doherty, 2008). The calibration process with Tikhonov is proposed as a restricted minimization process that decreases φ for a specific target set by the user. To ensure that Tikhonov's regularization process provides numerical stability to the model, the limits for the model must be between sub-spaces $S1$ and $S2$ so that the sensitivity matrix values are high. If this condition is not accomplished, φ is minimized without taking consideration of the conditions specified by the user, adjusting the weights to a-priori information.

The Objective Function (φ) is defined in order to optimize iteratively model parameters and fit model output and observed values. The goodness-of-fit uses the φ written in Eq. 4-13.

$$\varphi = \varphi_r + \gamma\varphi_m, \tag{4-13}$$

here, φ_r is the regularization of φ, φ_m is the minimization of the φ and γ is the Lagrange multiplier.

To solve this problem, φ_r is minimized while φ_m is maintained at an upper limit selected by the user. All the results generated below these limits allow us to consider that the model is calibrated.

Formal definition of the φ (Medina et al., 2001; Carrera et al., 2005) in this research is written in Eq 4-14.

$$\begin{aligned}\varphi = \mu_j \sum_{i=1}^{PP}\sum_{t=1}^{n}(P_{ti} - P_{ti}^*)V_p^{-1}(P_{ti} - P_{ti}^*) + w_h \sum_{i=1}^{OP}\sum_{t=1}^{n}(h_{ti} - h_{ti}^*)V_h^{-1}(h_{ti} - h_{ti}^*),\\ Constraint\ P_j^l \leq P_j \leq P_j^u,\end{aligned} \tag{4-14}$$

where, i is the number of observation points (OP), t is the observed time interval, h^* is the hydraulic head vector at the OP, h is the simulated hydraulic head vector, μ is the associated weight, P is the parameter to estimate, p^* is the prior estimate of PP values, V is the covariance matrix, w_h is the observations weights which has a value of one in our case, l and u are the lower and upper parameters limits and j is a node of PP.

In the Minimization of φ, was used *GLMA* algorithm (Gauss-Levenberg-Marquardt). This search algorithm linearize state variables dependencies in model parameters, imposing at the same time a change on p^k in every iteration (Eq. 4-15) (Finsterle & Zhang, 2011; Yao & Guo, 2014).

$$(H^k + \delta^k I) \triangle P^k = -g^k, \tag{4-15}$$

here, H^k represents an approximation of Hessian matrix of φ. g^k is the gradient in the model parameter's vector in k iteration, I is the identity matrix and δ^k is the Marquardt parameter.

After each iteration, the model parameter's vector is updated. Before consolidating this step, it is checked if the vector parameters components by iteration meet the assigned upper limit (Doherty, 2004). This process is iterative until: 1.) if $i \leq 0.0001$, where i is the φ value at the end of the optimization iteration i-th, 2.) when the number of iteration reaches 30, it is set as the maximum number of optimization iterations, 3.) if $\frac{\varphi_i - \varphi_{min}}{\varphi_i} \leq 0.1$, where φ_{min} it is the lowest φ reached so far.

Although the only guarantee of minimizing the objective function is to obtain a value of cero, it is also valid to analyze the convergence of the parameters to their optimum values. Thus, number 1 has been selected as the convergence control for this model. This convergence control was selected because allow to analyze the objective function itself behavior, showing whether there is a reduction in several successive iterations. That is, if the iterations are producing changes below the set value, there is probably little to gain by continuing with the optimizer execution.

In models with lack of information, sensitivity analyzes based on a plausible range of values or observations for calibration are the only way to restrict a parameter. It is proposed in this model to adopt for the statistical analysis the methodology by Alcolea et al. (2006a) that assess maximum likelihood equation's minimization (Eq. 4-16) using different weight values, in order to evaluate the model's results.

$$S = N + Ln(H) + NLn(\frac{\varphi}{N}) - \sum_j n_i Ln(w_i) - \sum_j k_i Ln(\mu_i), \tag{4-16}$$

here, N is the total number of data, n_i and k_i are the number of state variable and H is the first order approximation of Hessian matrix of φ at the optimization process end.

4.3. Model Development

4.3.1. Geological Model

MMV basin geology has been described by Gómez et al. (2003); Morales (1958); Sarmiento-Rojas (2011). This geological basin represents a depression that contains sedimentary formations deposited from the Cretaceous, emplaced in a Jurassic igneous and metamorphic basement. The tectonic evolution of the basin has been proposed by Cooper et al. (1995). The Jurassic crystalline basement is composed of intrusive igneous and associated metamorphic rocks consisting for the most part of Segovia Batolite.

Cretaceous sedimentary rocks were formed in a rift system during the Mesozoic in consequence to back-arc extension and marine transgression, in order to that in the basin were deposited a sequence of mostly shales, limestones, and chert beds (Luna and Umir Formations). Late Cretaceous–early Paleocene tectonic inversion from extensional to compressive regime marks a significant change in depositional environments from marine to continental in the incipient foreland basin (Lisama Formation).

Marine transgression occurred during the Oligocene epoch, during which the MMV area was flooded. The sediments laid down in these waters are known as La Paz, Esmeraldas, Mugrosa, and Colorado Formations, but except for their connate water, they are essentially of continental facies (Morales, 1958). Changes in plate tectonic motion documented in the late Oligocene to early Miocene causes by the reactivation of the middle Eocene structures created an upper Miocene unconformity. During this deformation phase, the Eastern Cordillera was uplifted and eroded, erosional deposits in MMV are lithic fluvial sands derived from the Central Cordillera dominate (Real Group) (Gómez et al., 2005). Major deformation of the Eastern Cordillera and Llanos Foothills began at approximately 10.5 millions of years (Late Miocene) and resulted from Panama's collision with Nazca plate (Cooper et al., 1995). The Pliocene Mesa Group rests conformably upon the Real Group and is reportedly composed of massive conglomerates, cross-bedded lithic sandstones, and mudstone layers; this unit is 575 m thick (Morales, 1958).

Result of this geological background, the MMV area is tilted towards the East, having a monoclinal structure, disturbed by some folds and faults (Servicio Geológico Colombiano, 2014). At this basin, clastic sediments of alluvial type, and sedimentary rocks of Quaternary and Tertiary age developed. The main characteristic of this material is the low consolidation and sediments predominance such as sand and gravel, interspersed with fine-grained materials such as clays and silt. In the MMV basin, groundwater is extracted from units that function as an aquifer. These units are recent alluvial and terrace deposits that emerge

in the Magdalena River proximity with an average productive thickness of 150 m (Gallego et al., 2015), whose origin is associated with Magdalena river, the Mesa formation and Real group, and unconsolidated sediments (sandstones and conglomerates).

The underlying rock represented at the East limit is used as a vertical and lateral no-slip boundary condition for every aquifer formation, which is not continuous through the whole domain. The following aspects were taken into account for the conceptual model integration: (*i*) the relationship between each formation material, (*ii*) homogeneity of hydraulic properties for regional scales, (*iii*) a resistivity analysis for each formation material, and (*iv*) common permeability values. At a regional scale, the geological reinterpretation of the study area led to a simpler model of hydrogeological basin. This model included depth of sedimentary formations, the Salina-Buitima fault, and every main fold. In addition, interpolation algorithms were used including secondary information from seismic and magnetotellurics studies, superficial geological interpretations, and stratigraphic from drilling well. In the end, seven layers resulted from this exercise, each one separated from the other by lithological contacts or erosive surfaces. Near-surface formations are considered the most important given the current water resource exploitation from those aquifers.

The model had been constructed by geological interpretation and analysis of spatial distributions of the formations and include major fault Buitama-Salina fault zone. Owing to confidentiality of information by oil companies, this work only uses public information. Base information has been collected by previous studies such as surface geology, geological maps scale 1:100 000 (Figure **4-2**) that have been development by the Colombian Geological Service (SGC), model area are cover by eight maps (Beltrán & Quintero, 2008; Beltrán et al., 2014; Gavidia et al., 2008; Ward et al., 1977). Each of these maps is accompanied by an interpreted geological cross-section (Figure **4-3**). Balanced geological cross-sections have been proposed by Moreno et al. (2013) in order to analyze the geometry of the Nuevo Mundo Synclinal and The Opon oilfield. The Nuevo Mundo Syncline is located at north-east part of study area. La Salina Fault bounding the western margin of the syncline and separates the Cenozoic strata from Cretaceous outcrop of the Eastern cordillera. In this work, three balanced sections of Moreno et al. (2013) are included in order to have subsurface information on the Guayabito fault, the Guayabito syncline, and the Armas syncline.

Magnetotelluric study has been carried by (INGENIERIA GEOTEC, 2016), as a result they proposed six geological-geophysics profile that were collected in the north part of the study area, these interpreted profiles show the interaction between Dos Hermanos fault and distribution of Quaternary deposits, Mesa formation and Real Group.

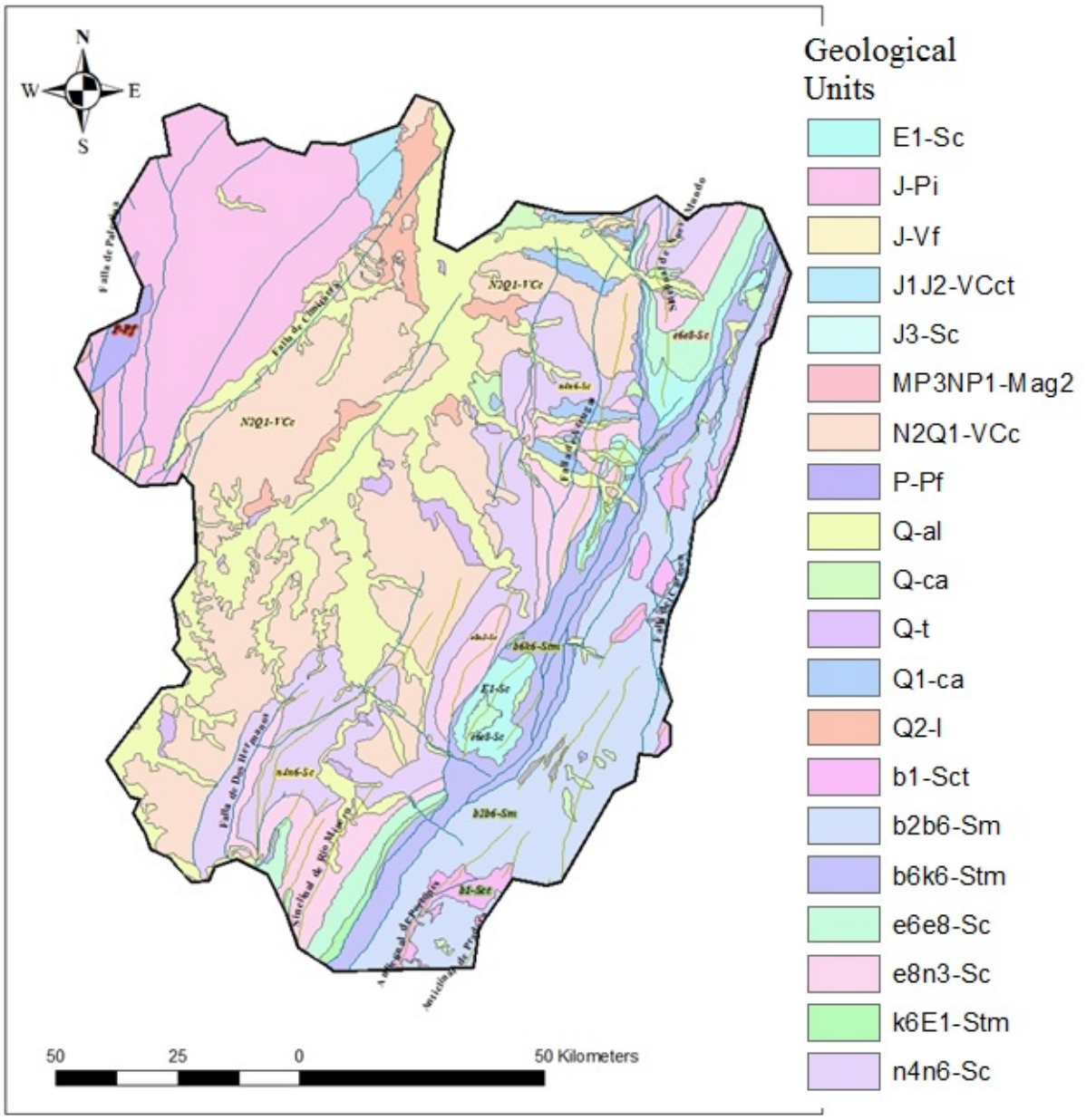

Figure **4-2**.: Geological map, scale 1:500 000. Source: SGC & MINMINAS (2016)

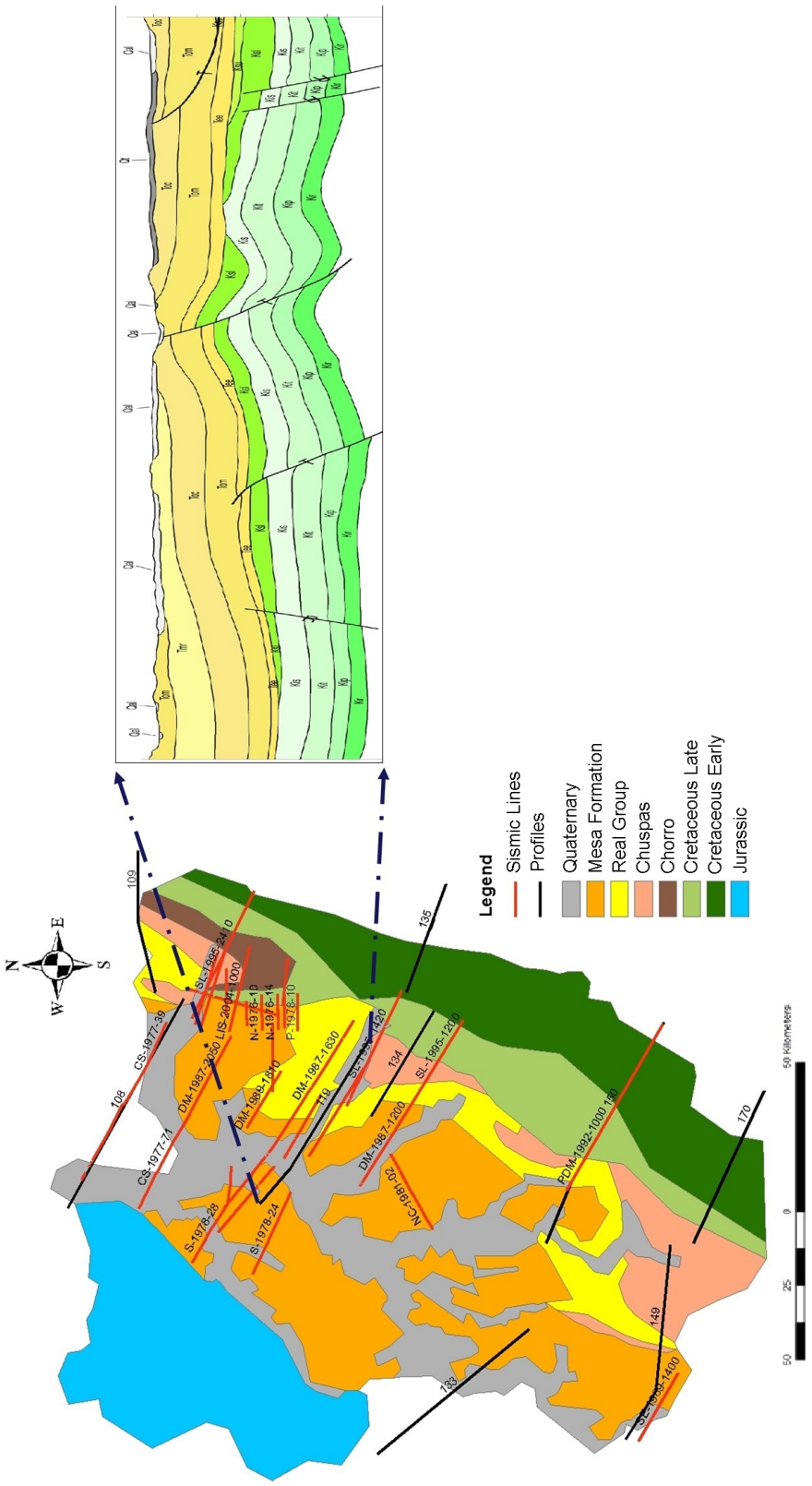

Figure **4–3**.: Simplified geological map and cross section available: 18 seismic lines, 17 interpreted and 6 magnetotelluric profiles and example of data interpreted cross-section from geology map N. 119.

Seismic surveys and stratigraphic well data were obtained by the Seismic Atlas of Colombia (Cediel et al., 1998) and from the seismic interpretation on oilfields Lisama, Tesoro, Nutria and Peroles (Ortiz et al., 2009). As a result 19 seismic lines were collected, in order to integrate the seismic lines with cross-section and geological map, the time-depth conversion was carried out using the velocity plot corresponding to the sonic log of 6 soundings in the area (Romero et al., 2015). To estimate depth in seismic lines it was used the quadratic function described in Eq. 4-17.

$$y = 0.00096v^2 + 1.9v + 41, \tag{4-17}$$

where, y is the depth in meters and v is the velocity (m/s).

Seismic lines are useful for estimating geometrical, dips, major structures, discontinuities, erosional surfaces and faults zones (Figure **4-4**). In order to simplify the model, units were combined that can represent homogeneous properties on a regional scale, these units are divided by major surfaces such as unconformities and lithology. This division from younger to older: Mesa formation, Real group, Chuspas Group, Lisama formation and Late Cretaceous, Early Cretaceous, and Jurassic Basement. Seven layers were created, and the division of rocks units correspond by lithological contacts or erosional surfaces, considering that shallow formations have more hydrogeological importance due to its current exploitation. With the intention of simplified model, faults were represented by folds using the dip separation and true displacement of the strata.

4.3.2. Hydrogeological Conceptual Model

Figure **4-5** represents the conceptual application model area. The zone is limited to the East and West by the limits of VMM aquifer system that acts as an impermeable boundary due to its igneous-metamorphic nature (Ideam, 2014). The South and North limits of model act as an inflow and outflow, respectively, in the different zone sections. The groundwater flow was estimated by Darcy's law (Karay & Hajnal, 2015; Şen, 2015) using piezometric data. The elevation in the focus zone descends smoothly in south-north direction, conserving the properties of an alluvial valley and, therefore, provoking a regional movement of groundwater throughout this depression (Ingrain, 2012). Additionally, there is a register of low scale domestic and industrial use of groundwater collection obtained with pumping equipment (Gonzalez et al., 2010). Most recharge of groundwater occurs at the mountain ranges, from rainfall infiltration, and at the low-lands, from channel drainage losses.

Figure 4-4.: Geological Model. The model had been constructed by geological interpretation and analysis of spatial distributions of formations. Source: Arenas-Bautista et al. (2018c).

The region presents high temperatures, especially during the dry season, which causes a loss of water in the form of evapotranspiration (Asociacion Colombiana del Petroleo, 2008).

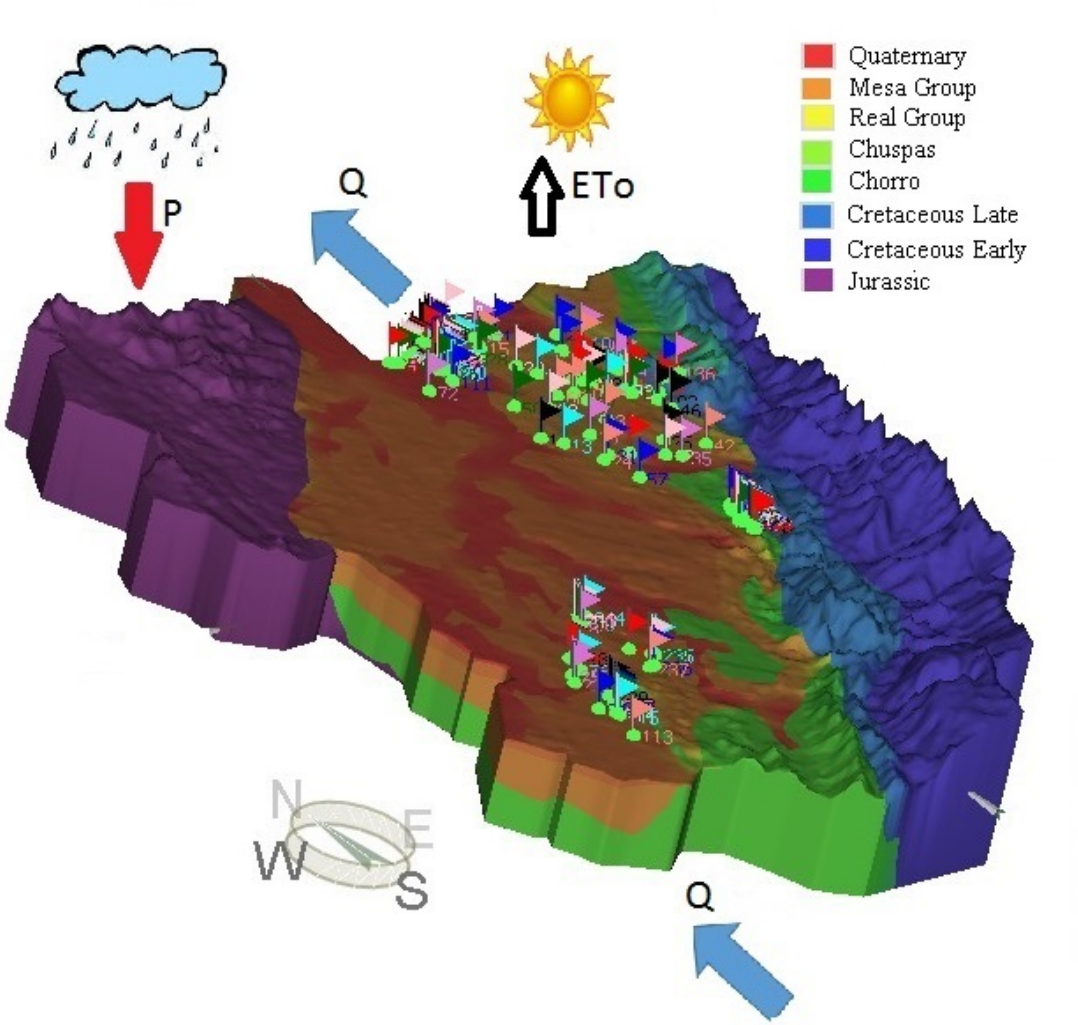

Figure **4-5**.: Hydrogeological Conceptual Model. P is the precipitation, Q represents the flow, and ET_o is the evapotranspiration.

The geostatistical model was defined by the transmissivity variogram in the model domain. The soil texture details for different depth profiles were available from well-logs. This data was used to establish the initial values of different hydraulic parameters in each hydrogeological zone, (Freeze & Cherry, 1979). The K values obtained vary between 10^{-5} to 35 $m\ day^{-1}$. It was defined 167 observation points based on piezometric levels (Figure **4-6**) because of values recorded in piezometers were not continuous in twelve years of analysis, an average data level was used as a reference in the numerical model in steady-state. For transient state, a measurement grouping by month was made. This grouping assumes that levels in the same months of different years, exhibit a similar behavior due to results of the

hydrological analysis. Finally, a series of monthly data was consolidated for an average year. The extraction data comes from 78 independent pumping tests in the wells where information was found within the model domain (Figure **4-6**). Pumping rates range between 10^{-2} m^3/day and 250 m^3/day (Annex 1).

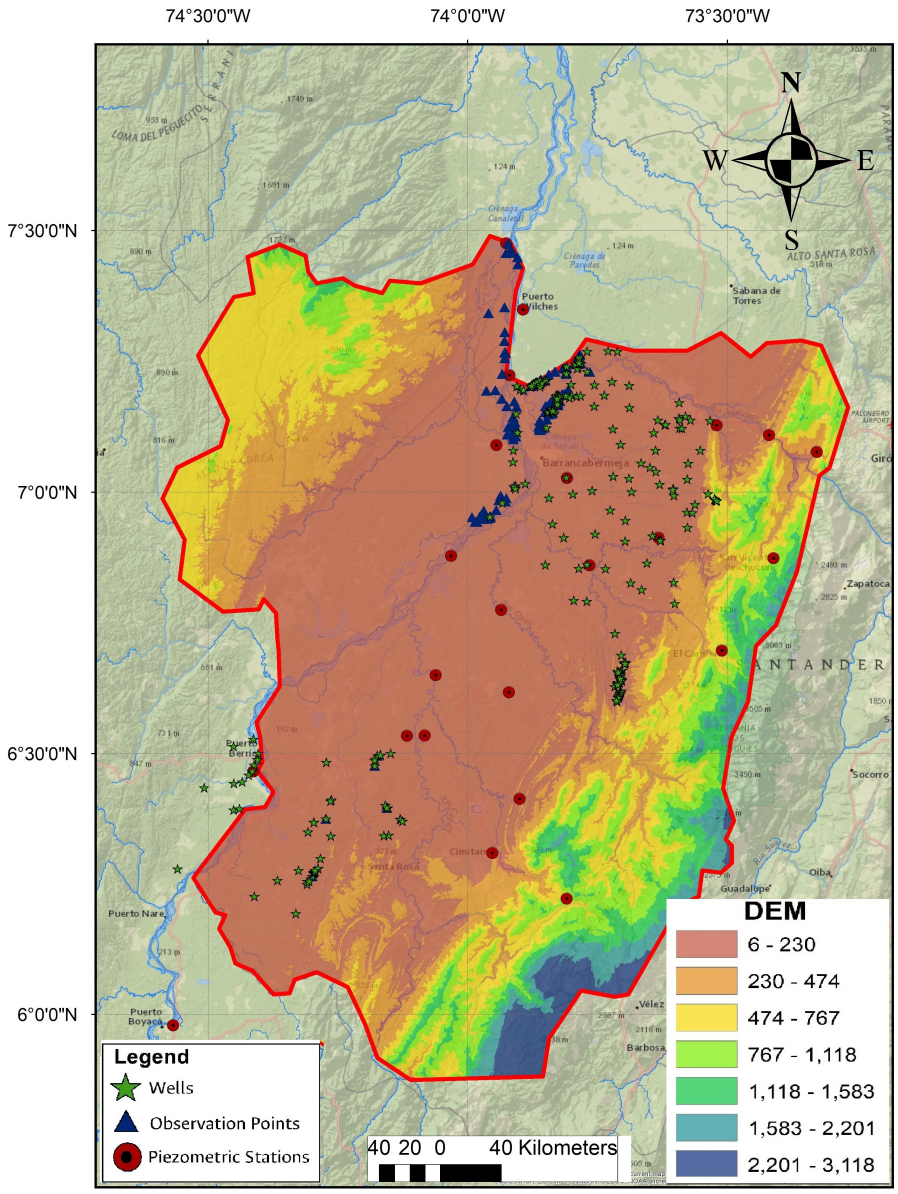

Figure **4-6**.: Locations of piezometric levels (red points), Limnimetric stations (blue triangles), and Wells (green stars).

The hydraulic properties of the aquifer system make possible to identify areas with primary and secondary porosity and characterize them as units able to store and transmit water with relative ease. The horizontal (x axis) permeability is an order of magnitude higher than the vertical (Han & Cao, 2018; Xie et al., 2006). The system total porosity ranges between 25% and 3%, with an average specific yield of around 14%. The test holes pumping results and the lithological analysis allow us to conclude that the hydraulic conductivity varies from 20 $m\ day^{-1}$ to 0.1 $m\ day^{-1}$.

4.3.3. Numerical Implementation

The objective of this chapter is to identify the variability of K in a real case regional flow model with respect to the number of PP and analyze whether plausibility contributes to the identification of heterogeneity in the model. The results are explored within the conception of a regional flow model that presents high soil hydraulic and temporal-space parameter variability, and hydrometeorological characteristics conditioned to the presence of the Inter-Tropical Confluence Zone (ITCZ).

The information was consolidated on a spatial scale of 6 km x 6 km resulting from hydrological modeling. The recharge is assigned as a material associated property, which becomes variable in time for transient model. The loading boundary conditions (Figure **4-7**) were assigned as a first type variable Dirichlet condition in south and north edges from the model domain, according to water level historical records. For the seven consolidated rivers in the model domain a Cauchy boundary condition was applied. This requires the hydraulic conductance of the riverbed material and its geometry procurement, which were obtained establishing the initial conductivity from the pumping tests and the cross section geometry, supplied by the limnmetric stations in the area. The East and West model limits were conditioned by the application of Neumann boundary conditions; given they are considered as a watershed. The inlet and outlet flow sections and the model domain flow were identified using piezometric water level contours, and applying Darcy's law. Finally, pumping wells were assigned as a well edge condition where a defined extraction was applied to a node.

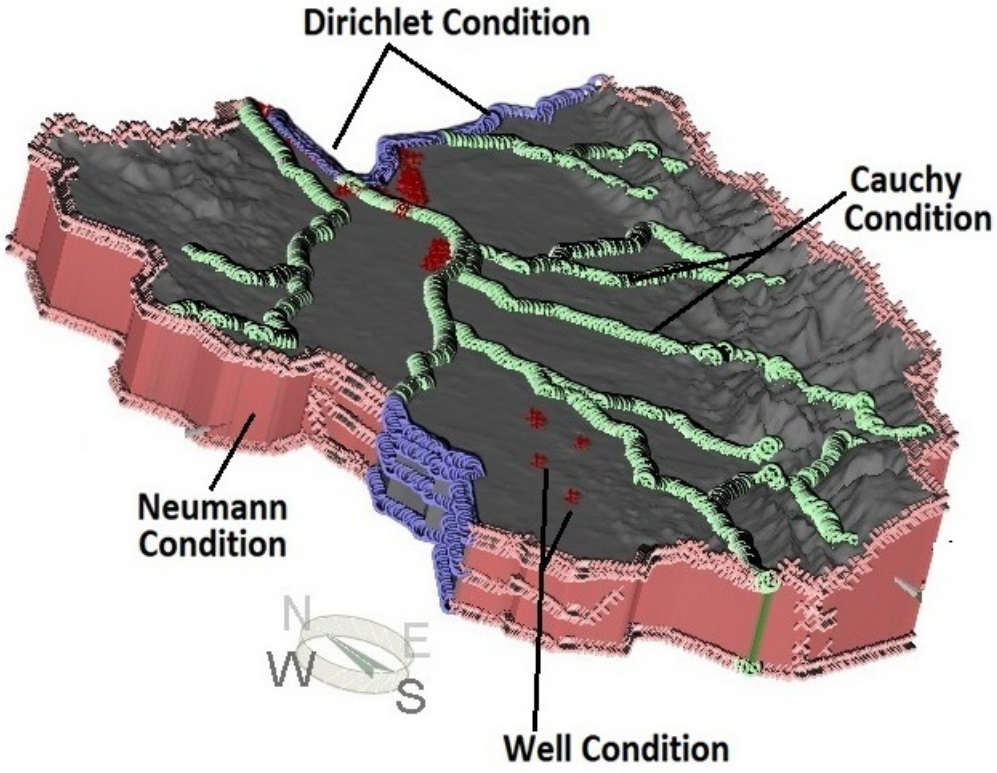

Figure **4-7**.: Boundary conditions used in the hydrogeological Conceptual Model. Source: Donado et al. (2018)

For *CZ* application a pattern on materials disposition according to the hydrogeological units was defined (Figure **4-8**-A). In the *PP* technique, it was observed that it was not possible to obtain a defined pattern for the same materials, so the initial values for *PP* were define assuming that the hydraulic conductivity value resulting in the pump tests represents the expected. To correlate these values, the semivariogram was used with an exponential model, a range of 2000 m and a variance of 2 without nugget effect. The K values obtained vary from 10^{-5} to 35 $m\ day^{-1}$. Then, the information was spatialized via Kriging (Tsai & Yeh, 2011). This technique was used given its additional use for regularization processes, which are based on the same variogram used for regionalization (Tsai, 2006; Kashyap & Vakkalagadda, 2009; Janetti et al., 2010; Riva et al., 2009). For the development of this model, each layer was treated as a single zone and tested with a variable number of *PP* to evaluate the response model. The principle of parsimony dictates that the numbers of parameters involved in an estimation process must be kept to a minimum (Merritt et al., 2005; Tonkin et al., 2007; Golmohammadi et al., 2015). However, when *PP* is used in conjunction with regularization, this number tends to increase (Panzeri et al., 2012). In the regularization process, the assignment by preferred value was used to restrict the variation of parameter value depending

on the limits established by pump tests in the geological units. This method was combined with the use of the covariance matrix to find a base that represented the data optimally.

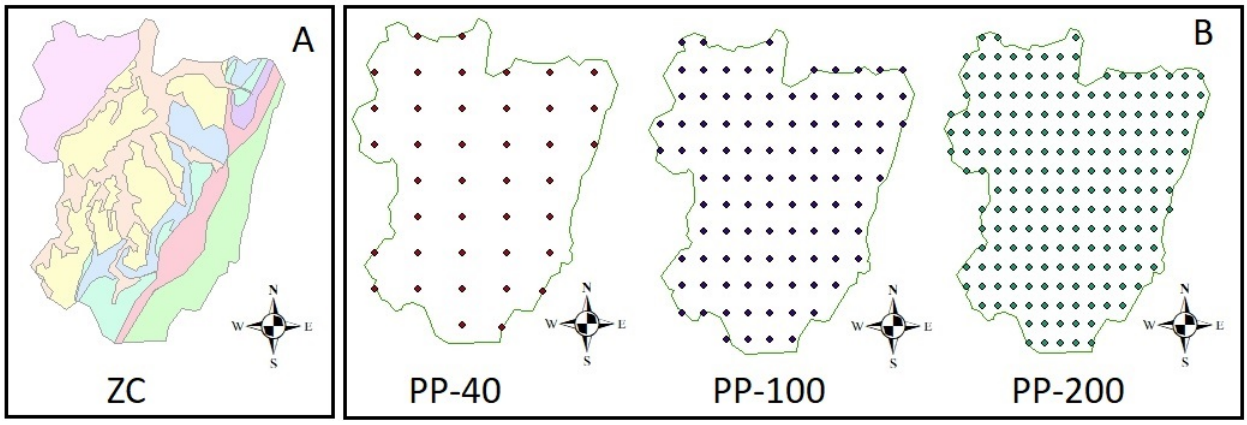

Figure **4-8**.: A-. Definition of geological units for *CZ*. B-. location of the *PP* according to the number of points.

In the model development, 40 *PP*, 100 *PP*, and 200 *PP* were randomly generated with a uniform distribution throughout the model domain (figure **4-8**-B). The fundamental principle of this constraint is to prefer homogenous distributions of parameters whose values show as small a deviation as possible from those expected. In a geological context, a PP should preferably have a similar value to its neighbors within a certain distance. This distance and the strength of correlation are defined through a semi-variogram. In this research, due to the study area does not have sufficient and reliable data throughout the domain, and the available data are pooled in small areas of the study area, was decided to generate the PPs with uniform distribution. The model ran 50 times, and in each run the PPs were distributed so that their locations were different (x, y, z), but the space between them was constant. It means that a rectangular pattern was used for every run, but the PP locations changed after every run, always keeping the same pattern. The random location of PPs with a uniform distribution allowed to represent without bias the locations that had no field measurements in the calibration process and the post-calibration analysis identified the parameter contributions to the uncertainty. To corroborate the calibration process results, an uncertainty analysis consisting of two phases was performed. The first phase consisted of a basic analysis where the model error was estimated computing the *RMSE*, the Pearson coefficient and *MAE*. In the second phase, the goal was to analyze how the plausibility would improve the identification of heterogeneity of K and, if it would be sensitive to the number of *PP*, plausibility was evaluated by computing the S factor, obtained from μ values between 10^{-3} and 10^{2}.

Additionally, nine experiments were performed, responding to regularization method changes

and the *PPs* numbers used in the initial model proposed. Then, to the best response to each variation, six adjustments were made for changing the ponderation factor μ in order to explore the plausibility term influence. The μ values oscillated between 10^{-3} and 10^{2}, taking into account that the optimal value for μ must be equal to one on an error-free geostatistical model.

4.4. Results and Discussions

4.4.1. *CZ* and *PP*

The two models calibration (*CZ* and *PP*) is compared briefly in their value parameters, model fit and predictions. This comparison focuses on model ability to simulate the real system and to show conceptual differences. The model residuals respect to the observation points allows us to infer that model calibration allows to adequately represent the assumptions presented in the conceptual model, both in the *CZ* and in the *PP* technique (Figure **4-9**-A).

The average residual differences in *PP* results is lower than 1 m. the *CZ* technique exhibits oddment points between 1 and 3 m. The possible reason for these mayor differences, would be associated with the large number of wells in this region, which pumps extensively the groundwater. Therefore, the possibility of an occasional partial inflow across the study area boundaries, especially on the eastern and western boundaries, could not be well represented by the input/output flow limits conditions. The error obtained in the observation points is summarized in Table **4-1**.

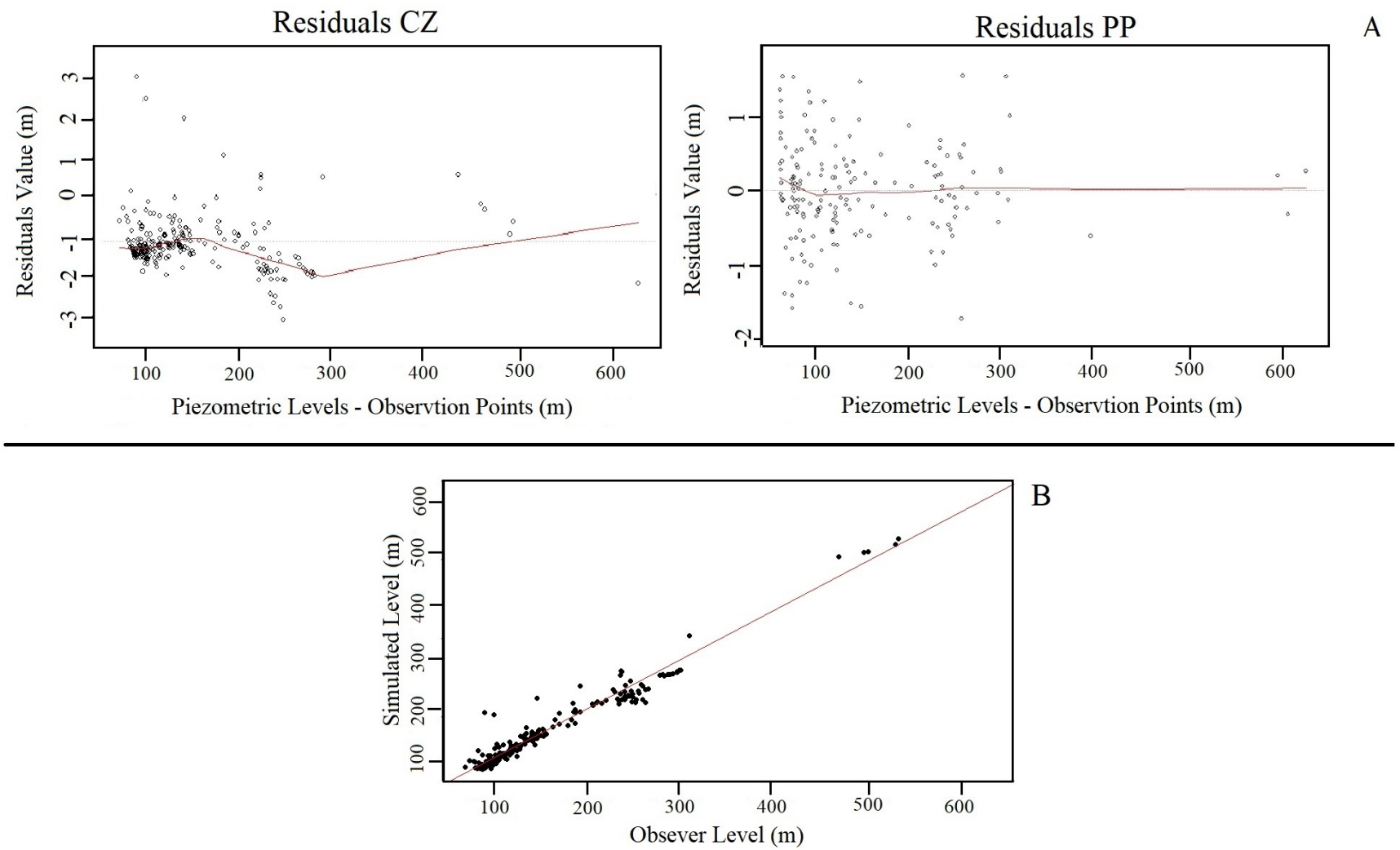

Figure **4-9**.: The conceptual model results from the residual values of the numerical model. A-. Shows the model residuals respect to observation points in the *CZ* and *PP* techniques. The red lines represents the mean. B-. Shows the result of a graphical fitting of observed and simulated heads at the observation points with $R^2 = 0.93$.

Table **4-1**.: Description of the experiments evaluated and results of the statistical metrics.

Experiment	Description	φ_m	φ_r	ϕ	MAE	$RMSE$	R^2
CZ	geological units	145.4	178.6	323.9	0.25	0.93	1
PP	40 PP	114.3	159.4	273.6	0.25	0.81	1

These results include R^2, MAE and $RMSE$. The value of R^2 for the calibration model is 0.99; likewise, MAE, which is an efficiency of calibration indicator, is 0.25. Figure **4-9**-B allows to evidence optimal simulation results, as the observation values are adequately represented under the numerical model assumptions, and the Figure **4-10** presents the results of transient-state calibration. The hydrographs of simulated versus observed heads over time show a relatively good match between observed and simulated heads, even if the model tends to overestimate the piezometric levels. The general behavior of PP technique offers average values of 142 m in the OF. However, the results obtained in CZ show a variation of 6 m above the results with respect to values obtained from PP. These results are in agreement with the findings of Alcolea et al. (2006a) where it is concluded that the PP technique offers better results for the analysis of heterogeneity.

The hydraulic conductivity analysis (Figure **4-11**) in the model shows that in the Quaternary, the average K_x values in CZ is different from the average PP values. This occurs because of the ignorance of hydraulic properties of outcrop geological units in the zone. The most information and monitoring compiled for this model has an 80 m depth (for mesa formation and real group); because of this, the model representation fits with higher certainty to reality. In the seven model units remaining, the K_x values assignment does not represent a direct link either with CZ nor PP. This is due to the ignorance of depths of hydraulic properties higher than 600 m. Additionally, the scarce available information is focused on specific influence areas, which gives another struggle for its representation. Finally, results show that in lower model units there can be generated equifinality issues when the same model performance with a different parameter for the same node is generated.

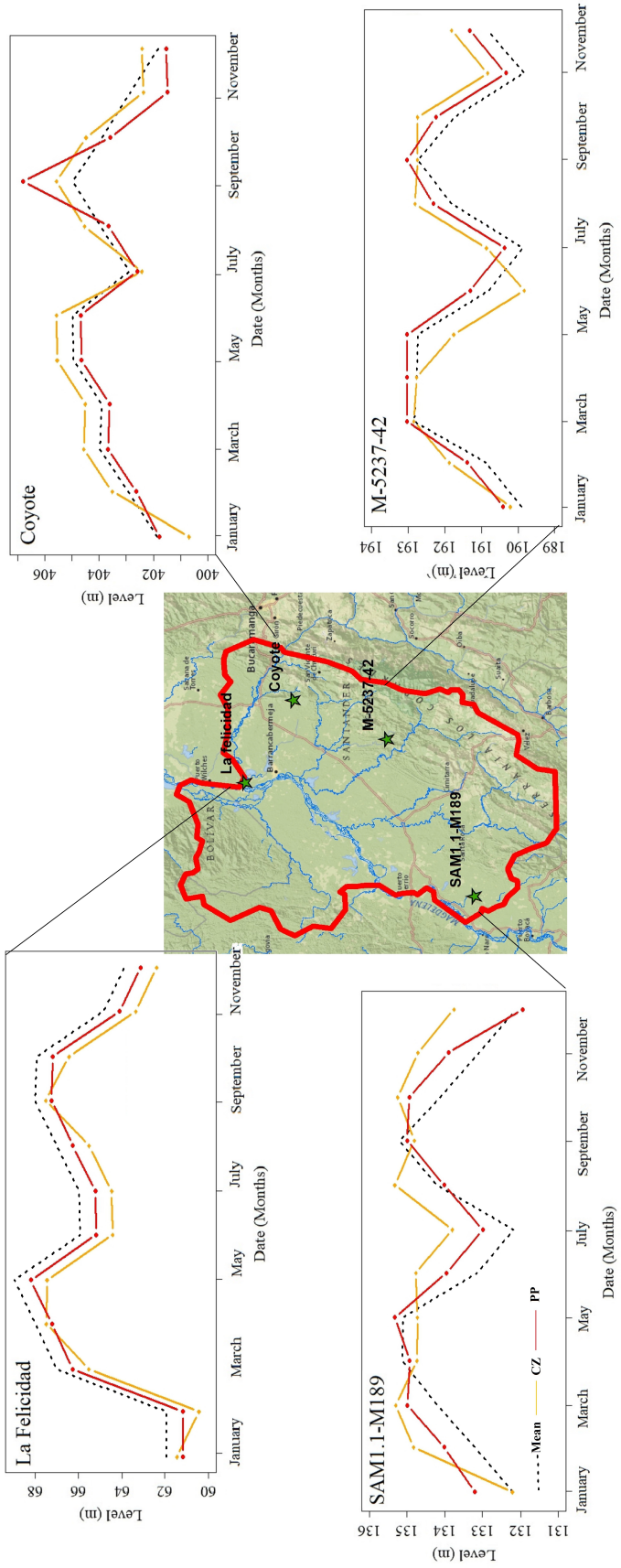

Figure **4-10**.: Result of observed and simulated levels in the model for transient state. The results are shown for four wells (green stars) because these are the most representative in the area and have consolidated information over time. These wells are: Felicidad, Coyote, SAM1.1 and M-5237.

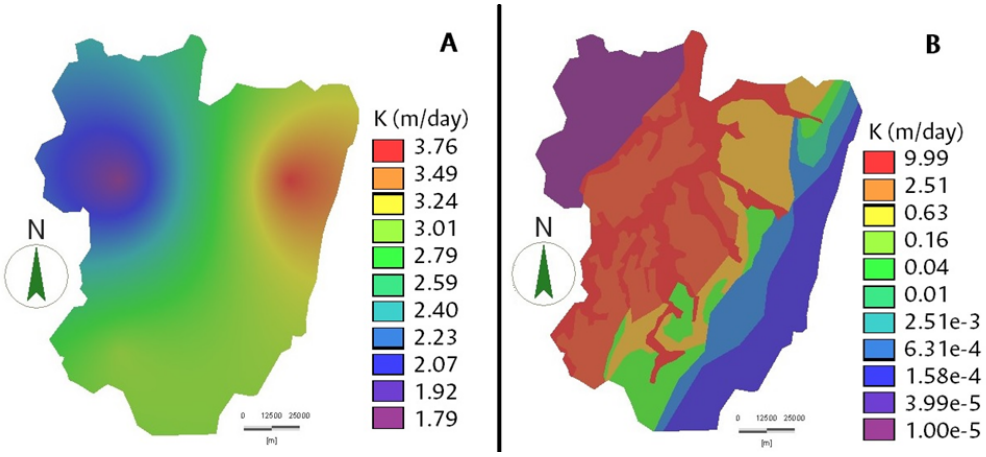

Figure **4-11**.: Result of K in the proposed hydrogeological model. A-. The model development with PP. B-. The model development with CZ.

Additionally, is evident a strong separation of the Quaternary aquifer and Mesa formation with values of 10 $m\ day^{-1}$ and 2.5 $m\ day^{-1}$ respectively. The PP calibration process presents a K three times higher than the CZ model. In general, the K values for all hydrogeological units are within the reported range in literature. Comparing the two methods evaluated through the CZ and PP, they show similar model characteristics: (i) The east and west regions of the model, corresponding to Jurassic and Early Cretaceous units, have a uniformly low conductivity, which corroborates the conceptual model assumption establishing those zones as water divisions, (ii) The model presents small areas of high conductivity in the north and central part and, (iii) The highest conductivity is found in Quaternary and Mesa formation. An interesting fact is that the estimated field begins to reflect some large known scale geological structures also perceived on the CZ model. The storage term does not significantly influence the hydraulic head during the one-day simulation period. Therefore, it can be concluded that K is the only definitive parameter in hydraulic head modeling.

In summary, compared to the previous CZ technique, PP approach is not only able to provide satisfactory matches for all measured heads and reproduce large-scale and local features of the measured groundwater level, but it can also extract more information of heterogeneity at several scales using the same amount of measured information. All the results shown above indicate that PP approach provides a more realistic model to simulate river-groundwater interactions based on parameters. Takin into account the parameters calibrated in both techniques the ratio between the horizontal and vertical hydraulic conductivity is at the center of its range with a value of around 0.1. Therefore, the vertical flow in the aquifer is ten times slower than the horizontal flow that coincides with the regional dips (sub-horizontal layers).

4.4.2. Regularization Methods

The φ_m behavior was evaluated for simulations in a transient state (Figure **4-12**) for the *PP* set in each applied regularization. This plot shows that, in general, 200 *PP* technic offers a better φ_m value with respect to 40 *PP*. The SVD method does not show improvement in φ_m value reduction since stabilized after the third interaction. SVD general behavior in all *PP* experiments is notably alike, showing average φ_m values of 115 m. The difference between Tikhonov and SVD-assist method application is focused on the number of interactions for φ_m stabilization. The Tikhonov method allows to make evident a lower φ_m value when 200 *PP* are used. These results are in accordance with the findings by Alcolea et al. (2006b), where it is concluded that within a bigger number of *PP* better φ_m results will be obtained. SVD-assist method analysis also reports a better model performance using 200 *PP*.

The "lever" for how well SVD does regularization is the number of singular values used (equal to the number of "super parameters"). This is chosen implicitly using the FEPEST EIGTHRESH variable. Therefore EIGTHRESH was probably set to $5x10^{-7}$ by FEPEST (Doherty, 2003). This is suggested as the lowest possible value to stop over-fitting where noise is strictly numerical (i.e. measurement noise is not taken into account). The model does SVD only once and then defines super parameters on the basis of this. This is not optimal because model nonlinearity may alter the optimal definition of super parameters as parameter change; however, it is convenient. The error obtained in the observation points is summarized in Table **4-2**.

Table **4-2**.: Description of the experiments evaluated and results of the statistical metrics.

Experiment	Method	φ_m	φ_r	ϕ	S	MAE	$RMSE$
40 PP	SVD	114.3	159.4	273.7	28.4	0.251	0.827
	Tikhonov	109.9	104.9	214.8	27.52	0.189	0.658
	SVD-assist	109.6	18.97	128.6	22.04	0.136	0.457
100 PP	SVD	72.31	273.5	345.8	28.82	0.26	0.81
	Tikhonov	62.95	234.7	297.6	28.27	0.209	0.613
	SVD-assist	57.61	61.41	119	23.73	0.141	0.412
200 PP	SVD	34.93	206.4	241.3	27.52	0.267	0.811
	Tikhonov	28.35	150	178.4	26.39	0.196	0.587
	SVD-assist	20.27	41.49	61.76	23.44	0.121	0.356

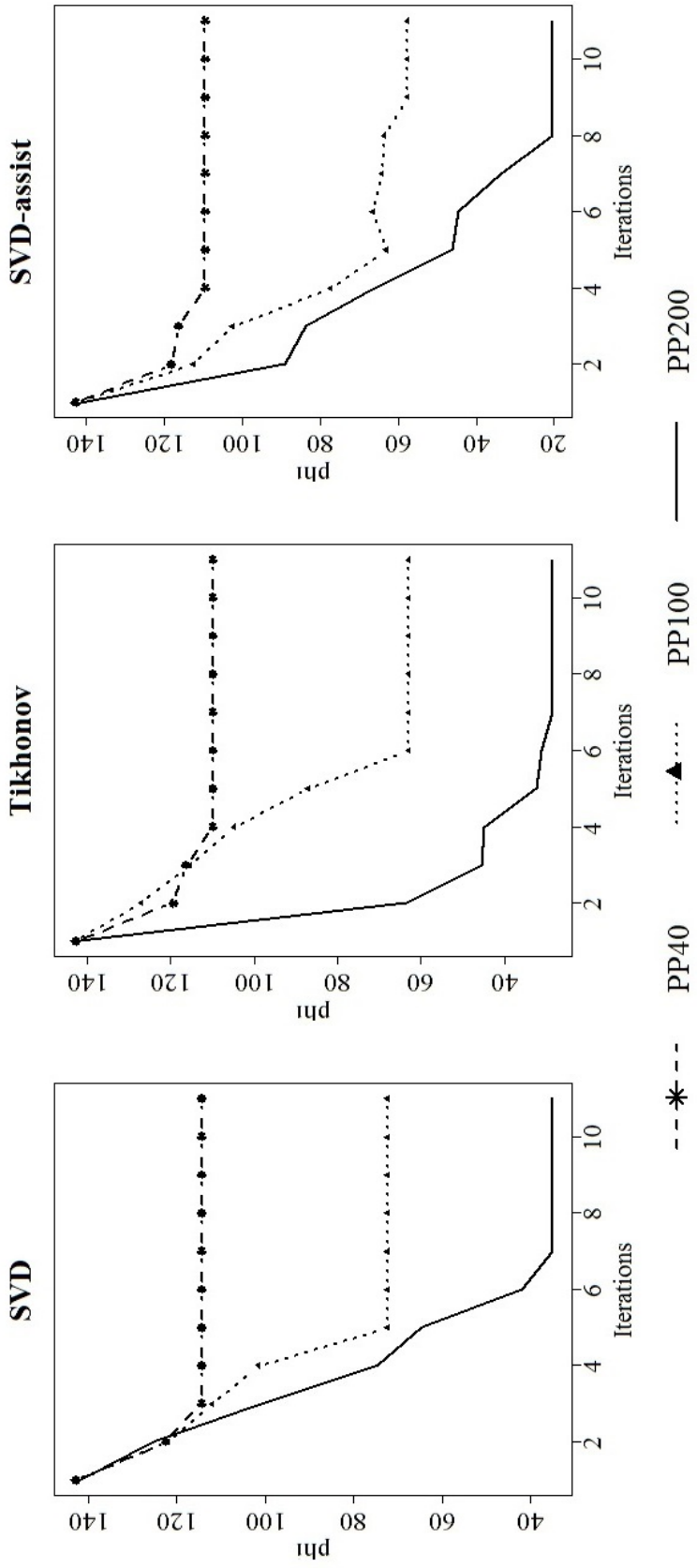

Figure **4-12**.: Model performance for regularization used under transient state conditions. This figure compares the number of iterations needed in each regularization to achieve the best value of φ_r

A further results review can be achieved through the boxplot analysis for each geological unit (Figure **4-13**). In the Quaternary, among *PP* models the range values are really close whatsoever. The most information available for the present model has an 80 m average depth (for Mesa formation and Real group), thus, the model representation fits with higher certainty to reality in this depth. However, the influence of observed data spatial configuration is unknown, and it could lead to different inverse problem results and model performance, but this subject is out of the scope of this research. In the seven remaining model units, the K_y values assignment does not represent a direct link with different *PP* quantities. This is due to the ignorance of hydraulic properties at depths greater than 600 m. Additionally, the scarce available information is focused on specific influence areas, which results in another struggle for its representation. Finally, the results show that in the deep unit model equifinality problems can be generated when the same model performance is generated with a different value of a parameter in the same node.

Following those reasons, it is not enough to evaluate φ_m to conclude which is the best method. As an additional tool of evaluation, φ_r and S were also calculated (Table **4-3**) for the *PP* experiments. The lower value of φ_r for all the experiments is got by the SVD-assited method, and the calculation of S corroborates this result. It is important to remark that all the experiments perform similarly on the likelihood function minimization, which calls into question the relationship between execution time and model's performance in the model with the least *PP*.

These results had already been reported in (Donado et al., 2018) when the Impact of the PP number was evaluated (Figure **4-14**). These characteristics correspond to the idea of maintaining a low hydraulic conductivity in the geological units that were characterized as a watershed. The model presents a limitation by not defining the limits of the geological units where surface aquifers are present. However, the model represents high conductivities in the central part of the study area. Therefore, it can be concluded from the representation of K that this parameter is important in the modeling of hydraulic heads.

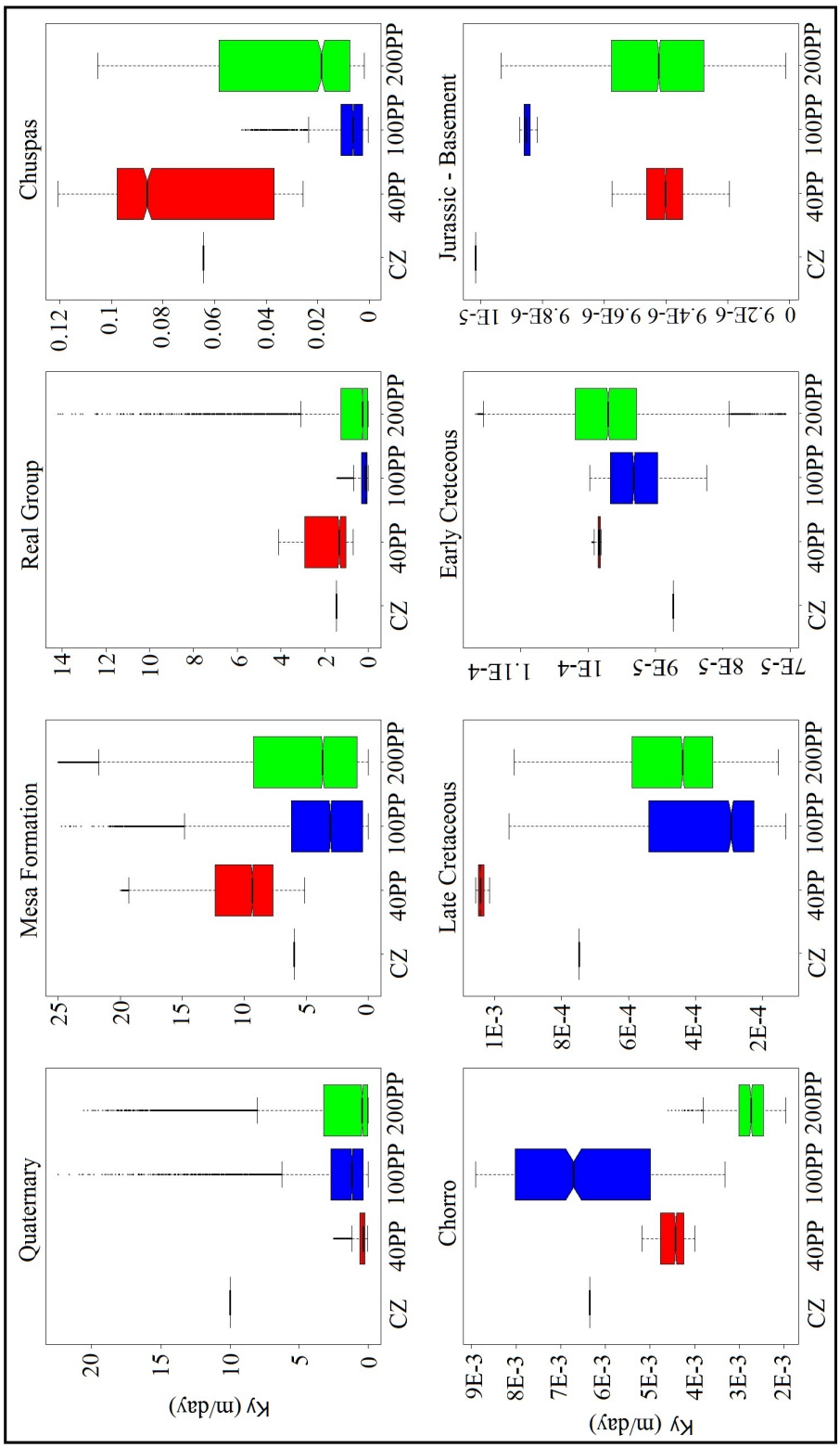

Figure **4-13**.: Box-plot for the geological units analysis in the model. The red color shows the distribution of data in different geological units using a normal distribution with 40 *PP*. The blue color shows the distribution of data in different geological units using a normal distribution with 100 *PP* and the green color shows the distribution of data in different geological units using a normal distribution with 200 *PP*. Parameters values correspond to the nodes parameters values.

Figure **4-14**.: Conductivity values estimates as of hydrogeological model applying SVD-assisted regularization methods.

4.4.3. Plausibility Effect

A sensitivity analysis of the *PP* model was performed with the variation of factor μ. Table **4-3** summarizes the total results concerning the identification of heterogeneity. The data analysis shows the ponderation factor effect μ in the consolidation of φ and the likelihood minimization. The results show that the use of lower values of μ generates constantly low values of φ. Likewise, high values of μ provoke a high error in K estimation, *i.e.*, the biggest errors are generated for values of $\mu = 10^2$ for any amount of *PP*, except for the 100 *PP* model, where the largest error is generated by $\mu = 10^{-3}$. Nevertheless, there were no restrictions in the plausibility term, and thus the estimated values in *PP* locations vary extensively, generating thicker solutions. Although this result does not constitute the optimum reply awaited, authors as (Alcolea et al., 2006b; Zhang & Burbey, 2016) obtain similar estimations and propose as solving methodology to vary the *PP* locations. Also, as expected, the use of higher values of μ generates higher values of φ (Table **4-3**). In this case, the results tends to bring about a smooth representation, because it is biased and contains little information about the real variability of the true field.

Table **4-3**.: Results of the sensitivity analysis to the weighting factor μ and to the number of pilot points.

PP	μ	φ_m	φ_r	ϕ	S	MAE_r	$RMSE_r$	MAE_h	$RMSE_h$
40	0.001	149.2	88.8	149.3	21.3	0.57	1.51	0.24	0.945
	0.01	**149.5**	**18.3**	**149.6**	**17.8**	**0.61**	**1.69**	**0.24**	**0.946**
	0.1	116.5	55.4	122.1	21.2	0.614	1.71	0.27	0.835
	1	109.6	18.9	128.6	22.1	0.133	0.697	0.268	0.811
	10	151.3	10.1	252.27	24.17	0.04	0.17	0.295	0.952
	100	217.5	285.9	28804	37.24	1.226	2.7	0.409	1.141
100	0.001	160.6	141.2	160.7	21.6	0.236	1.042	0.216	0.981
	0.01	**160.6**	**72.84**	**161.3**	**17.2**	**0.125**	**0.749**	**0.216**	**0.981**
	0.1	160.5	52.08	165.7	19.4	0.216	0.98	0.216	0.98
	1	57.6	61.41	119.0	23.7	0.026	0.687	0.197	0.587
	10	241.9	22.92	471.1	22.7	0.017	0.42	0.393	1.203
	100	341.1	57.67	6108	35.5	0.088	0.66	0.365	1.429
200	0.001	146.3	243.7	146.5	15.42	0.276	1.082	0.174	0.936
	0.01	63.5	102.9	16.5	0.087	0.553	0.084	0.783	0.783
	0.1	**85.1**	**117.0**	**21.9**	**0.034**	**0.64**	**0.102**	**0.806**	**0.806**
	1	41.5	61.76	23.4	0.053	0.447	0.121	0.357	0.357
	10	93.9	1080.3	26.7	0.041	0.672	0.287	0.92	0.92
	100	172.6	17426	40.1	0.196	0.911	0.35	1.008	1.008

The optimum results generated from the S criteria analysis, is obtained when $\mu = 10^{-2}$ (Table **4-3**). The analysis show that the difference of S for values between 100 *PP* and 200 *PP* is minimal, and so could be related to the random generation of the *PP*. In addition, this

results can also be due to the field transmissivity measurements location which were used to build the initial interpolation. Singh et al. (2008); Pool et al. (2015); Khaninezhad et al. (2018) demonstrated that a reduction on μ from its theoretical optimum leads to a robust solution regarding the geostatistical model.

If μ is not adequately weighted in correspondence to the real system conditions, the heterogeneity identification of the hydraulic properties fails, even reaching worse values than estimations from numerical model interpolation. However, minimization of the maximum likelihood function allows to identify if a weighted is adequate and to exclude the bias from the number of *PP* used.

Regarding the optimum number of *PP*, the error decreases when *PP* increase. Figure **4-15**-A shows error and variance decreasing in hydraulic head measurements, corroborating that the more *PP*s, the better the system representation. Figure **4-15**-B shows error and variance of measurements on the *PP*s of each model and it is evident there is no discernible differences between the 100 *PP* and 200 *PP* models. Heterogeneity identification performance increases with the *PP* number until 100 *PP* are reached but variations between 100 *PP* and 200 *PP* are depreciable (Figure **4-16**). Results from synthetic models (Alcolea et al., 2006b; Riva et al., 2010; Yoon & McKenna, 2012; Carniato et al., 2015; Jiménez et al., 2016; Klaas et al., 2017; Bao et al., 2018) also suggest that in the development of synthetic models a reduction of the objective function is evidenced as the number of *PP* increases, leading to a better relationship with the regularization data and heterogeneity identification. However, in this model and under the real conditions of the application area, although there is a significant change in the identification of heterogeneity in the use of 40 and 100 PP, the reduction of the objective function is not significant between 100 and 200 PP, and has required more time to generate the model solution.

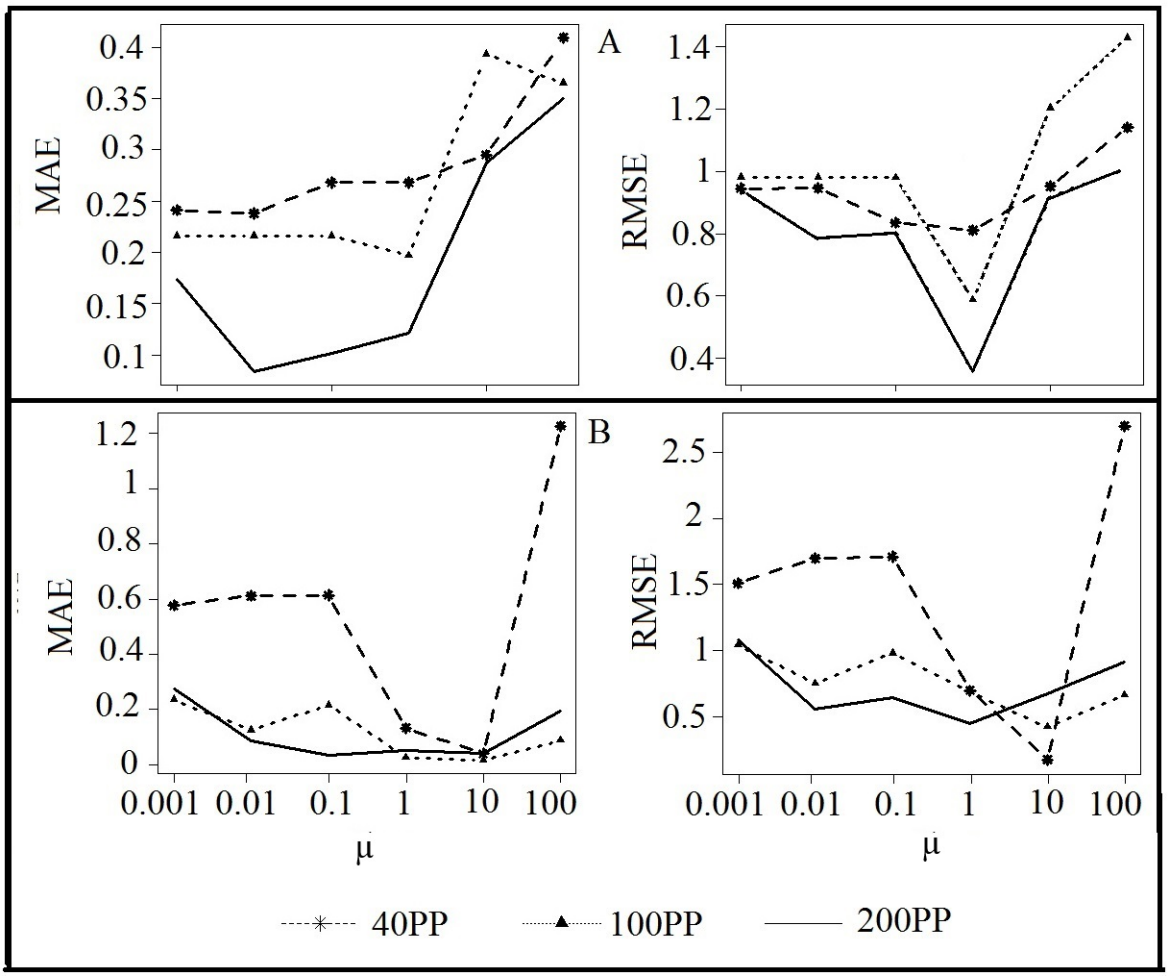

Figure **4-15**.: K estimation errors versus μ. (Left) mean absolute error. (Right) root mean square error. A-. Shows the analysis for hydraulic head and, B-. Shows the analysis for K values assigned to each PP in the model.

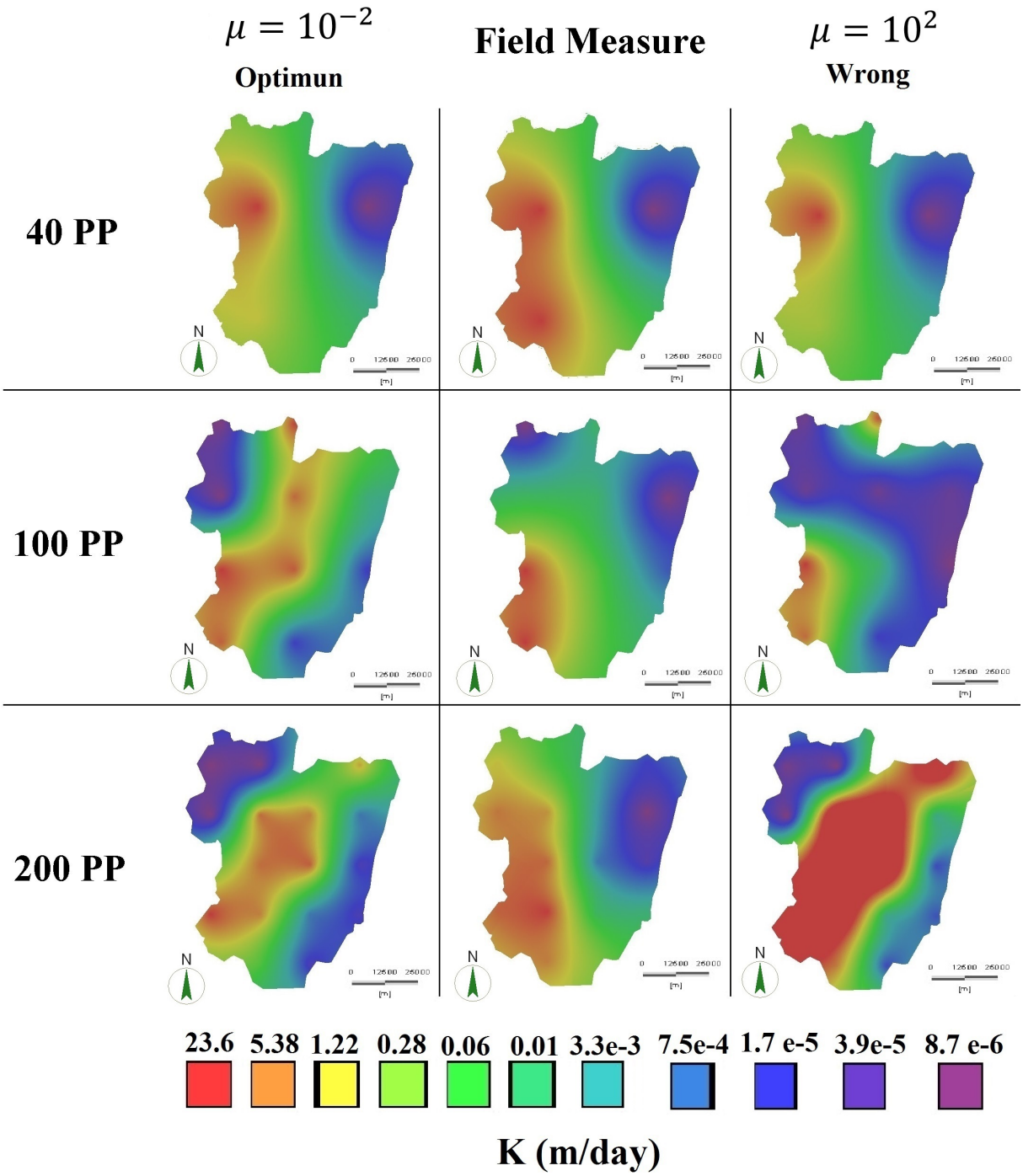

Figure **4-16**.: Qualitative comparison of spatial heterogeneity of K based on the plausibility analysis. Each row shows the $log - K$ for different PP numbers and each column shows the result when varying μ. The middle column is field generated from the field measurements and Kriging.

4.5. Conclusions

The characterization of complex groundwater systems tends to be interpreted with multiple models, but they are affected by data scarcity and limited knowledge, adding uncertainty to the model results. Therefore, the model uncertainty significantly affects the prediction of the groundwater system behavior. Given this complexity and the direct link between surface and groundwater flow, the real impact of groundwater extraction only can be accurately measured using a regional flow model. An adequate geological characterization and the proper extraction point representation and water injection, are essential for model calibration, and to provide tools for water resources administration in the study area.

The use of a highly parameterized inverse model offers a guide to estimate heterogeneity in the hydraulic conductivity as an anisotropic variable in non-confined aquifers. The application of real data as appropriated aquifer initial parameters and the inverse model restriction with parameters upper and lower limits reduces the number of necessary interactions to minimize φ, improving potential estimations and estimating possible convergence.

The results of inverse model calibration prove a better response in real system representation. The error in the hydraulic head is reduced by 3% compared with the developed conceptual model. Even though the state variable minimum square error is minimized in the observation points, the model validation evidence coherent results in the validation points. This supports the generated model solution, the model calibration through *PP* is more robust and flexible in contrast con *CZ* parameterization given its lower subjectivity, and lower representation of hydraulic properties heterogeneity.

Although the *PP* method reduces the homogeneity produced by *CZ*, it has some limitations, e.i., to overlook other sources of model error and result in an over-parameterization or equifinality. An important uncertainty of the PP method is the choice of the number and location of the *PP*s, as well as the effect it has on reducing the variability of the parameters in the model during the investment problem. Although there is no defined guideline for generating these points, the results of this article indicate that better results can be obtained using a uniform pattern, reducing the spaces between them which is useful to correlate the hydraulic properties as a guide for the separation distance. In the same way, the interpolated fields of K resulting from the application of the PP method function properly for the estimation of the flow at the regional scale; however, it can lead to significant limitations for other applications, such as solute transport modeling.

The use of a focused methodology in the parameters estimation through *PP* technique in accordance with a highly parameterized inverse model offers a guide to estimate heterogeneity

in hydraulic anisotrophic conductivity in non-confined aquifers. The application of real data as appropriated aquifer initial parameters and the inverse model restriction with parameters upper and lower limits reduces the number of necessary iterations to minimize φ.

The sensitivity analysis shows that K is the most influent hydraulic parameter in comparison with η and S_s. Nevertheless, this sensitivity directly depends on location and the model layers' configuration: the sensitivity of different observation points highlight Quaternary and Mesa unites as the ones with particular prevalence.

A modification has been proposed in the evaluation of the *PP* technique, which includes a plausibility term in the optimization process. The suggested method was tested on a real basin with in-situ data, and three elements regarding heterogeneity identification were explores: (*i*) the plausibility term influence, (*ii*) sensibility to the number of pilot points and, (*iii*) the effect that reducing the parameters variability had on the model during the inversion problem.

The standard *PP* method does not includes the plausibility term, which leads to a better adjustment of the reduction data but also to an unstable identification of model parameters as well. This instability means higher parameter variations and can be qualitatively described as rough field's estimations. On the contrary, too much prevalence to the plausibility term bias the solution toward an unreal system. If the geostatistical model contains less information of the real variability patters, like this case, the estimated field will also fail on identifying heterogeneities.

5. Integrated Water Resources Optimization Model

This chapter presents the hydro-economic model consolidation. This model allows us to maximize the value of water consumption in the study area. Throughout this chapter, you will find the optimization model in a current mean condition, at thirty years, fifty years and a hundred years.

Water resources management must be in all cases effective, efficient and sustainable, especially when considering the effects of climate change and variability. Achieving this is a challenge that is tackled in this chapter with a hydro-economic optimization model, which can be used as a decision-making tool for water assignment between several users. The model has been developed by integrating hydrological aspects (surface and groundwater) in an economical optimization framework for water allocation and water quality management. The model also has the purpose of maximizing the value for water consumption that integrates multiple water supplies (surface and groundwater), and water demands. For hydro-economic analysis, the model contemplates four main study scenarios: (*i*) current mean condition ($ESC1$), (*ii*) at thirty years ($ESC2$), (*iii*) at fifty years ($ESC3$) and, (*iv*) at 100 years (ESC4). These scenarios show fluctuation in water demand, and water supply based on the population increase. Water resources management is often limited to studying water quantity, although both quantity and quality of water have to be considered in order to improve decision making. The incorporation in the model of a water quality parameter in hydro-economic optimization increases its complexity and uncertainty.

5.1. Introduction

The constant increase of water demand for energy, agriculture, industrial development, and environmental sustainability, has constraint water resources throughout the world (Tortajada et al., 2019; Davis, 2007). This rise is strongly attached to quality worsening, according to the requirements necessary for each use, given the relationship between quantity and quality in water supply (Davidsen et al., 2015; Martinsen et al., 2019; Walker et al., 2015). Water quantity stored in hydrographic basins depends on the hydrological process and the water quality depends on the interaction with punctual or diffuse contamination sources, produced in the industrial development processes.

Water quality spoilage is related to the increase in supply costs (Cánovas et al., 2017; Davidsen et al., 2015; Maliva, 2014). This increases summed to a demand increment for water in specific areas have shown the necessity to apply more efficient processes in the water allocation methods (Assaf & Saadeh, 2008; Metcalfe et al., 2017; Pulido-Velazquez et al., 2008). According to, Integrated Water Resources Management (*IWRM*) concept is used to express the relation between water offer and demand based on availability; integrating quantitative and qualitative conditions (Al-Jawad et al., 2019; Ferreira et al., 2019; Wongsa, 2015; Rogers et al., 2003).

In recent years, one of the *IWRM* biggest challenge is to provide an efficient water allocation, due to the up-growth that agricultural, aquaculture, livestock, O&G, industrial, mining and domestic demand has turned towards the water availability (Dessu et al., 2019; Pérez-Blanco & Gutiérrez-Martín, 2017; Pérez-Uresti et al., 2019). *IWRM* uses optimization models that can integrate the hydrological modelation (surface water and groundwater), the economic evaluation of water, and mathematical optimization. This focus provides a cheap analysis tool to assess water allocation within the study area, which could help in decision-making and in the understanding of the system behavior (Al-Jawad et al., 2019; Li et al., 2019; Pulido-Velazquez et al., 2008). The water quality incorporation in the water resources optimization process allows to restrict the water allocation according to its use (Davidsen et al., 2015; Fu et al., 2017; Martinsen et al., 2019). Nevertheless, literature reviews showed few studies related to quality and quantity water optimization.

Hydro-economic models combine the economic system of regions and the engineering concepts for water resources modeling in order to analyze water allocation inside a cost-benefits appraisal under hydrology parameters (Booker et al., 2012; Harou et al., 2009; Reynaud & Leenhardt, 2008). Optimization models that incorporate economic objectives are widely used to evaluate decisions in water resources planning and management (Al-Jawad et al., 2019; Fu et al., 2017; Mohtar et al., 2019). The applications of hydro-economic

optimization models are numerous. Authors as Harou et al. (2009) provide a complete description of hydro-economic modeling concepts and Labadie (1975) gives a revision of the mathematical optimization process for water resource planning. Punctual water sources analysis is useful to determine and analyze the system operation, except for a regional scale water resources planning process, where optimization of various water sources is required.

Hydro-economic optimization models that integrate water quality, focus in administration strategies that minimize the pollution or improve water allocation management to limit the pollutant loads. Authors as Ferreira et al. (2019); Gunawardena et al. (2018); Morales-Marín et al. (2017); Peña-Haro et al. (2011) present studies that emulate water quality as a result of different management strategies. Those strategies seek to optimize the optimization model outcomes under imposed quality restrictions. Water quality standards may also be fulfilled using allocations and its impacts in water quality.

Modelling effects over water allocations regimes that involve several users and sources is complex and interdisciplinary. Various studies establish models related to economy, hydrology, hydrogeology, and ecology, and even though all studies aim to integrate different disciplines, each of them focuses in a particular subject. For example authors like Velázquez et al. (2003) focuses in determination of values to evaluate water shortage; Switzman et al. (2015) centers in availability and salinity of water for irrigation purposes; Jia et al. (2018) centers in create optimal strategies for water allocation between users; Lopez-Nicolas et al. (2018) determines prices and institutional limitations for water allocation in irrigation purposes; Blanco-Gutiérrez et al. (2013) focus their studies in integration of economy and ecology and Maliva (2014) shows the relationship between economic activities and water quality.

5.2. Methodology

IWRM is interpreted as the maximization of net profits in a regional model (García-González et al., 2007), seeking to achieve an economic efficiency (optimal) water allocation for all users. In this research, an integrated water management approach was performed in order to: (*i*) obtain an economic solution for allocation and optimization of hydro-economic models, (*ii*) to evaluate maximum profits of users in the region, and (*iii*) to analyze the impacts of water shortage base on the quality parameters. In this sense, the model explains optimal water allocation within economic sectors, based mainly in the population up growth. Moreover, when including physical and economic restrictions, the model provides a cost estimation for water allocation with different availability levels. Thereupon, are explained the main elements of the model: water use profits in each sector, relevant restrictions, and the relations that represent surface and groundwater flow.

5.2.1. Parameters Associated with Water Usage

Optimization model parameters determination has been performed in a municipality level scale, to evaluate benefits and costs related to water management and usage in regional level. The model results show optimal water levels, profits, and costs of the system for water allocation in the region. Nonetheless, most of the parameters correspond to 2018 which is considered the reference year of this work. Some prices are adjusted to reflect projection values at thirty, fifty and a hundred years, with a 3.33% increment based in consumer price index analysis (*PIA*) reported by DANE (2019).

As in most cases, the rates vary according to water use type (commercial or domestic), in this research it was used the ordinance N. 1155 by the environment and sustainable development Ministry issued in 2017 (Ministerio de Ambiente y Desarrollo Sostenible, 2017), to calculate the water rates in each sector. The estimated cost for service (VP) is formed by water use price rates (TU – $MUSD/Mm^3$) and volume of water collected (V – Mm^3). This volume is equivalent to demand satisfied in each economic sector, in a period of time t, corrected by the cost of opportunity factor (*Fop*) (Eq. 5-1)

$$Vp = (TU)(V)(Fop), \tag{5-1}$$

where, *Fop* factor (Eq. 5-2) takes in whether the users make adequate usage of the water or not. For this model, it was analyzed a non-returning water basin scenario.

$$Fop_{returtning} = \frac{V_c - V_v}{V_c}; \qquad Fop_{non-returtning} = 1, \tag{5-2}$$

Additionally, TU (Eq. 5-3) is expressed by multiplication between minimum rate – TM (0.0032 USD/m^3) and the regional factor (FR) (Eq. 5-4), that compiles the water availability factors, basin investment requirements, and social and economic community condition.

$$TU = (TM)(FR), \tag{5-3}$$

$$FR = [1 + (C_k + C_e)C_s]C_u, \tag{5-4}$$

where, C_k is investment coefficient (Eq. 5-5) and represents the total cost of basin management (Basin Management Plan, in Spanish POMCA - order N. 1279 of 2002). C_{pmc} is the annual total costs for the management plan of previous year, and C_{TM} shows the

annual billing of water use. In absence of POMCA, the investment coefficient value will be zero.

$$C_k = \frac{C_{pmc} - C_{TM}}{C_{pmc}}; 0 < C_k < 1, \tag{5-5}$$

C_e is the shortage coefficient (Eq. 5-6) and varies depending the source (surface or groundwater). This coefficient is considered from the water usage index, which reflects the relation between offer and demand reported by each municipality, for the area affected by the POMCA.

$$\begin{aligned} C_{e_{surface}} = & \\ 0 \quad & \rightarrow \quad I_{es} < 0.1 \\ \frac{5/6}{1-(5/3)I_{es}} \quad & \rightarrow \quad 0.1 < I_{es} > 0.5 \\ 5 \quad & \rightarrow \quad I_{es} > 0.5 \end{aligned} \tag{5-6}$$

$$\begin{aligned} C_{e_{groundwater}} = & \\ 0 \quad & \rightarrow \quad I_{eg} < 0.1 \\ \frac{40}{49-90I_{eg}} \quad & \rightarrow \quad 0.1 < I_{eg} > 0.5 \\ 10 \quad & \rightarrow \quad I_{eg} > 0.5 \end{aligned}$$

C_s is a social and economic conditions coefficient (Eq. 5-7) and is differentiating the domestic supplying and the other kinds of water usage trough the unsatisfied basic needs index (DANE, 2017).

$$C_s = \frac{100 - NBI}{100}; \quad 0 < C_s < 1, \tag{5-7}$$

And finally, C_u is usage coefficient, that varies according to final water use in each sector. For domestic, agricultural, livestock, aquaculture and energy generation, $C_u = 0.0775$, for the other usages $C_u = 0.2$ (Ministerio de Ambiente y Desarrollo Sostenible, 2017).

5.2.2. Water Demand and Quality

The domestic sector demand was based on the allocation of water provision for human consumption of the Technical Regulation of the Drinking Water and Basic Sanitation

Sector - RAS 2000 (Order 2320 of 2009 - Ministry of Environment, Housing and Territorial Development) and the National Census of Population and Housing, 2018. The projected domestic sector demand was performed trough the construction of a population up growth scenario from reference levels in 2018 reported for DANE (2019) and following the Eq. 5-8.

$$GP = P_{base}(1+g)^t, \tag{5-8}$$

where, P_{base} refers to population in 2018. This information is spatially distributed throughout the model area. g is the projected growth rate in the period. This information is geo-referenced by the municipality and spatially distributed in a 6 km by 6 km grid in the model area by Kriging method.

The estimation of the agricultural and aquaculture demand was carried out following the methodology of (IDEAM, 2019) (Eq. 5-9). This methodology consists in the assignment of a water footprint to the products sown and produced in the area. The green water footprint is used exclusively in the agricultural sector and is based on the natural use of water from the soil moisture. The blue water footprint refers to water that is extracted from rivers or lakes and that does not return to the source (IDEAM, 2019).

$$D_{total} = \%P(HH_{blue} + HH_{green})\%MA, \tag{5-9}$$

where, D_{total} is the total water demand in the agricultural or aquaculture sector. P represents the farming production in the municipality, HH_{blue} is the blue water footprint and HH_{green} is the green water footprint, and MA is the municipality area. This information is geo-referenced by the municipality and spatially distributed in a 6 km by 6 km grid in the model area by Kriging method.

To calculate the livestock sector demand, water consumption was classified by type of animal. In the case of beef cattle, Table **5-1** shows the water amount considered, which includes in a global way the water used in breeding, raising, fattening, benefit and slaughter. Table **5-2** shows the water consumption for other species. This consumption must be multiplied by the percentage of the municipality area.

Table **5-1**.: Daily water demand for beef cattle (Ideam, 2014).

Age (years)	Demand (l/day)
< 1	30
1-2	45
2-3	110
>3	115

Table **5-2**.: Daily water demand for animals for other animals (Ideam, 2014)

Species	Demand (l/day)
Swine	30
buffalo	82.1
Goats	10
Sheep	5
Equine	50
Birds	2.4

Construction, mining, industrial, and services sectors monthly demand were obtained from data reported by DANE (2019) and compared with data addressed by the National Water Study (IDEAM, 2019). O&G sector demand was compiled from data registered in extraction wells reported in the study area (Annex 4).

Water quality for the domestic sector was classified by the water quality index (WQI) (Eq. 5-10). This index represents the numerical value that qualifies the water quality of a surface current based on the measurements obtained for a set of five variables recorded in a monitoring station j at time t.

$$WQI_{njt} = \sum_{i=1}^{n} (W_i)(I_{ijt}), \tag{5-10}$$

where, W_i is the weighting or relative weight assigned to the quality variable i; I_{ijt} is the calculated value of variable i (obtained by applying the corresponding functional curve or equation), at the monitoring station j, recorded during the measurement made in the period of time t;and n is the number of quality variables involved in the calculation of the indicator; for this research, n is equal to 5.

The variables used in the computation of the WQI were: dissolved oxygen (DO), total suspended solids (TSS), chemical oxygen demand (COD), electrical conductivity (EC) and pH. The weighting of each variable was 0.2. The optional values that the index can take have been classified into categories, according to these values, the quality of the surface water is rated between 0 (non-viable by sanitary standard) and 1 (Free risk) (Table **5-3**) (Ministerio de Ambiente, 2007).

Table **5-3**.: Classification of the health risk level according to WQI.

Classification	Risk Level	Alert signal
0 - 0.25	Sanitarily Inviable	Red
0.25 - 0.5	High	Orange
0.5 - 0.7	Medium	Yellow
0.7 - 0.9	Low	Green
0.9 - 1	Risk free	Blue

This information was obtained from 380 samples in the influence area for the year 2018 (Instituto Nacional de Salud, 2018). 54% of this data corresponds to samples in the urban area (Figure **5-1**). Water quality in the other sectors (O&G, mining and industry) was analyzed through the HCO_3, SO_4, Cl, Na, Ca, Mg and K. This information was obtained from samples in the surface and groundwater spots in the area and the quality data registered in the environmental fulfillment reports delivered to the ANLA as reported by Malagón-Navarro (2017).

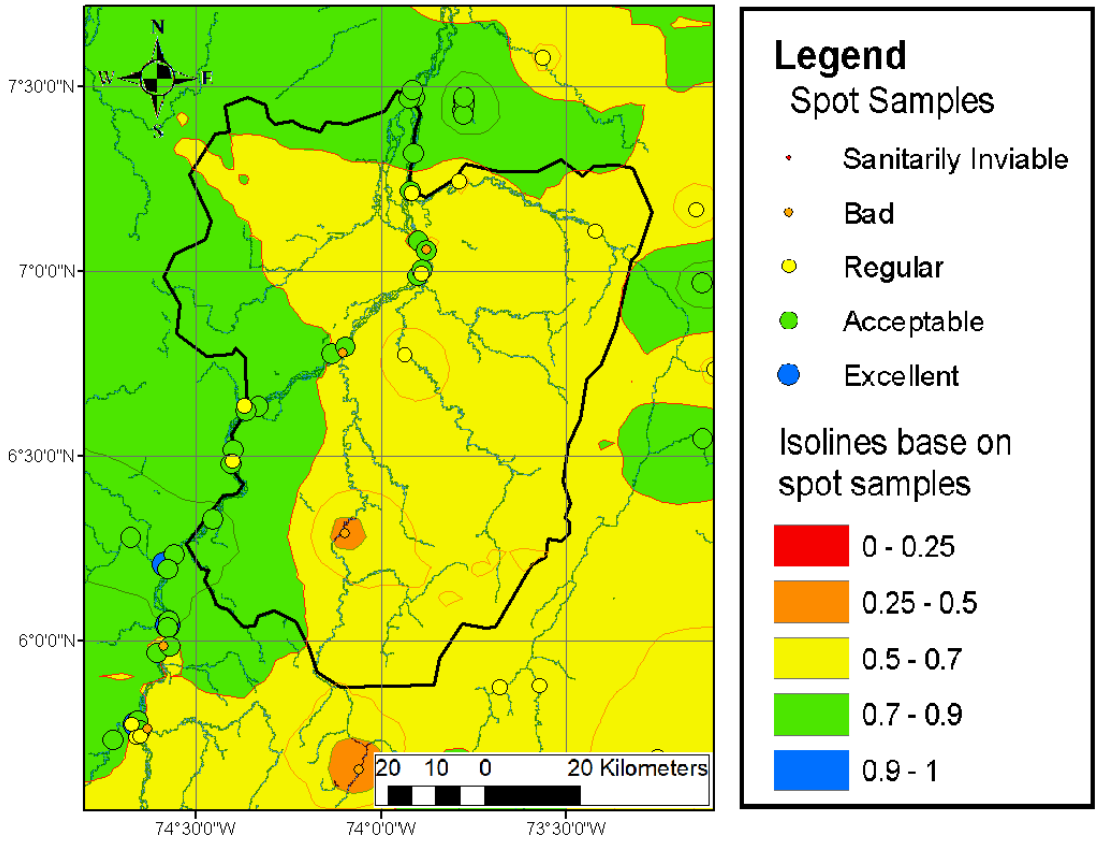

Figure **5-1**.: Water quality behavior in the study area, based on the WQI.

According to the results obtained by Malagón-Navarro (2017), the average pH behavior in the study area (Figure **5-2**-pH) is slightly acidic ($pH = 6$). These results indicate to dissolution processes are facilitated in the area and the main pH decrease factor is the industrial activities. The liquid waste discharge that contains nitrates and sulfates affects the natural weathering rates, and reduces the soils and rocks attenuation capacity, inducing a rise in the acidity of shallow groundwater, especially in areas with carbonated minerals deficiency such as the Quaternary units. Additionally, these results showed low values of the electrical conductivity (EC) (Figure **5-2**-EC), common of the aquifers with shallow groundwater levels and short residence times. However, the study area showed areas with high EC values, located in the influence area of the O&G fields.

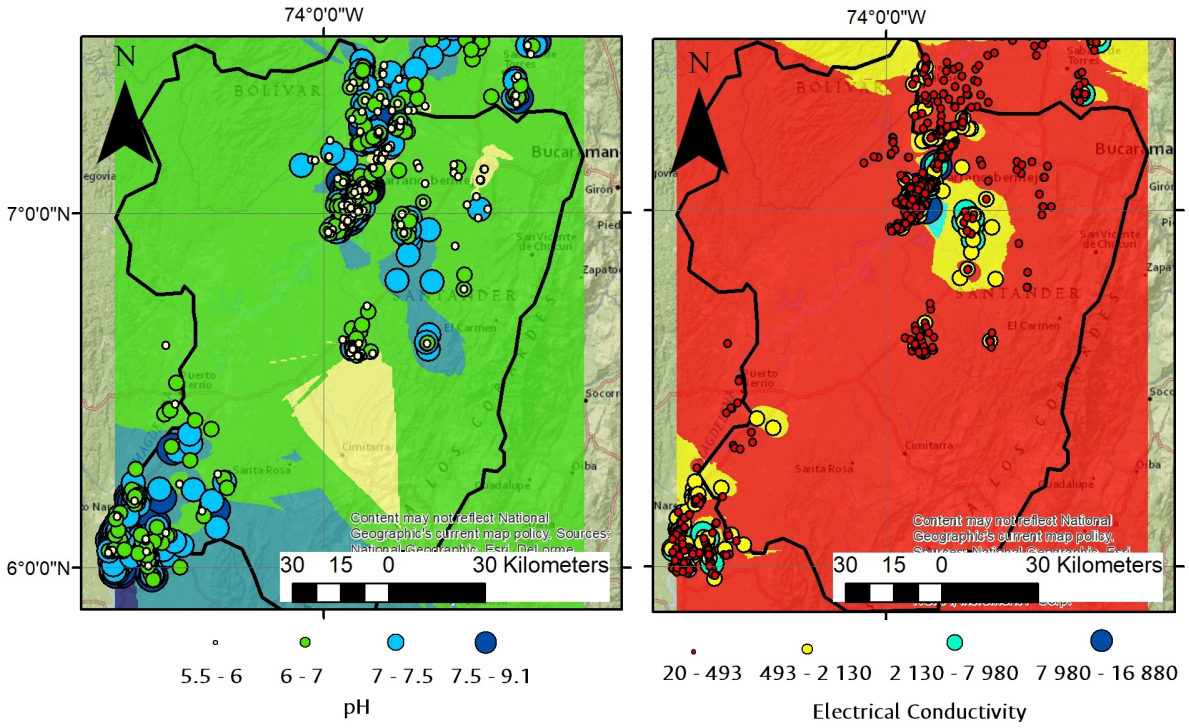

Figure **5-2**.: Groundwater quality behavior in the study area base on Electrical Conductivity and pH. Adapted from Malagón-Navarro (2017).

The hydrochemical classification results were analyzed by Malagón-Navarro (2017) based on the Piper diagram (Figure **5-3**). These results determined that the calcium bicarbonate hydrogeochemical facie is the water type dominant in the MMV area. Additionally, these results relate to the behavior of the Quaternary deposits present in the study area in a manner consistent with shallow groundwater behavior and short residence times.This water type represents a recent infiltration and its chemical signature is not different from the rainfall water. The sodium bicarbonate water is also important in the area, and are located in the Magdalena River floodplain deposits, in which silicate dissolution processes occur.

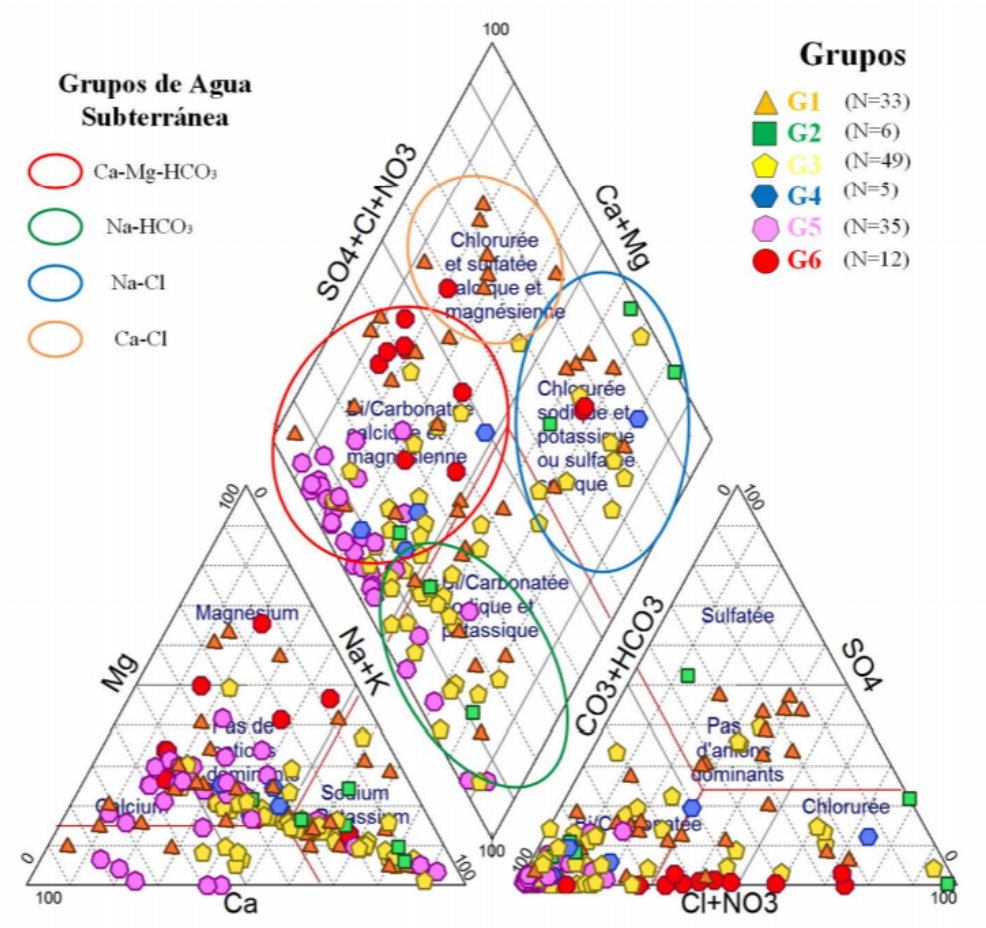

Figure **5-3**.: Piper diagram according to the six groups established. The samples are found in the calcium bicarbonate water domains and in a smaller proportion for sodium bicarbonate water type and calcium-sodium chloride. Group 1: Shallow samples with short residence times. Group 2, 3 and 4: Samples with intermediate depths and EC. Group 5: Deep wells. Mineralized samples and extracted at greater depth. Group 6: Piezometers. Shallow samples with a higher mineralization degree. Source: Malagón-Navarro (2017)

Based on the behavior analyzed above, a water quality variation was proposed to thirty, fifty, and a hundred years scenarios, that allowed to propose a water price change. These scenarios constituted a possibility to analyze the basin behavior, under a deficit situation. This change is described in Table **5-4**.

5.3. Baseline and Optimization Model

In this stage, it was created a simple code in the R software to solve the optimization model. This model seeks to find the values of the decision variables that maximize the profit in water allocation. The baseline model ($ESC1$) maximizes the water usage benefit in the social and economic current conditions ($Bwater$) conditioned to the aforementioned restrictions. The baseline optimization model structure is based on the subtraction between, total income and the total cost (Eq. 5-11). The total income, is in function of the water productivity and deficit. The total cost, is in function of water price and a penalty for not meeting the water demand.

$$\begin{aligned} & Max(B_{water}) \\ B_{water} = \quad & I_{total} - C_{total} \end{aligned} \tag{5-11}$$

In areas with water shortage, the total demand exceeds the availability thus, the requirements from every user cannot be fulfilled. This situation is not evenly distributed, doing necessary to use regulations that allow prioritizing and organizing the assignment. For this, the model propose has contemplated an economical penalty related to the deficit.

The I_{total} (Eq. 5-12) obtained by water usage is based on water productivity by each user (u_i) and used water amount (R_u). The water used is the difference between demand water amount (WD_u) and the water deficit in each sector. Economic value for productivity in the domestic sector is cero. These data were obtained following the methodology used by DANE (2017).

$$\begin{aligned} I_{total} &= \sum_t \sum_u R_{u,t}(WD_{u,t} - \sum_s Deficit_{u,t}), \\ I_{total} &= \sum_t \sum_u R_{u,t} WD_{u,t} - \sum_t \sum_u \sum_s (WD_{u,t} - WS_{u,t}), \end{aligned} \tag{5-12}$$

where, t represents the time, s is the water extraction source (surface or groundwater) and WS represents water availability by each source.

Likewise, the C_{total} obtained, refers to water shortage costs (Eq. 5-13).

$$C_{total} = \sum_t \sum_u \sum_s Pr_{u,t,S} WS_{t,S} - PE(WD_{u,t} + WS_{t,S}), \tag{5-13}$$

where, Pr is water price that every user must pay, and this will depend on the water source. PE is the penalty that takes into account the cost of not supplying the water demand by the users.

The general model restrictions focus on four axes: (*i*) the environmental flow, (*ii*) the water availability in a period, (*iii*) the minimal domestic provisioning and (*iv*) the price variation with respect to water quality. The environmental flow was determined as 3% of water supply. This flow is used as a necessary ecological flow for environment conservation (MAVDT, 2013; Parra & Carvajal, 2012). That each source can be sent to different demands' destinations, but it can not exceed the total source availability (Eq. 5-14).

$$\sum_{t,S} WA \leq WS, \tag{5-14}$$

where, WA represents the water allocation for each source (s) in a period of time t, and WS is the water availability by source.

Minimum domestic water supply restriction is defined according to the current normative. This normative establishes the minimum water quantity must be provided for each person per day is 50 liters (in the study area conditions) (Ministerio de Vivienda Ciudad y Territorio, 2018). Thus, water quantity that comes to every domestic demand unit must be equal higher that legal requirement. Finally, quality restriction considered a 5% rising in the price when WQI is less than 0.7.

The hydro-economic model was solved through a lineal optimization process, that links all available water resources and all water demands (Annex 4), under the limitations of demand rising, water quality variance and offer decrease. The objective function maximizes the profit in the MMV basin during a planning period of a year. The water demands may be supplied with surface or groundwater. Nonetheless, given its high variability for each usage, is necessary to evaluate the water source quality. The system considers the monthly water demand from each user and a penalty for no satisfy it.

Each scenario described under-here, provide variations in the basic results in order to evaluate availability or water demand changes. The $ESC2$, $ESC3$ y $ESC4$, to a 30, 50 and 100-year projection respectively and they consider: (*i*) rise in water demand based on the population growth (2% annual), (*ii*) changes in the water resource availability based on the results obtained by Arboleda-Obando (2018), where water availability was evaluated by changes in the climatic patrons, and change in the land use (1% for every 10 years) and (*iii*) changes in price estimation as result of the relationship among the availability, demand, quality.

The generation of these scenarios is an internal and consistent vision of the modeler on how the demand for water could be, based on the climate change analyzes shown by Arboleda-Obando (2018). This model implementation is based on recreated data displayed in Table **5-4**.

Table **5-4**.: Scenarios proposed in the integration of the economic aspects.

Experiment	Demand	Availability	Price
$ESC2$: to 30 years	+60%	+3%	+5%
$ESC3$: to 50 years	+100%	+5%	+7%
$ESC4$: to 100 years	+200%	+10%	+10%

5.4. Modeling Results and Discussions

In this section, it shows the results of the water allocations (surface and groundwater) and profits, highlighting: water deficit in the study area, supply and demand, water availability, and benefit maximization at the basin. The four scenarios analyzed shown in the optimal solution the profit spatial distribution in the MMV Basin (Figure **5-4**). This figure shows that the $ESC1$ (Figure **5-4**- 1A), presents positive yields in the analysis period as long as there is no deficit in any productive sector. Nonetheless, is evident that some areas from the oriental zone, have high values profit mainly due to water quality (Figure **5-1**). The maximum average profit is of 52 000 USD/year, and in a monthly basis, the highest profit is presented in march (Figure **5-4**- 2A). This allows ascertaining that the maximum profit associated with water use is obtained when the 53.8% surface water and 57.6% groundwater are assigned to the agricultural sector.

All scenarios present a deficit (Figure **5-5**) in some economic sector, which is translated in a penalty in the system leading to months with negative yields. In $ESC1$ and $ESC2$, the water deficit (Figure **5-5**-A and B) is slanted towards the east limit of the model. This tendency is maintained over the years ($ESC3$ - figure **5-5**-C and $ESC4$ - figure **5-5**-D), and the deficit tends to cover the center of the area. The month with more profit is February, the lowest is March, and the annual average profits in each scenario are 52, 1 457, 1 112, and -117 thousand USD, respectively (Figure **5-4**). This data shows that in $ESC4$ the system is not sustainable given the demand increase by the population variation and the water quality affectation.

In $ESC2$, the projected rise in water demand has a rate of 2%. In this scenario, the analyzed basin presents a 2% deficit to supply the user's requirements (Figure **5-5**-B). However, is

evident that water quality worsening (Figure **5-1**), limiting the surface and groundwater allocation.

In this scenario, it can be seen that the economic impact associated with water quality worsening is crucial in the election of the supply source. The maximum obtained profit in this scenario with respect to the baseline scenario ($ESC1$) show a significant difference of 1.4 MUSD generated by the demand variation and water quality. Arboleda-Obando (2018) suggests in his hydrological analysis of this area, that water availability variation and its relation with demand, provides in the MMV basin a change in the land-use regimes that can be settled to obtain a better water quality. The analysis also shows that variation in water quality is presented close to the industrial, mining and O&G extraction and exploitation developing points, located mainly in the central and oriental area at the model.

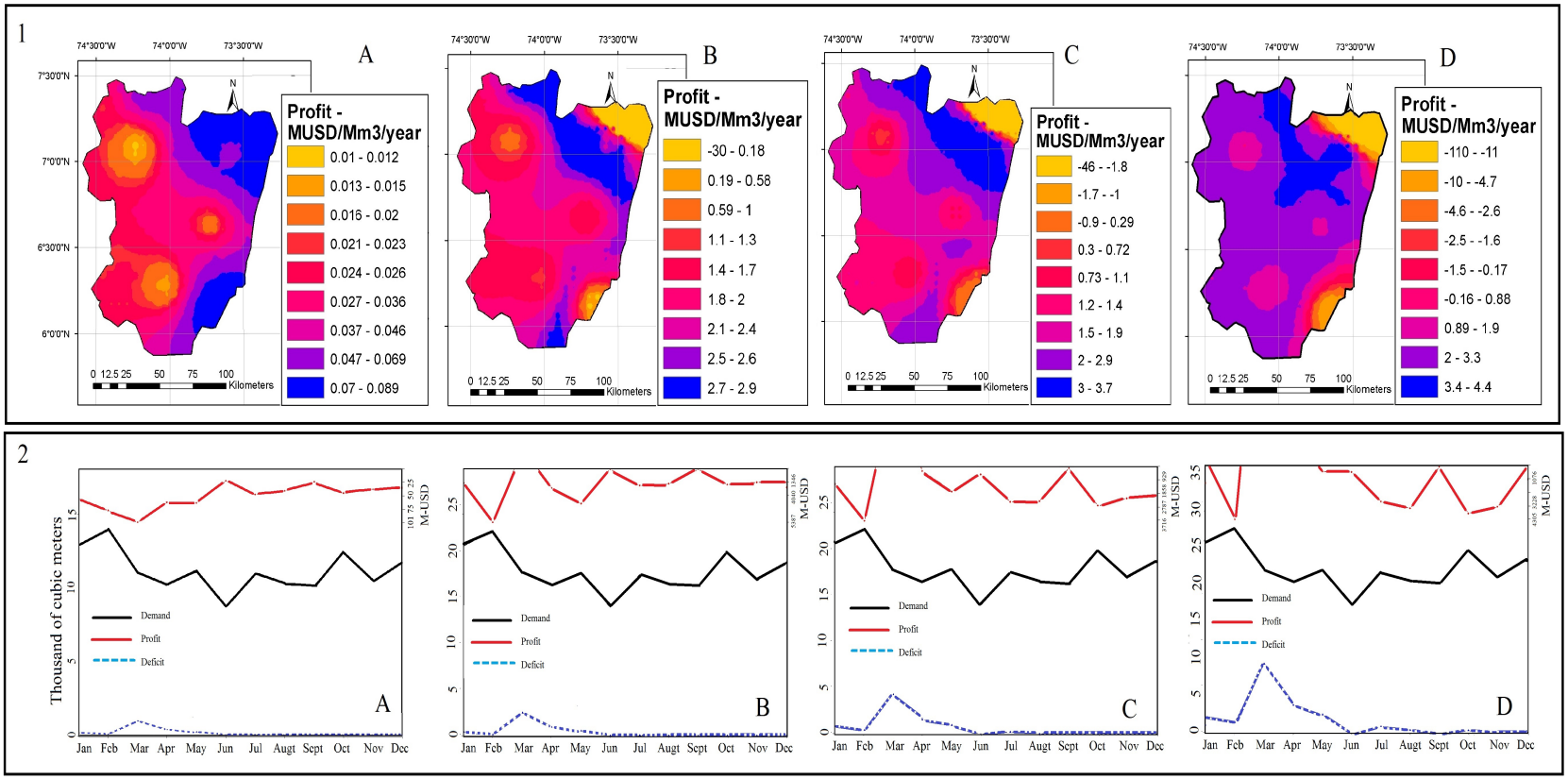

Figure **5-4**.: Results of economic aspects integration in the hydrological model. The numeral one, shows the profit in the optimal solution and the numeral 2 shows the behavior over time of demand, deficit, and profit in the study area.

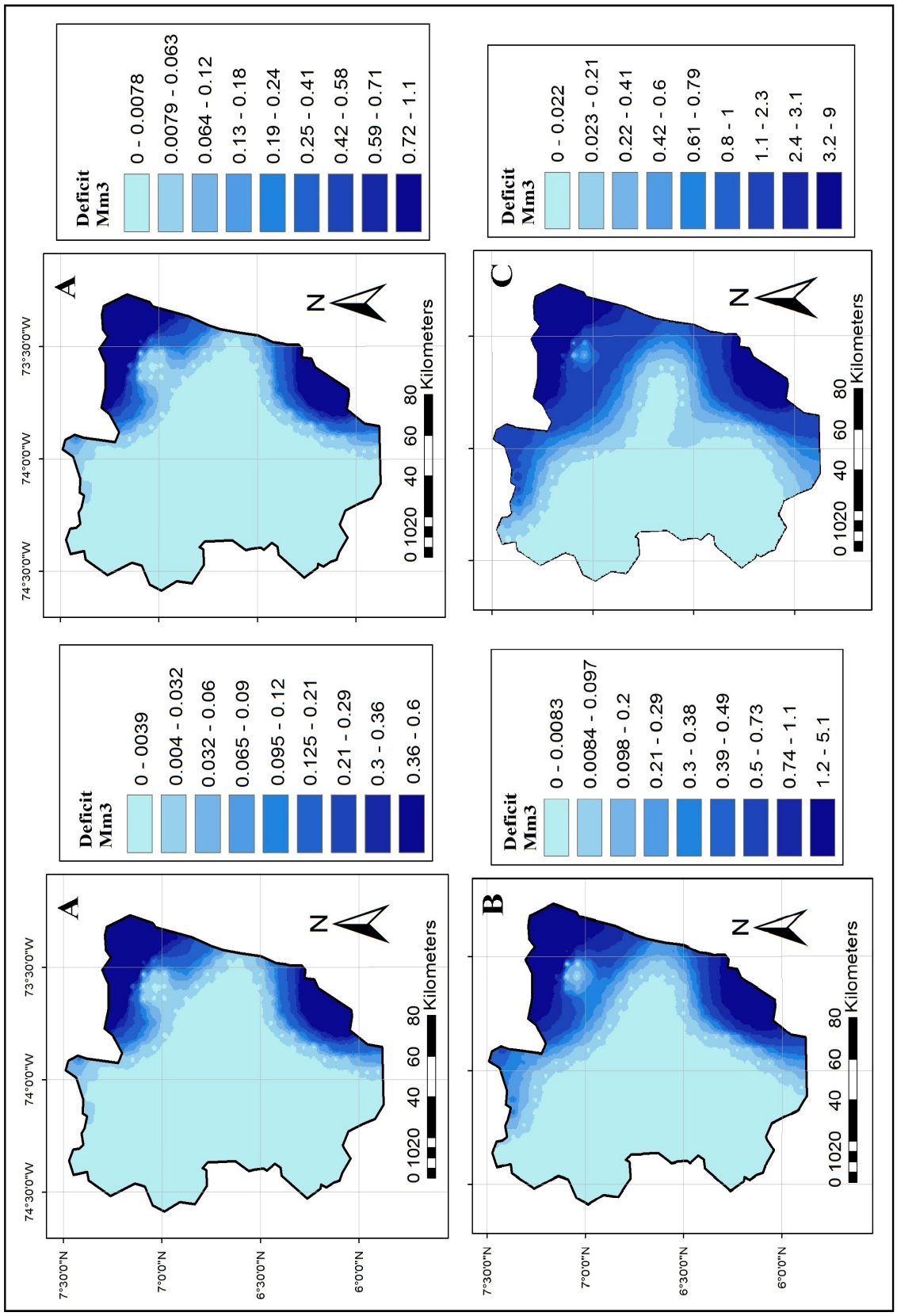

Figure **5-5**.: Average annual deficit per scenario. A- shows deficit in current situation. B- shows deficit in projection to 30-years. C- shows deficit in projection to 50-years. D- shows deficit in projection to 100-years.

Figure **5-4**-2B shows that the water deficit is higher in March with 2.5 Mm^3. This allows us to conclude that in March the penalty fee in the system is higher and thus the profit is lower. Additionally, in the aquaculture and livestock sectors are not a deficit due to the water quality and amount for each sector. The $ESC2$ results show that the higher deficit is in the agricultural sector (1.8 Mm^3) due it is the sector that needs more water. The O&G sector (0.48 Mm^3), industry (1.15 Mm^3) and mining (0.33 Mm^3) have a low deficit due to lower demand and the cost associated to obtain a higher water supply. In $ESC3$, the basin presents a 3% water deficit to supply the users needs (Figure **5-5**-C). The comparison among the $ESC3$, $ESC1$ and the projection to 30 years ($ESC2$) scenarios, shows that the deficit is approximately double.

This analysis permits to show that the economic impact associated with water quality spoilage is important in the supply source choice. Results comparison in this scenario with respect to the previous ones shows a 300 000 USD/year difference approximately in profit obtained for demand variation and water quality. Further analysis of this variation will lead to defining the importance of the land-use changes and the economic impact in the region. This scenario shows that water quality variation behaves similarly to the results showed in $ESC2$, where the higher spoilage is produced around the industrial, mining, and O&G sectors.

Figure **5-4**-2C shows that higher deficit is in March with 4.3 Mm^3, and supports the results previously generated in the $ESC2$. In this scenario, the livestock sector has not water deficit due to the relation demand/cost that the model evaluates. Sectors with biggest deficits are: industrial (2 Mm^3), O&G (0.9 Mm^3) and mining (0.6 Mm^3) due to the model penalizes with lower cost in these sectors, the non-fulfillment of water needs. This result shows that the O&G and mining deficits doubled with respect to the $ESC2$ results. Finally, the $ESC4$ showed a 6% water deficit to supply the user's needs (Figure **5-5**-D). The comparison of this scenario with prior ones indicates that spoilage behavior in water quality and supply deficit in all sectors is similar. Results comparison obtained in this scenario with respect to previous outcomes, shows a significant difference of -200 000 USD/yr in the profit obtained for the demand variations and water quality.

Figure **5-4**-2D shows that deficit continues to higher in March with 9.5 Mm^3, which represents the double deficit than in $ESC3$. In this scenario, the aquaculture sector has not deficit. This trend correlated to relation demand/cost. The sectors with a higher deficit are: agriculture (9.9 Mm^3), industrial (4.5 Mm^3) and O&G (2 Mm^3). Here, is evident that the model no longer responds to restriction applied in supply, and although the agriculture sector must be prioritized for allocation, the required water volumes are no longer viable given the population water demand increase.

5.5. Further Model Development and Limitations

A paramount concern in water resources management is uncertainty about future water. Allocation control and water demand fulfillment associated with phenomena as droughts and floods are often the main objectives of water management. The model results presented in this research were optimized throughout an annual middle period, that cannot capture the essence of all-weather variability in the area. Studies made in the same area (Arboleda-Obando, 2018) have found that the future weather of MMV basin will be influenced by changes in evapotranspiration, temperature, and some alterations in precipitation patrons. These changes lead to changes in water usage perspectives and living conditions adjustments in the communities regarding water quality and cost. The model results may interfere with some possible future climatic changes, of those who we cannot be certain of. Also, the model framework assumes a perfect prevision throughout the whole planning period, which does not actually occur in reality. The water managers and planners will not have a perfect prevision and will be restricted by the reach of the forecasts data available in the moment. The main focus of this chapter was to compare different scenarios of water allocation and not to generate operative decision backing. The perfect prevision will underestimate real water prices, and the appraisal of this cost must be identified with higher limits.

Input data and model optimization have nonlinear reliance with results water allocation scheme. This improves the computational performance of the model but has a risk of losing sight of general changes effects in water allocation. The model optimization can not capture the effects in recharge, given the changing conditions in agricultural irrigation, the water quality, return flows of domestic, and industrial sectors and agricultural nutrients filtration. This limits the computational resources and uncertainty introduced starting from parametrization and this interactions modelling. In the water management process, any important change in the system must be identified, and the model has to be updated with new information. Adaptation towards more sustainable groundwater allocation will result in important changes in the system. Therefore, the model results must be evaluated as a starting point for future analysis of water management in the area for decision making.

5.6. Conclusions

The general analysis of the studied scenarios establishes a series of important ideas about the global effects of economic activities that must be prioritized in the study area and the required infrastructure design projects to guarantee water allocation, bases on the hydro-economic dynamics of the basin.

This part of the research shows that, in the $ESC4$ drastically alters the distribution of profits in basin water resources management, affecting significantly domestic consumption, and agricultural production. Through this analysis and assuming the behavior under a mean hydrologic year, an 11% reduction in the agricultural, domestic, livestock, and industrial sectors be would achieve an 8% in the system profits. Additionally, availability decrease (surface water and groundwater) and water quality, reduce the profits in one million dollars approximately. In this way, the concerns associated with total demand, allocation, and fulfillment in a middle and long term basis does not seem excessive.

A remarkable discovery of the presented analysis is that there are significant differences between the stakeholders allocation regimes. This has been identified between domestic and agricultural sectors, but not between commercial activities. In conclusion, a general analysis that would contemplate variable rates for each sector according to its productivity must be updated. It is important to highlight that the whole system was optimized under an equitable distribution in allocation and costs, and thus, the resulting profits would improve results to satisfy all economic sectors.

6. Water Resources Management and Planning

This chapter presents the management strategies of the optimization model. These strategies allow us to characterize the water system with respect to allocation, availability, supply, and demand (surface and groundwater) from an intensity levels assessment in the study area. Throughout this chapter, you will find the indices presented to determine the possible strategies of management, planning, and adaptation in water systems, and the management strategies proposed for the allocation process.

A Integrated Water Resources Management *IWRM* tool, offers: (*i*) hydrological consolidation (surface water and groundwater), (*ii*) management strategies design, planning, and (*iii*) adaptation provide a solution in decision making that leads to efficient water allocation, and to protect and preserve the ecosystems at a regional scale. In this chapter, it describes a methodology appropriation to determine the management strategies for joint use of water resources at a regional scale, from problem identification. For that purpose, it describes four indices that allow characterizing the water system with respect to allocation, availability, supply, and demand (surface and groundwater) from an intensity levels assessment. The analyzed scenarios are based on the results obtained in the optimization model presented in the previous chapter.

6.1. Introduction

There is a growing concern regarding the unawareness of water offer (surface water and groundwater), its quality, and the necessity to satisfy the future need for water especially in the regions of high climatic variability (as a tropical countries) (Pérez-Sánchez & Senent-Aparicio, 2015). The attention to this problematic in water resources management has emerged in recent years as a key element to guarantee sustainable regional growth and constitutes a transcendental and dynamic matter in societies (Rogers et al., 2003). This has been made evident from the moment in which societies had to acquire political compromises and promote agreements that allow responding to the growing tension and concern about the actual a future state of water resources and their role in the development for the communities (Al-Jawad et al., 2019).

The joined actions and efforts of governments are leading to improve the institutional framework, including key subjects as: (*i*) implementation of coordinated agreements for assignment and water usage, (*ii*) revision of legal an institutional groundwork regarding the water subject, and (*iii*) promotion in the concept of economic value of water, thus, the world is living a new legal development period towards: (*a*) regional lowland regulation, (*b*) *IWRM*, and (*c*) sustainability of market and usage, based in an efficient allocation, the optimization in profiteering, and satisfaction of required demand. These actions, represent then an opportunity to build relationships between different state institutions for regional water use, considering the local, regional and national synergies.

Water management systems evolution tend to the adaptation of the natural, political, social and economic reality of the regions, including functional concepts, mechanisms, models and strategies to satisfy the need of regions, the existence of competition between users and economic sectors by water, and characterize the system problems. Thus, the main load and incidence of resource assignation and determination of its management by the economical actors, will determine its future, also including the economic activities associated to its use. For this, hydroeconomic models may lead to analyze and interpret the system behavior to identify planning, adaptation and water management strategies.

Given the fact that inclusion of these models to lead the orientation towards decision making and policies design is pretty recent, the literature indicates a few revisions, analysis and research studies that show the impact that generates these models in planning and management for water resources. As an example, Payne et al. (2004) analyzed the implications of different scenarios of climate change using simulation models. Subsequent studies about water management and its impact on the climatic change also were based in simulation models (Tzabiras et al., 2016). Another approach to this analysis, is the

optimization models like the one used by Xie et al. (2018) to manage water resources in agriculture and land use management, presented by Pérez-Uresti et al. (2019) to optimize water resources management in shortage areas or the one showed by Martinsen et al. (2019) to make a jointed optimization of assignments and water quality to satisfy the final users demand.

To help the evaluation process of system performance and in the planning and management process, several authors have proposed different strategies based on the indices results, which allow to condense the impact of modelling in the water resource system management. For example, Hashimoto et al. (1982) defined some indices to describe the reliability, resilience and vulnerability of the water system. More recent research proposes methods to calculate a series of the index that allows studying the water shortage in water resources systems, using the results of an optimization model (Martin-Carrasco & Garrote, 2006). Considering that these methods also have derived in research focused on identifying management, planning, and adaptation of water systems that allows reducing the impacts as was showed by Pulido-Velazquez et al. (2011); Du et al. (2018); Pedro-Monzonís et al. (2015).

Some of the previously proposed indices in the mentioned studies useful to analyze the effects of the up-rise in demand, the variability of water quality and water availability in the system. In this chapter, is presented a series of management strategies generated from the incorporation of a methodology based on the index appropriation, those index evaluate water assignment between different users to define management and planning strategies to a regional scale, that contributes to the system improvement and the reduction in the impact with respect to quality and availability.

6.2. Management Strategies

The four indices presented to determine the possible strategies of management, planning, and adaptation in water systems are proposed by Martin-Carrasco & Garrote (2006); Pulido-Velazquez et al. (2011). The inclusion of these indexes allows diagnosing the system behavior after the water allocation to identify the current problems scenario, in thirty, fifty and a hundred years.

- Demand Satisfaction Index (I_s): is the relation between assigned water quantity (S) to each user (u) in an analyzed time period, and the total water demand (D) generated by this user in the same period of time (6-1).

$$I_s = \frac{S}{D}, \tag{6-1}$$

when the water volume delivered is equal to the demand the relation tends to 1 and is presumed that there is no vulnerability in the water resource.

- Reliability in Demand Index (I_r): is the relation between water availability to be assigned to users, with respect to the total demand in time period t (Eq. 6-2).

$$I_r = \frac{S_r}{D}, \tag{6-2}$$

In this index, it is considered that there is no reliability in the water offer when the water available in the system is lower than 70% of demand. Values close to zero in this relation indicates that the system cannot satisfy the demands in a reliable manner, hence the system is prone to water shortage.

With the appropriation of those two indexes, it is possible to diagnose the system management strategies, but in some cases, it is also necessary to identify the source or cause of the problem in a more assertive approach, which can be achieved with the incorporation of the extraction index and the extraction usage index.

- Extraction Index (I_w): is defined (Eq. 6-3) as the relation between the total extracted water volume from each of the system sources (Y_{sup} and Y_{base}), without considering stored water in different structures with respect to total water demand.

$$I_w = \frac{Y_{sup} + Y_{base}}{D}, \tag{6-3}$$

values close to zero in this relation indicate problems with water supply, therefore strategies must focus in determine and assign complementary resources.

- Extraction Usage Index: this relation is defined to evaluate the percentage of water resources extracted in the system to satisfy the demand (Eq. 6-4).

$$I_u = \frac{S}{Y_{sup} + Y_{base}}, \tag{6-4}$$

low values in this index show that more water is extracted from the system that necessary, leading to a higher system regulation need.

6.3. Strategies for Planning and Management of Water Resources.

Identification of problems evidenced as a response to indices analyzed, allow us to establish different management strategies, planning, and adaptation. For this, considered three intensity levels proposed in a qualitative scale: high (70%), intermediate (70% and 40%) and low (less than 40%). Management problems are described trough four indexes that allow characterizing the basin problems, giving a series of management, planning and adaptation strategies (Figure **6-1**).

System characterization starting from I_s and I_r indices establishes that a problem associated to resource availability (deficit, water insufficiency, rationing, and vulnerability), generate in the worst scenario, problems with a shortage in the system (low qualification in I_s and I_r indices). In these cases, useful to use index I_w and I_u to identify the source of the problems (Figure **6-2**). Problems associated with low values of those indexes make reference to excesses in the extraction flows, generating supply regulation, storage and infrastructure problems in the system. These indexes (I_w and I_u) will be qualified as high and low.

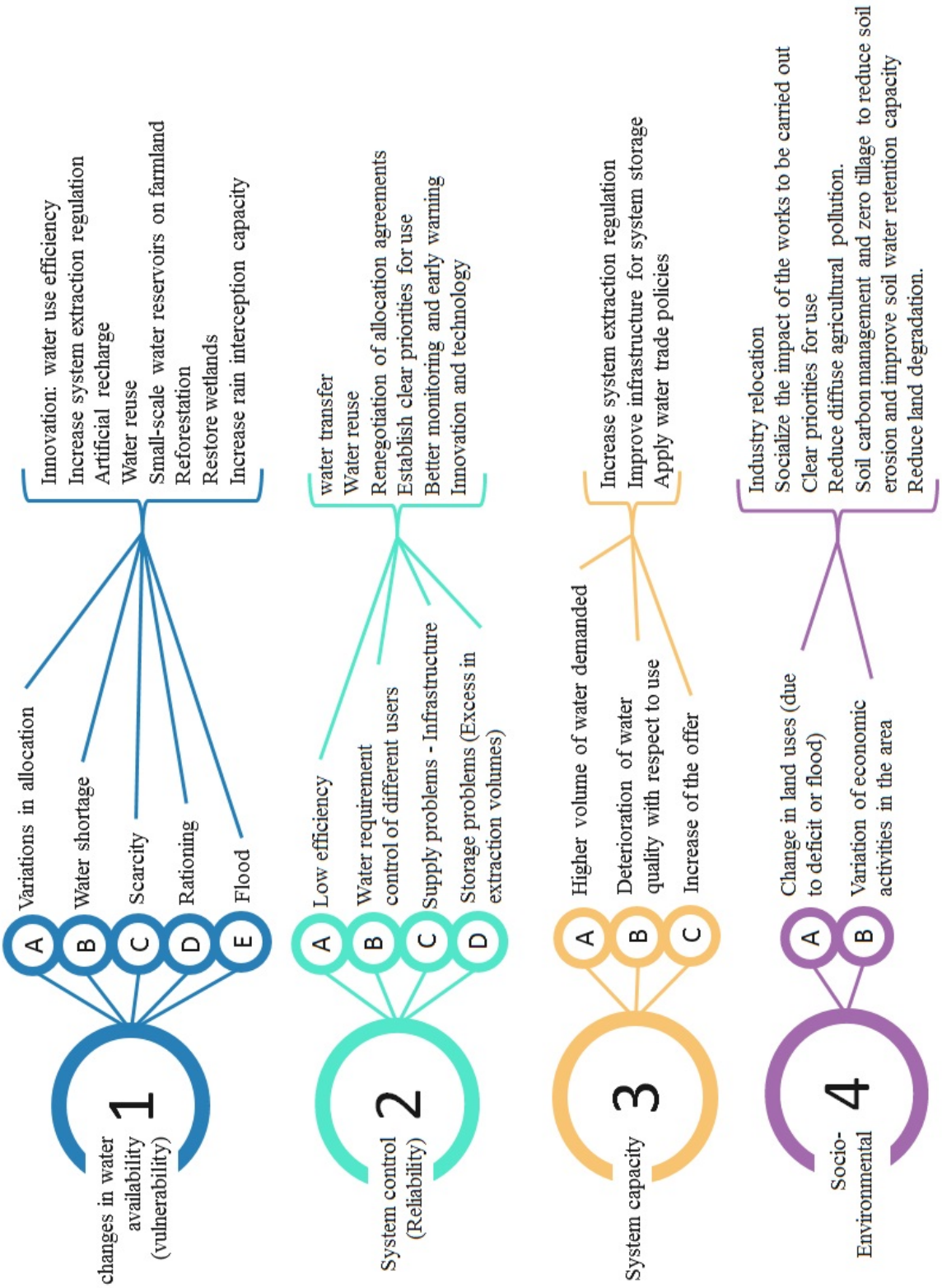

Figure **6-1**.: Management, planning, and adaptation strategies used in the model.

Is	Iw	Iu	Ir		
			High	Intermediate	Low
High	High	High		1 A	1 A-B
		Low		1A 2C	1 A 2 B-C
	Low	High		1 A	1 B 2 A-B-C
Intermediate	High	Low	1 B 3 A	1 B C	1 C D
	Low	High	1 A 2 C D 3C	1 A E 2 D 3C	1 A 2 D 3 C 4 A B
Low	High	Low	1 A B C 4 A B	2 A B C 4 A B	1 B C D 2B 4 A B
	Low	High	1 A E 2 A B 3 B C 4 A B	1 A 2A B C 4 A B	1 C D 2 A B C 3 B 4 A B
		Low	1 A B C 2 C 3 B 4 A B	2 C D 3 C 4 A B	1 A 2 A B C 4 A B

Figure **6-2**.: System characterization through to problems identification base on the management, planning, and adaptation strategies used in the model at the study area. Adapted from Pulido-Velazquez et al. (2011)

6.4. Results

6.4.1. Management strategies proposed for allocation process.

The management model was used to calculate the described indices in the previous section, in a current scenario, and in the three scenarios (defined with the combination of future estimated hydrology, and different hypothesis regarding possible demand, and water quality and availability). Indexes obtained for those scenarios were calculated on a monthly basis, assuming an average medium behavior of the current condition that was evaluated. Figure **6-3** shows the correlation between I_s and I_r indexes. The results from $ESC1$ (Figure **6-3**-A)

do not evidence problems of vulnerability and reliability, given the fact that water availability and the offer *vs* demand relation is high. In $ESC2$ (Figure **6-3**-B) correlation values are presented for the indexes I_s and I_r between 80% and 60%, which indicates that there are changes in water availability, problems of system control, and possible affectations around its capacity.

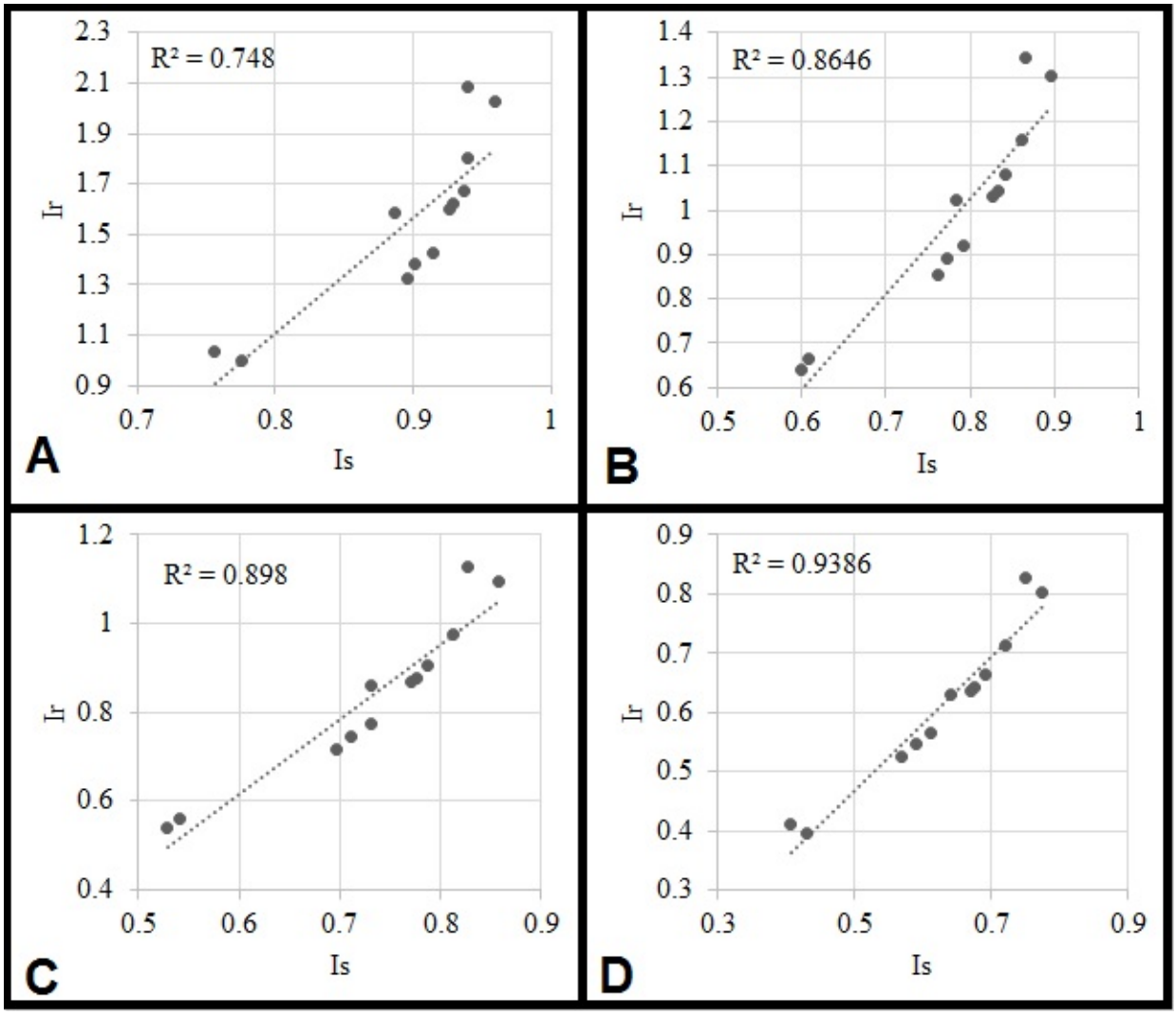

Figure **6-3**.: Correlation between I_s and I_r indices. A- Shown the correlation in the current situation. B- Shown the correlation at thirty years. C- Shown the correlation at one hundred years. D- shown the correlation at two hundred years.

The I_w and I_u indexes analysis (Figure **6-4**-A), shows that for this scenario the main cause of the problem is given by the low values of I_w that linked the changes in water availability with variations in the assignment and possible problems of flooding.

Additionally, this scenario may present system control problems given the excesses in the

volumes of water extraction. Given the management, planning, and adaptation strategies the $ESC2$ would find itself in the situation proposed in Figure **6-5**- Black Line.

The $ESC3$ and $ESC4$ present the same tendency of $ESC2$ and the correlation values in the indexes I_s and I_r can be found between 40% and 60% (Figure **6-3**-C and D). In these scenarios, the indexes I_w and I_u analysis (Figure **6-4**-C and D) show that the problems of the system may be associated to the low delivery efficiency and the water transit in the system, also to the lack of control of the water requirements between different users. Given the management, planning and adaptation strategies, the $ESC3$ and $ESC4$ will be encountered in the situation established in Figure **6-5**- Red Line.

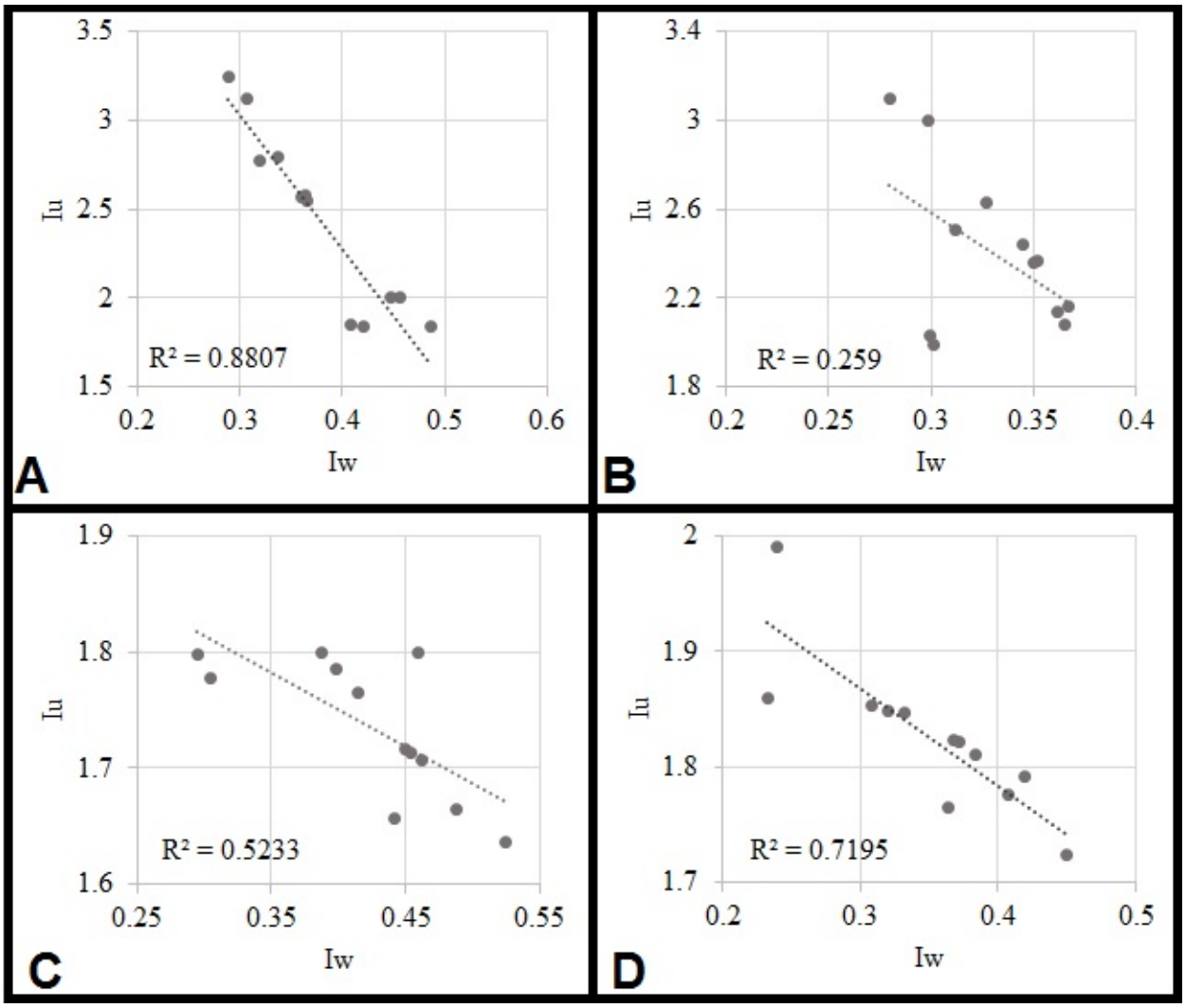

Figure **6-4**.: Correlation between I_w and I_u indices. A- Shown the correlation in the current situation. B- Shown the correlation at thirty years. C- Shown the correlation at one hundred years. D- shown the correlation at two hundred years.

Is	Iw	Iu	Ir: High	Ir: Intermediate	Ir: Low
High	High	High		1 A	1 A-B
		Low		1A 2C	1 A 2 B-C
	Low	High		1 A	1 B 2 A-B-C
Intermediate	High	Low	1 B 3 A	1 B C	1 C D
	Low	High	1 A 2 C D 3C	1 A E 2 D 3C	1 A 2 D 3 C 4 A B
Low	High	Low	1 A B C 4 A B	2 A B C 4 A B	1 B C D 2B 4 A B
	Low	High	1 A E 2 A B 3 B C 4 A B	1 A 2A B C 4 A B	1 C D 2 A B C 3 B 4 A B
		Low	1 A B C 2 C 3 B 4 A B	2 C D 3 C 4 A B	1 A 2 A B C 4 A B

Figure **6-5**.: Management strategies for scenarios $ESC1$, $ESC2$, $ESC3$ and $ESC4$ based on problem identification. The red line represents the expected situation for scenarios $ESC1$ and $ESC2$. The black line represents the system analysis for $ESC3$ and $ESC4$.

The results showed, allow us to infer that high values in domestic water demand (as a result of the $ESC2$, $ESC3$ and $ESC4$) may produce an increase in the necessity of water extraction, therefore the system responds with high values of I_u. Additionally, the evaluated system evidences that the values of I_s and I_r indexes will increase in accordance, as the extraction rates get higher. If the management strategies contemplate the possibility of making more

flexible the joined water usage by different users or increase the reuse rates (decreasing the pressure and restrictions of extraction volumes), the demand in $ESC2$ and $ESC3$ will be supplied with less.

6.4.2. Management Strategies Analysis.

Analysis by scenario of the management, planning and adaptation strategies, based on the risks and the potential benefits are shown in the Table (**6-1**). The strategies suggested, do not necessarily constitute an exhaustive list, or restricts in any way the adaptation and inclusion of others instead of the proposal here. These strategies do not make up a set of policies but try to reflect an idea that may be appropriated within different political or institutional guidelines to edifice the variables of impact in future scenarios. In this analysis is required that implementation of management planning and adaptation strategies, depend on local, regional, and national conditions. The regions with social and economic inequality must contribute to the management policies to be focused on efficient and fair water assignment, that produce economic and health benefits.

The lastly detailed strategies allow inferring that the water assignment processes, the interventions, and regulation must consider in the solutions the water supply and the demand (Navarro-Chaparro et al., 2015; Ki-moon et al., 2014; Harmanny & Malek, 2019). In so far as to the offer, the planning, adaptation and management strategies involve an increase in the storage volume or the water extraction. In demand, the strategies focus on how to increase the efficiency of water allocation to ensure that the economic and social benefit is maximized throughout the usage in sectors of higher value (Gleick & Palaniappan, 2010; Lionboui et al., 2018). This allows to stand out that the importance of the water resource in productive and social scopes require that policies and management strategies are well aware of the generalized impacts of water.

Considering the scenarios with variable conditions to availability and water quality, it is evident that the reallocation of water resources is a key action of adaptation to approach the possible problems of water shortage. In parallel, it could be considered as potential solutions in the changes and improvements of infrastructure, the land use or the definition of usage priorities (Iglesias et al., 2018; Iglesias & Garrote, 2015; Alameddine et al., 2018). Additionally, it is necessary to consider that these processes of allocation and decision making might lead to conflicts between different users, it is essential to incorporate the interests of the different parties (Pulido-Velazquez et al., 2018; de Sousa Fragoso & de Almeida Noéme, 2018; Pereira et al., 2019).

Table **6-1**.: Management strategies to different scenarios with risks and opportunities.

Scenario	Index	Problem	Strategies.	Level[1]	Category[2]	Time Scale[3]	Technical Difficulty[4]	Potential Cost[5]	Potential Benefits[6]
$ESC1$	1	A	Innovation: water usage efficiency.	Us, Mu	Mg	M	M	M	H
		E	Increase the system extraction regulation and increase the regulation volume available for water conservation.	P, Mu	Mg	M, L	H	H	H
	2	C	Water reservoirs and water allocation for environmental and consumptive uses.	Us, Mu, P	Mg, In	L	M	H	H
		D	Better monitoring and early alert.	Mu, P	Mg	M	M	M	H
			Increase the system extraction regulation	Mu, P	Mg	M	M	M	H
	3	C	Improve infrastructure for storage in the system.	Mu	In	M, L	H	H	H
$ESC2$	1	A	Innovation: water usage efficiency.	Us, Mu	Mg	M	M	M	H
	2	A	Increase the system extraction regulation and increase the regulation volume available for water conservation.	P, Mu	Mg	M, L	H	H	H
		C	Water reservoirs and water allocation for environmental and consumptive uses.	Us, Mu, P	Mg, In	L	M	H	H
		D	Better monitoring and early alert.	Mu, P	Mg	M	M	M	H
	3	C	Increase the system extraction regulation.	Mu, P	Mg	M	M	M	H
	4	A	Improve infrastructure for storage in the system.	Mu	In	M, L	H	H	H
		B	Industry relocation.	Mu	Mg	L	H	H	H
			Clear priorities for usage.	P	Mg	M	L	L	H
$ESC3$ and $ESC4$	1	C	Innovation: water usage efficiency.	Us, Mu	Mg	M	M	M	H
		D	Increase the system extraction regulation.	P, Mu	Mg	M, L	H	H	H
	2	A	Water reservoirs and water allocation for environmental and consumptive uses.	Us, Mu, P	Mg, In	L	M	H	H
		B	Better monitoring and early alert.	Mu, P	Mg	M	M	M	H
		C	Increase the regulation volume available for water conservation.	P, Mu	Mg	M, L	H	H	H
	3	B	Improve infrastructure for storage in the system.	Mu	In	M, L	H	H	H
	4	A	Industry relocation.	Mu	Mg	L	H	H	H
		B	Clear priorities for usage.	P	Mg	M	L	L	H
			Socialize the impact of future works to be performed.	P	Mg	M	L	L	H

Users level (Us), policy level (P), and Municipality Level (Mu); [2] Management (Mg) or infrastructural (In); [3] short time (S), medium time (M) or long time (L); [4–6] low (L), medium (M) or high (H).

Reference processes around the water policies design have been establishing in several countries. For example, in Europe, the EUWFD promotes public participation in the allocation processes, decision making and policies around the management and handling of water. Relly & Sabharwal (2009); Choi (2018); Garrido-Rodríguez et al. (2019) assures that the users and communities demand more bluntly to be included in the processes used to assign resources and watch for these to be transparent, based on scientific evidence and to give results that can be of public interest. For that, a better comprehension of how the user perceives the water system, its changes and needs, the adaptation policies and the factors that influence in the support to those management, planning and adaptation policies, may be a useful tool in the development of these political decisions. In the United States exists the reference to the design of water policies with an analytic focus. In this case, the general concern of communities for the state of the environment has increased the interest in participatory decision making.

The local and regional necessities and capabilities are based on the potential to develop new systems (Sordo-Ward et al., 2019; Garrote, 2017), implement efficient and adaptable technologies to the conditions and needs of the system (Fabre et al., 2016), ideas and technologic development to re-use water (González-Zeas et al., 2019), different alternatives of water management generation of groundwater (Hernández-Bedolla et al., 2017), water recollection techniques (López et al., 2019) and capacity to develop water markets (Harmanny & Malek, 2019).

With this, integration of the community, the environmental analysis of the systems, and the demands of water in the joint systems, permits the jointed management of surface and groundwater to overcome the dry periods and to provide sturdiness in the water resources systems (Pulido-Velazquez et al., 2011). Even though the local needs determine the scenario for adaptation, planning, and management, the cooperation is a priority that allows enlarging the knowledge transference generating local and regional resilience in the management strategies (Hashimoto et al., 1982; Escriva-Bou et al., 2017). Finally, given the costs and the lack of incentives associated with management planning and adaptation promotion capacity, is unlikely that water management would be enforced through the introduction of new independent policies, but rather through the revision and adaptation of existing policies (Iglesias et al., 2011, 2018).

6.5. Discussion and Conclusions

The main limitations of the management, planning and adaptation strategies for the handling of water systems, are set by the definition of metrics in all the analysis units. The main difficulty to develop efficiently this definition is ruled by the acting areas of the water resource within the communities and ecosystems.

In this research, it is evidenced the importance of quantifying the surface and groundwater offer to guarantee the economic development of the communities. Additionally, the offer quantification leaves open the necessity to regulate and determine the available water amount that can be used to cover the demand of communities and the environment. Likewise, it is evidenced that the water demand is influenced by social and economic factors of the community and in order to improve the efficient allocation processes it must acknowledge the bias that the economic value of water may generate to users with low acquisition capacities.

The analyzed scenarios show that the population up growth enlarge the existing demand patterns, which leads to the need of implementing planning, adaptation and management strategies that maximize the benefit in the domestic and agricultural sectors and that reduce the areas that in the future may present high levels of water stress. The analysis presented in this research does not contemplate projections of technologic change that optimize or improve the proposed scenarios. The assumption that the technological context and the development of current water infrastructure will be valid in the future is evidently wrong. The technologic change and innovation in the management of water resources will determine and will reorient the adaptation, planning, and management strategies that were considered here. Additionally, the analysis of the relation of cost-benefit of different strategies in management requires information about social and economic changes in the communities that are not contemplated in this research.

The political definition of clear guidelines that express the water rights may lead to the sustainability of different economic sectors trough research methods (Tian et al., 2016). Nevertheless, it has to consider that a favorable and equal governability may not be applied around the water resource management. Even though policies that develop financial incentives may lead to short term profits, they also may encourage unsuspected behaviors between users that may generate negative impacts. For this linking, engineering and economics around a social context are important, considering that the policies that are based in objectively verifiable indicators, will result to be adequate.

The analysis presented in this chapter gives an evaluation of the main management strategies, that can respond to risks and opportunities of future scenarios, in high variability climatic

zones. The results here consigned show that the most interesting management, planning, and adaptation strategies in terms of effort–benefit ratio are focused to: (*i*) improve the systems of groundwater monitoring, (*ii*) establish clear priorities of usage among different users and, (*iii*) regulate the water allocation between users to ensure a minimal conservation for the environment. Additionally, the results may also evidence that the beneficial management strategies in a regional scale are: (*i*) generation of a water marketplace, (*ii*) the improvement of infrastructure for water storage and, (*iii*) the negotiation of agreements for water assignment between users in an inclusive manner.

7. Conclusions and Outlook

7.1. Conclusions

The importance of characterize the water systems (surface water and groundwater) is based in the implicit need of communities to survive and develop. Water as a vital subject for sustainable development is determinant for social and economic development, water also is a main concern when climate changing are faced. Given this situation, the water resource is constituted as the main link between society and the environment, and thus, it generates the need for conciliate the water demands. This impose the necessity for works and methods that allow to understand the behavior of water systems, and also to foresee several explanations to their complex behavior. Within those systems, groundwater flow in shallow aquifers are part of the hydrological cycle, and they are affected by variability in recharge processes and by human intervention. In the last years, water (mainly groundwater) has emerged as an important topic given the increase in activities that requires provisioning from a water source. Water supply to communities, agricultural development, mining, industry, and exploration and production of O&G have led to seek different techniques that provide information in specific scales. These techniques have analyzed the water systems based in simulations, transformations, mathematical expressions, numeric models, and geo-statistical correlations, without focusing in obtaining equivalent models and parameters that can be totally reliable to represent different conditions.

This document is an attempt to characterize a water system (surface water and groundwater) in an economical framework to determine strategies of management in a regional scale. This objective involved to perform different tests and analysis that allowed to integrate those aspects. To evaluate the efficiency of the proposed model and techniques, it was used the MMV as a real scenario. First the system was characterized and recharge was defined, taking in consideration that hydrological modelling is the base for integral water resource management, and also the fact that in basins of the valley there is a complex interaction of physical and chemical processes. For this, it was analyzed the interaction between the hydrological cycle and the climatic conditions, observing that the used modelling patterns in this research, even on other research made in the area, do not reproduce in an exact manner the singularities of analyzed hydrograms. These differences in hydrograms representation

were applied mainly in base flow simulation and this behavior was attributed to the ignorance of ground characteristics and the inability of the model to represent in detail deep percolation processes. To establish temporal and spatial relations for this parameters it was necessary to identify the range in which the parameters were adjusted to observed data and face them with a posterior simulation period to assure this correlation. Given this, the completed sensitivity analysis allowed to conclude that parameters that are involved in the model behavior and the interaction of surface water and groundwater are the transmissivity recession curve, the storage deficit in root zones, and the initial flow characteristics. These results were useful to understand the hydrological dynamic in the valley area, the initial flow is correlated with physical conditions of the basin, and that this flow vary depending in the analyzed period; although this conclusion is obvious given the fact that the hydrological cycle is dynamic, it was useful to establish similarities between different time periods in specified basin areas that provide ideas in how the drainage networks and the superficial runoff velocity are going to behave. The condition of saturation in the low end of the model caused a decrease in surface flow quantity, due to gradient soil moisture decrease, that in consequence, increased the superficial runoff. This allow to conclude that the influence of evapotranspiration in hydrological behavior in the area through soil moisture analysis.

The hydrological characterization results, added to the geologic description of the area, allowed to propose a conceptual hydrogeological model for MMV. In this model established the correlation of superficial conditions with the hydraulic conductivity. The conceptual model was validated trough a numeric model simulate groundwater flows and the flow directions, there, it was seen that the representation of hydraulic conductivity and the thickness of modelled aquifer variations were variables in time and space. This information led to evaluate geo-statistical techniques that allowed to represent in a more appropriate way, the zone characteristics. Although the MMV is a high ecologic, social and economic area of importance for the country, it does not show an adequate relation between groundwater information points, affecting flow behavior pattern determination. Additionally, groundwater system characterization allowed to conclude that geostatistical methods reduce the errors in determination of hydraulic properties. The sensitivity analysis performed, allowed to identify which parameters govern the model behavior and quantify the correlation with defined geological units. The hydrogeological modelling results allowed to conclude that hydraulic conductivity, the porosity and the specific storage directly rule the flows and flow directions in the aquifers. The conclusions about the hydraulic conductivity establishment, allowed to identify a clear correlation of superficial layers parameter that represent the Quaternary aquifer. The uncertainty in the identification of characteristics in higher depths than 600 m, biased the initial interpretation results established in the conceptual model. The results in this geological units allowed to identify equifinality problems in some areas specified in the model. The conclusion in the stage allowed to establish that flow directions are mainly direction from South to North. Additionally, some areas in the model add flows

of West and East limits. The Jurassic and Cretaceous units are identified as water dividers. This behavior is concluded from the low values of conductivity, an interesting fact is this model, is that the estimated field reflected defined geological structures in a large scale, which were perceive in the conceptual model trough the constant zone definition.

Finally, the integration of these aspects in the economic optimization model, allow to determine management strategies from an allocation process based in usage, amount, and water quality. These strategies were proposed in the development of four scenarios. The general analysis of these scenarios allowed to consolidate a series of important ideas about global effects of different economical activities that can be prioritized. The results of this integration showed that the demographic increase and the water need changes in economic developments raise the demand patterns. The general conclusions of this investigation are focused in provide strategies that allow to establish a balance between water resource use, and ecosystem protection. Thus, it is concluded that integral water management is restricted by: (*i*) the limitations in the allocation processes, (*ii*) information identification that allow to correlate problems to evaluate the management capacity and (*iii*) the difficulty to quantify the real offer and demand of water. The uncertainty in hydrological modelling (surface and groundwater) and long term planning are added to the complexity of management strategies. Because of this, the knowledge transference, and technology to define policies and rules, are essential to allow an adaptive action of water needs and usages. The need to strengthen the knowledge base towards hydrodynamic processes through investigation, will not be enough to modify and boost the management strategies in water resource planning.

With respect to specific impacts, it was concluded that there are significant variations between allocation regimes of users. Because of that, is evident that the need of involve the interested parties, trough the development of proper methodologies to evaluate the impacts, vulnerabilities and planning as a requirement for a profitable management. The direct influences in the water users' behavior, as changes in the demand, allocation and rate regulation, must be considerate in conjunction with variations of water offer. This allow to conclude that even though the strategies must be sustainable and participative, they also must be appropriated and relevant in relation with specific factors of each economic sector.

The outlook presented in this investigation allow to conclude in a general manner that the demographical increase raises the existing demand patrons. This leads to the necessity of implement planning strategies, adaptation and management that maximize the social benefits in the domestic and agricultural sectors. The analysis of the major strategies of management proposals in this investigation, respond to problems of different economic sectors in the area. These results allowed to conclude that the main management, planning, and adapting strategies in terms of effort-benefit ratio are centered in: (*i*) improve the monitoring systems for groundwater. Priorization of monitoring systems that allow to

understand and characterize the best existing conditions, the current and potential problems and establish priorities, policies and viable strategies for water resource management. (*ii*) establish clear priorities in usage between different users. The process of water management and planning must be dynamic and iterative, and must allow the interaction, learning and feedback between different users. This strategy will allow the simultaneous implementation of practices and activities according the needs of users without losing sight of the general context. And finally (*iii*) regulate the water allocation between users to guarantee a minimal conservation for the environment. To balance the increasing water demand between the aquatic and land ecosystems and the base flow in the upstream sections, will allow to analyze the bidirectional relations between the macroeconomic policies, the social and environmental objectives, the development, and the management and use of surface and groundwater. A last consideration about the implementation cost of management strategies allow to conclude that they are from low to medium cost and technically manageable in regional planning for the basin. Nevertheless, is also evident that there are strategies that require a large scale effort, either in the distribution network management or in the infrastructure development.

Finally, the novelty in this work is the combination and coupling of several tool of modelling and analysis, to a real case study in a tropical basin. The technics and metrics of validation used in this investigation, must be enlarged to guarantee their representativeness and to improve the hydrological and hydrogeological characterization, and the identification of allocation and usage problems. This way, there will be establish more reliable parameters, and more more accurate results.

7.2. Outlook

Characterization of MMV water system presented in this document allows to suggest future research focused on the following subjects.

- Hydrological models and coupled hydrodynamics and physically based that allow to identify hydraulic parameters in different scales. Evaluate the correlation of these parameters and establish mathematical models that represent the general characteristics of the systems must be addressed in new researches.
- The variation in water quality, that may interfere in surface water quality or worsen the groundwater quality. To analyze the interactions in the water systems and analyzes the decrease on flow velocity that raise the presence of dispersion phenomena. A study about the fluids re injection in aquifers must be approached to add planning tools, and decision making management.

- Generalized application of geo-statistical methods to hydro geologically characterize water systems, will allow to consider correlations of parameters and analyze the mathematical model behavior that allow to escalate the hydraulic conductivity. These studies will allow to reduce the uncertainty in areas where there is not a detailed information monitoring.
- Dynamic price policies could be established trough multi scale studies of integral water management, that include strategical environmental evaluations in different economic sectors

A. Annex: Initial Data

Hydrology Data

Name	Code Number	Category	Latitude	Longitude	Z	Missing Data (%)
Nus	23085080	CP	6.49	-74.84	835	5.25
Virginias	23090020	PM	6.39	-74.68	639	5.29
El Tigre	23100030	PM	6.84	-74.79	994	2.65
Apto OTU	23175020	SS	7.01	-74.72	718	7.03
El Bosque	27030090	PM	7.32	-74.84	220	0.74
Palma de Coco	27030140	PM	7.24	-74.81	100	3.98
La Sierra	24025030	CP	5.97	-73.16	2700	1.72
Pto Berrio	23095010	CP	6.47	-74.41	150	4.50
La Verde	23120010	PM	6.41	-73.90	305	1.22
Pto Araujo	23120200	PM	6.53	-74.08	159	8.34
Carare	23125050	CO	6.65	-74.06	168	6.50
Chucuri	23130010	PM	6.88	-74.03	100	1.80
Apto Yariguies	23155030	SP	7.03	-73.81	126	8.70
Yondó	23160010	PM	7.09	-73.94	140	5.15
Sabana Torres	23180070	PM	7.39	-73.49	176	6.39
Eloy Valenzuela	23180080	PM	7.49	-73.68	132	1.84
Villa Leiva	23185010	CP	7.46	-73.54	328	9.72
El Playon	23190140	PM	7.46	-73.20	500	7.55
El Picacho	23190300	PM	7.11	-72.97	3310	1.50
Matajira	23190340	PM	7.21	-73.06	996	0.02
Portachuelo	23190360	PM	7.33	-73.17	800	8.54
La Galvicia	23190400	PM	7.12	-73.06	1779	3.91
El Naranjo	23190440	PM	7.21	-73.30	825	4.29
El Pantano	23190600	PM	7.00	-73.23	1280	1.34
Piedecuesta	23190700	PG	6.99	-73.07	1000	1.95
Vivero Surata	23195090	CO	7.37	-72.99	1725	4.36
Llano Grande	23195110	CO	7.03	-73.17	777	6.44
Palonegro	23195130	SP	7.12	-73.18	1189	2.09
Cachiri	23195200	CO	7.47	-72.99	1850	2.84
La Comoda	24010110	PM	6.08	-73.47	1242	4.66
Confines	24010230	PM	6.36	-73.24	1523	5.81
Bolivar	24010640	PM	5.99	-73.77	2260	8.85
Olival	24010650	PM	6.15	-73.34	1502	1.49
Simacota	24010660	PM	6.44	-73.33	1050	1.80
Suaita	24010760	PM	6.10	-73.44	1617	6.36

Continued on the next page

Name	Code Number	Category	Latitude	Longitude	Z	Missing Data (%)
Guavata	24010820	PM	5.96	-73.70	2018	5.52
Chima	24015260	CO	6.36	-73.37	1090	4.08
Coromoro	24020120	PM	6.30	-73.04	1520	2.30
El Cucharo	24025020	CP	6.53	-73.20	975	9.55
Mogotes	24025040	CP	6.47	-72.97	1673	3.24
Cepita	24030300	PM	6.75	-72.98	600	3.55
El Tope	24030330	PM	6.94	-72.93	2050	3.21
Sta Isabel	24040050	PM	6.64	-73.21	1300	0.31
La Putana	24050070	PM	7.13	-73.52	150	1.46
Albania	24050110	PM	6.91	-73.63	300	0.94
Zapatoca	24055030	CO	6.79	-73.28	1810	4.49
Aguasclaras	24060040	PM	7.26	-73.55	188	0.65
La Mesa	24060050	PM	6.76	-73.09	1460	0.94
La Paz	24060060	PM	7.11	-73.42	180	1.22
La Parroquia	24060070	PG	7.08	-73.33	267	8.92
Hda Brisas	24065010	CO	7.25	-73.79	138	12.81
Campo Capote	23125040	CO	6.62	-73.92	180	13.23
Landazuri	23125130	CO	6.22	-73.81	1085	2.92
Pte Ferrocarril	23140040	PM	6.77	-73.94	90	3.74
Pto Wilches	23180020	PM	7.35	-73.89	128	6.11
El Porvenir	23180040	PM	7.45	-73.48	154	1.04
La Coquera	23180120	PM	7.22	-73.92	170	2.29
Tona	23190130	PM	7.20	-72.97	1910	2.01
Laguna	23190260	PM	7.08	-73.21	1050	8.58
Palo Gordo	23190280	PM	6.97	-73.13	950	0.33
Llano de Palmas	23190350	PM	7.24	-73.20	778	0.97
Palmas	23190380	PM	7.21	-73.22	855	3.06
Cooperativo	23205020	CO	7.48	-73.93	165	5.37
Oiba	24010240	PM	6.26	-73.30	1400	2.18
La Laja	24015250	CO	6.24	-73.42	1400	3.26
Velez Granja	24015270	CO	6.00	-73.67	2170	2.35
Encino	24020040	PG	6.14	-73.10	1814	8.64
San José	24020080	PM	6.44	-73.14	1300	0.40
Curiti 2	24020130	PM	6.60	-73.06	1626	1.07
Charala	24025050	CO	6.27	-73.15	1350	8.37
Remolino	24040060	PM	6.61	-73.28	630	0.82
San vicente	24050060	PM	6.87	-73.41	721	0.62
La Fuente	24050100	PM	6.71	-73.28	815	3.36
Pto Boyacá	23115010	CO	5.98	-74.57	350	8.68
Pto Berrio-Aut	23097030	LG	6.49	-74.40	108	0.67
San Pablo-Aut	23207040	LG	7.48	-73.92	64	19.62

Points Inventory - Observation Points in Steady State

x	y	Q (m^3)	Level	Depth	Radius	Z	top	bottom
975497	1184466	9.07	6.0	38	0.0762	146.2	140.2	108.2
978367	1196624	146.88	18.3	38	0.0762	150.0	131.7	112.0
991395	1198951	80.64	17.1	25	0.0508	160.8	143.7	135.8
988823	1207855	103.68	7.9	20	0.0508	122.9	115.0	102.9
989394	1209989	80.64	18.3	38	0.0508	135.6	117.3	97.6
1010571	1259484	15.26	2.0	8.91	0.1651	73.1	71.1	64.2
1010191	1259529	9.50	0.8	7.15	0.0127	77.8	77.0	70.7
1012465	1260133	4.78	1.3	4.5	0.0127	76.9	75.7	72.4
1012153	1260146	53.28	4.4	7	0.0127	91.4	87.0	84.4
1012800	1260184	1.44	0.5	1.54	0.01524	92.6	92.1	91.1
1013313	1260320	39.74	3.4	4.2	0.0127	76.5	73.1	72.3
1009463	1260467	20.16	3.8	0.12	0.3175	94.9	91.1	94.8
1013196	1260494	26.21	3.4	30	0.0127	86.5	83.1	56.5
1013224	1260503	11.81	3.0	4	0.0127	87.6	84.6	83.6
1013284	1260513	12.10	3.4	90	0.002032	90.6	87.2	0.6
1013451	1260656	15.84	102.0	1	0.01905	84.9	-17.1	83.9
1011176	1260660	10.37	0.5	1	0.01778	77.5	77.0	76.5
1011832	1260737	9.79	2.6	2	0.0127	84.1	81.6	82.1
1011534	1261027	12.38	3.1	24	0.001524	81.5	78.4	57.5
1012010	1261836	79.78	1.3	31	0.001524	86.0	84.7	55.0
1014643	1261973	6.34	0.9	2	0.00762	78.9	78.0	76.9
1016614	1263818	3.74	2.5	358	0.003175	86.3	83.8	-271.7
1015233	1264063	15.84	4.4	50	0.000762	98.6	94.2	48.6
1015537	1264162	2.88	2.2	388	0.003175	92.5	90.3	-295.5
1016819	1264484	11.81	1.3	32	0.001524	87.3	86.0	55.3
1015625	1265058	9.50	10.5	1.6	0.023495	67.7	57.2	66.1
1018309	1276957	7.32	1.8	7.5	0.001143	71.6	69.8	64.1
1018293	1277517	6.91	3.2	7	0.001143	72.7	69.5	65.7
1018692	1277546	4.90	2.4	9	0.001143	74.0	71.7	65.0
1018809	1277605	16.99	0.9	11	0.001524	73.6	72.7	62.6
1018691	1277656	11.81	2.7	11	0.000762	72.8	70.1	61.8
1018432	1277676	10.08	1.1	16	0.000762	76.5	75.4	60.5
1017014	1277931	12.10	4.4	3	0.0127	71.3	66.9	68.3
1018736	1278595	23.90	2.2	8	0.0127	66.3	64.2	58.3
1018700	1278846	10.66	1.9	6.5	0.001524	67.0	65.1	60.5
1024130	1278908	15.84	5.5	8	0.01397	71.8	66.4	63.8
1023910	1278981	7.78	3.5	6	0.0127	75.3	71.8	69.3
1018438	1279046	8.93	2.1	12	0.001524	62.7	60.6	50.7
1023907	1279056	288.00	8.8	43	0.00129	77.5	68.7	34.5
1018719	1279125	15.84	2.5	9	0.001143	73.0	70.5	64.0
1023853	1279268	57.60	9.9	11	0.015875	81.0	71.1	70.0
1024572	1279277	23.90	2.7	6	0.01397	75.6	72.9	69.6
1024147	1279443	19.01	9.6	13.5	0.01397	81.5	71.9	68.0
1018773	1279485	0.04	2.3	9	0.002286	68.8	66.5	59.8

Continued on the next page

x	y	Q (m^3)	Level	Depth	Radius	Z	top	bottom
1024023	1279585	10.08	6.9	10	0.01397	82.1	75.3	72.1
1017263	1279610	47.81	3.8	3.7	0.0127	72.9	69.1	69.2
1023687	1279663	11.52	6.5	9	0.01397	77.1	70.7	68.1
1018696	1279706	3.74	2.0	9	0.001524	69.8	67.8	60.8
1018396	1279806	8.35	3.5	7	0.001524	71.2	67.7	64.2
1024075	1279831	3.17	10.5	13	0.01397	83.1	72.6	70.1
1018425	1279906	8.35	3.3	12	0.001524	70.8	67.5	58.8
1023999	1279961	23.90	10.0	12	0.01397	81.0	71.0	69.0
1024223	1280182	7.78	1.7	2.66	0.0127	69.2	67.6	66.6
1024228	1280378	23.90	2.1	5	0.0127	70.8	68.7	65.8
1018685	1280536	7.78	2.1	11	0.000762	71.5	69.5	60.5
1023829	1280821	23.90	4.0	6	0.01397	74.0	70.1	68.0
1018388	1280847	24.48	1.0	7.5	0.001143	73.8	72.8	66.3
1025423	1281125	31.68	10.5	14	0.01397	97.8	87.3	83.8
1018326	1281567	8.35	2.0	4.3	0.0127	61.1	59.1	56.8
1018189	1281607	37.15	2.8	21	0.001524	74.7	71.9	53.7
1025800	1282203	11.81	6.5	8	0.01397	94.4	87.9	86.4
1026374	1282333	11.81	8.8	12	0.01397	97.1	88.3	85.1
1026294	1282446	23.90	2.7	5	0.01143	95.4	92.6	90.4
1026247	1282467	15.84	2.7	4	0.01397	94.4	91.7	90.4
1025774	1282649	47.81	6.0	8.25	0.01397	90.6	84.7	82.4
1026332	1282673	31.68	1.4	2.5	0.01397	89.2	87.8	86.7
1025030	1282724	47.81	0.7	3.2	0.01397	76.1	75.4	72.9
1025518	1282726	39.74	5.6	7.38	0.01397	83.0	77.4	75.6
1025431	1282797	7.78	0.6	2.77	0.01397	80.1	79.6	77.4
1026334	1282797	15.84	1.0	3.5	0.01397	87.5	86.5	84.0
1026570	1282817	23.90	1.3	4.38	0.01397	76.1	74.8	71.7
1026448	1282820	10.66	1.4	2.5	0.0254	87.0	85.6	84.5
1026080	1282929	7.20	3.9	9.4	0.01397	90.1	86.2	80.7
1025924	1283042	0.75	3.5	10	0.01397	87.3	83.8	77.3
1026378	1283164	46.08	1.2	3	0.0127	88.4	87.2	85.4
1026123	1283184	15.84	2.2	3.2	0.0127	85.2	83.0	82.0
1026829	1283243	46.08	2.3	3.5	0.01524	72.2	69.9	68.7
1025747	1283578	11.81	2.8	9	0.01397	81.3	78.5	72.3
1025819	1283824	11.81	1.9	4.1	0.01397	76.7	74.8	72.6
1019033	1283854	8.35	1.2	5	0.0508	80.1	78.9	75.1
1016905	1283971	9.22	3.2	30	0.000254	69.7	66.6	39.7
1025115	1283994	31.68	5.6	7	0.01397	76.5	70.9	69.5
1025562	1284008	6.34	3.7	6	0.01397	77.2	73.5	71.2
1027796	1284192	31.68	1.5	7.15	0.01397	80.2	78.6	73.0
1027647	1284332	15.84	0.7	7	0.01397	85.1	84.4	78.1
1027652	1284505	24.77	2.7	5.3	0.01397	87.0	84.3	81.7
1027815	1284615	7.78	1.0	4.3	0.01397	89.6	88.6	85.3
1027278	1284674	7.78	0.9	4	0.01397	77.5	76.6	73.5
1026142	1284714	63.36	3.3	7	0.01397	75.4	72.1	68.4
1027560	1284816	11.81	0.9	3.12	0.01397	85.2	84.3	82.1

Continued on the next page

x	y	Q (m^3)	Level	Depth	Radius	Z	top	bottom
1018518	1284976	63.36	0.6	3.32	0.0127	69.1	68.5	65.8
1026385	1284993	23.90	3.0	5	0.01397	79.6	76.6	74.6
1028172	1285067	95.04	4.8	6	0.01397	77.4	72.5	71.4
1026659	1285089	15.84	2.4	7	0.01397	93.5	91.1	86.5
1027555	1285211	23.90	1.7	4.73	0.01397	83.2	81.5	78.5
1027890	1285432	23.90	1.1	5	0.01397	79.2	78.1	74.2
1015844	1285504	15.26	2.0	0.8	0.02667	62.0	60.0	61.2
1028024	1286164	95.04	8.0	14	0.0127	94.5	86.5	80.5
1028755	1286383	15.84	1.2	3	0.01143	78.9	77.7	75.9
1027562	1286404	17.86	1.0	4	0.01397	72.9	71.9	68.9
1029190	1286436	7.78	1.1	2.8	0.0127	81.5	80.4	78.7
1028632	1286462	15.84	0.9	4	0.0127	77.0	76.1	73.0
1029095	1286547	46.08	1.8	6	0.0127	80.1	78.2	74.1
1012601	1287242	8.06	1.9	2.5	0.0127	73.9	71.9	71.4
1014458	1287378	10.08	0.5	24	0.001524	67.2	66.7	43.2
1029971	1287509	66.24	5.0	9	0.02032	82.7	77.7	73.7
1022068	1288246	0.99	8.0	9	0.0762	68.3	60.3	59.3
1022343	1288503	11.81	3.0	7	0.000806	68.6	65.6	61.6
1022616	1288667	8.06	6.0	12	0.000484	77.0	71.0	65.0
1022672	1288693	7.20	7.0	12	0.000484	74.4	67.4	62.4
1023159	1288901	4.03	6.0	11	0.000484	68.5	62.5	57.5
1023014	1288948	28.80	6.0	10	0.000484	76.9	70.9	66.9
1023270	1288957	0.79	1.7	3	0.00635	71.0	69.3	68.0
1023353	1289024	15.84	4.5	10	0.000484	69.5	65.0	59.5
1023835	1289314	6.05	4.0	10	0.000484	73.3	69.3	63.3
1024918	1289330	11.52	1.2	7	0.000484	72.8	71.6	65.8
1024178	1289612	3.74	4.0	10	0.000484	72.4	68.4	62.4
1025800	1290658	12.67	2.4	8	0.01397	74.7	72.3	66.7
1029543	1290781	2.43	1.5	3.5	0.009779	75.6	74.1	72.1
1015894	1290804	5.76	0.4	32	0.001524	68.4	67.9	36.4
1029520	1291054	2.38	2.2	4.5	0.00635	70.0	67.8	65.5
1027087	1291217	17.28	4.0	7	0.0127	79.9	75.9	72.9
1034557	1291223	31.68	2.5	7	0.01397	80.8	78.3	73.8
1027160	1291230	13.25	3.9	10	0.01397	75.5	71.6	65.5
1029215	1291943	9.50	7.9	14	0.0127	81.4	73.5	67.4
1028821	1292016	23.90	0.9	7.15	0.01143	85.0	84.1	77.9
1029521	1292138	0.39	3.5	8.5	0.017399	85.4	81.9	76.9
1029592	1292270	0.59	4.0	6	0.01524	89.8	85.8	83.8
1031457	1292857	0.99	6.0	15	0.0127	94.7	88.7	79.7
1032120	1292890	15.84	8.5	10	0.01524	84.2	75.7	74.2
1031697	1293002	31.68	6.5	13	0.01524	92.1	85.6	79.1
1032695	1293017	6.30	5.0	8.57	0.019812	84.0	79.0	75.4
1032100	1293097	15.84	7.0	14	0.0127	83.9	76.9	69.9
1032413	1293354	23.90	2.5	5	0.0127	84.0	81.5	79.0
1032200	1293914	2.38	1.4	4.28	0.01524	92.7	91.3	88.4
1032230	1294105	0.49	2.9	6.25	0.02032	94.9	92.1	88.7

Continued on the next page

x	y	Q (m^3)	Level	Depth	Radius	Z	top	bottom
1016469	1294132	44.93	5.0	4.6	0.0127	62.0	57.0	57.4
1032272	1294384	2.16	2.4	5.69	0.02032	97.4	95.0	91.7
1032071	1294490	5.76	4.7	6	0.01397	96.0	91.3	90.0
1032375	1294755	28.80	2.3	10	0.01397	92.4	90.1	82.4
1032463	1294910	27.65	1.9	10	0.01397	92.2	90.4	82.2
1016684	1295258	4.61	2.7	237	0.003175	61.6	59.0	-175.4
1016452	1295362	26.50	0.7	13	0.001524	64.5	63.8	51.5
1016443	1297743	10.66	2.7	18	0.000762	67.8	65.1	49.8
1016505	1299592	18.72	1.5	10.8	0.001524	66.4	64.9	55.6
1013014	1303611	23.33	1.9	2.6	0.0127	59.7	57.8	57.1
1016392	1304903	9.50	0.9	2.5	0.0127	61.8	60.9	59.3
1019212	1313972	9.22	1.6	3.05	0.0127	57.8	56.2	54.7
1019151	1315474	5.47	1.2	3	0.0127	60.9	59.7	57.9
1016738	1316342	7.20	7.9	27	0.001524	61.3	53.4	34.3
1018227	1316397	6.91	1.5	33	0.001143	58.6	57.1	25.6
1017665	1316929	18.43	3.5	27	0.000762	59.5	56.0	32.5
1017142	1318401	19.87	4.6	6.49	0.0127	71.6	67.1	65.1

Observation Points in Transient State

X	Y	Jan	Febr	Mar	Apr	May	Jun	Jul	Aug	Sept	Oct	Nov	Dec
996087	1144836	157	154	177	219	232	191	162	151	165	215	238	201
1003087	1144836	146	143	164	203	217	181	154	145	158	203	222	187
1010087	1144836	139	136	154	192	206	176	151	144	156	194	209	176
1017087	1144836	151	148	164	200	215	190	168	160	172	204	214	184
1024087	1144836	167	165	179	213	228	208	188	179	190	217	225	196
989087	1151836	164	162	186	230	244	201	169	157	172	226	251	212
996087	1151836	154	152	175	217	231	191	161	150	165	215	237	199
1003087	1151836	144	142	162	203	217	181	152	143	158	203	222	186
1010087	1151836	135	133	152	191	205	173	146	138	154	193	208	174
1017087	1151836	129	127	144	181	196	168	144	137	151	186	198	165
1024087	1151836	126	124	140	177	192	167	144	137	151	182	192	161
989087	1158836	161	160	183	229	243	200	167	155	172	225	249	210
996087	1158836	152	150	172	216	230	190	158	147	165	214	236	198
1003087	1158836	143	141	162	204	218	181	151	141	159	205	223	186
1010087	1158836	137	135	154	195	209	175	146	138	156	197	212	177
1017087	1158836	131	129	148	188	202	170	143	136	153	191	204	169
1024087	1158836	126	125	143	183	197	168	141	134	151	187	197	164
1031087	1158836	124	123	141	182	197	167	140	133	150	186	196	162
961087	1165836	184	185	212	266	281	236	203	182	196	257	290	247
968087	1165836	181	181	208	260	274	229	195	176	191	252	283	240
975087	1165836	174	175	201	251	265	219	185	168	185	244	273	231
982087	1165836	167	166	191	240	254	209	174	160	178	235	261	220
989087	1165836	158	157	181	228	242	198	164	152	171	225	248	208
996087	1165836	151	149	172	217	231	189	156	145	166	216	236	197
1003087	1165836	144	143	164	207	221	182	150	141	161	208	226	188
1010087	1165836	139	137	158	201	215	178	146	138	159	202	218	181
1017087	1165836	135	134	153	196	211	175	145	137	157	199	212	176
1024087	1165836	132	131	151	195	210	175	145	137	157	198	210	173
1031087	1165836	131	131	152	197	212	176	146	138	158	200	211	173
1038087	1165836	131	132	154	200	215	179	148	140	159	202	213	174
1045087	1165836	133	135	157	205	220	182	152	143	162	206	216	176
961087	1172836	186	187	215	270	285	240	206	186	201	262	294	249
968087	1172836	182	182	209	263	277	231	197	178	196	256	286	242
975087	1172836	175	176	202	253	268	222	186	170	189	248	276	233
982087	1172836	167	167	192	242	256	211	175	160	181	238	264	221
989087	1172836	159	158	182	230	244	199	164	151	174	228	251	209
996087	1172836	151	150	173	219	233	190	155	144	167	218	238	198
1003087	1172836	145	144	166	211	225	183	149	140	163	212	229	190
1010087	1172836	142	141	162	207	222	181	147	138	162	209	225	186
1017087	1172836	139	139	161	207	222	182	148	139	163	210	224	184
1024087	1172836	139	139	162	209	225	185	151	142	165	212	226	185
1031087	1172836	140	141	164	213	229	188	154	145	168	216	229	186
1038087	1172836	141	143	167	217	234	193	159	150	172	220	232	189
1045087	1172836	144	147	171	223	240	198	164	156	178	226	237	192

Continued on the next page

X	Y	Jan	Febr	Mar	Apr	May	Jun	Jul	Aug	Sept	Oct	Nov	Dec
954087	1179836	203	205	234	293	307	261	228	205	222	285	317	269
961087	1179836	198	199	227	283	298	253	219	198	216	276	307	261
968087	1179836	191	192	219	273	288	242	207	189	208	267	296	252
975087	1179836	183	183	210	262	277	231	195	178	199	257	285	241
982087	1179836	174	173	199	249	264	217	181	166	189	246	271	228
989087	1179836	162	162	186	235	249	203	166	153	178	233	256	213
996087	1179836	152	151	174	222	236	190	153	142	169	221	241	200
1003087	1179836	147	147	169	216	230	186	149	139	166	217	235	194
1010087	1179836	146	145	168	218	233	188	150	141	168	220	237	194
1017087	1179836	146	146	170	220	237	192	154	145	171	224	240	195
1024087	1179836	147	148	172	224	241	197	159	149	176	229	243	197
1031087	1179836	149	151	175	228	246	201	164	155	181	233	246	199
1038087	1179836	152	155	180	234	253	207	171	162	187	240	251	203
1045087	1179836	156	160	185	241	260	214	178	169	194	246	256	208
1052087	1179836	160	165	191	247	267	220	185	176	200	253	262	212
954087	1186836	231	231	260	319	334	288	255	234	253	315	345	296
961087	1186836	218	219	247	304	319	274	240	219	238	298	329	281
968087	1186836	209	209	235	290	306	261	226	207	227	285	314	269
975087	1186836	197	197	223	276	292	246	210	193	215	272	299	255
982087	1186836	185	184	209	261	276	230	192	177	202	259	284	239
989087	1186836	170	170	194	245	259	212	173	160	187	243	266	222
996087	1186836	155	154	178	227	240	192	153	142	172	226	246	203
1003087	1186836	152	151	176	227	242	193	152	141	172	229	248	202
1010087	1186836	152	152	177	231	249	199	157	146	177	235	254	205
1017087	1186836	153	154	179	235	253	204	162	152	182	241	257	207
1024087	1186836	155	156	182	238	258	209	168	159	188	246	260	209
1031087	1186836	158	160	186	243	264	215	175	166	194	252	264	213
1038087	1186836	162	166	192	250	271	222	183	174	202	258	269	217
1045087	1186836	167	172	198	257	278	229	191	183	209	265	275	222
1052087	1186836	172	178	204	264	285	236	198	191	217	273	280	227
1059087	1186836	177	184	210	271	292	242	206	198	224	280	286	232
961087	1193836	250	249	276	333	350	306	273	253	271	329	359	313
968087	1193836	236	234	261	316	333	289	255	236	255	312	342	296
975087	1193836	221	220	246	300	317	272	235	218	241	298	325	279
982087	1193836	205	203	229	283	300	253	214	199	224	282	308	262
989087	1193836	188	187	212	266	283	234	192	179	208	267	291	244
996087	1193836	166	165	192	248	265	213	166	155	188	251	274	223
1003087	1193836	159	158	186	245	264	209	160	149	184	251	273	218
1010087	1193836	158	159	187	246	267	213	166	155	189	255	274	218
1017087	1193836	160	161	189	249	271	217	172	162	195	259	275	219
1024087	1193836	162	165	192	252	275	223	179	170	201	263	277	222
1031087	1193836	166	170	197	257	280	229	186	178	208	269	281	225
1038087	1193836	171	175	203	264	287	236	195	187	216	276	286	230
1045087	1193836	177	182	209	271	295	243	204	196	224	283	292	236
1052087	1193836	183	190	217	279	303	251	212	205	233	292	298	242
1059087	1193836	190	197	225	287	311	259	221	215	243	301	306	248

Continued on the next page

X	Y	Jan	Febr	Mar	Apr	May	Jun	Jul	Aug	Sept	Oct	Nov	Dec
968087	1200836	269	266	292	346	366	324	290	271	289	343	375	329
975087	1200836	249	246	273	328	349	304	266	248	270	328	358	310
982087	1200836	228	225	253	310	331	282	240	224	250	312	340	289
989087	1200836	204	202	231	291	312	259	211	197	228	295	322	267
996087	1200836	175	174	205	269	292	233	178	164	202	278	304	242
1003087	1200836	164	164	196	262	286	226	170	157	197	274	297	233
1010087	1200836	164	165	196	260	285	227	175	164	201	274	293	231
1017087	1200836	166	168	198	261	286	230	181	172	207	276	292	231
1024087	1200836	169	172	201	264	290	235	189	180	214	280	293	233
1031087	1200836	173	178	206	269	295	241	197	189	221	285	296	237
1038087	1200836	179	184	212	276	301	248	206	199	230	292	301	242
1045087	1200836	186	192	220	284	310	257	216	209	239	300	307	248
1052087	1200836	193	201	228	293	319	266	226	220	249	310	315	255
1059087	1200836	202	210	237	303	329	276	237	231	260	320	324	263
968087	1207836	299	295	320	374	396	357	323	304	320	373	405	360
975087	1207836	274	271	299	355	378	333	294	277	298	356	387	338
982087	1207836	252	250	280	341	364	313	268	252	278	343	374	319
989087	1207836	223	221	255	321	346	287	234	218	252	328	358	295
996087	1207836	183	182	218	291	319	253	189	174	217	305	334	262
1003087	1207836	170	170	205	277	306	240	178	165	209	295	320	247
1010087	1207836	169	171	203	272	301	239	184	173	213	292	311	242
1017087	1207836	170	174	205	272	300	241	190	181	219	293	308	241
1024087	1207836	174	179	208	275	303	246	198	190	226	295	307	243
1031087	1207836	179	185	213	280	307	252	207	200	233	300	310	247
1038087	1207836	185	192	220	286	314	260	217	210	242	307	314	252
1045087	1207836	193	201	228	295	323	269	227	222	253	316	321	259
1052087	1207836	202	210	238	305	333	279	239	233	264	326	330	267
1059087	1207836	213	221	249	316	345	291	251	246	276	338	341	277
1066087	1207836	225	234	261	330	359	303	264	259	290	352	353	288
968087	1214836	286	282	305	354	377	341	313	298	313	359	385	342
975087	1214836	287	284	313	368	389	345	310	296	314	368	398	349
982087	1214836	280	278	311	373	394	341	299	285	308	371	403	348
989087	1214836	260	259	296	364	388	326	273	259	289	366	400	335
996087	1214836	215	215	255	332	360	289	223	207	250	344	378	299
1003087	1214836	175	177	214	292	324	253	186	172	221	316	342	260
1010087	1214836	172	176	210	282	315	249	191	181	224	309	327	251
1017087	1214836	174	179	210	281	312	251	199	190	230	307	321	249
1024087	1214836	178	184	214	283	313	256	207	200	237	309	319	251
1031087	1214836	183	190	219	288	318	262	216	210	245	313	321	255
1038087	1214836	191	198	226	295	324	270	226	221	254	320	325	261
1045087	1214836	199	208	235	304	333	280	237	233	265	329	333	268
1052087	1214836	209	218	245	314	343	290	249	245	276	339	341	277
1059087	1214836	220	229	256	325	355	301	261	257	288	351	352	286
1066087	1214836	232	242	269	339	370	314	274	271	302	366	365	298
968087	1221836	258	254	274	313	335	307	287	280	293	326	341	303
975087	1221836	301	298	326	374	392	352	326	319	330	372	397	354

Continued on the next page

X	Y	Jan	Febr	Mar	Apr	May	Jun	Jul	Aug	Sept	Oct	Nov	Dec
982087	1221836	323	321	356	413	429	378	344	335	349	402	434	384
989087	1221836	323	323	364	428	444	382	338	328	348	416	453	393
996087	1221836	285	289	333	406	424	350	293	281	315	404	442	368
1003087	1221836	180	186	225	304	336	259	192	178	232	337	361	271
1010087	1221836	174	180	214	289	325	257	198	189	235	324	340	258
1017087	1221836	176	182	214	286	321	259	206	199	240	320	330	255
1024087	1221836	180	187	217	288	321	263	215	209	247	320	327	257
1031087	1221836	187	195	223	294	325	270	224	220	255	324	329	261
1038087	1221836	195	203	231	301	332	279	235	232	264	331	334	268
1045087	1221836	203	212	239	309	339	287	245	242	273	338	339	274
1052087	1221836	211	221	247	317	347	295	254	252	282	345	346	281
1059087	1221836	221	231	257	326	357	304	264	262	292	355	354	289
1066087	1221836	233	243	269	338	369	315	277	274	305	368	366	299
975087	1228836	320	318	345	385	397	363	348	348	351	377	398	363
982087	1228836	387	385	423	472	479	431	411	409	408	443	478	438
989087	1228836	421	422	468	526	531	469	440	437	438	487	531	483
996087	1228836	377	384	433	500	507	430	386	377	398	477	522	454
1003087	1228836	208	222	262	339	363	277	213	198	258	375	400	303
1010087	1228836	172	181	214	290	330	261	204	196	244	335	345	259
1017087	1228836	174	183	213	287	326	264	212	207	249	328	335	256
1024087	1228836	180	189	218	290	326	269	221	218	255	328	332	260
1031087	1228836	188	197	225	297	330	276	232	229	263	332	333	265
1038087	1228836	196	206	233	304	336	284	242	240	272	337	337	272
1045087	1228836	203	213	239	309	340	289	249	248	278	341	340	276
1052087	1228836	210	220	246	315	344	294	256	255	284	345	344	281
1059087	1228836	218	228	253	321	351	301	263	262	291	352	349	286
1066087	1228836	227	238	262	329	359	309	272	271	300	360	357	293
968087	1235836	201	197	208	233	254	239	233	237	250	263	259	230
975087	1235836	295	291	314	347	361	333	325	328	332	349	361	330
982087	1235836	414	412	449	491	495	452	442	446	436	456	488	457
989087	1235836	567	567	621	672	662	602	592	597	569	592	647	617
996087	1235836	481	484	536	596	597	529	505	506	499	545	593	544
1003087	1235836	326	334	375	442	465	395	356	353	376	445	472	402
1010087	1235836	187	198	229	302	347	280	230	227	270	353	358	270
1017087	1235836	168	177	205	278	324	265	217	215	256	331	330	249
1024087	1235836	177	187	215	287	326	272	227	226	262	331	330	258
1031087	1235836	187	198	225	297	331	280	238	238	270	335	333	267
1038087	1235836	196	207	232	303	334	286	246	246	276	339	336	273
1045087	1235836	201	212	237	306	335	288	250	250	279	339	335	274
1052087	1235836	205	216	240	307	335	289	253	253	280	338	335	275
1059087	1235836	210	221	244	309	336	291	256	256	283	339	336	276
1066087	1235836	215	226	248	311	339	294	260	260	286	342	338	278
1073087	1235836	220	231	251	313	342	296	262	262	289	345	341	279
954087	1242836	159	154	160	180	202	194	187	191	208	219	211	184
961087	1242836	187	182	191	215	237	224	217	220	235	249	244	216
968087	1242836	224	219	233	262	283	264	255	258	270	287	288	258

Continued on the next page

X	Y	Jan	Febr	Mar	Apr	May	Jun	Jul	Aug	Sept	Oct	Nov	Dec
975087	1242836	272	267	287	321	339	314	303	305	314	333	342	311
982087	1242836	332	327	355	395	409	376	362	363	367	390	409	377
989087	1242836	403	398	435	483	492	448	431	431	429	456	487	454
996087	1242836	454	450	495	550	557	503	482	481	475	509	550	513
1003087	1242836	399	398	442	504	522	462	433	431	437	484	517	467
1010087	1242836	263	267	300	367	408	350	311	311	337	396	406	338
1017087	1242836	162	171	196	266	323	268	225	228	265	330	321	241
1024087	1242836	172	183	208	279	321	272	232	235	267	330	322	252
1031087	1242836	186	198	223	294	326	281	243	245	274	334	328	266
1038087	1242836	194	206	230	300	328	284	248	250	277	335	329	272
1045087	1242836	195	207	230	297	322	281	246	249	274	329	324	269
1052087	1242836	196	207	229	293	317	277	244	246	270	323	318	264
1059087	1242836	196	207	227	288	311	272	241	243	266	317	312	259
1066087	1242836	195	205	224	281	305	267	237	238	261	310	306	253
1073087	1242836	193	202	220	273	298	260	231	232	254	303	299	245
954087	1249836	181	175	182	207	228	217	209	212	228	242	238	210
961087	1249836	206	200	211	239	260	246	235	238	253	270	269	239
968087	1249836	235	229	244	276	298	278	266	267	281	301	305	273
975087	1249836	269	262	282	318	339	314	300	300	312	335	344	311
982087	1249836	305	298	323	365	384	353	336	335	345	372	387	353
989087	1249836	341	334	365	412	430	392	372	369	378	409	431	395
996087	1249836	369	361	397	450	468	424	399	394	402	439	467	429
1003087	1249836	376	368	406	467	487	436	406	399	410	454	484	443
1010087	1249836	307	302	337	403	437	384	347	339	363	416	436	381
1017087	1249836	213	213	240	310	356	305	263	258	293	354	357	292
1024087	1249836	202	208	234	304	340	294	255	254	284	343	342	283
1031087	1249836	195	207	231	302	326	287	252	254	279	334	329	277
1038087	1249836	193	206	229	297	317	281	248	252	274	326	320	272
1045087	1249836	189	201	223	287	307	272	241	244	266	315	310	262
1052087	1249836	183	194	214	273	294	260	230	233	254	301	296	249
1059087	1249836	175	185	203	258	278	245	218	220	240	284	280	233
1066087	1249836	167	176	192	241	261	230	205	207	226	266	263	218
1073087	1249836	159	167	181	224	243	215	192	193	211	248	245	202
954087	1256836	195	189	197	224	246	234	224	226	243	259	257	229
961087	1256836	218	211	222	253	275	259	247	249	265	284	285	255
968087	1256836	242	235	249	284	307	287	273	273	288	311	316	283
975087	1256836	268	260	279	318	340	316	299	298	313	339	348	314
982087	1256836	293	286	308	352	374	345	325	322	337	367	380	344
989087	1256836	318	309	336	384	407	372	350	345	359	393	411	374
996087	1256836	335	326	357	411	434	394	367	360	375	414	437	397
1003087	1256836	340	330	364	423	449	404	372	361	380	425	451	409
1010087	1256836	319	306	341	407	437	389	350	335	361	414	439	395
1017087	1256836	253	245	275	344	381	334	292	279	313	372	386	334
1024087	1256836	224	225	254	324	354	311	272	263	292	350	359	307
1031087	1256836	223	231	256	325	348	311	276	274	301	354	355	304
1038087	1256836	208	217	240	303	324	292	260	261	285	333	330	282

Continued on the next page

X	Y	Jan	Febr	Mar	Apr	May	Jun	Jul	Aug	Sept	Oct	Nov	Dec
1045087	1256836	191	200	221	279	299	269	240	242	263	307	304	258
1052087	1256836	176	185	203	257	276	248	221	223	243	284	281	236
1059087	1256836	159	167	184	232	250	224	199	201	219	257	254	212
1066087	1256836	141	148	162	204	221	197	176	178	193	226	223	185
1073087	1256836	125	131	142	174	189	169	152	154	167	193	190	158
1080087	1256836	114	120	129	154	168	152	136	138	150	172	171	139
947087	1263836	189	181	186	213	235	226	216	219	236	252	249	222
954087	1263836	207	199	207	237	260	247	235	238	255	274	273	243
961087	1263836	226	219	230	263	287	271	257	258	275	297	299	267
968087	1263836	247	239	253	291	315	295	279	278	295	321	326	292
975087	1263836	268	260	277	318	344	319	300	298	315	344	353	317
982087	1263836	288	279	300	346	371	343	321	317	334	367	379	342
989087	1263836	306	297	321	371	397	364	339	333	351	388	404	364
996087	1263836	319	310	337	391	418	381	353	344	363	405	424	383
1003087	1263836	324	314	344	403	432	391	358	346	368	415	437	394
1010087	1263836	311	298	331	395	427	382	344	328	355	409	432	387
1017087	1263836	261	249	283	352	387	340	297	277	311	371	394	343
1024087	1263836	236	235	266	334	364	323	284	270	301	358	373	318
1031087	1263836	259	261	288	352	377	344	309	304	334	384	388	335
1038087	1263836	239	243	268	329	353	322	290	288	314	361	362	310
1045087	1263836	211	217	239	296	318	289	260	260	283	326	325	276
1052087	1263836	184	189	209	261	281	255	229	229	249	288	287	241
1059087	1263836	157	163	180	225	244	221	197	199	216	250	249	207
1066087	1263836	130	135	148	186	203	183	163	165	179	207	206	170
1073087	1263836	100	104	113	139	151	138	124	126	136	154	153	127
1080087	1263836	82	87	93	111	122	113	101	104	112	125	125	101
947087	1270836	199	191	196	225	249	239	227	231	248	267	265	236
954087	1270836	216	208	216	248	272	259	246	248	266	287	288	256
961087	1270836	234	226	236	272	297	281	265	266	284	309	312	278
968087	1270836	252	244	257	297	323	303	285	284	302	330	336	300
975087	1270836	270	261	278	321	348	324	303	301	320	351	360	322
982087	1270836	287	278	297	344	372	345	321	316	336	371	383	343
989087	1270836	302	292	315	366	395	363	337	330	350	389	404	362
996087	1270836	313	303	329	383	414	379	349	340	361	405	422	378
1003087	1270836	319	309	336	395	427	389	355	343	367	415	435	389
1010087	1270836	314	303	333	396	430	389	351	336	364	417	438	390
1017087	1270836	292	281	313	380	415	373	331	311	345	403	425	373
1024087	1270836	274	270	301	365	396	360	322	306	341	394	410	352
1031087	1270836	299	298	325	387	414	384	350	343	375	422	428	371
1038087	1270836	271	272	299	360	387	357	324	320	348	394	397	340
1045087	1270836	239	242	267	326	352	322	291	289	314	358	360	304
1052087	1270836	208	211	234	289	314	286	257	256	277	319	320	266
1059087	1270836	176	179	199	249	273	247	221	220	239	277	279	228
1066087	1270836	144	147	165	209	231	208	185	184	201	235	237	189
1073087	1270836	114	117	131	168	189	169	149	149	163	191	193	150
1080087	1270836	111	113	133	190	225	192	166	166	186	228	231	163

Continued on the next page

X	Y	Jan	Febr	Mar	Apr	May	Jun	Jul	Aug	Sept	Oct	Nov	Dec
961087	1277836	242	232	243	281	308	291	274	274	293	320	324	288
968087	1277836	258	249	262	303	332	311	291	290	310	341	346	309
975087	1277836	274	264	280	325	355	331	308	305	326	360	368	328
982087	1277836	289	279	298	347	377	350	324	319	341	379	390	347
989087	1277836	303	293	314	366	398	367	339	332	354	396	409	365
996087	1277836	314	303	327	383	416	382	351	341	365	411	427	380
1003087	1277836	321	311	337	396	430	394	360	347	373	423	440	392
1010087	1277836	325	313	341	404	439	402	364	349	377	431	450	400
1017087	1277836	327	316	345	409	446	408	367	350	383	439	458	405
1024087	1277836	420	409	431	481	509	493	460	453	494	529	535	483
1031087	1277836	349	344	374	434	463	436	402	396	429	473	477	418
1038087	1277836	300	299	330	394	423	392	358	353	381	428	431	369
1045087	1277836	263	263	293	356	386	353	320	316	341	388	391	328
1052087	1277836	229	230	258	317	347	315	284	281	303	348	351	290
1059087	1277836	197	198	223	279	308	277	248	245	266	309	312	252
1066087	1277836	167	168	190	242	272	243	215	212	232	273	278	217
1073087	1277836	139	140	161	212	245	215	186	183	204	247	253	188
1080087	1277836	122	123	141	188	218	190	165	163	182	220	225	166
961087	1284836	250	239	249	289	318	301	282	283	303	332	336	299
968087	1284836	265	255	267	311	341	320	299	298	319	352	358	318
975087	1284836	280	269	285	331	364	339	315	312	334	370	379	336
982087	1284836	294	283	301	352	385	357	330	325	348	388	399	354
989087	1284836	307	296	317	370	405	374	344	337	361	405	418	371
996087	1284836	318	308	330	387	423	390	357	347	373	420	435	386
1003087	1284836	328	317	342	402	439	404	368	355	383	434	450	400
1010087	1284836	336	325	351	414	452	416	377	362	391	446	464	412
1017087	1284836	347	337	364	429	467	431	390	374	405	461	480	426
1024087	1284836	398	388	416	475	507	482	446	436	471	516	525	468
1031087	1284836	373	368	403	469	500	469	434	429	459	505	508	443
1038087	1284836	316	315	352	420	452	416	382	376	401	452	455	387
1045087	1284836	277	277	311	376	408	372	339	334	357	406	410	343
1052087	1284836	243	243	274	335	365	331	300	295	317	364	368	304
1059087	1284836	212	213	240	296	326	294	264	260	280	325	330	268
1066087	1284836	184	185	209	260	289	259	231	227	247	289	294	234
1073087	1284836	159	161	180	224	251	224	199	196	214	252	257	202
1080087	1284836	137	139	153	190	214	191	169	167	183	216	221	173
954087	1291836	243	232	239	278	307	292	275	278	298	326	329	291
961087	1291836	258	247	257	299	330	312	292	292	314	345	349	310
968087	1291836	273	262	274	319	352	330	308	306	329	364	370	328
975087	1291836	287	276	291	339	374	349	323	319	343	382	390	346
982087	1291836	300	290	307	359	395	367	338	332	357	400	410	363
989087	1291836	313	302	323	377	415	384	352	344	370	417	429	379
996087	1291836	325	314	337	395	434	400	366	355	382	433	447	395
1003087	1291836	337	326	350	411	451	415	378	365	394	447	463	410
1010087	1291836	348	337	363	427	467	430	391	375	405	462	479	424
1031087	1291836	341	340	388	468	504	458	421	413	434	493	497	421

Continued on the next page

X	Y	Jan	Febr	Mar	Apr	May	Jun	Jul	Aug	Sept	Oct	Nov	Dec
1038087	1291836	308	308	351	425	458	416	381	374	395	450	454	382
1045087	1291836	278	278	315	380	412	374	341	335	356	407	411	344
1052087	1291836	248	248	280	339	369	334	304	299	318	365	370	307
1059087	1291836	220	221	248	300	328	296	269	264	282	326	331	272
1066087	1291836	195	197	219	264	289	261	236	232	249	288	293	240
1073087	1291836	176	178	194	231	252	229	208	204	220	254	259	213
1080087	1291836	156	158	170	198	216	197	179	176	190	219	223	185
954087	1298836	253	241	248	288	320	304	286	289	310	340	343	304
961087	1298836	267	255	265	309	342	323	302	302	325	359	363	321
968087	1298836	282	270	282	329	364	342	318	316	340	377	384	339
975087	1298836	295	284	299	349	386	360	333	329	354	395	404	356
982087	1298836	309	298	315	368	407	378	348	341	368	413	423	373
989087	1298836	322	311	331	387	428	395	362	354	381	430	442	390
996087	1298836	335	324	346	405	448	412	376	365	394	447	461	406
1003087	1298836	347	336	360	423	467	429	390	377	406	463	478	422
1010087	1298836	361	350	376	441	485	446	405	389	419	479	496	439
1017087	1298836	376	366	393	461	504	466	423	406	435	496	515	458
961087	1305836	277	265	274	320	355	335	313	313	337	373	378	334
968087	1305836	291	279	291	340	378	354	328	327	352	392	398	351
975087	1305836	306	294	308	360	400	373	344	340	366	410	418	369
982087	1305836	319	308	325	380	422	391	359	353	380	428	438	385
989087	1305836	333	321	341	399	443	409	374	365	394	446	458	402
996087	1305836	346	335	357	418	464	427	389	377	407	463	477	419
1003087	1305836	360	349	373	437	485	445	404	390	421	481	496	436
1010087	1305836	374	364	390	457	506	464	420	404	435	498	515	453
1017087	1305836	389	379	407	476	523	482	438	419	448	513	534	472
968087	1312836	303	290	302	353	393	368	341	339	365	407	414	365
1010087	1312836	390	379	407	475	529	482	436	420	453	520	536	469
1017087	1312836	405	394	424	495	550	502	453	434	467	538	556	487

Hydraulic Data - Pumping Test

In this section, indicates the pumping test information from six wells. The specific yield and transmissivity parameters were estimated using Theis and Neuman methods.

San Antonio Well

Parameters	Theis method
X	978474
Y	1208615
Q (l/s)	1,6
Depth (m)	40
Diameter (inch)	6
Estatic Level (m)	9,66
Dinamic Level (m)	14.08
Drawdown (m)	4,48
Q - Pumping test (l/s)	0.18
Pumping Time (hours)	14
Drawdown Time (hours)	13
Transmisivity (m^2/día)	2.37
Conductivity (m/día)	0.0674
Storage Coefficient	$3.37*10^{-5}$
Aquifer type	Confinado
Aquifer Name	Mesa

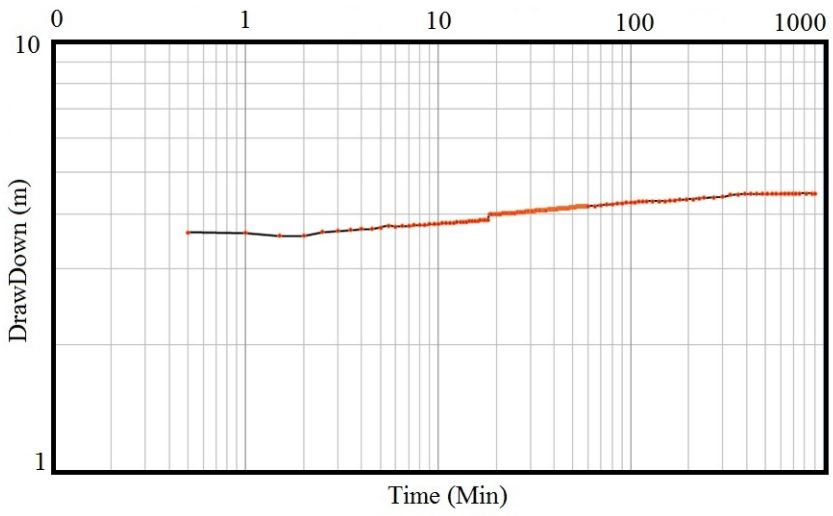

Las Mercedes Well

Parameters	Theis method
X	989394
Y	1209989
Q (l/s)	1,6
Depth (m)	38
Diameter (inch)	4
Estatic Level (m)	18.27
Dinamic Level (m)	23.68
Drawdown (m)	5.41
Q - Pumping test (l/s)	1.7
Pumping Time (hours)	14
Drawdown Time (hours)	14
Transmisivity (m^2/día)	38.4
Conductivity (m/día)	0.64
Storage Coefficient	$2.96*10^{-5}$
Aquifer type	Confinado
Aquifer Name	Mesa

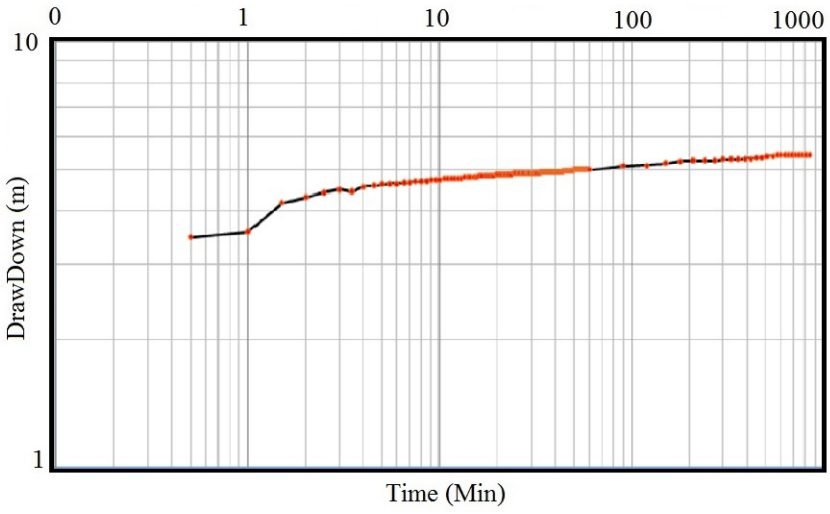

Penjamo Well

Parameters	Neuman method
X	978367
Y	1196624
Q (l/s)	1.7
Depth (m)	38
Diameter (inch)	6
Estatic Level (m)	16.81
Dinamic Level (m)	18.8
Drawdown (m)	1.99
Q - Pumping test (l/s)	0.6
Pumping Time (hours)	24
Drawdown Time (hours)	15
Transmisivity (m^2/dia)	25.6
Conductivity (m/dia)	0.427
Storage Coefficient	--
Aquifer type	Free
Aquifer Name	Real

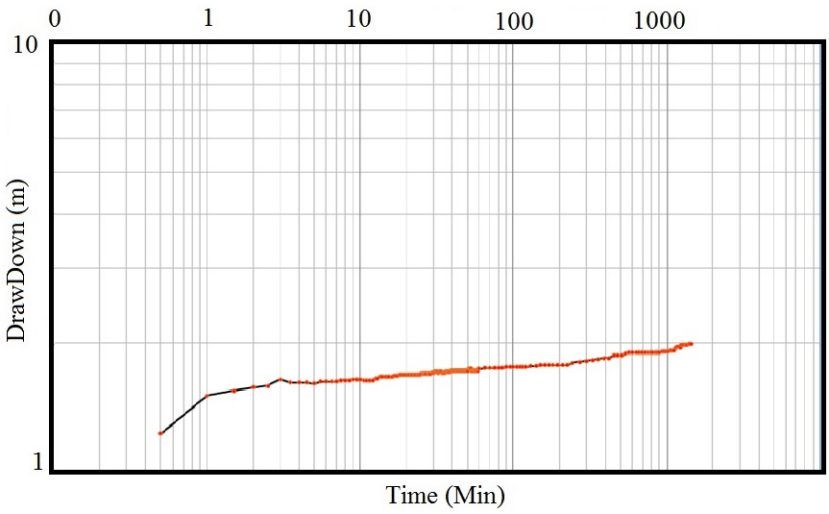

La Ponderosa Well

Parameters	Hantush method
X	988823
Y	1207855
Q (l/s)	1.2
Depth (m)	20
Diameter (inch)	4
Estatic Level (m)	17.13
Dinamic Level (m)	20.84
Drawdown (m)	3.71
Q - Pumping test (l/s)	1.64
Pumping Time (hours)	24
Drawdown Time (hours)	12
Transmisivity (m^2/dia)	49.3
Conductivity (m/dia)	0.98
Storage Coefficient	--
Aquifer type	Free
Aquifer Name	Real

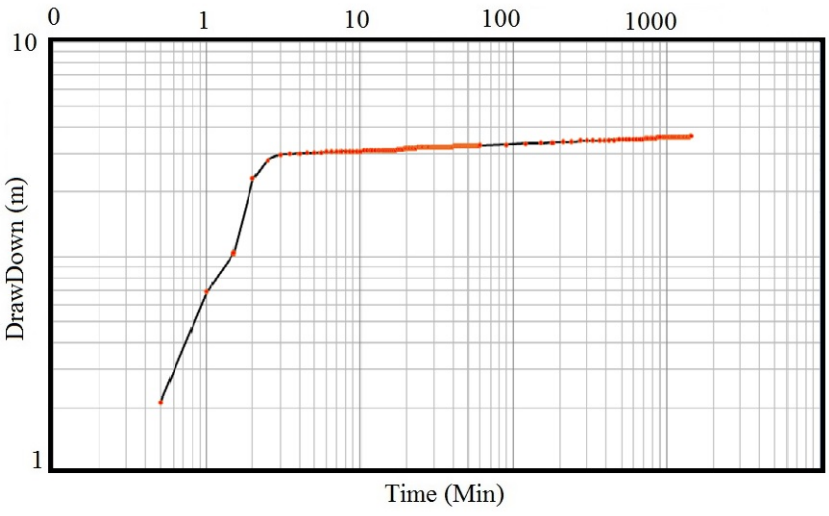

Campo Seco Well

Parameters	Hantush method
X	975497
Y	1184466
Q (l/s)	0.18
Depth (m)	38
Diameter (inch)	6
Estatic Level (m)	6
Dinamic Level (m)	9.36
Drawdown (m)	3.36
Q - Pumping test (l/s)	0.45
Pumping Time (hours)	14
Drawdown Time (hours)	9
Transmisivity (m^2/día)	11.4
Conductivity (m/día)	0.19
Storage Coefficient	6.91*10-4
Aquifer type	Semi-Confined
Aquifer Name	Mesa

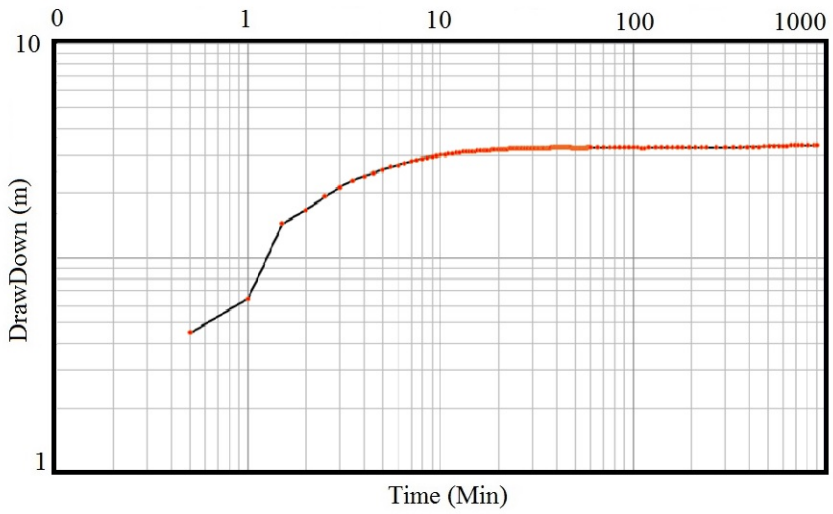

Socorro Well

Parameters	Neuman method
X	991395
Y	1198951
Q (l/s)	1.6
Depth (m)	25
Diameter (inch)	4
Estatic Level (m)	17.13
Dinamic Level (m)	20.84
Drawdown (m)	3.71
Q - Pumping test (l/s)	1.64
Pumping Time (hours)	14
Drawdown Time (hours)	12
Transmisivity (m^2/dia)	49.3
Conductivity (m/dia)	0.98
Storage Coefficient	--
Aquifer type	Free
Aquifer Name	Real

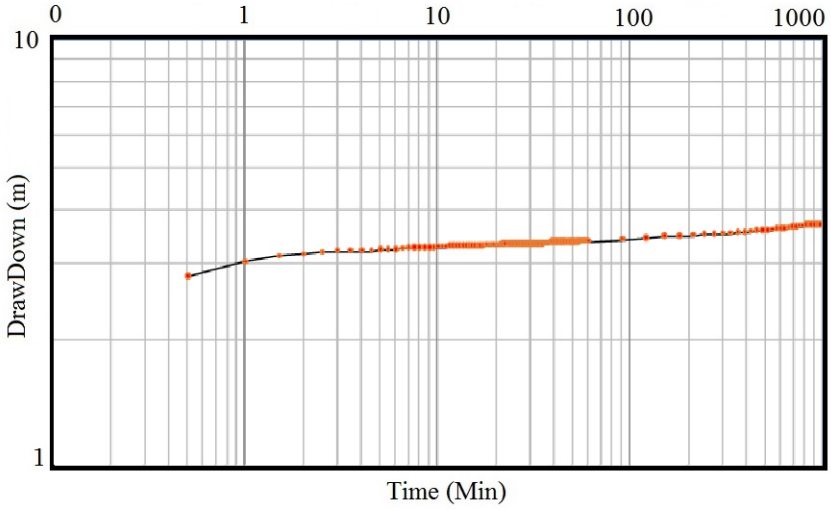

B. Annex: Statistical Analysis of the Hydrological Model

AMA and Sobol' Indices Series for each Parameter

Parameters	$AMAE$	$AMAV$	AMA_γ	AMA_K	Sobol'
qso	0.00785132	0.02195257	0.01612656	0.0572445	0.00018611
$LnTe$	0.00711278	0.02082543	0.01589391	0.05800311	0.00017285
m	0.00879224	0.02077318	0.01395075	0.05217205	0.00023078
Sro	0.00731151	0.01876407	0.01389315	0.04903818	0.00018132
Sr_{max}	0.00703534	0.02425542	0.01281027	0.05354968	0.00015073
td	0.00720454	0.02285963	0.01409881	0.05340454	0.0002027
vch	0.00898599	0.02904335	0.01415603	0.05518942	0.0002894
vr	0.00808449	0.01829092	0.01587576	0.04834258	0.00019543
ko	0.0079966	0.0222415	0.01330691	0.05682577	0.00017769
CD	0.00691153	0.02106544	0.0096962	0.03976828	0.00015061

Analysis of the Four Statistical Moments

Day	Mean	Variance	Skewness	Kurtosis
1	1.80E-03	1.09E-06	3.29E-03	1.80E+00
150	6.21E-03	4.35E-06	4.48E-01	4.48E+00
300	6.76E-03	1.41E-06	1.79E+00	5.84E+00
1000	3.77E-03	1.25E-06	2.16E+00	6.76E+00
1250	4.66E-03	1.78E-06	2.00E+00	6.02E+00
1500	2.28E-03	8.99E-08	1.37E+00	4.91E+00
2000	7.02E-03	9.61E-07	1.94E+00	5.93E+00
2600	2.03E-03	1.07E-07	1.24E+00	5.63E+00
3000	2.00E-03	9.92E-07	3.44E-01	3.44E+00

Comparison of Index Values by Decomposition and Integral

Index	day	Descomposition			Integral			Index	Descomposition			Integral		
		qso	m	Sr_{max}	qso	m	Sr_{max}		qso	m	Sr_{max}	qso	m	Sr_{max}
	1	0.4993	0.0055	0.0053	0.4528	0.0053	0.0052		3.7846	3.6115	3.2578	3.7352	3.2703	3.1475
	150	0.1297	0.0560	0.1859	0.1114	0.0507	0.1610		3.1867	0.1590	5.5022	3.0052	0.1488	5.1229
	300	0.0063	0.0043	0.1240	0.0050	0.0038	0.1085		0.1192	0.0491	3.5936	0.1005	0.0445	3.4480
	1000	0.0029	0.0167	0.2061	0.0027	0.0153	0.1781		0.0149	0.0130	0.9485	0.0139	0.0121	0.9016
$AMAE$	1250	0.0028	0.0368	0.2013	0.0026	0.0335	0.1749	AMA_{γ}	0.0156	0.0300	0.8890	0.0146	0.0294	0.8419
	1500	0.0011	0.0565	0.0839	0.0011	0.0511	0.0735		0.0197	0.3240	1.0517	0.0190	0.3084	1.0003
	2000	0.0013	0.0025	0.0971	0.0012	0.0023	0.0844		0.0149	0.0137	0.9693	0.0138	0.0127	0.9213
	2600	0.0012	0.0675	0.0963	0.0012	0.0602	0.0836		0.0282	0.6934	2.0245	0.0267	0.6618	1.9243
	3000	0.0037	0.3367	0.1868	0.0035	0.3108	0.1615		0.0467	4.5832	4.2107	0.0438	4.4152	4.0070
	1	0.9975	0.0084	0.0083	0.9470	0.0081	0.0080		0.0066	0.0063	0.0058	0.0060	0.0059	0.0057
	150	0.3539	0.0470	0.6126	0.3308	0.0422	0.5774		0.3058	0.0473	0.9649	0.2789	0.0427	0.7772
	300	0.0655	0.0369	0.9382	0.0494	0.0328	0.8925		0.0254	0.0289	11.8009	0.0232	0.0278	11.3524
	1000	0.0200	0.0745	0.9736	0.0187	0.0687	0.9277		0.0234	0.0226	0.6355	0.0218	0.0208	0.6034
$AMAV$	1250	0.0185	0.0342	0.9653	0.0174	0.0333	0.9183	AMA_{K}	0.0243	0.0300	0.6599	0.0227	0.0297	0.6273
	1500	0.0171	0.2464	0.7295	0.0164	0.2351	0.6998		0.0215	0.0930	0.6041	0.0204	0.0891	0.5748
	2000	0.0182	0.0681	0.9456	0.0174	0.0602	0.9006		0.0212	0.0234	0.5944	0.0195	0.0214	0.5662
	2600	0.0187	0.2505	0.6910	0.0180	0.2460	0.6641		0.0185	0.1779	0.3127	0.0175	0.1728	0.2968
	3000	0.0177	0.6246	0.5384	0.0169	0.5864	0.4846		0.0098	0.9353	0.3044	0.0094	0.9009	0.2880
	1	1.0448	0.0001	0.0001	1.0448	0.0001	0.0001							
	150	0.3100	0.0389	0.6450	0.3100	0.0389	0.6450							
	300	0.0051	0.0010	0.9885	0.0051	0.0010	0.9885							
	1000	0.0001	0.0043	1.0300	0.0001	0.0043	1.0300							
Sobol	1250	0.0001	0.0228	1.0200	0.0001	0.0228	1.0200							
	1500	0.0001	0.2600	0.7686	0.0001	0.2600	0.7686							
	2000	0.0001	0.0005	0.9960	0.0001	0.0005	0.9960							
	2600	0.0001	0.2645	0.7279	0.0001	0.2645	0.7279							
	3000	0.0001	0.6579	0.2871	0.0001	0.6579	0.2871							

C. Annex: Hydrogeologic Model

Results Regularization Methods

Observation Points	X	Y	Measure	CZ			40 -PP			100 -PP			200 -PP		
				SVD	Tikh.	SVD-a	SVD	Tikh.	SVD-a	SVD	Tikh.	SVD-a	SVD	Tikh.	SVD-a
Coyote	1059674	1265494	405.174	406.89	406.89	406.89	406.89	406.89	406.89	406.89	406.89	406.89	406.89	406.89	406.89
12 Oct	1032200	1293914	90.9937	92.2	92.32	92.31	92.3	92.42	92.43	92.24	92.36	92.33	92.31	92.55	92.45
Pte. Sogamoso	1032212	1293128	69.3122	69.99	69.99	69.99	69.98	69.99	69.99	69.98	69.99	69.99	70.17	70.03	70.01
Bello Monte 2	1025355	1289443	68.5806	68.96	68.96	68.96	68.96	68.96	68.97	68.96	68.96	68.96	69.11	69	68.98
Bello Monte	1024625	1289121	125.35	127.01	127.01	127.01	127	127.01	127	127	127	127	127	127	127
Bocas de Sog.	1019662	1287460	148.262	148.85	148.85	148.85	148.85	148.85	148.85	148.85	148.85	148.85	148.85	148.85	148.85
Bufalera	1032060	1292207	171.955	172.27	172.27	172.27	172.27	172.27	172.27	172.27	172.27	172.27	172.27	172.27	172.27
Ponderosa	988823	1207855	127.134	125.62	125.62	125.62	125.62	125.62	125.62	125.62	125.62	125.62	125.62	125.62	125.62
Cantagallo	1040376	1295548	117.674	115.86	115.86	115.86	115.86	115.86	115.86	115.86	115.86	115.86	115.86	115.86	115.86
Campo Seco	975497	1184466	113.178	114.24	114.24	114.24	114.24	114.24	114.24	114.24	114.24	114.24	114.24	114.24	114.24
Coyote	1047880	1256558	113.599	113	113	113	113	113	113	113	113	113	113	113	113
Coyote	1042872	1288351	112.158	112.12	112.12	112.12	112.12	112.12	112.12	112.12	112.12	112.12	112.12	112.12	112.12
Coyote	1037608	1286282	114.336	114.8	114.8	114.8	114.8	114.8	114.8	114.8	114.8	114.8	114.8	114.8	114.8
Coyote	1026557	1259046	114.039	114.57	114.57	114.57	114.57	114.57	114.57	114.57	114.57	114.57	114.57	114.57	114.57
Coyote	1055225	1268549	97.6181	96.59	96.59	96.59	96.59	96.59	96.59	96.59	96.59	96.59	96.59	96.59	96.59
Coyote	1035630	1256907	101.218	101.23	101.23	101.23	101.23	101.23	101.23	101.23	101.23	101.23	101.23	101.23	101.23
Coyote	1052395	1265100	106.195	107.01	107.01	107.01	107.01	107.01	107.01	107.01	107.01	107.01	107.01	107.01	107.01
Coyote	1047276	1271021	93.9767	93.85	93.85	93.85	93.85	93.85	93.85	93.85	93.85	93.85	93.85	93.85	93.85
Coyote	1049411	1267467	131	130.48	130.48	130.48	130.48	130.48	130.48	130.48	130.48	130.48	130.48	130.48	130.48
Coyote	1053508	1284723	101.333	102.67	102.67	102.67	102.67	102.67	102.67	102.67	102.67	102.67	102.67	102.67	102.67
Coyote	1038895	1261988	93.604	93.66	93.66	93.66	93.66	93.66	93.66	93.66	93.66	93.66	93.66	93.66	93.66
Coyote	1032195	1249690	84.9609	85.01	85.01	85.01	85.01	85.01	85.01	85.01	85.01	85.01	85.01	85.01	85.01
Coyote	1046672	1250824	92.2162	92.94	92.94	92.94	92.94	92.94	92.94	92.94	92.94	92.94	92.94	92.94	92.94
Coyote	1045435	1271996	82.3175	82.52	82.52	82.52	82.52	82.52	82.52	82.52	82.52	82.52	82.52	82.52	82.52
Coyote	1039207	1289151	102.894	102.1	102.09	102.1	102.09	102.08	102.1	102.07	102.11	102.11	102.09	102.11	102.12
Coyote	1035433	1283961	97.7521	98.72	98.72	98.72	98.72	98.72	98.72	98.72	98.72	98.72	98.72	98.72	98.72
Coyote	1039398	1279164	100.019	101.51	101.51	101.51	101.51	101.51	101.51	101.51	101.51	101.51	101.51	101.51	101.51
Coyote	1041091	1275895	86.4685	87.17	87.17	87.17	87.17	87.17	87.17	87.17	87.17	87.17	87.17	87.17	87.17
Coyote	1033985	1250501	208.854	210.72	210.72	210.72	210.72	210.72	210.72	210.72	210.72	210.72	210.72	210.72	210.72
Coyote	1042059	1259841	87.531	87.5	87.5	87.5	87.5	87.5	87.5	87.5	87.5	87.5	87.5	87.5	87.5
Coyote	1048583	1270162	88.025	88.51	88.51	88.51	88.51	88.51	88.51	88.51	88.51	88.51	88.51	88.51	88.51

Continued on the next page

Observation Points	X	Y	Measure	CZ			40 -PP			100 -PP			200 -PP		
				SVD	Tikh.	SVD-a	SVD	Tikh.	SVD-a	SVD	Tikh.	SVD-a	SVD	Tikh.	SVD-a
Coyote	1048518	1274638	71.3773	73.04	73.04	73.04	73.04	73.04	73.04	73.04	73.04	73.04	73.04	73.04	73.04
Coyote	1045559	1245147	128.733	129.24	129.24	129.24	129.24	129.24	129.24	129.24	129.24	129.24	129.24	129.24	129.24
Coyote	1053609	1279361	208.72	209.81	209.81	209.81	209.81	209.81	209.81	209.81	209.81	209.81	209.81	209.81	209.81
Coyote	1043381	1265883	130.401	129.55	129.55	129.55	129.55	129.55	129.55	129.55	129.55	129.55	129.55	129.55	129.55
Coyote	1035018	1266105	138.213	138.82	138.82	138.82	138.82	138.82	138.82	138.82	138.82	138.82	138.82	138.82	138.82
Coyote	1026421	1283408	116.813	118.17	118.17	118.17	118.17	118.17	118.17	118.17	118.17	118.17	118.17	118.17	118.17
Coyote	1057996	1274691	113.216	113.6	113.6	113.6	113.6	113.6	113.6	113.6	113.6	113.6	113.6	113.6	113.6
Coyote	1047880	1256558	100.028	100.43	100.43	100.43	100.43	100.43	100.43	100.43	100.43	100.43	100.43	100.43	100.43
Coyote	1052346	1246725	103	103.87	103.87	103.87	103.87	103.87	103.87	103.87	103.87	103.87	103.87	103.87	103.87
Coyote	1042036	1255430	123.697	123.7	123.7	123.7	123.7	123.7	123.7	123.7	123.7	123.7	123.7	123.7	123.7
Coyote	1042944	1283661	76.9657	76.82	76.82	76.82	76.82	76.82	76.82	76.82	76.82	76.82	76.82	76.82	76.82
Coyote	1052631	1242242	86.1388	86	86.19	86.18	86.06	86.15	86.16	85.98	86.04	85.96	85.7	86.37	86.13
Coyote	1055345	1258333	161.685	162.12	162.12	162.12	162.11	162.12	162.11	162.09	162.09	162.09	162.12	162.11	162.11
Coyote	1039884	1235905	70.0088	68.27	68.22	68.22	68.58	69.82	69.86	68.59	69.83	69.7	68.28	69.78	70.05
Coyote	1037860	1249611	70.1585	71.29	71.29	71.29	71.29	71.29	71.29	71.29	71.29	71.29	71.29	71.29	71.29
Coyote	1055462	1271893	132.943	136.23	136.22	136.22	136.2	136.16	133.67	136.18	132.99	136.15	136.18	133.15	132.97
Coyote	1029556	1268887	150.126	146.61	147.28	147.28	146.95	150.19	150.31	146.74	150.11	150.27	146.75	150.13	150.16
Coyote	1030678	1286282	74.8362	76.58	76.58	76.58	76.58	76.58	76.58	76.58	76.58	76.58	76.58	76.58	76.58
Coyote	1031122	1242879	83.9126	84.08	84.08	84.08	84.08	84.08	84.08	84.08	84.08	84.08	84.08	84.08	84.08
Coyote	1052300	1266521	84.0521	85.17	85.16	85.16	84.71	84.18	84.11	84.69	84.24	84.25	84.41	84.08	84.14
Coyote	1025074	1250409	69.3534	69.8	69.8	69.8	69.8	69.8	69.8	69.8	69.8	69.8	69.8	69.8	69.8
Coyote	1030907	1265404	69.1798	70.53	70.53	70.53	70.53	70.53	70.53	70.53	70.53	70.53	70.53	70.53	70.53
Coyote	1031734	1286051	68.9996	70.5	70.5	70.5	70.5	70.5	70.5	70.5	70.5	70.5	70.5	70.5	70.5
Coyote	1033897	1242729	69.0886	70.28	70.28	70.28	70.28	70.28	70.28	70.28	70.28	70.28	70.28	70.28	70.28
Coyote	1048130	1278346	69.4922	69.62	69.62	69.62	69.62	69.62	69.62	69.62	69.62	69.62	69.62	69.62	69.62
Coyote	1049641	1255613	73.7402	72.5	72.51	72.51	72.52	72.53	72.52	72.51	72.55	72.55	72.56	72.56	72.56
Coyote	1039477	1269166	69.6045	70.54	70.54	70.54	70.53	70.53	70.53	70.53	70.53	70.53	70.53	70.53	70.53
Coyote	1030522	1288586	70.5502	71.06	71.08	71.08	71.01	70.98	70.98	71	70.95	70.95	71.11	71.04	70.99
Coyote	1035506	1288469	95.3403	94.21	94.35	94.34	94.5	95.25	95.24	94.42	95.14	95.09	94.59	94.99	95.01
Coyote	1025846	1264554	94.0048	93.3	93.45	93.45	93.47	93.67	93.68	93.41	93.57	93.54	93.53	93.84	93.75
Coyote	1053472	1281422	70.4663	70.55	70.55	70.55	70.55	70.55	70.55	70.55	70.55	70.55	70.55	70.55	70.55
Coyote	1060084	1280926	104.869	104.45	104.45	104.45	104.45	104.45	104.45	104.45	104.45	104.45	104.45	104.45	104.45

Continued on the next page

Observation Points	X	Y	Measure	CZ			40 -PP			100 -PP			200 -PP		
				SVD	Tikh.	SVD-a	SVD	Tikh.	SVD-a	SVD	Tikh.	SVD-a	SVD	Tikh.	SVD-a
Coyote	1043211	1246611	96.0018	97.17	97.17	97.17	97.17	97.17	97.17	97.17	97.17	97.17	97.17	97.17	97.17
Coyote	1028977	1256175	154.834	155.97	155.97	155.97	155.97	155.97	155.97	155.97	155.97	155.97	155.97	155.97	155.97
El esfuerzo	1024923	1289333	81.0006	81.32	81.32	81.32	81.32	81.32	81.32	81.32	81.32	81.32	81.32	81.32	81.32
el progreso 2	1029521	1292138	110.517	110.43	110.43	110.43	110.43	110.43	110.43	110.43	110.43	110.43	110.43	110.43	110.43
el progreso 3	1029592	1292270	145.581	145.9	145.9	145.9	145.9	145.9	145.9	145.9	145.9	145.9	145.9	145.9	145.9
Hda Ponderosa	991395	1198951	126.355	127.48	127.48	127.48	127.48	127.48	127.48	127.48	127.48	127.48	127.48	127.48	127.48
Escuela la lucha	1022847	1288743	94.303	94.14	94.14	94.14	94.14	94.14	94.14	94.14	94.14	94.14	94.14	94.14	94.14
Guane	1018862	1282366	87.0677	87.58	87.58	87.58	87.58	87.58	87.58	87.58	87.58	87.58	87.58	87.58	87.58
Guane	1020430	1287299	155.274	156.91	156.91	156.91	156.91	156.91	156.91	156.91	156.91	156.91	156.91	156.91	156.91
Las Mercedes	989394	1209989	83.0301	83.4	83.4	83.4	83.41	83.44	83.42	83.4	83.44	83.43	83.4	83.39	83.44
Penjamo	978367	1196624	79.8569	79.8	79.8	79.8	79.8	79.8	79.8	79.8	79.8	79.8	79.8	79.8	79.8
San Antonio	978474	1208615	82.0645	80.99	81.18	81.17	81.36	81.07	81.06	81.28	81.1	81.14	81.34	81.22	81.2
Hortensia	1031873	1291928	89.9279	88.9	88.92	88.92	88.94	88.88	88.88	88.92	88.88	88.89	88.91	88.89	88.86
La cascadera	1032695	1293017	85.4097	83.64	83.69	83.69	83.74	83.62	83.62	83.69	83.61	83.63	83.68	83.63	83.57
la ceiba	1022068	1288246	81.6372	81.15	81.58	81.56	81.93	81.4	81.4	81.8	81.46	81.54	81.9	81.74	81.69
la esmeralda	1022071	1288244	83	84.58	84.75	84.75	84.93	84.4	84.41	84.73	84.37	84.43	84.66	84.46	84.2
la esperanza 2	1031457	1292857	83.2303	83.39	83.64	83.63	83.89	83.24	83.25	83.65	83.22	83.32	83.57	83.31	83.01
La felicidad	1018987	1288157	84.6765	83.89	84.3	84.27	84.69	84.55	84.55	84.68	84.57	84.9	84.63	84.48	84.56
La felicidad	1019017	1288214	80.3412	79.93	79.93	79.93	79.93	79.93	79.94	79.92	79.88	79.88	79.89	79.88	79.88
La felicidad 2	1019012	1288214	81.5892	81.9	82.09	82.07	82.25	82.2	82.2	82.25	82.14	82.29	82.2	82.12	82.15
La lucha	1022205	1288404	82.1163	82.1	82.09	82.09	82.09	82.09	82.09	82.1	82.24	82.2	82.2	82.24	82.28
La lucha 4	1024111	1288555	87.318	87.19	87.18	87.18	87.17	87.16	87.15	87.2	87.23	87.21	87.22	87.22	87.24
La lucha 2	1022464	1288569	82.2149	80.85	80.85	80.85	80.85	80.85	80.85	80.85	80.85	80.85	80.85	80.85	80.85
La lucha 3	1022673	1288694	91.9346	91.33	91.29	91.3	91.26	91.27	91.26	91.26	91.28	91.26	91.27	91.29	91.29
la lucha 5	1023170	1288895	90.483	90.16	90.16	90.16	90.15	90.15	90.15	90.15	90.14	90.14	90.14	90.14	90.14
La lucha 6	1023972	1289417	90.0462	90.31	90.31	90.31	90.31	90.31	90.31	90.31	90.31	90.31	90.31	90.31	90.31
Las delicias	1024076	1288522	618.984	619.08	619.08	619.08	619.08	619.08	619.08	619.08	619.08	619.08	619.08	619.08	619.08
los mogalos	1032272	1294384	638.293	638.96	638.96	638.96	638.96	638.96	638.96	638.96	638.96	638.96	638.96	638.96	638.96
los mogalos 2	1032230	1294105	607.704	608.31	608.31	608.31	608.31	608.31	608.31	608.31	608.31	608.31	608.31	608.31	608.31
lucha	1022539	1288505	109.741	111.68	111.68	111.68	111.68	111.68	111.68	111.68	111.68	111.68	111.68	111.68	111.68
M-0007-14-101	1052159	1266329	266.269	266.57	266.57	266.57	266.57	266.57	266.57	266.57	266.57	266.57	266.57	266.57	266.57
M-0007-14-109	1032536	1286180	227.828	228.44	228.44	228.44	228.44	228.44	228.44	228.44	228.44	228.44	228.44	228.44	228.44

Continued on the next page

Observation Points	X	Y	Measure	CZ			40 -PP			100 -PP			200 -PP		
				SVD	Tikh.	SVD-a	SVD	Tikh.	SVD-a	SVD	Tikh.	SVD-a	SVD	Tikh.	SVD-a
M-0007-14-11	1053689	1281102	317.976	319.24	319.24	319.24	319.24	319.24	319.24	319.24	319.24	319.24	319.24	319.24	319.24
M-0007-14-119	1050456	1280052	307.893	309.42	309.42	309.42	309.42	309.42	309.42	309.42	309.42	309.42	309.42	309.42	309.42
M-0007-14-120	1050652	1280092	313.992	315.77	315.77	315.77	315.77	315.77	315.77	315.77	315.77	315.77	315.77	315.77	315.77
M-0007-14-125	1042828	1268734	307.298	307.85	307.85	307.85	307.85	307.85	307.85	307.85	307.85	307.85	307.85	307.85	307.85
M-0007-14-129	1049540	1255546	257.57	257.73	257.73	257.73	257.73	257.73	257.73	257.73	257.73	257.73	257.73	257.73	257.73
M-0007-14-137	1055198	1261560	305.329	307.19	307.19	307.19	307.19	307.19	307.19	307.19	307.19	307.19	307.19	307.19	307.19
M-0007-14-140	1056335	1261488	304.622	304.86	304.86	304.86	304.86	304.86	304.86	304.86	304.86	304.86	304.86	304.86	304.86
M-0007-14-141	1056903	1263197	243.602	243.71	243.71	243.71	243.71	243.71	243.71	243.71	243.71	243.71	243.71	243.71	243.71
M-0007-14-147	1055957	1281024	239.587	239.35	239.35	239.35	239.35	239.35	239.35	239.35	239.35	239.35	239.35	239.35	239.35
M-0007-14-148	1054881	1281862	243.01	243.47	243.47	243.47	243.47	243.47	243.47	243.47	243.47	243.47	243.47	243.47	243.47
M-0007-14-15	1030162	1285752	242.506	243.42	243.42	243.42	243.42	243.42	243.42	243.42	243.42	243.42	243.42	243.42	243.42
M-0007-14-19	1029372	1286160	245.35	244.78	244.78	244.78	244.78	244.78	244.78	244.78	244.78	244.78	244.78	244.78	244.78
M-0007-14-47	1027008	1282516	255.679	255.34	255.34	255.34	255.34	255.34	255.34	255.34	255.34	255.34	255.34	255.34	255.34
M-0007-14-73	1025299	1279402	236.991	236.26	236.26	236.26	236.26	236.26	236.26	236.26	236.26	236.26	236.26	236.26	236.26
M-0007-14-9	1048986	1281049	252.417	252.6	252.6	252.6	252.6	252.6	252.6	252.6	252.6	252.6	252.6	252.6	252.6
M-0033-14-192	971967	1176580	253.787	253.52	253.52	253.52	253.52	253.52	253.52	253.52	253.52	253.52	253.52	253.52	253.52
M-2249-314	1027563	1286294	265.172	263.75	263.75	263.75	263.75	263.75	263.75	263.75	263.75	263.75	263.75	263.75	263.75
M-2249-315	1027268	1286107	263.24	263.97	263.97	263.97	263.97	263.97	263.97	263.97	263.97	263.97	263.97	263.97	263.97
M-2249-316	1027920	1286287	267.988	268.85	268.85	268.85	268.85	268.85	268.85	268.85	268.85	268.85	268.85	268.85	268.85
M-2249-317	1027618	1285767	236.52	237.09	237.09	237.09	237.09	237.09	237.09	237.09	237.09	237.09	237.09	237.09	237.09
M-2249-318	1027584	1285560	211.143	211.44	211.44	211.44	211.44	211.44	211.44	211.44	211.44	211.44	211.44	211.44	211.44
M-2249-319	1027939	1286126	264.601	265.29	265.29	265.29	265.29	265.29	265.29	265.29	265.29	265.29	265.29	265.29	265.29
M-2249-320	1028131	1285705	241.519	242.33	242.33	242.33	242.33	242.33	242.33	242.33	242.33	242.33	242.33	242.33	242.33
M-2249-321	1028112	1285781	234.233	234.05	234.05	234.05	234.05	234.05	234.05	234.05	234.05	234.05	234.05	234.05	234.05
M-2249-322	1027789	1285421	237.009	237.44	237.44	237.44	237.44	237.44	237.44	237.44	237.44	237.44	237.44	237.44	237.44
M-2249-323	1027557	1284818	244.632	244.94	244.94	244.94	244.94	244.94	244.94	244.94	244.94	244.94	244.94	244.94	244.94
M-2249-324	1027775	1284202	193.058	193.39	193.39	193.39	193.39	193.39	193.39	193.39	193.39	193.39	193.39	193.39	193.39
M-2249-325	1027608	1284348	281.691	281.92	281.92	281.92	281.92	281.92	281.92	281.92	281.92	281.92	281.92	281.92	281.92
M-2249-326	1025426	1282796	271.56	271.58	271.58	271.58	271.58	271.58	271.58	271.58	271.58	271.58	271.58	271.58	271.58
M-2249-327	1025549	1282686	266.915	268.68	268.68	268.68	268.68	268.68	268.68	268.68	268.68	268.68	268.68	268.68	268.68
M-2249-328	1025664	1282748	259.921	259.95	259.95	259.95	259.95	259.95	259.95	259.95	259.95	259.95	259.95	259.95	259.95
M-2249-329	1026367	1283144	251.541	251.34	251.34	251.34	251.34	251.34	251.34	251.34	251.34	251.34	251.34	251.34	251.34

Continued on the next page

Observation Points	X	Y	Measure	CZ			40 -PP			100 -PP			200 -PP		
				SVD	Tikh.	SVD-a	SVD	Tikh.	SVD-a	SVD	Tikh.	SVD-a	SVD	Tikh.	SVD-a
M-2249-330	1026451	1282824	250.217	250.92	250.92	250.92	250.92	250.92	250.92	250.92	250.92	250.92	250.92	250.92	250.92
M-2249-332	1026638	1282968	240.032	240.48	240.48	240.48	240.48	240.48	240.48	240.48	240.48	240.48	240.48	240.48	240.48
M-2249-63	1027584	1285560	237.513	237.67	237.67	237.67	237.67	237.67	237.67	237.67	237.67	237.67	237.67	237.67	237.67
M-4236-2	1061332	1264005	232.682	232.12	232.12	232.12	232.12	232.12	232.12	232.12	232.12	232.12	232.12	232.12	232.12
M-4236-3	1061281	1264074	183.13	183.03	183.03	183.03	183.03	183.03	183.03	183.03	183.03	183.03	183.03	183.03	183.03
M-4236-4	1061120	1264241	258.561	258.47	258.47	258.47	258.47	258.47	258.47	258.47	258.47	258.47	258.47	258.47	258.47
M-4236-5	1061070	1264389	278.079	278.58	278.58	278.58	278.58	278.58	278.58	278.58	278.58	278.58	278.58	278.58	278.58
M-4236-6	1061551	1263940	315.63	315.79	315.79	315.79	315.79	315.79	315.79	315.79	315.79	315.79	315.79	315.79	315.79
M-4644-4	1038432	1295689	108.473	108.33	108.33	108.33	108.33	108.33	108.33	108.33	108.33	108.33	108.33	108.33	108.33
M-5237-1	1040640	1225176	81.8296	80.84	80.91	80.9	80.78	80.71	80.7	80.75	80.67	80.65	80.62	80.77	80.7
M-5237-10	1041936	1229461	74.8237	73.09	73.06	73.06	73.3	74.31	74.08	73.01	74.48	74.47	74.24	74.32	74.66
M-5237-11	1041325	1228063	134.654	134.76	134.76	134.76	134.76	134.76	134.69	134.76	134.67	134.76	134.76	134.68	134.67
M-5237-12	1041342	1228135	128.471	128.37	128.37	128.37	128.37	128.37	128.37	128.37	128.37	128.37	128.37	128.37	128.37
M-5237-13	1041193	1227867	156.796	155.48	155.48	155.48	155.48	155.48	155.48	155.48	155.48	155.48	155.48	155.48	155.48
M-5237-14	1041004	1227679	156.431	156.1	156.1	156.1	156.1	156.1	156.1	156.1	156.1	156.1	156.1	156.1	156.1
M-5237-15	1040950	1227427	140.898	141.42	141.42	141.42	141.42	141.42	141.42	141.42	141.42	141.42	141.42	141.42	141.42
M-5237-16	1041049	1227442	140.241	140.25	140.25	140.25	140.25	140.25	140.25	140.25	140.25	140.25	140.25	140.25	140.25
M-5237-17	1040940	1227195	143.264	143.71	143.71	143.71	143.71	143.71	143.71	143.71	143.71	143.71	143.71	143.71	143.71
M-5237-18	1041039	1227340	143.845	143.8	143.8	143.8	143.8	143.8	143.8	143.8	143.8	143.8	143.8	143.8	143.8
M-5237-19	1041023	1227224	126.714	125.52	125.52	125.52	125.52	125.52	125.52	125.52	125.52	125.52	125.52	125.52	125.52
M-5237-2	1040602	1225288	145.704	144.42	144.42	144.42	144.42	144.42	144.42	144.42	144.42	144.42	144.42	144.42	144.42
M-5237-20	1040955	1227137	143.87	144.79	144.79	144.79	144.79	144.79	144.79	144.79	144.79	144.79	144.79	144.79	144.79
M-5237-21	1040949	1226799	149.932	150.29	150.29	150.29	150.29	150.29	150.29	150.29	150.29	150.29	150.29	150.29	150.29
M-5237-22	1040972	1226800	178.059	178.75	178.75	178.75	178.75	178.75	178.75	178.75	178.75	178.75	178.75	178.75	178.75
M-5237-23	1041171	1223732	165.781	165.39	165.39	165.39	165.39	165.39	165.39	165.39	165.39	165.39	165.39	165.39	165.39
M-5237-24	1041162	1223612	168.806	168.81	168.81	168.81	168.81	168.81	168.81	168.81	168.81	168.81	168.81	168.81	168.81
M-5237-25	1041114	1223519	130.586	130.36	130.36	130.36	130.36	130.36	130.36	130.36	130.36	130.36	130.36	130.36	130.36
M-5237-26	1041128	1223509	128.427	128.8	128.8	128.8	128.8	128.8	128.78	128.8	128.78	128.8	128.8	128.78	128.78
M-5237-27	1041080	1223529	128.956	128.93	128.93	128.93	128.93	128.93	128.93	128.93	128.93	128.93	128.93	128.93	128.93
M-5237-28	1040947	1223228	128.928	128.79	128.79	128.79	128.79	128.79	128.7	128.79	128.67	128.79	128.79	128.68	128.67
M-5237-29	1040969	1223113	105.781	106.75	106.75	106.75	106.75	106.75	106.75	106.75	106.75	106.75	106.75	106.75	106.75
M-5237-3	1040890	1225474	126.19	126.56	126.56	126.56	126.56	126.56	126.56	126.56	126.56	126.56	126.56	126.56	126.56

Continued on the next page

Observation Points	X	Y	Measure	CZ			40 -PP			100 -PP			200 -PP		
				SVD	Tikh.	SVD-a	SVD	Tikh.	SVD-a	SVD	Tikh.	SVD-a	SVD	Tikh.	SVD-a
M-5237-30	1040861	1222823	140.597	140.67	140.67	140.67	140.67	140.67	140.67	140.67	140.67	140.67	140.67	140.67	140.67
M-5237-31	1040722	1222654	128.654	129.44	129.44	129.44	129.44	129.44	129.44	129.44	129.44	129.44	129.44	129.44	129.44
M-5237-32	1040684	1222484	124.859	126.53	126.53	126.53	126.53	126.53	126.53	126.53	126.53	126.53	126.53	126.53	126.53
M-5237-33	1040628	1222426	153.983	156.07	156.07	156.07	156.07	156.07	156.07	156.07	156.07	156.07	156.07	156.07	156.07
M-5237-34	1040585	1222277	71.3105	71.36	71.36	71.36	71.36	71.36	71.36	71.36	71.36	71.36	71.36	71.36	71.36
M-5237-35	1040828	1225478	72.2645	72.35	72.34	72.34	72.31	72.22	72.23	72.31	72.15	72.15	72.32	72.18	72.19

D. Annex: Optimization Model Data

Water Demand and Deficit

	Demand				Deficit			
Month	$ESC1$	$ESC2$	$ESC3$	$ESC4$	$ESC1$	$ESC2$	$ESC3$	$ESC4$
January	6172	9875	12344	18516	-1503	-3878	-5667	-9710
February	6658	10653	13317	19975	-1490	-4276	-6272	-11368
March	5302	8483	10603	15905	-334	-1341	-2261	-4888
April	4913	7860	9826	14738	-202	-822	-1399	-3317
May	5312	8500	10624	15937	-456	-1763	-2853	-6197
June	4179	6686	8357	12536	-474	-1444	-2242	-4510
July	5236	8377	10472	15708	-518	-1897	-3023	-6430
August	4945	7912	9890	14835	-352	-1321	-2207	-4810
September	4883	7813	9766	14649	-298	-1041	-1696	-3671
October	5965	9544	11930	17895	-362	-1327	-2249	-4971
November	5040	8064	10080	15120	-374	-1399	-2313	-4994
December	5636	9018	11272	16908	-589	-2157	-3427	-7267
Total year	64240	102784	128481	192721	-6951	-22665	-35610	-72132

Water Allocation

	Surface water allocation				Groundwater allocation			
Month	$ESC1$	$ESC2$	$ESC3$	$ESC4$	$ESC1$	$ESC2$	$ESC3$	$ESC4$
January	2156	3048	2924	4384	2514	2950	3753	4422
February	2369	3174	3129	3979	2799	3203	3916	4628
March	3043	4220	3457	4935	1925	2921	4885	6081
April	3205	4693	3279	4801	1506	2346	5148	6620
May	2438	3623	3370	4468	2418	3114	4401	5272
June	2373	3157	2425	3483	1332	2085	3691	4543
July	2376	3451	3280	4260	2342	3030	4169	5017
August	2791	3808	3200	4522	1802	2783	4482	5502
September	3176	4589	3588	4856	1409	2183	4482	6122
October	3599	5096	3866	5652	2004	3122	5814	7272
November	2854	3843	3244	4575	1812	2822	4522	5551
December	2310	3573	3488	4442	2738	3288	4357	5199
Total year	32690	46274	39250	54359	24600	33845	53621	66230

Deficit by Economic Sectors

	ESC1								
	Aquac.	Agricult.	Const.	Domest.	O&G	Indust.	Minner	Livestock	Serv.
January	196	867	18	73	28	21	15	276	8
February	217	839	10	75	13	19	4	310	4
March	68	156	0	24	0	0	0	87	0
April	43	90	0	16	0	0	0	52	0
May	81	235	0	30	0	1	0	110	0
June	65	302	1	25	0	0	0	81	0
July	89	277	0	32	0	1	0	118	0
August	64	183	0	23	0	0	0	82	0
September	50	164	0	20	0	0	0	64	0
October	65	192	0	24	0	0	0	80	0
November	67	198	0	24	0	0	0	86	0
December	101	316	0	36	0	1	1	134	0

	ESC2								
	Aquac.	Agricult.	Const.	Domest.	O&G	Indust.	Minner	Livestock	Serv.
January	464	1434	112	153	212	498	163	714	129
February	542	1404	135	175	249	588	195	843	146
March	202	305	43	53	79	197	61	355	48
April	125	182	28	34	53	126	37	205	31
May	268	421	56	66	106	267	79	440	59
June	196	451	43	50	81	203	62	314	44
July	285	481	58	70	109	283	90	454	66
August	193	326	40	49	75	187	59	344	48
September	151	278	32	39	59	146	46	256	34
October	193	335	42	51	77	190	61	330	48
November	207	347	42	52	80	199	62	360	51
December	320	546	68	81	125	328	102	510	76

	ESC3								
	Aquac.	Agricult.	Const.	Domest.	O&G	Indust.	Minner	Livestock	Serv.
January	696	3031	74	302	150	243	127	940	104
February	774	3415	71	345	143	223	117	1080	102
March	370	1131	8	160	15	46	12	509	11
April	231	726	3	106	5	17	4	305	1
May	437	1427	17	190	34	82	34	600	32
June	309	1229	11	127	32	30	32	446	27
July	440	1561	16	190	35	79	41	629	32
August	356	1114	7	154	13	43	14	487	19
September	265	941	0	122	1	6	1	353	7
October	371	1153	5	162	9	34	8	495	14
November	367	1181	7	158	13	46	18	503	21
December	495	1759	20	216	47	91	47	710	43

	ESC4								
	Aquac.	Agricult.	Const.	Domest.	O&G	Indust.	Minner	Livestock	Serv.
January	1086	5415	122	510	265	390	212	1527	184
February	1241	6536	130	593	270	408	233	1746	211
March	693	2562	29	312	58	128	59	994	53
April	540	1651	12	231	21	80	26	732	24
May	925	3129	41	414	101	189	94	1220	84
June	593	2411	47	247	99	140	81	830	62
July	948	3303	50	415	110	193	103	1223	86
August	696	2470	28	313	71	125	67	983	59
September	522	2026	6	231	21	36	32	762	35
October	736	2549	26	316	61	129	64	1032	59
November	716	2580	29	325	76	129	72	1004	62
December	1051	3721	61	456	135	229	119	1398	97

Groundwater Allocation by Economic Sectors

	ESC1								
	Aquac.	Agricult.	Const.	Domest.	O&G	Indust.	Minner	Livestock	Serv.
January	140	1122	94	119	179	420	135	196	109
February	142	1256	114	129	216	469	161	186	127
March	131	952	65	46	121	259	89	192	70
April	100	771	46	46	87	188	63	153	52
May	167	1146	81	101	152	322	113	244	92
June	80	628	50	26	97	211	66	127	48
July	151	1109	81	96	153	327	114	221	91
August	125	866	62	41	115	246	85	194	68
September	85	732	46	23	87	184	64	135	53
October	135	996	67	45	125	270	91	202	73
November	122	867	63	42	118	252	86	192	70
December	178	1301	94	115	177	381	130	256	105

	ESC2								
	Aquac.	Agricult.	Const.	Domest.	O&G	Indust.	Minner	Livestock	Serv.
January	187	1093	82	749	155	278	100	223	82
February	160	1384	77	827	151	251	97	168	88
March	339	709	108	497	193	431	123	433	90
April	316	447	76	380	138	329	96	490	74
May	288	856	109	638	205	392	146	363	118
June	213	549	69	415	125	261	83	298	71
July	262	870	105	641	198	367	134	337	116
August	316	664	105	495	186	408	122	396	91
September	261	482	77	370	141	313	93	372	74
October	401	675	107	525	190	457	122	548	96
November	312	689	107	505	189	408	125	394	93
December	271	987	109	728	209	375	143	342	123

	ESC3								
	Aquac.	Agricult.	Const.	Domest.	O&G	Indust.	Minner	Livestock	Serv.
January	20	1843	172	232	319	678	218	92	179
February	10	1851	195	221	362	750	255	69	203
March	175	2335	201	184	382	753	281	346	228
April	271	2573	188	149	356	725	258	420	208
May	78	2220	194	188	368	718	262	163	210
June	156	1724	155	165	281	604	197	248	161
July	76	2081	192	189	360	706	250	110	206
August	145	2151	189	180	359	697	259	297	205
September	229	2086	176	179	334	664	245	376	194
October	277	2816	229	200	436	855	319	431	252
November	143	2168	192	184	366	708	261	293	207
December	65	2184	205	201	380	757	267	83	215

	ESC4								
	Aquac.	Agricult.	Const.	Domest.	O&G	Indust.	Minner	Livestock	Serv.
January	4	1993	236	316	415	938	289	4	226
February	0	1925	270	329	489	1044	326	0	247
March	105	2981	287	280	543	1061	383	132	309
April	184	3235	280	272	534	1025	383	399	310
May	16	2545	277	262	504	1009	352	23	282
June	82	2186	203	240	376	824	268	140	224
July	20	2356	264	262	486	991	336	28	274
August	67	2720	268	261	491	993	346	76	280
September	231	2846	273	256	508	1020	356	351	283
October	138	3623	329	318	613	1212	433	258	348
November	68	2728	273	264	496	1013	349	78	283
December	14	2413	277	280	506	1045	354	18	290

Surface water Allocation by Economic Sectors

	ESC1								
	Aquac.	Agricult.	Const.	Domest.	O&G	Indust.	Minner	Livestock	Serv.
January	70	1402	12	437	28	46	22	114	24
February	80	1563	10	475	24	38	22	136	22
March	151	1806	41	470	81	159	60	224	51
April	180	1838	52	439	100	200	74	261	61
May	102	1539	26	410	49	96	36	150	30
June	130	1366	32	375	62	119	50	189	48
July	106	1490	24	406	46	85	33	158	29
August	137	1668	37	440	73	144	54	193	45
September	187	1788	51	455	98	201	72	264	59
October	193	2090	52	539	101	200	76	284	64
November	143	1704	38	447	73	146	55	201	46
December	93	1479	19	423	37	63	27	145	25

	ESC2								
	Aquac.	Agricult.	Const.	Domest.	O&G	Indust.	Minner	Livestock	Serv.
January	0	2899	2	105	8	3	14	0	16
February	0	3066	1	83	5	2	6	0	11
March	19	3647	18	315	51	42	54	18	57
April	77	3690	53	387	108	165	87	51	76
May	5	3393	5	162	12	12	13	4	18
June	32	2673	21	216	48	64	42	22	38
July	5	3251	4	143	11	11	11	5	11
August	13	3357	12	262	39	29	40	11	43
September	103	3533	46	387	96	158	80	114	72
October	36	4234	42	396	95	106	84	28	75
November	13	3394	12	265	38	30	39	12	42
December	3	3422	3	110	8	8	7	4	9

	ESC3								
	Aquac.	Agricult.	Const.	Domest.	O&G	Indust.	Minner	Livestock	Serv.
January	0	2899	2	105	8	3	14	0	16
February	0	3066	1	83	5	2	6	0	11
March	19	3647	18	315	51	42	54	18	57
April	77	3690	53	387	108	165	87	51	76
May	5	3393	5	162	12	12	13	4	18
June	32	2673	21	216	48	64	42	22	38
July	5	3251	4	143	11	11	11	5	11
August	13	3357	12	262	39	29	40	11	43
September	103	3533	46	387	96	158	80	114	72
October	36	4234	42	396	95	106	84	28	75
November	13	3394	12	265	38	30	39	12	42
December	3	3422	3	110	8	8	7	4	9

	ESC4								
	Aquac.	Agricult.	Const.	Domest.	O&G	Indust.	Minner	Livestock	Serv.
January	98	1909	0	723	0	54	0	139	1
February	94	2051	0	791	0	77	0	115	1
March	154	2360	2	736	5	38	4	152	5
April	146	2100	6	747	12	33	12	207	16
May	186	2190	0	704	1	39	1	245	2
June	86	1638	2	560	5	26	4	99	5
July	175	2112	1	689	2	41	2	255	2
August	151	2169	2	673	3	40	3	155	3
September	150	2339	19	694	36	101	27	199	24
October	139	2587	4	854	9	52	7	206	8
November	154	2189	2	685	4	42	3	161	4
December	183	2250	1	731	1	41	1	277	2

Demands by Economic Sectors

	ESC1								
	Aquac.	Agricult.	Const.	Domest.	O&G	Indust.	Minner	Livestock	Serv.
January	407	3391	123	629	234	487	173	586	142
February	439	3658	133	678	253	525	186	632	153
March	350	2913	106	540	201	418	148	503	122
April	324	2699	98	501	187	388	137	466	113
May	350	2919	106	541	202	419	149	504	122
June	276	2296	83	426	159	330	117	397	96
July	345	2877	105	534	199	413	146	497	120
August	326	2717	99	504	188	390	138	469	114
September	322	2683	98	498	185	385	137	463	112
October	393	3278	119	608	226	471	167	566	137
November	332	2769	101	514	191	398	141	478	116
December	372	3097	113	574	214	445	158	535	129

	ESC2								
	Aquac.	Agricult.	Const.	Domest.	O&G	Indust.	Minner	Livestock	Serv.
January	651	5426	197	1006	375	779	276	937	227
February	702	5853	213	1086	404	841	298	1011	245
March	559	4661	169	864	322	669	237	805	195
April	518	4319	157	801	298	620	220	746	181
May	560	4670	170	866	323	671	238	807	195
June	441	3674	134	681	254	528	187	635	154
July	552	4603	167	854	318	661	234	795	192
August	522	4347	158	806	300	624	221	751	182
September	515	4293	156	796	297	617	219	741	180
October	629	5244	191	973	362	753	267	906	219
November	532	4431	161	822	306	636	226	765	185
December	595	4955	180	919	342	712	252	856	207

	ESC3								
	Aquac.	Agricult.	Const.	Domest.	O&G	Indust.	Minner	Livestock	Serv.
January	814	6782	247	1258	469	974	345	1172	284
February	878	7317	266	1357	506	1051	372	1264	306
March	699	5826	212	1080	403	837	297	1006	244
April	648	5399	196	1001	373	775	275	933	226
May	701	5838	212	1083	403	838	297	1008	244
June	551	4592	167	852	317	660	234	793	192
July	690	5754	209	1067	398	826	293	994	241
August	652	5434	198	1008	375	781	277	939	227
September	644	5366	195	995	371	771	273	927	224
October	787	6555	238	1216	453	942	334	1132	274
November	665	5538	201	1027	383	796	282	957	232
December	743	6193	225	1149	428	890	315	1070	259

	ESC4								
	Aquac.	Agricult.	Const.	Domest.	O&G	Indust.	Minner	Livestock	Serv.
January	98	1909	0	723	0	54	0	139	1
February	94	2051	0	791	0	77	0	115	1
March	154	2360	2	736	5	38	4	152	5
April	146	2100	6	747	12	33	12	207	16
May	186	2190	0	704	1	39	1	245	2
June	86	1638	2	560	5	26	4	99	5
July	175	2112	1	689	2	41	2	255	2
August	151	2169	2	673	3	40	3	155	3
September	150	2339	19	694	36	101	27	199	24
October	139	2587	4	854	9	52	7	206	8
November	154	2189	2	685	4	42	3	161	4
December	183	2250	1	731	1	41	1	277	2

References

Agencia Nacional de Hidrocarburos - ANH (2012). Escenarios de Oferta y Demanda de Hidrocarburos en Colombia. Technical report, Agencia Nacional de Hidrocarburos.

Ahmed Suliman, A., Gumindoga, W., Katimon, A., & Darus, I. (2014). Semi-distributed rainfall-runoff modeling utilizing ASTER DEM in Pinang catchment of Malaysia. *Sains Malaysiana*, 43(9).

Al-Jawad, J. Y., Alsaffar, H. M., Bertram, D., & Kalin, R. M. (2019). A comprehensive optimum integrated water resources management approach for multidisciplinary water resources management problems. *Journal of Environmental Management*, 239:211–224.

Alameddine, I., Fayyad, A., Abou Najm, M., & El-Fadel, M. (2018). Sustainability of basin level development under a changing climate. *International Journal of Sustainable Development and Planning*, 13(3):394–405.

Alberti, L., Colombo, L., & Formentin, G. (2018). Null-space Monte Carlo particle tracking to assess groundwater PCE (Tetrachloroethene) diffuse pollution in north-eastern Milan functional urban area. *Science of The Total Environment*, 621:326–339.

Alcolea, A., Carrera, J., & Medina, A. (2006a). Inversion of heterogeneous parabolic-type equations using the pilot points method. *International Journal for Numerical Methods in Fluids*, 51(9-10):963–980.

Alcolea, A., Carrera, J., & Medina, A. (2006b). Pilot points method incorporating prior information for solving the groundwater flow inverse problem. *Advances in Water Resources*, 29(11):1678–1689.

Alcolea, A., Carrera, J., & Medina, A. (2008). Regularized pilot points method for reproducing the effect of small scale variability: Application to simulations of contaminant transport. *Journal of Hydrology*, 355(1-4):76–90.

Allen, R. G., Pereira, L. S., Raes, D., & Smith, M. (1998). Crop evapotranspiration-guidelines fo computing crop water requirements. *FAO Irrigation and Drainage Paper*, 56:1–15.

Álvarez Mendiola, E. (2010). *Diseño de una política eficiente de precios del agua integrando*

costes de oportunidad del recurso a escala de cuenca. Aplicación a la Directiva Marco europea del Agua. PhD thesis, Universidad Politecnica de Valencia.

Amini, M., Johnson, A., Abbaspour, K. C., & Mueller, K. (2009). Modeling large scale geogenic contamination of groundwater, combination of geochemical expertise and statistical techniques. In *International Congress on Modelling and Simulation: Interfacing Modelling and Simulation with Mathematical and Computational Sciences*, pages 4100–4106. Geochmica et Cosmochimica Acta.

Andersen, J., Refsgaard, J. C., & Jensen, K. H. (2001). Distributed hydrological modelling of the Senegal River Basin — model construction and validation. *Journal of Hydrology*, 247(3-4):200–214.

Anderton, S., Latron, J., & Gallart, F. (2002). Sensitivity analysis and multi-response, multi-criteria evaluation of a physically based distributed model. *Hydrological Processes*, 16(2):333–353.

Arboleda-Obando, P. F. (2018). *Determinando los efectos del cambio climático y del cambio en usos del suelo en la Macro Cuenca Magdalena Cauca utilizando el modelo de suelo-superficie e hidrológico MESH*. PhD thesis, Universidad Nacional de Colombia ? Sede Bogotá.

Arenas-Bautista, M., Pescador-Arévalo, J., Donado, L., Saavedra-Cifuentes, E., & Arboleda-Obando, P. (2020). Hydrogeological Modeling in Tropical Regions via FeFlow. *Earth Sciences Research Journal*, 24(1):42–52.

Arenas-Bautista, M. C., Arboleda Obando, P. F., Duque-Gardeazábal, N., Guadagnini, A., Riva, M., & Donado, L. D. (2017). Hydrological Modelling the Middle Magdalena Valley (Colombia). In *American Geophysical Union*, New Orleans.

Arenas-Bautista, M. C., Arboleda-Obando, P. F., Duque-Gardeazábal, N., Guadagnini, A., Riva, M., & Donado, L. D. (2018a). Sensitivity Analysis to uncertain Parameters of TopModel in Tropical Regions with application to the Middle Magdalena Valley (Colombia). In *European Geosciences Union*, Vienna.

Arenas-Bautista, M. C., Arboleda Obando, P. F., Duque-Gardeazábal, N., Saavedra, E., & Donado, L. D. (2018b). Hydrological Modeling in Tropical Regions via TopModel. Study Case: Central Sector of the Middle Magdalena Valley - Colombia. In EGU, editor, *EGU*, Vienna. Preprints.

Arenas-Bautista, M. C., Pescador-Arévalo, J. P., Donado, L. D., Guadagnini, A., & Riva, M. (2018c). Three-dimensional geological model applied for groundwater flow simulations in the Middle Magdalena Valley, Colombia. In *AGU Fall Meeting*.

Asociacion Colombiana del Petroleo (2008). Historia del Petróleo En Colombia. Technical report, ACIPET.

Assaf, H. & Saadeh, M. (2008). Assessing water quality management options in the Upper Litani Basin, Lebanon, using an integrated GIS-based decision support system. *Environmental Modelling and Software*, 23(10-11):1327–1337.

Ayantobo, O. O., Li, Y., Song, S., & Yao, N. (2017). Spatial comparability of drought characteristics and related return periods in mainland China over 1961–2013. *Journal of Hydrology*, 550:549–567.

Badjana, H., Fink, M., Helmschrot, J., Diekkrüger, B., Kralisch, S., Afouda, A., & Wala, K. (2017). Hydrological system analysis and modelling of the Kara River basin (West Africa) using a lumped metric conceptual model. *Hydrological Sciences Journal*, 62(7).

Ballinas-González, H., Alcocer-Yamanaka, V., & Pedrozo-Acuña, A. (2016). Uncertainty analysis in data-scarce urban catchments. *Water (Switzerland)*, 8(11).

Bao, J., Hou, Z., Ray, J., Huang, M., Swiler, L., & Ren, H. (2018). Soil moisture estimation using tomographic ground penetrating radar in a MCMC–Bayesian framework. *Stochastic Environmental Research and Risk Assessment*, 32(8):2213–2231.

Barthel, R. & Banzhaf, S. (2016). Groundwater and Surface Water Interaction at the Regional-scale – A Review with Focus on Regional Integrated Models. *Water Resources Management*, 30(1):1–32.

Beltrán, A., Lancheros, A., Lopez, C., Chaque, C., Patino, A., Guerra, A., Cabreras, J., Quintero, C., & Molano, S. (2014). Plancha Geologica 149- Puerto Serviez.

Beltrán, A. & Quintero, C. (2008). Plancha Geologica 119- Barrancabermeja.

Benoit, N., Marcotte, D., Boucher, A., D'Or, D., Bajc, A., & Rezaee, H. (2018). Directional hydrostratigraphic units simulation using MCP algorithm. *Stochastic Environmental Research and Risk Assessment*, 32(5):1435–1455.

Betancur, T., Mejia, O., & Palacio, C. (2009). Conceptual hydrogeology model to Bajo Cauca antioqueño: a tropical aquifer system. *Revista Facultad de Ingeniería*, 48:107–118.

Beven, K. & Freer, J. (2001a). A dynamic TOPMODEL. *Hydrological Processes*, 15(10):1993–2011.

Beven, K. & Freer, J. (2001b). Equifinality, data assimilation, and uncertainty estimation in mechanistic modelling of complex environmental systems using the GLUE methodology. *Journal of Hydrology*, 249(1-4):11–29.

Blanco-Gutiérrez, I., Varela-Ortega, C., & Purkey, D. R. (2013). Integrated assessment

of policy interventions for promoting sustainable irrigation in semi-arid environments: a hydro-economic modeling approach. *Journal of environmental management*, 128:144–60.

Booker, J. F., Howitt, R. E., Michelsen, A. M., & Young, R. A. (2012). Economics And The Modeling Of Water Resources And Policies. *Natural Resource Modeling*, 25(1):168–218.

Borgonovo, E., Lu, X., Plischke, E., Rakovec, O., & Hill, M. C. (2017). Making the most out of a hydrological model data set: Sensitivity analyses to open the model black-box. *Water Resources Research*, 53(9):7933–7950.

Boskidis, I., Gikas, G. D., Sylaios, G. K., & Tsihrintzis, V. A. (2012). Hydrologic and Water Quality Modeling of Lower Nestos River Basin. *Water Resources Management*, 26(10):3023–3051.

Bossa, A., Diekkrüger, B., Giertz, S., Steup, G., Sintondji, L., Agbossou, E., & Hiepe, C. (2012). Modeling the effects of crop patterns and management scenarios on N and P loads to surface water and groundwater in a semi-humid catchment (West Africa). *Agricultural Water Management*, 115:20–37.

Brouwer, R. & Hofkes, M. (2008). Integrated hydro-economic modelling: Approaches, key issues and future research directions. *Ecological Economics*, 66(1):16–22.

Bulot, D., Gumiere, S., Périard, Y., Lafond, J. A., Gallichand, J., ARMALY-ST-GELAIS, M.-H., & Caron, J. (2016). Relationships between soil hydraulic properties, drainage efficiency and cranberry yields. *Canadian Journal of Soil Science*, pages 2016–0020.

Buytaert, W. (2011). topmodel: Implementation of the hydrological model TOPMODEL in R.

Buytaert, W. & Beven, K. (2011). Models as multiple working hypotheses: hydrological simulation of tropical alpine wetlands. *Hydrological Processes*, 25(11):1784–1799.

Cai, X. (2008). Implementation of holistic water resources-economic optimization models for river basin management - Reflective experiences. *Environmental Modelling and Software*, 23(1):2–18.

Cánovas, C. R., Macías, F., Olías, M., López, R. P., & Nieto, J. M. (2017). Metal-fluxes characterization at a catchment scale: Study of mixing processes and end-member analysis in the Meca River watershed (SW Spain). *Journal of Hydrology*, 550:590–602.

Carniato, L., Schoups, G., Van De Giesen, N., Seuntjens, P., Bastiaens, L., & Sapion, H. (2015). Highly parameterized inversion of groundwater reactive transport for a complex field site. *Journal of Contaminant Hydrology*, 173:38–58.

Carrera, J., Alcolea, A., Medina, A., Hidalgo, J., & Slooten, L. (2005). Inverse problem in hydrogeology. *Hydrogeology Journal*, 13(1):206–222.

Carrera, J., Hidalgo, J., Slooten, L., & Vázquez-Suñé, E. (2010). Computational and conceptual issues in the calibration of seawater intrusion models | Problèmes conceptuels et de calibration des modèles d'intrusion marines. *Hydrogeology Journal*, 18(1):131–145.

Carrera, J., Mousavi, S., Usunoff, E., Sánchez-Vila, X., & Galarza, G. (1993). A discussion on validation of hydrogeological models. *Reliability Engineering and System Safety*, 42(2-3):201–216.

Carrera, J. & Neuman, S. (1986). Estimation of Aquifer Parameters Under Transient and Steady State Conditions: 2. Uniqueness, Stability, and Solution Algorithms. *Water Resources Research*, 22(2):211–227.

Casadevall, S. R. (2016). Improving the management of water multi-functionality through stakeholder involvement in decision-making processes. *Utilities Policy*, 43:71–81.

Cediel, F., Barrero, D., & Caceres, C. (1998). Seismic Atlas of Colombia.

Chen, M., Izady, A., Abdalla, O. A., & Amerjeed, M. (2018). A surrogate-based sensitivity quantification and Bayesian inversion of a regional groundwater flow model. *Journal of Hydrology*, 557:826 – 837.

Cherry, J. A., Parker, B. L., Bradbury, K. R., Eaton, T. T., Gotkowitz, M. G., Hart, D. J., & Borchardt, M. A. (2004). Role of Aquitards in the Protection of Aquifers from Contamination: A "State of the Science" Report. *AWWA Research Foundation Report*, pages 1–144.

Choi, J. M. (2018). Factors influencing public officials' responses to requests for information disclosure. *Government Information Quarterly*, 35(1):30–42.

Christensen, S. & Doherty, J. (2008). Predictive error dependencies when using pilot points and singular value decomposition in groundwater model calibration. *Advances in Water Resources*, 31(4).

Cobourn, K. M., Elbakidze, L., & Ghosh, S. (2017). Chapter 3.1.2 - Conjunctive Water Management in Hydraulically Connected Regions in the Western United States. In Ziolkowska, J. R. & Peterson, J. M., editors, *Competition for Water Resources*, pages 278–297. Elsevier.

Cooper, M. A., Addison, F. T., Alvarez, R., Coral, M., Graham, R., Hayward, A., Howe, S., Martinez, J., Naar, J., Peñas, R., Pulham, A., & Taborda, A. (1995). Basin development and tectonic history of the Llanos basin, and Middle Magdalena Valley, Colombia. *Petroleum basins of South America. AAPG. Memoir no. 62*, 10(10):659–666.

Crespo, P., Feyen, J., Buytaert, W., Célleri, R., Frede, H.-G., Ramírez, M., & Breuer, L. (2012). Development of a conceptual model of the hydrologic response of tropical Andean

micro-catchments in Southern Ecuador. *Hydrology and Earth System Sciences Discussions*, 9(2):2475–2510.

Custodio, E., Andreu-Rodes, J. M., Aragón, R., Estrela, T., Ferrer, J., García-Aróstegui, J. L., Manzano, M., Rodríguez-Hernández, L., Sahuquillo, A., & Del Villar, A. (2016). Groundwater intensive use and mining in south-eastern peninsular Spain: Hydrogeological, economic and social aspects. *The Science of the total environment*, 559:302–316.

da Silva, M. G., de Aguiar Netto, A. d. O., de Jesus Neves, R. J., do Vasco, A. N., Almeida, C., & Faccioli, G. G. (2015). Sensitivity Analysis and Calibration of Hydrological Modeling of the Watershed Northeast Brazil. *Journal of Environmental Protection*, 06(08):837–850.

Dai, H., Ye, M., Walker, A., & Chen, X. (2017). A new process sensitivity index to identify important system processes under process model and parametric uncertainty. *Water Resources Research*, 53(4).

Dakhlaoui, H., Ruelland, D., Tramblay, Y., & Bargaoui, Z. (2017). Evaluating the robustness of conceptual rainfall-runoff models under climate variability in northern Tunisia. *Journal of Hydrology*, 550:201–217.

DANE (2016). Metodología General Tercer Censo Nacional Agropecuario. Technical report, Departamento Adminsitrativo Nacional de Estadistica, Bogotá D.C.

DANE (2017). Hoja metodológica de indicadores Productividad hídrica. Technical report, Departamento Nacional de Estadísticas, Bogotá D.C.

DANE (2019). Boletín Técnico de Índice de Precios. Technical report, Departamento Administrativo Nacional de Estadistica, Bogotá D.C.

Davidsen, C., Liu, S., Mo, X., Holm, P. E., Trapp, S., Rosbjerg, D., & Bauer-Gottwein, P. (2015). Hydroeconomic optimization of reservoir management under downstream water quality constraints. *Journal of Hydrology*, 529:1679–1689.

Davis, M. D. (2007). Integrated water resource management and water sharing. *Journal of Water Resources Planning And Management-Asce*, 133(5):427–445.

De O. Torres, M., Howitt, R., & Rodrigues, L. N. (2016). Modeling the economic benefits and distributional impacts of supplemental irrigation. *Water Resources and Economics*, 14:1–12.

de Sousa Fragoso, R. M. & de Almeida Noéme, C. J. (2018). Economic effects of climate change on the Mediterranean's irrigated agriculture. *Sustainability Accounting, Management and Policy Journal*, 9(2):118–138.

Dell'Oca, A., Riva, M., & Guadagnini, A. (2017). Moment-based Metrics for Global

Sensitivity Analysis of Hydrological Systems. *Hydrology and Earth System Sciences Discussions*, pages 1–41.

Dessu, S. B., Melesse, A. M., Bhat, M. G., Price, R. M., Seid, A. H., Debebe, S. A., & McClain, M. E. (2019). Development and application of a priority rated optimization model (PROM) for multi-sector water resource management systems. *Environmental Modelling & Software*, 113:84–97.

Dewandel, B., Jeanpert, J., Ladouche, B., Join, J. L., & Maréchal, J. C. (2017). Inferring the heterogeneity, transmissivity and hydraulic conductivity of crystalline aquifers from a detailed water-table map. *Journal of Hydrology*, 550:118–129.

Dewandel, B., Maréchal, J., Bour, O., Ladouche, B., Ahmed, S., Chandra, S., & Pauwels, H. (2012). Upscaling and regionalizing hydraulic conductivity and effective porosity at watershed scale in deeply weathered crystalline aquifers. *Journal of Hydrology*, 416-417:83–97.

Doherty, J. (2003). Ground water model calibration using pilot points and regularization. *Ground Water*, 41(2):170–177.

Doherty, J. (2004). *PEST Model-Independent Parameter Estimation*. Watermark Numerical Computing, Idaho, 5th edition.

Donado, L. D., Arenas-Bautista, M. C., Pescador-Arévalo, J. P., Guadagnini, A., & Riva, M. (2018). Hydrogeological Characterization in Tropical Regions with lack of information subject to competing uses of groundwater. In *AGU Fall Meeting*, Washington.

Du, M., Zavattero, E., Ma, Q., Gourbesville, P., & Delestre, O. (2018). Groundwater Modeling for a Decision Support System: The Lower Var Valley, Southeastern France. In *Advances in Hydroinformatics*, pages 273–283. Springer Nature.

Dunne, T. (1983). Relation of field studies and modeling in the prediction of storm runoff. *Journal of Hydrology*, 65(1):25–48.

Ehtiat, M., Mousavi, S., & Ghaheri, A. (2015). Ranking of conceptualized groundwater models based on model information criteria. *Journal of Water Supply: Research and Technology - AQUA*, 64(6):670–687.

Escriva-Bou, A., Pulido-Velazquez, M., & Pulido-Velazquez, D. (2017). Economic value of climate change adaptation strategies for water management in Spain's Jucar Basin. *Journal of Water Resources Planning and Management*, 143(5).

Fabre, J., Ruelland, D., Dezetter, A., & Grouillet, B. (2016). Sustainability of water uses in managed hydrosystems: Human- and climate-induced changes for the mid-21st century. *Hydrology and Earth System Sciences*, 20(8):3129–3147.

Fajraoui, N., Ramasomanana, F., Younes, A., Mara, T. A., Ackerer, P., & Guadagnini, A. (2011). Use of global sensitivity analysis and polynomial chaos expansion for interpretation of nonreactive transport experiments in laboratory-scale porous media. *Water Resources Research*, 47(2):1–14.

Ferreira, D. M., Fernandes, C. V. S., Kaviski, E., & Fontane, D. (2019). Water quality modelling under unsteady state analysis: Strategies for planning and management. *Journal of Environmental Management*, 239:150–158.

Finsterle, S. & Zhang, Y. (2011). Error handling strategies in multiphase inverse modeling. *Computers & Geosciences*, 37(6):724 – 730.

Freeze, R. & Cherry, J. (1979). *Groundwater*. Prentice-Hall.

Friedel, M. & Iwashita, F. (2013). Hybrid modeling of spatial continuity for application to numerical inverse problems. *Environmental Modelling and Software*, 43:60–79.

Fu, Z. H., Zhao, H. J., Wang, H., Lu, W. T., Wang, J., & Guo, H. C. (2017). Integrated planning for regional development planning and water resources management under uncertainty: A case study of Xining, China. *Journal of Hydrology*, 554:623–634.

Gaganis, P. & Smith, L. (2006). Evaluation of the uncertainty of groundwater model predictions associated with conceptual errors: A per-datum approach to model calibration. *Advances in Water Resources*, 29(4):503–514.

Gallego, J., Jaramillo, H., & Patiño, A. (2015). Servicios Intensivos en Conocimiento en la Industria del Petróleo en Colombia. Technical report, Banco Interamericano de Desarrollo.

García-González, M. L., Carvajal-Escobar, Y., & Jiménez-Escobar, H. (2007). Integrated water resource management as a strategy for adaptation to climate change. *Ingeniería y Competitividad*, 29(1):19–29.

Garrido-Rodríguez, J. C., López-Hernández, A. M., & Zafra-Gómez, J. L. (2019). The impact of explanatory factors on a bidimensional model of transparency in Spanish local government. *Government Information Quarterly*, 36(1):154–165.

Garrote, L. (2017). Managing Water Resources to Adapt to Climate Change: Facing Uncertainty and Scarcity in a Changing Context. *Water Resources Management*, 31(10):2951–2963.

Gavidia, A., Porras, J., Perez, O., Pacheco, S., Mesa, L., Talero, C., Fuquen, J., Farfan, E., & Fonseca, H. (2008). Plancha Geologica 133- Puerto Berrio.

George, B., Malano, H., Davidson, B., Hellegers, P., Bharati, L., & Massuel, S. (2011). An integrated hydro-economic modelling framework to evaluate water allocation strategies I: Model development. *Agricultural Water Management*, 98(5):733–746.

Gil Morales, E. G. & Tobón Marín, C. (2016). Hydrological modelling with TOPMODEL of Chingaza páramo, Colombia. *Revista Facultad Nacional de Agronomía*, 69(2).

Gleick, P. H. & Palaniappan, M. (2010). Peak water limits to freshwater withdrawal and use. *Proceedings of the National Academy of Sciences*, 107(25):11155–11162.

Gogu, R., Carabin, G., Hallet, V., Peters, V., & Dassargues, A. (2001). GIS-based hydrogeological databases and groundwater modelling. *Hydrogeology Journal*, 9(6):555–569.

Golmohammadi, A., Khaninezhad, M.-R., & Jafarpour, B. (2015). Group-sparsity regularization for ill-posed subsurface flow inverse problems. *Water Resources Research*, 51(10):8607–8626.

Gómez, E., Jordan, T. E., Allmendinger, R. W., Hegarty, K., & Kelley, S. (2005). Syntectonic Cenozoic sedimentation in the northern middle Magdalena Valley Basin of Colombia and implications for exhumation of the Northern Andes. *Bulletin of the Geological Society of America*, 117(5-6):547–569.

Gómez, E., Jordan, T. E., Allmendinger, R. W., Hegarty, K., Kelley, S., & Heizler, M. (2003). Controls on architecture of the Late Cretaceous to Cenozoic southern Middle Magdalena Valley Basin, Colombia. *Bulletin of the Geological Society of America*, 115(2):131–147.

Gonzalez, M., Sladarriaga, G., & Jaramillo, O. (2010). Estimación de la demanda del agua: Conceptaulización y dimensionamiento de la demanda hídrica sectorial. *Estudio Nacional del Agua*, pages 169–228.

González-Zeas, D., Erazo, B., Lloret, P., De Bièvre, B., Steinschneider, S., & Dangles, O. (2019). Linking global climate change to local water availability: Limitations and prospects for a tropical mountain watershed. *Science of the Total Environment*, 650:2577–2586.

Groves, D. G., Yates, D., & Tebaldi, C. (2008). Developing and applying uncertain global climate change projections for regional water management planning. *Water Resources Research*, 44(12):n/a–n/a.

Gunawardena, A., White, B., Hailu, A., Wijeratne, E., & Pandit, R. (2018). Policy choice and riverine water quality in developing countries: An integrated hydro-economic modelling approach. *Journal of Environmental Management*, 227:44–54.

Gupta, H. V. & Razavi, S. (2018). Revisiting the Basis of Sensitivity Analysis for Dynamical Earth System Models. *Water Resources Research*, 54(11):8692–8717.

H. Hargreaves, G. & A. Samani, Z. (1985). Reference Crop Evapotranspiration from Temperature. *Applied Engineering in Agriculture*, 1(2):96–99.

Han, D. & Cao, G. (2018). Phase difference between groundwater storage changes and

groundwater level fluctuations due to compaction of an aquifer-aquitard system. *Journal of Hydrology*, 566:89–98.

Hanemann, W. M. (2006). The economic conception of water. In *Water Crisis: Myth or Reality*, number 1, chapter 4, pages 60–91. University of California, Berkeley.

Hargreaves, G. & Samani, Z. (1982). Estimating potential evapotranspiration. *Journal of the Irrigation & Drainage Division*, 108(IR3):225–230.

Hargreaves, G. H. & Allen, R. G. (2003). History and Evaluation of Hargreaves Evapotranspiration Equation. *Journal of Irrigation and Drainage Engineering*, 129(1).

Harmanny, K. S. & Malek, Z. (2019). Adaptations in irrigated agriculture in the Mediterranean region: an overview and spatial analysis of implemented strategies. *Regional Environmental Change*, 19(5):1401–1416.

Harou, J. J., Pulido-Velazquez, M., Rosenberg, D. E., Medellín-Azuara, J., Lund, J. R., & Howitt, R. E. (2009). Hydro-economic models: Concepts, design, applications, and future prospects. *Journal of Hydrology*, 375(3-4):627–643.

Hashimoto, T., Loucks, D. P., & Stedinger, J. R. (1982). Reliability , Resiliency , Robustness , and Vulnerability Criteria for Water Resource Systems. *Water Resources Research*, 18(1):14–20.

Hassane, M. & Ackerer, P. (2017). Groundwater flow parameter estimation using refinement and coarsening indicators for adaptive downscaling parameterization. *Advances in Water Resources*, 100:139–152.

He, L., Huang, G., Lu, H., Wang, S., & Xu, Y. (2012). Quasi-Monte Carlo based global uncertainty and sensitivity analysis in modeling free product migration and recovery from petroleum-contaminated aquifers. *Journal of hazardous materials*, 219-220:133–40.

Hernandez, A., Neuman, S., Guadagnini, A., & Carrera, J. (2003). Conditioning mean study state flow on hydraulic head and conductivity through geostatistical inversion. *Stochastic Environmental Research and Risk Assessment*, 17(5):329–338.

Hernández-Bedolla, J., Solera, A., Paredes-Arquiola, J., Pedro-Monzonís, M., Andreu, J., & Sánchez-Quispe, S. T. (2017). The Assessment of Sustainability Indexes and Climate Change Impacts on Integrated Water Resource Management. *Water (Switzerland)*, 9(3).

Hollanda, M., Cecílio, R., Campanharo, W., Zanetti, S., de Andrade, L., & Garcia, G. (2015). Evaluation of TOPMODEL for prediction of the runoff of a watershed under different land uses | Avaliação do TOPMODEL na estimativa do escoamento superficial em microbacia hidrográfica em diferentes usos. *Revista Brasileira de Engenharia Agricola e Ambiental*, 19(5).

Hou, T., Zhu, Y., Lü, H., Sudicky, E., Yu, Z., & Ouyang, F. (2015). Parameter sensitivity analysis and optimization of Noah land surface model with field measurements from Huaihe River Basin, China. *Stochastic Environmental Research and Risk Assessment*, 29(5).

Hu, Z. & Chan, C. W. (2015). In-situ bioremediation for petroleum contamination: A fuzzy rule-based model predictive control system. *Engineering Applications of Artificial Intelligence*, 38:70–78.

Hughes, D. (2016). Hydrological modelling, process understanding and uncertainty in a southern African context: lessons from the northern hemisphere. *Hydrological Processes*, 30(14).

Hutcheson, R. S. & McAdams, D. A. (2010). A Hybrid Sensitivity Analysis for Use in Early Design. *Journal of Mechanical Design*, 132(11):111007.

Ibarra-Zavaleta, S., Landgrave, R., Romero-López, R., Poulin, A., & Arango-Miranda, R. (2017). Distributed hydrological modeling: Determination of theoretical hydraulic potential & streamflow simulation of extreme hydrometeorological events. *Water (Switzerland)*, 9(8).

Ideam (2014). Estudio Nacional del Agua 2014. Technical report, Instituto de Hidrología, Meteorología y Estudios Ambientales.

IDEAM (2019). Estudio Nacional del Agua 2018. Technical report, Instituto de Hidrología, Meteorología y Estudios Ambientales – IDEAM, Bogotá D.C.

Iglesias, A. & Garrote, L. (2015). Adaptation strategies for agricultural water management under climate change in Europe. *Agricultural Water Management*, 155:113–124.

Iglesias, A., Garrote, L., Diz, A., Schlickenrieder, J., & Martin-Carrasco, F. (2011). Re-thinking water policy priorities in the Mediterranean region in view of climate change. *Environmental Science & Policy*, 14(7):744–757.

Iglesias, A., Santillán, D., & Garrote, L. (2018). On the Barriers to Adaption to Less Water under Climate Change: Policy Choices in Mediterranean Countries. *Water Resources Management*, 32(15):4819–4832.

INGENIERIA GEOTEC, S. (2016). ESTUDIO DE IMPACTO AMBIENTAL PARA LAS ACTIVIDADES EXPLORATORIAS A DESARROLLARSE EN EL BLOQUE VMM-9. Technical report, PAREX, Bogota.

Ingrain (2012). Cuenca del Valle Medio del Magdalena - Integración Geológica de la Digitalización y Análisis de Núcleos. Technical report, Agencia Nacional de Hidrocarburos.

Instituto Nacional de Salud (2018). Boletin de vigilancia de calidad del agua en colombia. Technical report, Instituto Nacional de Salud, Bogotá D.C.

Irsa, J. & Zhang, Y. (2012). A direct method of parameter estimation for steady state flow in heterogeneous aquifers with unknown boundary conditions. *Water Resources Research*, 48(9).

Islam, M., Firoz, A., Foglia, L., Marandi, A., Khan, A., Schüth, C., & Ribbe, L. (2017). A regional groundwater-flow model for sustainable groundwater-resource management in the south Asian megacity of Dhaka, Bangladesh | Modèle régional d'écoulement des eaux souterraines pour une gestion durable des ressources en eaux souterraines dans la mé. *Hydrogeology Journal*, 25(3):617–637.

Jafarpour, B. (2013). Sparsity-promoting solution of subsurface flow model calibration inverse problems. *Advances in Hydrogeology*, 9781461464:73–94.

Janetti, E., Riva, M., Straface, S., & Guadagnini, A. (2010). Stochastic characterization of the Montalto Uffugo research site (Italy) by geostatistical inversion of moment equations of groundwater flow. *Journal of Hydrology*, 381(1-2):42–51.

Jardani, A., Dupont, J., Revil, A., Massei, N., Fournier, M., & Laignel, B. (2012). Geostatistical inverse modeling of the transmissivity field of a heterogeneous alluvial aquifer under tidal influence. *Journal of Hydrology*, 472-473:287–300.

Jenson, S. K. (1991). Applications of hydrologic information automatically extracted from digital elevation models. *Hydrological Processes*, 5(1):31–44.

Jeong, H. & Adamowski, J. (2016). A system dynamics based socio-hydrological model for agricultural wastewater reuse at the watershed scale. *Agricultural Water Management*, 171:89–107.

Jeziorska, J. & Niedzielski, T. (2015). Applicability of TOPMODEL in the mountainous catchments in the upper Nysa Kłodzka River basin (SW Poland). *Acta Geophysica*, 66(2):203–222.

Jia, Z., Cai, Y., Chen, Y., & Zeng, W. (2018). Regionalization of water environmental carrying capacity for supporting the sustainable water resources management and development in China. *Resources, Conservation and Recycling*, 134:282–293.

Jiao, J. & Zhang, Y. (2016). Direct Method of Hydraulic Conductivity Structure Identification for Subsurface Transport Modeling. *Journal of Hydrologic Engineering*, 21(10).

Jiménez, S., Mariethoz, G., Brauchler, R., & Bayer, P. (2016). Smart pilot points using reversible-jump Markov-chain Monte Carlo. *Water Resources Research*, 52(5):3966–3983.

Jung, Y., Ranjithan, R., & Mahinthakumar, G. (2011). Subsurface characterization using a D-optimality based pilot point method. *Journal of Hydroinformatics*, 13(4):775–793.

Karay, G. & Hajnal, G. (2015). Modelling of Groundwater Flow in Fractured Rocks. *Procedia Environmental Sciences*, 25:142 – 149.

Karlsson, I. B., Sonnenborg, T. O., Refsgaard, J. C., Trolle, D., Børgesen, C. D., Olesen, J. E., Jeppesen, E., & Jensen, K. H. (2016). Combined effects of climate models, hydrological model structures and land use scenarios on hydrological impacts of climate change. *Journal of Hydrology*, 535:301–317.

Kashyap, D. & Vakkalagadda, R. (2009). New model of variogram of groundwater hydraulic heads. *Journal of Hydrologic Engineering*, 14(8):872–875.

Kauffeldt, A., Wetterhall, F., Pappenberger, F., Salamon, P., & Thielen, J. (2016). Technical review of large-scale hydrological models for implementation in operational flood forecasting schemes on continental level. *Environmental Modelling & Software*, 75:68–76.

Kellner, J., Multsch, S., Kraft, P., Houska, T., Mueller, C., & Breuer, L. (2015). Uncertainty Analysis of a Coupled Hydrological-plant Growth Model for Grassland under Elevated CO2. *Procedia Environmental Sciences*, 29:79–80.

Khaninezhad, M. & Jafarpour, B. (2018). Field-scale history matching with sparse geologic dictionaries. *Journal of Petroleum Science and Engineering*, 170:967–991.

Khaninezhad, M., Jafarpour, B., & Li, L. (2012). Sparse geologic dictionaries for subsurface flow model calibration: Part II. Robustness to uncertainty. *Advances in Water Resources*, 39:122–136.

Khaninezhad, M.-R., Golmohammadi, A., & Jafarpour, B. (2018). Discrete Regularization for Calibration of Geologic Facies Against Dynamic Flow Data. *Water Resources Research*, 54(4):2523–2543.

Khorashadi Zadeh, F., Nossent, J., Sarrazin, F., Pianosi, F., van Griensven, A., Wagener, T., & Bauwens, W. (2017). Comparison of variance-based and moment-independent global sensitivity analysis approaches by application to the SWAT model. *Environmental Modelling and Software*, 91.

Ki-moon, B., Bokova, I., Jarraud, M., & Miletto, M. (2014). Water and Energy. Technical report, UNESCO.

Kirshen, P., Aytur, S., Hecht, J., Walker, A., Burdick, D., Jones, S., Fennessey, N., Bourdeau, R., & Mather, L. (2018). Integrated urban water management applied to adaptation to climate change. *Urban Climate*, 24:247–263.

Klaas, D. K. S. Y., Imteaz, M. A., Sudiayem, I., Klaas, E. M. E., & Klaas, E. C. M. (2017). Novel approaches in sub-surface parameterisation to calibrate groundwater models. *IOP Conference Series: Earth and Environmental Science*, 82(1):012014.

Kpegli, K. A. R., Alassane, A., van der Zee, S. E., Boukari, M., & Mama, D. (2018). Development of a conceptual groundwater flow model using a combined hydrogeological, hydrochemical and isotopic approach: A case study from southern Benin. *Journal of Hydrology: Regional Studies*, 18:50 – 67.

Labadie, J. (1975). A Surrogate-Parameter Approach to Modeling Groundwater Basins. *JAWRA Journal of the American Water Resources Association*, 11(1):97–114.

Lamb, R., Beven, K., & Myrabo, S. (1998). Use of spatially distributed water table observations to constrain uncertainty in a rainfall–runoff model. *Advances in Water Resources*, 22(4):305–317.

Le Ravalec-Dupin, M. (2010). Pilot block method methodology to calibrate stochastic permeability fields to dynamic data. *Mathematical Geosciences*, 42(2):165–185.

Le Ravalec-Dupin, M. & Roggero, F. (2012). Parameterization in history matching: State of the art and perspectives. In *Integrated Reservoir Modelling: Are We Doing it Right?*

Li, H. & Zhang, Y. (2017). Regionalising rainfall-runoff modelling for predicting daily runoff: Comparing gridded spatial proximity and gridded integrated similarity approaches against their lumped counterparts. *Journal of Hydrology*, 550:279–293.

Li, T., Yang, S., & Tan, M. (2019). Simulation and optimization of water supply and demand balance in Shenzhen: A system dynamics approach. *Journal of Cleaner Production*, 207:882–893.

Linde, N., Ginsbourger, D., Irving, J., Nobile, F., & Doucet, A. (2017). On uncertainty quantification in hydrogeology and hydrogeophysics. *Advances in Water Resources*, 110:166 – 181.

Linde, N., Lochbühler, T., Dogan, M., Van Dam, R. L., & Dam, R. L. V. (2015). Tomogram-based comparison of geostatistical models: Application to the Macrodispersion Experiment (MADE) site. *Journal of Hydrology*, 531:543–556.

Lionboui, H., Benabdelouahab, T., Elame, F., Hasib, A., & Boulli, A. (2018). Estimating the economic impact of climate change on agricultural water management indicators. *Pertanika Journal of Science and Technology*, 26(2):749–762.

Liu, J., Zhu, A.-X., Qin, C.-Z., Wu, H., & Jiang, J. (2016). A two-level parallelization method for distributed hydrological models. *Environmental Modelling & Software*, 80:175–184.

Llopis-Albert, C., Merigó, J., & Xu, Y. (2016). A coupled stochastic inverse/sharp interface seawater intrusion approach for coastal aquifers under groundwater parameter uncertainty. *Journal of Hydrology*, 540:774–783.

Loosvelt, L., De Baets, B., Pauwels, V. R., & Verhoest, N. E. (2014). Assessing hydrologic

prediction uncertainty resulting from soft land cover classification. *Journal of Hydrology*, 517:411–424.

López, S. T., de los Angeles Barrionuevo, M., & Rodríguez-Labajos, B. (2019). Water accounts in decision-making processes of urban water management: Benefits, limitations and implications in a real implementation. *Sustainable Cities and Society*, 50:101676.

Lopez-Nicolas, A., Pulido-Velazquez, M., Rougé, C., Harou, J. J., & Escriva-Bou, A. (2018). Design and assessment of an efficient and equitable dynamic urban water tariff. Application to the city of Valencia, Spain. *Environmental Modelling & Software*, 101:137–145.

Loucks, D. P., Beek, E. V., Stedinger, J. R., Dijkman, J. P., & Monique T. Villars (2005). *Water Resources Systems Planning and Management: An Introduction to Methods, Models and Applications*. UNESCO, Paris.

Lund, J. R. & Israel, M. . (1995). Water Transfers in Water Resource Systems. *Journal of Water Resources Planning and Management*, 121(2).

Ma, W. & Jafarpour, B. (2017). Conditioning multiple-point geostatistical facies simulation on nonlinear flow data using pilot points method. In *SPE Western Regional Meeting Proceedings*, volume 2017-April, pages 288–305.

Ma, W. & Jafarpour, B. (2018). Pilot points method for conditioning multiple-point statistical facies simulation on flow data. *Advances in Water Resources*, 115:219–233.

Mahmoud, F. & Saleem, M. (1993). Regularization method for solving radon integral equations. *Computers and Mathematics with Applications*, 25(4):3–13.

Malagón-Navarro, J. P. (2017). *Análisis hidrogeoquímico-multivariado del agua subterránea del sistema acuífero del Valle Medio del Magdalena Colombia*. PhD thesis, Universidad Nacional de Colombia - Sede Bogotá.

Maliva, R. G. (2014). Economics of managed aquifer recharge. *Water (Switzerland)*, 6(5):1257–1279.

Marchant, B. P. & Bloomfield, J. P. (2018). Spatio-temporal modelling of the status of groundwater droughts. *Journal of Hydrology*, 564:397 – 413.

Martin-Carrasco, F. & Garrote, L. (2006). Drought-Induced Water Scarcity in Water Resources Systems. In NATO Science Series, editor, *Extreme Hydrological Events: New Concepts for Security*, pages 301–311. Springer Netherlands, Dordrecht, 78 edition.

Martinsen, G., Liu, S., Mo, X., & Bauer-Gottwein, P. (2019). Joint optimization of water allocation and water quality management in Haihe River basin. *Science of The Total Environment*, 654:72–84.

MAVDT (2013). Metodología para la estimación y evaluación del caudal ambiental en

proyectos que requieren Licencia Ambiental. Technical report, Ministerio de Medio Ambiente Vivienda y Desarrollo TerritoriL, Bogotá D.C.

Mazzoleni, M., Alfonso, L., Chacon-Hurtado, J., & Solomatine, D. (2015). Assimilating uncertain, dynamic and intermittent streamflow observations in hydrological models. *Advances in Water Resources*, 83:323–339.

Medina, A., Galarza, G., Carrera, J., Jódar, J., & Alcolea, A. (2001). The inverse problem in hydrogeology: Applications | El problema inverso en hidrología subterránea. Aplicaciones. *Boletin Geologico y Minero*, 112(SPECIAL ED):93–106.

Meeks, J., Moeck, C., Brunner, P., & Hunkeler, D. (2017). Infiltration under snow cover: Modeling approaches and predictive uncertainty. *Journal of Hydrology*, 546:16–27.

Meerveld, I. T. v. & Weiler, M. (2008). Hillslope dynamics modeled with increasing complexity. *Journal of Hydrology*, 361(1-2):24–40.

Merritt, W., Croke, B., & Jakeman, A. (2005). Sensitivity testing of a model for exploring water resources utilisation and management options. *Environmental Modelling & Software*, 20(8):1013–1030.

Metcalfe, P., Beven, K., & Freer, J. (2015). Dynamic TOPMODEL: A new implementation in R and its sensitivity to time and space steps. *Environmental Modelling & Software*, 72:155–172.

Metcalfe, P., Beven, K., Hankin, B., & Lamb, R. (2017). A modelling framework for evaluation of the hydrological impacts of nature-based approaches to flood risk management, with application to in-channel interventions across a 29 km2 scale catchment in the United Kingdom. *Hydrological Processes*, 31(9):1734–1748.

Meyer, R., Engesgaard, P., Høyer, A.-S., Jørgensen, F., Vignoli, G., & Sonnenborg, T. O. (2018). Regional flow in a complex coastal aquifer system: Combining voxel geological modelling with regularized calibration. *Journal of Hydrology*, 562:544 – 563.

Ministerio de Ambiente, V. y. D. T. (2007). Resolucion N. 2115 del 2007. Technical report, MAVDT, Bogotá D.C.

Ministerio de Ambiente y Desarrollo Sostenible (2017). Decreto 1155 de 2017.

Ministerio de Vivienda Ciudad y Territorio (2018). Resolución CRA 825 de 2017. Technical report, Ministerio de Vivienda, Ciudad y Territorio, Bogotá D.C.

Mishra, V. & Lilhare, R. (2016). Hydrologic sensitivity of Indian sub-continental river basins to climate change. *Global and Planetary Change*, 139:78–96.

Mockler, E. M., O'Loughlin, F. E., & Bruen, M. (2016). Understanding hydrological

flow paths in conceptual catchment models using uncertainty and sensitivity analysis. *Computers & Geosciences*, 90:66–77.

Mohtar, W. H. M. W., Maulud, K. N. A., Muhammad, N. S., Sharil, S., & Yaseen, Z. M. (2019). Spatial and temporal risk quotient based river assessment for water resources management. *Environmental Pollution*, 248:133–144.

Morales, L. (1958). General Geology and Oil Occurrences of Middle Magdalena Valley, Colombia: South America. *Asociación Colombiana de Geólogos y Geofisicos del Petróleo (ACGGP)*, page 55.

Morales-Marín, L. A., Wheater, H. S., & Lindenschmidt, K. E. (2017). Assessment of nutrient loadings of a large multipurpose prairie reservoir. *Journal of Hydrology*, 550:166–185.

Moreno, N., Silva, A., Mora, A., Tesón, E., Quintero, I., Rojas, L. E., Lopez, C., Blanco, V., Castellanos, J., Sanchez, J., Osorio, L., Namson, J., Stockli, D., & Casallas, W. (2013). Interaction between thin- and thick-skinned tectonics in the foothill areas of an inverted graben. The Middle Magdalena Foothill belt. *Geological Society, London, Special Publications*, 377(1):221–255.

Mukherjee, S., Mukherjee, S., Garg, R., Bhardwaj, A., & Raju, P. (2013). Evaluation of topographic index in relation to terrain roughness and DEM grid spacing. *Journal of Earth System Science*, 122(3).

Mukundan, R., Acharya, N., Gelda, R. K., Frei, A., & Owens, E. M. (2019). Modeling streamflow sensitivity to climate change in New York City water supply streams using a stochastic weather generator. *Journal of Hydrology: Regional Studies*, 21:147–158.

Navarro-Chaparro, K., Rivera, P., & Sánchez, R. (2015). Water management analysis of the city of Tijuana , Baja California : Critical factors and challenges Análisis del manejo de agua en la ciudad de Tijuana , Baja California : Factores críticos y retos. *Estudios Fronterizos Nueva Época*, 17(33):1–20.

Neverre, N. & Dumas, P. (2015). Projecting and valuing domestic water use at regional scale: A generic method applied to the Mediterranean at the 2060 horizon. *Water Resources and Economics*, 11:33–46.

Ortiz, R., Luis, J., Ruiz, S., & Ricardo, J. (2009). Modelo Geológico De Los Campos Maduros De Lisama, Tesoro, Nutria Y Peroles, Valle Medio Del Magdalena. Colombia. *... Exploracion Petrolera en ....*

Padrón, R. S., Wilcox, B. P., Crespo, P., & Célleri, R. (2015). Rainfall in the Andean Páramo: New Insights from High-Resolution Monitoring in Southern Ecuador. *Journal of Hydrometeorology*, 16(3):985–996.

Panzeri, M., Guadagnini, A., & Riva, M. (2012). Optimization of pilot points location for

geostatistical inversion of groundwater flow. In *IAHS-AISH Publication*, volume 355, pages 34–40.

Parra, E. A. & Carvajal, I. A. (2012). *Modelamiento y manejo de las interacciones entre la hidrología, la ecología y la economía en una cuenca hidrográfica para la estimación de caudales ambientales*. PhD thesis, Universidad Nacional de Colombia.

Payne, J. T., Wood, A. W., Hamlet, A. F., Palmer, R. N., & Lettenmaier, D. P. (2004). Mitigating the Effects of Climate Change on the Water Resources of the Columbia River Basin. *Climatic Change*, 62(1-3):233–256.

Pedro-Monzonís, M., Ferrer, J., Solera, A., Estrela, T., & Paredes-Arquiola, J. (2015). Key issues for determining the exploitable water resources in a Mediterranean river basin. *Science of The Total Environment*, 503-504:319–328.

Pedro-Monzonís, M., Solera, A., Ferrer, J., Andreu, J., & Estrela, T. (2016). Water accounting for stressed river basins based on water resources management models. *Science of The Total Environment*, 565:181–190.

Peña-Haro, S., Pulido-Velazquez, M., & Llopis-Albert, C. (2011). Stochastic hydro-economic modeling for optimal management of agricultural groundwater nitrate pollution under hydraulic conductivity uncertainty. *Environmental Modelling and Software*, 26(8):999–1008.

Peña-Haro, S., Pulido-Velazquez, M., & Sahuquillo, A. (2009). A hydro-economic modeling framework for optimal management of groundwater nitrate pollution from agriculture. *Journal of Hydrology*, 373(1-2):193–203.

Pereira, H., Figueira, J. R., & Marques, R. C. (2019). Multiobjective Irrigation Model: Alqueva River Basin Application. *Journal of Irrigation and Drainage Engineering*, 145(7).

Pérez-Blanco, C. D. & Gutiérrez-Martín, C. (2017). Buy me a river: Use of multi-attribute non-linear utility functions to address overcompensation in agricultural water buyback. *Agricultural Water Management*, 190:6–20.

Pérez-Sánchez, J. & Senent-Aparicio, J. (2015). Integrated water resources management on a local scale: a challenge for the user community—a case study in Southern Spain. *Environmental Earth Sciences*, 74(7):6097–6109.

Pérez-Uresti, S. I., Ponce-Ortega, J. M., & Jiménez-Gutiérrez, A. (2019). A multi-objective optimization approach for sustainable water management for places with over-exploited water resources. *Computers & Chemical Engineering*, 121:158–173.

Pianosi, F., Beven, K., Freer, J., Hall, J. W., Rougier, J., Stephenson, D. B., & Wagener, T. (2016). Sensitivity analysis of environmental models: A systematic review with practical workflow. *Environmental Modelling & Software*, 79:214–232.

Pianosi, F., Sarrazin, F., & Wagener, T. (2015). A Matlab toolbox for Global Sensitivity Analysis. *Environmental Modelling and Software*, 70.

Pool, M., Carrera, J., Alcolea, A., & Bocanegra, E. (2015). A comparison of deterministic and stochastic approaches for regional scale inverse modeling on the Mar del Plata aquifer. *Journal of Hydrology*, 531:214–229.

Pulido-Velazquez, D., Collados-Lara, A.-J., & Alcalá, F. J. (2018). Assessing impacts of future potential climate change scenarios on aquifer recharge in continental Spain. *Journal of Hydrology*, 567:803–819.

Pulido-Velazquez, D., Garrote, L., Andreu, J., Martin-Carrasco, F.-J. J., & Iglesias, A. (2011). A methodology to diagnose the effect of climate change and to identify adaptive strategies to reduce its impacts in conjunctive-use systems at basin scale. *Journal of Hydrology*, 405(1-2):110–122.

Pulido-Velazquez, M., Andreu, J., Sahuquillo, A., & Pulido-Velazquez, D. (2008). Hydro-economic river basin modelling: The application of a holistic surface–groundwater model to assess opportunity costs of water use in Spain. *Ecological Economics*, 66(1):51–65.

Räsänen, A., Juhola, S., Monge Monge, A., Käkönen, M., Kanninen, M., & Nygren, A. (2017). Identifying mismatches between institutional perceptions of water-related risk drivers and water management strategies in three river basin areas. *Journal of Hydrology*, 550:704–715.

Refsgaard, J. C. (1997). Parameterisation, calibration and validation of distributed hydrological models. *Journal of Hydrology*, 198(1-4):69–97.

Relly, J. E. & Sabharwal, M. (2009). Perceptions of transparency of government policymaking: A cross-national study. *Government Information Quarterly*, 26(1):148–157.

Reynaud, A. & Leenhardt, D. (2008). MoGIRE : A Model for Integrated Water Management. *American Geophysical Union*, 2:576–583.

Riva, M., Guadagnini, A., De Gaspari, F., & Alcolea, A. (2010). Exact sensitivity matrix and influence of the number of pilot points in the geostatistical inversion of moment equations of groundwater flow. *Water Resources Research*, 46(11).

Riva, M., Guadagnini, A., Neuman, S., Janetti, E., & Malama, B. (2009). Inverse analysis of stochastic moment equations for transient flow in randomly heterogeneous media. *Advances in Water Resources*, 32(10):1495–1507.

Riva, M., Panzeri, M., Guadagnini, A., & Neuman, S. P. (2011). Role of model selection criteria in geostatistical inverse estimation of statistical data- and model-parameters. *Water Resources Research*, 47(7).

Rogers, B. P., Hall, A. W., & Global Water Partnership (2003). Effective Water Governance. Technical Report 7, Global Water Partnership.

Romero, J., Jerez, S., Muñoz, O., Castro, O., Bermudez, C., & Pardo, Y. (2015). Mapa Sismotectónico en el Sector Norte del Valle Medio del Magdalena. Technical report, Servicio Geológico Colombiano -SGC, Bogotá D.C.

Rosenberg, D. E., Howitt, R. E., & Lund, J. R. (2008). Water management with water conservation, infrastructure expansions, and source variability in Jordan. *Water Resources Research*, 44(11):1–11.

Ruelland, D., Ardoin-Bardin, S., Billen, G., & Servat, E. (2008). Sensitivity of a lumped and semi-distributed hydrological model to several methods of rainfall interpolation on a large basin in West Africa. *Journal of Hydrology*, 361(1-2):96–117.

Sahoo, S. & Jha, M. (2017). Numerical groundwater-flow modeling to evaluate potential effects of pumping and recharge: implications for sustainable groundwater management in the Mahanadi delta region, India | Modélisation numérique des écoulements d'eau souterraine pour évaluer les . *Hydrogeology Journal*, 25(8):2489–2511.

Salazar, J. (2016). *Una metodología para la estimación de curvas de duración de caudales (cdc) en cuencas no instrumentadas. Caso de aplicación para Colombia en los departamentos de Santander y norte de Santander.* PhD thesis, Universidad Nacional de Colombia.

Sanchez-León, E., Leven, C., Haslauer, C., & Cirpka, O. (2016). Combining 3D Hydraulic Tomography with Tracer Tests for Improved Transport Characterization. *Groundwater*, 54(4):498–507.

Sarmiento-Rojas, L. F. (2011). Middle Magdalena Basin-Vol. 11 Petroleum Geology of Colombia. Technical report, Agencia Nacional de Hidrocarburos, Bogotá D.C.

Schwabe, K., Knapp, K., & Luviano, I. (2017). Chapter 2.1.2 - The Water–Energy Nexus and Irrigated Agriculture in the United States: Trends and Analyses. In Ziolkowska, J. R. & Peterson, J. M., editors, *Competition for Water Resources*, pages 80–104. Elsevier.

Şen, Z. (2015). Basic Porous Medium Concepts. In *Practical and Applied Hydrogeology*, chapter Water Scie, pages 43–97. Elsevier.

Servicio Geológico Colombiano (2014). Plan Estratégico del Conocimiento Geológico del territorio Colombiano. Technical report, Servicio Geológico Colombiano, Bogotá.

Servicios Integrales Hidrogeológicos, S. (2015). Elaborar la Caracterización Hidrológica e Hidrogeológica de las Áreas de Interés de las Zonas Hidrográficas del Meta y Magdalena Medio en el Marco del Estudio Nacional del Agua en el Marco del Estudio Nacional del Agua. Technical report, IDEAM, Bogota.

SGC & MINMINAS (2016). Historia geológica de los Andes colombianos en los alrededores de Ibagué. Technical Report July, Servicio Geologico Colombiano, Bogota.

Sheikholeslami, R., Yassin, F., Lindenschmidt, K.-E., & Razavi, S. (2017). Improved understanding of river ice processes using global sensitivity analysis approaches. *Journal of Hydrologic Engineering*, 22(11).

Sieber, J., Yates, D., Huber-Lee, a., & Purkey, D. (2005). WEAP a demand, priority, and preference driven water planning model: Part 1, model characteristics. *Water International*, 30(4):487–500.

Sigdel, A., Jha, R., Bhatta, D., Abou-Shanab, R. A. I. Sapireddy, V. R., & Jeon, B. H. (2011). Applicability of TOPMODEL in the catchments of nepal: Bagmati river basin. *Geosystem Engineering*, 14(4):181–190.

Simmons, J., Harley, M., Marshall, L., Turner, I., Splinter, K., & Cox, R. (2017). Calibrating and assessing uncertainty in coastal numerical models. *Coastal Engineering*, 125.

Singh, A., Walker, D., Minsker, B., & Valocchi, A. (2008). Interactive multi-objective inverse groundwater modelling - Incorporating subjective knowledge and conceptual uncertainty. In *World Environmental and Water Resources Congress 2008: Ahupua'a - Proceedings of the World Environmental and Water Resources Congress 2008*, volume 316.

Sobol, I. (2001). Global sensitivity indices for nonlinear mathematical models and their Monte Carlo estimates. *Mathematics and Computers in Simulation*, 55(1-3):271–280.

Sobol, I. M. (1993). Sensitivity analysis for nonlinear mathematical models. *Math. Model. Computer.Exp*, 1(4):407–414.

Sochala, P. & Le Maître, O. (2013). Polynomial Chaos expansion for subsurface flows with uncertain soil parameters. *Advances in Water Resources*, 62:139–154.

Song, X., Zhang, J., Zhan, C., Xuan, Y., Ye, M., & Xu, C. (2015). Global sensitivity analysis in hydrological modeling: Review of concepts, methods, theoretical framework, and applications. *Journal of Hydrology*, 523.

Sordo-Ward, A., Granados, A., Iglesias, A., Garrote, L., & Bejarano, M. D. (2019). Adaptation effort and performance of water management strategies to face climate change impacts in six representative basins of Southern Europe. *Water (Switzerland)*, 11(5).

Spulber, D. F. (1988). Optimal environmental regulation under asymmetric information. *Journal of Public Economics*, 35(2):163–181.

Sudret, B. (2008). Global sensitivity analysis using polynomial chaos expansion. *Reliability Engineering & System Safety*, 93:964–979.

Suliman, A., Katimon, A., Darus, I., & Shahid, S. (2016). TOPMODEL for Streamflow

Simulation of a Tropical Catchment Using Different Resolutions of ASTER DEM: Optimization Through Response Surface Methodology. *Water Resources Management*, 30(9).

Sun, D., Zhao, C., Wei, H., & Peng, D. (2011). Simulation of the relationship between land use and groundwater level in Tailan River basin, Xinjiang, China. *Quaternary International*, 244(2):254–263.

Sun, L., Nistor, I., & Seidou, O. (2015). Streamflow data assimilation in SWAT model using Extended Kalman Filter. *Journal of Hydrology*, 531:671–684.

Switzman, H., Coulibaly, P., & Adeel, Z. (2015). Modeling the impacts of dryland agricultural reclamation on groundwater resources in Northern Egypt using sparse data. *Journal of Hydrology*, 520:420–438.

Tavakoli, R. & Reynolds, A. (2009). History matching with parametrization based on the SVD of a dimensionless sensitivity matrix. In *SPE Reservoir Simulation Symposium Proceedings*, volume 1, pages 455–476.

Teng, J., Jakeman, A., Vaze, J., Croke, B., Dutta, D., & Kim, S. (2017). Flood inundation modelling: A review of methods, recent advances and uncertainty analysis. *Environmental Modelling and Software*, 90.

Tian, Y., Zheng, Y., & Zheng, C. (2016). Development of a visualization tool for integrated surface water and groundwater modeling. *Computers & Geosciences*, 86:1–14.

Tiedeman, C. & Green, C. (2013). Effect of correlated observation error on parameters, predictions, and uncertainty. *Water Resources Research*, 49(10):6339–6355.

Tonkin, M., Doherty, J., & Moore, C. (2007). Efficient nonlinear predictive error variance for highly parameterized models. *Water Resources Research*, 43(7).

Tortajada, C., González-Gómez, F., Biswas, A. K., & Buurman, J. (2019). Water demand management strategies for water-scarce cities: The case of Spain. *Sustainable Cities and Society*, 45:649–656.

Tóth, A., Havril, T., Simon, S., Galsa, A., Monteiro-Santos, F. A., Muller, I., & Mádl-Szonyi, J. (2016). Groundwater flow pattern and related environmental phenomena in complex geologic setting based on integrated model construction. *Journal of Hydrology*, 539:330–344.

Tsai, F.-C. (2006). Enhancing random heterogeneity representation by mixing the kriging method with the zonation structure. *Water Resources Research*, 42(8).

Tsai, F.-C. & Yeh, W.-G. (2011). Model calibration and parameter structure identification in

characterization of groundwater systems. *Groundwater Quantity and Quality Management*, pages 159–202.

Tzabiras, J., Vasiliades, L., Sidiropoulos, P., Loukas, A., & Mylopoulos, N. (2016). Evaluation of Water Resources Management Strategies to Overturn Climate Change Impacts on Lake Karla Watershed. *Water Resources Management*, 30(15):5819–5844.

Usman, M., Reimann, T., Liedl, R., Abbas, A., Conrad, C., & Saleem, S. (2018). Inverse parametrization of a regional groundwater flow model with the aid of modelling and GIS: Test and application of different approaches. *ISPRS International Journal of Geo-Information*, 7(1).

Valdés-Pineda, R., Pizarro, R., García-Chevesich, P., Valdés, J. B., Olivares, C., Vera, M., Balocchi, F., Pérez, F., Vallejos, C., Fuentes, R., Abarza, A., & Helwig, B. (2014). Water governance in Chile: Availability, management and climate change. *Journal of Hydrology*, 519(APRIL):2538–2567.

Valencia, C. (2014). Más petróleo, menos agua.

Van Der Heijden, S. & Haberlandt, U. (2015). A fuzzy rule based metamodel for monthly catchment nitrate fate simulations. *Journal of Hydrology*, 531:863–876.

Vargas, N. (2006). Zonas Hidrogeológicas Homogéneas de Colombia. *Boletín Geológico y Minero*, 117(1):47–61.

Vargas Martínez, N. O., Campillo Pérez, A. K., García Herrán, M., & Jaramillo Rodríguez, O. (2013). *Aguas Subterráneas en Colombia: una Visión General*. IDEAM, Bogota.

Velázquez, M. A. P., Álvarez, J. A., & Herraiz, A. S. (2003). *Optimización económica de la gestión del uso conjunto de aguas superficiales y subterráneas en un sistema de recursos hídricos: contribución al análisis económico propuesto en la Directiva Marco Europea del Agua*. PhD thesis, Universidad Politecnica de Valencia.

Vieira, S. M. (2009). World Water Assesment Programme. *The United Nations World Water Development Report*, 5(3):153.

Wagner, P. D., Fiener, P., Wilken, F., Kumar, S., & Schneider, K. (2012). Comparison and evaluation of spatial interpolation schemes for daily rainfall in data scarce regions. *Journal of Hydrology*, 464-465:388–400.

Walker, D., Jakovljević, D., Savić, D., & Radovanović, M. (2015). Multi-criterion water quality analysis of the Danube River in Serbia: A visualisation approach. *Water research*, 79:158–72.

Wang, S., Huang, G., Baetz, B., & Huang, W. (2015). A polynomial chaos ensemble

hydrologic prediction system for efficient parameter inference and robust uncertainty assessment. *Journal of Hydrology*, 530:716–733.

Wang, X., Jardani, A., & Jourde, H. (2017a). A hybrid inverse method for hydraulic tomography in fractured and karstic media. *Journal of Hydrology*, 551:29 – 46.

Wang, X.-S., Wan, L., Jiang, X.-W., Li, H., Zhou, Y., Wang, J., & Ji, X. (2017b). Identifying three-dimensional nested groundwater flow systems in a Tóthian basin. *Advances in Water Resources*, 108:139 – 156.

Ward, D., Goldsmith, R., Jimeno, A., Cruz, J., Restrepo, H., & Gomez, E. (1977). Plancha Geologica 109- Rionegro.

Ward, F. A. (2009). Economics in integrated water management. *Environmental Modelling & Software*, 24(8):948–958.

White, J. T. (2018). A model-independent iterative ensemble smoother for efficient history-matching and uncertainty quantification in very high dimensions. *Environmental Modelling & Software*, 109:191–201.

White, J. T., Fienen, M. N., & Doherty, J. E. (2016). A python framework for environmental model uncertainty analysis. *Environmental Modelling & Software*, 85:217 – 228.

Wiant, H. V. J. & Harner, E. J. (1979). Percent Bias and Standard Error in Logarithmic Regression. *Forest Science*, 25(1):167–168.

Wongsa, S. (2015). Impact of Climate Change on Water Resources Management in the Lower Chao Phraya Basin, Thailand. *Journal of Geoscience and Environment Protection*, 03(10):53–58.

Woodrow, K., Lindsay, J. B., & Berg, A. A. (2016). Evaluating DEM conditioning techniques, elevation source data, and grid resolution for field-scale hydrological parameter extraction. *Journal of Hydrology*, 540:1022–1029.

Wu, Q., Liu, S., Cai, Y., Li, X., & Jiang, Y. (2017). Improvement of hydrological model calibration by selecting multiple parameter ranges. *Hydrology and Earth System Sciences*, 21(1).

Wu, X., Jeuland, M., & Whittington, D. (2016). Does political uncertainty affect water resources development? The case of the Eastern Nile. *Policy and Society*, 35(2):151–163.

Xie, S., Hu, Y., Jiang, M., & Liu, Q. (2006). Study on the inverse method to permeability coefficient of groundwater system: A case study of uranium gangue site in Southern China. In *5th International Conference on Environmental Informatics, ISEIS 2006*.

Xie, Y., Cook, P. G., Simmons, C. T., Partington, D., Crosbie, R., & Batelaan, O. (2018).

Uncertainty of groundwater recharge estimated from a water and energy balance model. *Journal of Hydrology*, 561:1081–1093.

Xue, L., Yang, F., Yang, C., Wei, G., Li, W., & He, X. (2018). Hydrological simulation and uncertainty analysis using the improved TOPMODEL in the arid Manas River basin, China. *Scientific Reports*, 8(1):1–12.

Yao, L. & Guo, Y. (2014). Hybrid algorithm for parameter estimation of the groundwater flow model with an improved genetic algorithm and gauss-newton method. *Journal of Hydrologic Engineering*, 19(3):482–494.

Yasari, E., Pishvaie, M. R., Khorasheh, F., Salahshoor, K., & Kharrat, R. (2013). Application of multi-criterion robust optimization in water-flooding of oil reservoir. *Journal of Petroleum Science and Engineering*, 109:1–11.

Yeh, W.-G. (2015). Review: Optimization methods for groundwater modeling and management | Revue: Méthodes d'optimisation pour la modélisation et la gestion des eaux souterraines | Revisão: Métodos de otimização para modelagem e gerenciamento de águas subterrâneas | Revisión. *Hydrogeology Journal*, 23(6):1051–1065.

Yi, L., Zhang, W.-C., & Yan, C.-A. (2017). A modified topographic index that incorporates the hydraulic and physical properties of soil. *Hydrology Research*, 48(2):370–383.

Yoon, H. & McKenna, S. (2012). Highly parameterized inverse estimation of hydraulic conductivity and porosity in a three-dimensional, heterogeneous transport experiment. *Water Resources Research*, 48(10).

Young, R. (1996). Measuring economic benefits for water investments and policies. *World Bank technical paper*, 1(338):140.

Zhang, J., Fan, S.-k., Yang, J.-c., Du, X.-m., Li, F.-s., & Hou, H. (2014). Petroleum contamination of soil and water, and their effects on vegetables by statistically analyzing entire data set. *The Science of the total environment*, 476-477:258–65.

Zhang, M. & Burbey, T. (2016). A comparison of three hydraulic parameter optimization schemes for Las Vegas valley. *Environmental and Engineering Geoscience*, 22(3):173–194.

Zhang, X., Sun, A. Y., & Duncan, I. J. (2016). Shale gas wastewater management under uncertainty. *Journal of Environmental Management*, 165:188–198.

Zhou, H., Gómez-Hernández, J. J., & Li, L. (2014). Inverse methods in hydrogeology: Evolution and recent trends. *Advances in Water Resources*, 63.

Zimmerman, J. (2016). GIS Topographic Wetness Index (TWI) Exercise Steps.